

# 3D Characterization of Human Knee Cartilage affected by Osteoarthritis Using Laser Scanning Microscopy

**Author:**

Baena Vargas, Juan Carlos

**Publication Date:**

2014

**DOI:**

<https://doi.org/10.26190/unsworks/17219>

**License:**

<https://creativecommons.org/licenses/by-nc-nd/3.0/au/>

Link to license to see what you are allowed to do with this resource.

Downloaded from <http://hdl.handle.net/1959.4/54078> in <https://unsworks.unsw.edu.au> on 2024-05-03

# **3D Characterization of Human Knee Cartilage Affected by Osteoarthritis Using Laser Scanning Microscopy**

**by**

**Juan Carlos Baena Vargas**

A thesis fulfilment of the requirements for the degree of

Master by Research



**School of Mechanical and Manufacturing Engineering**

**Faculty of Engineering**

**The University of New South Wales, Sydney, Australia**

**December 2014**

## Abstract

Osteoarthritis (OA) is a degenerative and the most common joint disease that is affecting a large population nowadays. The cartilage surfaces affected by OA contain information about its degradation process and the different factors that cause this process. Studying the surface topography of human cartilage in different OA grade conditions, using 3D texture parameters, will reveal the surface features of diseased cartilage in a quantitative and objective manner and assist in understanding the degradation process. The purposes of this project were (a) to develop sample preparation procedures for imaging hydrated human cartilage samples using laser scanning confocal microscopy, and (b) to identify the numerical parameters that could effectively describe the distinct cartilage surface morphologies for each OA grade. Human knee cartilage samples with three different OA grades (OA I, II and III) were imaged using laser scanning microscopy (LSM) and analysed using 35 numerical parameters. A statistical method called two-stage nested design was used to determinate the most effective numerical parameters that could describe changes in the surface conditions of human knee cartilage affected by OA. The most effective and reliable numerical parameter describing the progression of the degraded cartilage surface was the  $S_{dc10\_50}$  parameter followed by the  $S_q$  and  $S_a$  parameters. This study has demonstrated that the changes in the surface morphologies of OA cartilage can be characterised quantitatively and the distinctive surface feature is a bearing area related property. The surface feature described by the  $S_{dc10\_50}$  parameter can be used not only to describe the OA grade progression of human knee cartilage, but also to identify the influence of the different factor that increase the OA and to reveal any dependence of the surface topography and the structural condition of the articular cartilage.

## Acknowledgement

Although the realization of this thesis tested my dedication, knowledge and creativity, this project lied in a stable base created by people and institutions who directly or indirectly, allowed me to successfully materialize it.

My most deepest gratefulness to my parents, *Mary* and *Carlos Enrique*, who taught me the value of discipline and perseverance, and most importantly, for giving me that unconditional love. Even when my father is not with us, he is always in my hearth. I thank my wife, *Adriana*, for her support and patience.

I sincerely thank Dr Zhongxiao Peng of the School of Mechanical and Manufacturing Engineering at the University of New South Wales, Australia, for giving me the opportunity of being part of her team, working on such an important topic. Her guidance, advice and support through the whole project were essentials for its satisfactory completion.

Dr Ross Odell, Lecturer of Engineering Statistics and Experiment Design, Graduate School of Biomedical Engineering, UNSW, Australia, for his assistance with the statistical Analysis

Ms Lynn Ferris, Laboratory Manager of Graduate School of Biomedical Engineering at the University of New South Wales, is acknowledged for helping me with the SWP for the sample extraction procedure and allowing the sample extraction process in the PC2 Lab.

Mr Russell Overhall, Laboratory Manager of the School of Mechanical and Manufacturing Engineering at the University of New South Wales, is thanked for helping me to set up the Safe Work Procedure (SWP) for the image acquisition process, using the Laser Scanning Microscope (LSM) and for supplying the required training to use this technique.

The financial support from the Australian Research Council (ARC DP1093975 9) to this project is acknowledged.

I also thank all the others whose names have not been mentioned, but in different ways, they made their contributions to this project

## Table of Contents

<b>Abstract</b> .....	i
<b>Acknowledgement</b> .....	ii
<b>List of Abbreviations</b> .....	viii
<b>List of Figures</b> .....	x
<b>List of Tables</b> .....	xvi
<b>Chapter 1 Introduction</b> .....	1
1.1 Background .....	1
1.2 Aims and objectives .....	5
<b>Chapter 2 Literature Review</b> .....	6
2.1 Articular cartilage of human knee joints .....	6
2.1.1 Composition and structure of human cartilage .....	7
2.1.2 Mechanical function and properties of knee cartilage .....	8
2.2 Wear mechanisms and lubrication on knee articular cartilage (AC).....	10
2.2.1 Lubrication mechanism on AC .....	10
2.2.2 Wear and friction of AC .....	13
2.3 Osteoarthritis and diagnosis .....	14
2.3.1 Impact of OA on society .....	14
2.3.2 Factors influencing on the progression of OA.....	15
2.3.3 Criteria and techniques for osteoarthritis diagnosis.....	17
2.4 Image acquisition techniques for articular cartilage surfaces.....	19
2.4.1 Image acquisition of articular cartilage using scanning white light interferometry microscope (SWLI) .....	19
2.4.2 Image acquisition of articular cartilage using atomic force microscopy (AFM) .....	20
2.4.3 Image acquisition of articular cartilage using scanning electronic microscopy (SEM).....	21
2.4.4 Image acquisition of articular cartilage using ultrasound technique .....	22
2.4.5 Image acquisition of articular cartilage using laser scanning confocal microscopy (LSCM) .....	23

2.5 Surface characterization techniques .....	24
2.5.1 Importance of surface morphology for OA assessment.....	24
2.5.2. Numerical parameters for surface characterization .....	25
2.5.3 Existing studies on cartilage morphology characterization using numerical parameters.....	31
2.6 Summary .....	32
<b>Chapter 3 Materials and Methods.....</b>	<b>34</b>
3.1 Sample treatment.....	34
3.1.1 Sample extraction procedure .....	35
3.1.2 OA grade classification.....	37
3.2 Image acquisition procedure.....	39
3.2.1 Sample condition for image acquisition using laser scanning microscopy (LSM).....	39
3.2.2 Image acquisition using laser scanning microscopy.....	41
3.3 Surface characterization and statistical analysis technique .....	43
3.3.1 Image processing and characterization method .....	43
3.3.2 Criteria of evaluation and statistical procedure .....	44
3.4 Summary .....	47
<b>Chapter 4 Development of Sample Extraction and Image Acquisition Procedures .....</b>	<b>49</b>
4.1 Outcomes of the sample extraction procedure .....	49
4.1.1 Sample sizes and dehydration tests.....	50
4.1.2 Improvement of sample extraction procedure .....	54
4.2 Outcomes of the sample holder design and its functional tests.....	56
4.3 Setting up the laser microscope facility for image acquisition.....	57
4.3.1 Qualitative comparison of images taken with 10X and 20X magnification lens for OA grades III condition .....	57
4.3.2 Quantitative comparison of the data taken with 10X and 20X magnification lens for three different OA grades .....	60
4.4 Summary .....	62
<b>Chapter 5 Qualitative and Quantitative Characterization Results of Cartilage Surface Affected by OA .....</b>	<b>63</b>

5.1 Qualitative characterization of cartilage affected by OA .....	63
5.1.1 Image acquisition by using a 20X magnification objective lens .....	63
5.1.2 Qualitative information from larger image size.....	65
5.1.3 Qualitative description between surface morphologies for 3D stitched images of OA cartilage.....	66
5.2 Quantitative surface characterization and statistical analysis results .....	70
5.2.1 Classification process of the numerical parameters.....	70
5.2.2 Analysis of the selected parameters.....	72
5.2.3 Analysis of the correlated groups .....	74
5.2.4 OA grade evolution described by $S_{dc10\_50}$ parameter .....	76
5.3 Summary .....	77
<b>Chapter 6 Investigations of Micron and Sub-micron Wear Features of Diseased Human Cartilage Surfaces .....</b>	<b>79</b>
6.1 Qualitative characterization of surface morphologies of human knee cartilage by using AFM and LSM techniques.....	80
6.2 Quantitative characterization of surface morphologies of human knee cartilage in micro- and nano-metre scale .....	84
6.3 Summary .....	86
<b>Chapter 7 Discussion .....</b>	<b>88</b>
7.1 Procedures for sample extraction and image acquisition .....	89
7.1.1 Identification of the required sample size.....	89
7.1.2 Performance of the designed sample holder .....	90
7.1.3 Performance of the LSM.....	90
7.1.4 Criteria for the selected magnification.....	91
7.2 Qualitative and quantitative characterization of human knee cartilage at different OA grade levels .....	92
7.2.1 Qualitative surface assessment .....	92
7.2.2 Statistic analysis and quantitative results.....	93
7.2.3 Correlation between cartilage surface texture and its structural condition.....	96
7.3 Comparison between micron and sub-micron characterization of diseased human cartilage surface.....	97
7.4 Limitations of this project and suggestion for future work .....	99

<b>Chapter 8 Conclusions</b> .....	102
8.1 Outcomes of sample extraction process .....	102
8.2 Outcomes of the image acquisition process using LSM .....	103
8.3 Qualitative assessment of cartilage surface morphology .....	103
8.4 Quantitative assessment of cartilage surface morphology .....	105
8.5 Cartilage surface assessment at micron and sub-micron level .....	106
8.6 Significance and benefits of this project .....	107
<b>References</b> .....	108
Appendix A. Safe work procedure (SWP) .....	126
A.1 SWP for Sample extraction from human knee parts.....	126
A.2 SWP for image acquisition of human samples .....	133
Appendix B Selected 3D images of human knee cartilage surfaces affected by OA using LSM .....	140
B.1 Selected LSM images at 20X magnification of OA grade I. ....	140
B.2 LSM images at 20X magnification of OA grade II.....	143
B.3 LSM images at 20X magnification of OA grade III .....	146
Appendix C Numerical values of the studied OA grade condition .....	149
Appendix D Statistical result, using the Engineering statistical software, Minitab. .	164

## List of Abbreviations

Abbreviations	Full name
AC	Articular cartilage
AFM	Atomic force microscope
LSM	Laser scanning microscope
PBS	Phosphate buffered saline
PG	Proteoglycan
OA	Osteoarthritis
<i>Sa</i>	Arithmetical mean height
<i>Sq</i>	Root mean square
<i>Ssk</i>	Surface skewness
<i>Sku</i>	Surface kurtosis
<i>Sz</i>	Peak-peak
<i>S10z</i>	Ten Point Height
<i>Sv</i>	Max valley depth (largest valley depth value)
<i>Sp</i>	Max peak height (largest peak height value)
<i>Sds</i>	Density of summits of the surface
<i>Sal</i>	Autocorrelation Length
<i>Str</i>	Texture Aspect Ratio
<i>Std</i>	Texture direction

<i>Ssc</i>	Mean summit curvature
<i>Sdq</i>	Root mean square gradient
<i>Sdr</i>	Surface area ratio
<i>Sbi</i>	Surface bearing Index
<i>Sci</i>	Core fluid retention Index
<i>Svi</i>	Valley fluid retention Index
<i>Spk</i>	Reduced summit height
<i>Sk</i>	Core roughness depth
<i>Svk</i>	Reduced valley depth
<i>Sdcl-h</i>	l-h% height intervals of bearing curve
<i>Sds</i>	Density of summits
<i>Ssc</i>	Aritmetic mean peak curvature
<i>S5z</i>	Ten point height of surface
<i>S5p</i>	Five point peak height
<i>S5v</i>	Five point pit height
<i>Sva</i>	Closed void area
<i>Spa</i>	Closed peak area
<i>Svv</i>	Closed void volume
<i>Spv</i>	Closed peak volume

## List of Figures

Figure 2.1 Description of knee structure part (AAOO, 2011). <i>The Figure has been removed due to copyright restrictions.</i> .....	6
Figure 2.2 Structure of macromolecules that form a cohesive solid cartilage (Bergman, 2010). <i>The Figure has been removed due to copyright restrictions.</i> .....	8
Figure 2.3 Architectural layout of the articular cartilage, according to its various layers. Note the anisotropic distribution of the tissue in relation to the depth (Moore, 2014). <i>The Figure has been removed due to copyright restrictions.</i> .....	8
Figure 2.4 Strain variation of Cartilage samples from bovine knee, as a function of the permeability (Julkunen, 2007). <i>The Figure has been removed due to copyright restrictions.</i> .....	9
Figure 2.5 Adhesion and friction force of load bearing cartilage (M1) and non-load bearing cartilage (M4). (A) Friction force versus external normal load. (B) The adhesion force during the shearing, (C) cartilage surface roughness and dependence on the joint location (Chan et al., 2011). <i>The Figure has been removed due to copyright restrictions.</i> .....	11
Figure 2. 6 AFM Images of (A,B) load bearing cartilage (M1) and (C,D) non-load bearing cartilage (M4) after friction testing with (A,C) lowest (1.7 nN) and (B,D) the highest (6.8 nm) external normal load (Chan et al., 2011). <i>The Figure has been removed due to copyright restrictions.</i> .....	11
Figure 2.7 Start-up friction response of articular cartilage under three levels of load (Katta et al., 2007). <i>The Figure has been removed due to copyright restrictions.</i> .....	14
Figure 2.8 Dynamic model of friction response of articular cartilage under three different levels of stress, sliding speed of 4 m/s (Katta et al., 2007). <i>The Figure has been removed due to copyright restrictions.</i> .....	14
Figure 2.9 Loss of Proteoglycan in OA. Safranin O staining cartilage. (A) healthy adult showing staining of proteoglycans in all area. (B) OA cartilage with reduced staining in superficial section, caused by proteoglycan content loss (Pearle et al., 2005). <i>The Figure has been removed due to copyright restrictions.</i> .....	16

Figure 2.10 Transversal section of degraded cartilages, classified according to the ICRS (Kleemann et al., 2005). <i>The Figure has been removed due to copyright restrictions.</i> .....	18
Figure 2.11 3-D image of cartilage surface topography located in four regions on the bovine knee (Shekhawat et al., 2009). <i>The Figure has been removed due to copyright restrictions.</i> .....	20
Figure 2.12 3D AFM images showing a banding pattern of collagen fibrils from healthy (A, C) and OA cartilage (B, D). Images C and D are a magnification of images A and C respectively (Wen et al., 2012). <i>The Figure has been removed due to copyright restrictions.</i> .....	21
Figure 2.13 SEM images of collagen fiber orientation with reference to the horizontal cartilage-bone interface. (A) Superficial zone, (B) Deep zone, (C) transitional zone-oblique orientation, (D) no predominant orientation (transitional zone), (E) organized tissues on several directions, (E), orientated and non-orientated tissues were present. The length of the scale bar is equivalent to 500 nm (Changoor et al., 2011). <i>The Figure has been removed due to copyright restrictions.</i> .....	22
Figure 2.14 3D image acquisition of the cartilage. (a) Healthy cartilage, (b) cartilage with hypertrophy due to OA, (c) high degree of OA. The intensity of the colour represents the thickness of the cartilage, which is given in micrometers (Lefebvre et al., 1998). <i>The Figure has been removed due to copyright restrictions.</i> .....	23
Figure 2.15 3D LSCM image of an articular cartilage surface (Tian et al., 2011). <i>The Figure has been removed due to copyright restrictions.</i> .....	24
Figure 2.16 Roughness of osteoarthritic cartilage surfaces and the relation with the loss of proteoglycans in the cartilage structure (Shekhawat et al., 2009). <i>The Figure has been removed due to copyright restrictions.</i> .....	25
Figure 2.17 Several surface profiles with the same $R_a$ -value (Bhushan, 2001). <i>The Figure has been removed due to copyright restrictions.</i> .....	26
Figure 2.18 The ambiguity of the characterization of a 2D profile (Leach, 2010). <i>The Figure has been removed due to copyright restrictions.</i> .....	27

Figure 2.19 Spectrum of the polar graph representing the texture direction of a surface (Blateyron, 2013). <i>The Figure has been removed due to copyright restrictions.</i> .....	28
Figure 2.20 Bearing area curve with the reduced peak height, reduce core depth and reduced valley depth (Blateyron, 2013). <i>The Figure has been removed due to copyright restrictions.</i> .....	30
Figure 2.21 Feature parameter set, according to ISO 25178-2 (Scott, 2009). <i>The Figure has been removed due to copyright restrictions.</i> .....	30
Figure 2.22 Sliding condition test of human cartilage surface; a) before and b) after test with a normal load of 60 N and 300,000 cycles (Verberne et al., 2009). <i>The Figure has been removed due to copyright restrictions.</i> .....	32
Figure 3.1 Key steps to achieve the objectives of this thesis. ....	35
Figure 3.2 Cartilage sample extraction procedure. a) Biological hood prepared for the sample extraction, b) Cartilage samples collected from the hospital, and c) extracted a sample of a suitable size for 3D imaging. ....	36
Figure 3.3 Measurement of the cartilage thickness in the four sections of the samples to classify the OA grade condition in the cartilage sample.....	38
Figure 3.4 Image acquisition procedure using LSM. (a and b). Setting up of the work area and following the Safe Work Procedure for the image acquisition process of human samples; (c) A human sample located in the sample holder (Baena and Peng, 2014). ....	41
Figure 3.5 Stitching image process of human knee cartilage with OA grade III. (a) Twelve LSM images taken using a 20X objective lens; (b) The stitched image using Topostitch; (c) 3D image of the stitched image (Baena and Peng, 2014).....	42
Figure 3.6 Residual plot for the $S_a$ -parameter data. (a) Original data, and (b) transformed data, using the function nature log Ln. In both (a) and (b), 1 - The normal probability plot, 2 - The residual versus fits plot, 3 - Histogram, and 4 - The residual versus the order of the data.....	46

Figure 4.1 Variation of the surface texture for a sample imaged under dry conditions for a period of 15 minutes, using LSM. a) 5 mm human sample, b) the surface of the human sample imaged just taken out from the petridish and with a magnification lens of 10X. Surface roughness $R_a=69.26\text{ }\mu\text{m}$ measured across the red line, and c) image of the sample after 15 min of being taken out of the petridish and captured at a 10X magnification lens. Surface roughness $R_a=35.36\text{ }\mu\text{m}$ measured on the red line.....	51
Figure 4.2 Variation of the surface texture imaged under dry conditions for a period of 25 minutes, using LSM. a) 10 mm sheep sample, b) roughness measurement of a sheep sample, just taken out of the petri-dish, $R_a=12.5\text{ }\mu\text{m}$ measured across the blue line, 10X, c) roughness measurement of the sheep sample, after 25 minutes of being taken out of the petridish and captured at a 10X magnification lens. The roughness value of the blue line is $R_a=12.7\text{ }\mu\text{m}$ . .....	52
Figure 4.3 physical appearances of the samples under both conditions, with and without hydration for around 2 hours. a) and b) sample dry condition just taken out from the petri-dish and two hours after, respectively, c) and d) hydrated sample just taken out from the petri-dish and two hours after, respectively. ....	53
Figure 4.4 Cartilages used for sample extraction. a) Sheep cartilage attached to the femur, and b) collected human knee samples.....	54
Figure 4.5 Three different sample size extracted by different tools, a) 5 mm sample, manually extracted with a puncher, b) 10 mm sample with attached bone extracted with a hole-maker and a drill, c) 15 mm sample with attached bone, extracted with electric oscillating saw and a 10 mm stainless steel blade. ....	55
Figure 4.6 Improvement of the sample holder used for the image acquisition, a&d) first montages for image acquisition of 10mm sample in dry condition, b and f) designed sample holder for 10mm sample with hydration, c and g) improved sample holder for 15 x 15mm human sample with hydration.....	57
Figure 4.7 Images of a healthy cartilage of sheep samples at three different magnifications. a) 10X, b) 20X and c) 50X. ....	58

Figure 4.8 Images of a human cartilage with OA grade III at two magnifications on the same spot of the sample; (a and b) 2D images at 10X and 20X magnification objective lens respectively; (c and d) 3D images at 10X and 20X magnification objective lens respectively.....	59
Figure 4.9 Quantitative comparisons between the data reliability taken by 10X and 20X magnification objective lens. ....	62
The University provide the setting up your work station guide (OHS705) .....	134
Figure 5.1 Evolution of the surface morphology for degraded human knee cartilage for three different OA grade by using a 20X magnification objective lens. (a and b) OA grade I, 53 years old female and 65 years old male respectively (c and d) OA grade II, 64 years old male and 65 years old male respectively (e and f) OA grade III, 89 years old male and 76 years old female respectively.....	64
Figure 5.2 Image process of human knee cartilage surface with OA grade III of an 89 year old male, a) and c) specific regions of the surface with different surface features (Peaks and pits respectively) (b) 3D large stitched image. ....	67
Figure 5.3 Assembled images of diseased human knee cartilage surfaces imaged using LSM. (a) and (b) OA grade I, from 73 years old male and 53 years old female respectively, (c) and (d) OA grade II, from 65 Years old male and 65 years old male respectively, and (e) and (f) OA grade III, from 89 years old male and 53 years old female, respectively. ....	69
Figure 5.4 Ranking of the 16 selected numerical parameters based on the values supplied in Table 1. ....	74
Figure 5.5 Variations of the roughness values with the OA grades of the first correlated group of numerical parameters with the highest F-values. The numbers over the bars, represent the coefficient of variation (%).....	75
Figure 5.6 Variation of the roughness value with the OA grades of the second correlated group of numerical parameters with the lowest F-values. The presented values are dimensionless.....	76

Figure 5.7 Bearing area curves (BAC) illustrating the surface texture of three cartilage surfaces affected by OA. (a) OA grade I cartilage (73 years old male patient); (b) OA grade II (64 years old male); and (c) OA grade III (53 years old female). ..... 77

Figure 6.1 Evolution of the surface morphology with OA grade condition using both techniques, AFM and LSM; a, c and e) 3D images of cartilages in OA grades 1, 2 and 3 acquired using AFM; b, d and f) 3D images of cartilages in OA grades 1, 2 and 3 acquired using laser scanning microscopy. .... 81

Figure 6.2 Image of human knee cartilage surface with OA grade III a) AFM image, b) LSM image with 20x magnification objective lens and c) 3D large stitched image using LSM. .... 83

## List of Tables

Table 2.1 Classification of chondral injuries using the Outerbridge classification system (Kleemann et al., 2005). <i>The Table has been removed due to copyright restrictions.</i> .....	18
Table 2.2 Classification of chondral injuries by International cartilage repair society (ICRS) classification system (Zilkens et al., 2011; Robert, 2007). <i>The Table has been removed due to copyright restrictions.</i> .....	18
Table 2.3 Height parameter set according to SPIP classic roughness parameters for images (Image metrology, 2012; Blateyron, 2013). <i>The Table has been removed due to copyright restrictions.</i> .....	27
Table 2.4 Spatial parameters, according to SPIP Classic roughness parameters for images (Image metrology, 2012; Blateyron, 2013). <i>The Table has been removed due to copyright restrictions.</i> .....	28
Table 2.5 Hybrid parameters (Image metrology, 2012; Blateyron, 2013). <i>The Table has been removed due to copyright restrictions.</i> .....	29
Table 2.6 Functional parameters according to SPIP Classic roughness parameters for images (Image metrology, 2012; Blateyron, 2013). <i>The Table has been removed due to copyright restrictions.</i> .....	29
Table 4.1 Roughness value using Sa parameter for three different OA grade conditions by using two magnifications, 10X and 20X. ....	61
Table 5.1 Statistical results of the 28 Numerical parameters with Significant difference between OA grades (P-Value<0.05). The Standard deviation is represented by the Coefficient of Variation (CV). ....	71
Table 5.2 Pearson correlation coefficients between the selected numerical parameters with significant difference between pairs of OA means, using Tukey's test. ....	73
Table 6.1 The surface roughness ( $S_a$ ) values of the cartilage samples measured at the micro- and nano-metre scales. ....	85
Table 6.2 Distinctive features the three OA grades at the micron and nano-metre scales. ....	86

# **Chapter 1 Introduction**

## **1.1 Background**

Cartilage degradation involves increased loss of articular cartilage, and consequently, causes pain and a reduction in mobility. This degradation process is known as osteoarthritis (OA) which is the most common disease in joints. The progression of OA is not fully understood. This is because different variables, including mechanical behaviour, genetic propensity, ageing and unbalanced nutrition (Pearle et al., 2005), contribute to the cartilage wear. Most of the reported OA patients are over 50 years old (Merchan et al., 1993). However, the number of OA patients at the age of 45 years or less is increasing in the recent years (Jordan et al., 2007). Also, the knee joint, which has the most complex joint structure, has the highest number of reported injuries compared to any other joints (Peña et al., 2007).

Articular cartilage (AC) is a tissue that covers the articular part of the bones to conform the joint. This tissue avoids direct contact between the bones and allows a smooth movement in the joint with little friction (Wooley et al., 2005). It is a composite material made up of different elements such as collagen, proteoglycan and water to conform the cartilage tissue. The physical and mechanical characteristics of this tissue vary from the top surface to its deep level attached to the bone, with the superficial layer being the stiffest region of the cartilage (Ewing, 1990).

Due to the high social and economic impact of OA, understanding of the cartilage degradation process has become an important issue. Unfortunately, articular cartilage damage has been difficult to classify due to the lack of objective measurements. Different

criteria have been used to evaluate OA severities. Two popularly used criteria are the International Cartilage Repair Society (ICRS) scale and the Outerbridge scaling system. The Outerbridge classification, based on the size of the affected area (Outerbridge, 1961), is the most popular classification system used to describe the level of cartilage degradation. In comparison, the ICRS classification is based on the depth of the cartilage injury, and has four OA grades, being OA grades 1 and 2 for a partial cartilage loss, and grades 3 and 4 for nearly full or full-thickness defect (Kleemann et al., 2005).

Changes in the extracellular matrix and the cells of articular cartilage are important symptoms of the disease (Loeser et al., 2003; Byers et al., 1977; Setton et al., 1993). Cartilage fibrillation for different OA grade conditions has been studied at a macro and micro-scale by using arthroscopic (Nomura et al., 2004) and microscopic techniques with diverse magnifications (Loeser et al., 2003; Stoop et al., 2001; Hayami et al., 2003). Stoop et al. (2001) studied the change of fibrillation with the cartilage degradation by using images of the transverse section of the cartilage and magnifications from 100x to 400x. Optical microscopes were used to observe the cartilage fibrillation in the transversal section of the cartilage, reaching a resolution up to 0.24  $\mu\text{m}$  (Silver et al., 2004). The sizes of the studied cartilage section vary according to the objective lens being reported size of the studied transversal section between 0.9 mm to 1.8 mm approximately (Kleemann et al., 2005). However, the vertical section does not show the appearance of the fibrillation at the micro-scale when it is observed parallel to the surface (Meachim et al., 1974).

Cartilage surfaces contain valuable information on the cartilage wear history, and together with their mechanical properties, these features/properties are important to understand the process of cartilage degradation (Ghosh et al., 2012). For this reason, image acquisition techniques are widely used to study cartilage surface topography. These techniques allow

studying the wear of cartilage surfaces at a micro- and nano-metre scale. Some techniques such as the AFM, can also be used to evaluate the mechanical and biological characteristics of cartilages simultaneously (Darling et al., 2010). AFM has been considered to be one of the best methods for 3D image acquisition and quantitative roughness measurements at a sub-micron level (Coles et al., 2008). However, the small imaged area (e.g., an area of 50 x 50  $\mu\text{m}$  for a typical AFM scan) makes this technique unsuitable for studies where an image of a large area is required. This technique is suitable to evaluate nano-scaled surface features, friction and mechanical response (Coles et al., 2008). SEM has been used in the characterization of articular cartilage to evaluate the correlation between collagen arrangements with the biomechanical properties of the tissue (Changoor et al., 2011). The sample treatment required before the image acquisition is one of the limitation of this technique. In contrast, laser scanning microscopy (LSM) does not require a special treatment of the samples (Paddock, 1999), which is a significant advantage in respect to the mentioned techniques. Its capability of generating 3D quantitative images with a high resolution in a micro scale has made this technique highly competitive. Even though this technique has become widely used in biological research, it is not commonly employed as a tool for quantitative surface characterization of engineering and bio-engineering materials.

With the advancement of image acquisition techniques, numerical parameters have been developed to evaluate surface textures, and each parameter describes a particular surface feature. Cartilage surface morphology has been characterized by some surface texture parameters. Among them, an amplitude parameter  $R_a$  is the most widely used to describe the arithmetic average of the surface texture (Ghosh et al., 2012). Forster and Fisher (1999) state that the  $R_{3z}$  parameter (the vertical mean from the third highest peak to the

third lowest valley in each sample length over the assessment length) can supply the most accurate information about the surface condition of the cartilage morphology exposed to friction conditions in comparison to  $R_a$  and  $R_{tm}$  (mean of all the maximum peak-to-valley heights in each sampling length within the assessment length).

It has been recently reported that feature and field parameters can reveal and describe information about the surface degradation process by identifying surface characteristics of the surface such as peak density and trend direction of the surface texture (Blunt and Jiang, 2003; Tian et al., 2011). Wang et al. (2012) stated that a decreasing of the  $S_{dq}$  value reflected a slight diminution on the surface roughness. Furthermore, they also reported that the combination of increasing  $S_{ha}$  and decreasing  $S_{pd}$  value indicated that the surface became smoother with less peak density. These existing results show that although feature parameters such as  $S_{ha}$  have not been widely used to evaluate the wear progression of AC, they have the potential to describe changes in the surface conditions which may not be revealed using commonly used surface parameters  $R_a$  and  $R_q$ .

To date, existing OA assessments are primarily based on the visual inspection of the surface features, and the micro-scaled wear characteristics of human cartilage surfaces have not been well studied using a quantitative and objective method. The aim of this project was to study the main surface features of the AC samples of human knee joints using 3D imaging and numerical parameters. The LSM imaging technique was used to acquire 3D images of human cartilage samples at a micro-scale level. After the quantitative image analyses, a statistical method based on ANOVA was conducted to select numerical parameter(s) that could reveal the progression of the cartilage degradation.

## **1.2 Aims and objectives**

The main purpose of this research project was to characterize the osteoarthritis conditions of human knee cartilage surfaces at a micro scale by using laser scanning microscopy (LSM) and numerical parameters. To achieve the goal, five objectives of this project are specified below.

1. To develop a sample extraction procedure that can guarantee the integrity of the cartilage surface for LSM imaging.
2. To develop a sample preparation procedure for the image acquisition using the LSM technique and in a hydrate mode.
3. To identify the variables of the LSM for the image acquisition in order to obtain appropriate information about the surface conditions in three-dimensional (3D) images with a high quality.
4. To characterize qualitatively the surface morphologies of the OA cartilage in order to identify the main features of the cartilage surface.
5. To identify the most reliable parameter(s) that can reveal quantitatively the main features of the surface morphologies of diseased human cartilage with the OA progression.

## Chapter 2 Literature Review

The surface characterization process of human knee cartilage, affected by osteoarthritis, require a deep understanding of concepts related to the structural, mechanical and physical properties of cartilage and the factors that promote its degradation. The topics reviewed in this chapter include the definition of articular cartilage (AC) regarding to the structural, mechanical and physical behaviour, the factors that might be involved in the cartilage degradation and the different techniques and methods used to evaluate the diseased cartilage surface.

### 2.1 Articular cartilage of human knee joints

The knee is considered one of the most complex joints in the body with a higher probability of being injured than any other articular joint (Peña et al., 2007). The knee joint is conformed by four bones (tibia, femur, patella and fibula) and an arrangement of ligaments and tendon that allow the mechanical response to the different load requirements (Figure 2.1). Articular cartilage is a tissue that covers the end of the bone that is connected to another bone making a joint. This tissue allows a smooth movement between the bones with a minimum friction when it is in a normal condition.

**Figure 2.1** Description of knee structure part (AAOO, 2011). *The Figure has been removed due to copyright restrictions.*

### *2.1.1 Composition and structure of human cartilage*

Articular cartilage (AC) is a biphasic material (solid and liquid). The solid phase is formed by cells and two main macromolecules (collagen and proteoglycans) that are enmeshed together to make a solid and compact material (Ewing, 1990). There are evidences of other kind of macromolecules in this tissue similar to the proteoglycan such as perlecan, decorin and biglycan that have been detected in cartilages and might influence in their intrinsic properties (Knudson, 2001). Figure 2.2 shows the structure of these macromolecules above mentioned, which form an organised and enmeshed new solid phase with porosity and high permeability. These physical characteristics have an important influence on its mechanical response (Ewing, 1990).

The fluid phase that makes up the cartilage tissue contains water and solutes (nutrients and ions). It is estimated that there is more that 60% by wet weight of water in this tissue and there is a free interaction between the water molecule tissue and surrounding fluid (Ewing, 1990). This characteristic ensures the tissue highly hydrated with high permeability and low compressive stiffness. The tissue absorbs energy and uniformly distributes load to the bone.

Articular cartilage is an anisotropic material. The structure characteristics of this cartilaginous tissue change from the surface to the bone (Ewing, 1990). These changes are represented in 4 main segments named as superficial, middle, deep and calcified cartilage zones which are shown in Figure 2.3. The superficial segment of this tissue, estimated between 10% and 20% of the AC thickness, presents a high density of collagen fibers that are tangentially oriented to the surface. The orientation of the collagen fibers change to a perpendicular orientation to the top surface as they are closer to the deep layer

(with 30% of the AC thickness). The estimated middle layer thickness is between 40% and 60% (Yeh et al., 2005).

**Figure 2.2** Structure of macromolecules that form a cohesive solid cartilage (Bergman, 2010). *The Figure has been removed due to copyright restrictions.*

**Figure 2.3** Architectural layout of the articular cartilage, according to its various layers. Note the anisotropic distribution of the tissue in relation to the depth (Moore, 2014). *The Figure has been removed due to copyright restrictions.*

These cartilage structure and components ensure that the tissue has the required mechanical and physical properties such as low friction, load distribution and wear-resistance.

### *2.1.2 Mechanical function and properties of knee cartilage*

Knee joints are a sort of diarthrodial joints that have been affected by injuries because of the mechanical requirement related to work conditions, leisure activities and osteoarthritis. Diarthrodial joints transmit loads and allow the smooth movement between the bones. Cartilage stress is influenced by the joint contact force, the contact area, thickness and material properties of articular cartilage. All these variables have a

significant influence on the fatigue and consequently the degradation of articular cartilage. The mechanical properties of articular cartilage are related to the functional characteristics and the cartilage structure condition. Julkunen (2007) demonstrated that cartilage mechanical properties depend on the cartilage type. The humeral cartilage, for example, has a high stiffness but low permeability in contrast to the tibia cartilage that has a low stiffness but a high permeability. The cartilage permeability is highly correlated with both stiffness and strain. Figure 2.4 shows the variation of permeability with the articular cartilage type and the strain. The tibias cartilage has the highest permeability and it decreases significantly with strain. The patella cartilage has the lowest permeability and less strain-dependent. The patella was also reported to have the highest stiffness (Julkunen, 2007).

**Figure 2.4** Strain variation of Cartilage samples from bovine knee, as a function of the permeability (Julkunen, 2007). *The Figure has been removed due to copyright restrictions.*

AC has anisotropic properties and a complex geometry. The load distribution on the cartilage surface is not uniform, which requests a higher mechanical response on specific areas of the cartilage surface (Laasanen et al., 2003). The properties of the tibial cartilage, for example, change according to the location. The cartilage area covered by the meniscus is thinner and presents different mechanical properties to that in the region which is not covered by the meniscus (Thambyah et al., 2006).

The collagen network has a significant influence on the anisotropy and nonlinearly mechanical property of cartilages. Most of the tensile stiffness of cartilages is provided by collagen fibrils in all directions, but the collagen fibrils do not contribute significantly to compression resistance (Korhonen, 2003). Their mechanical properties depend on the direction that is evaluated. The elastic module parallel to the superficial zone of these articular cartilage is approximately 7.0 GPa and 2.21 GPa perpendicular to the cartilage surface (Kempson et al., 1973).

## **2.2 Wear mechanisms and lubrication on knee articular cartilage (AC)**

The wear of articular cartilage is the removal of material caused by physical contact surface, due to different mechanical actions that promote wear in a variety of forms, such as adhesive, abrasive, erosion and fatigue wear (Waters et al., 2003). Adhesive and abrasive wear mechanisms involve friction and lubrication. The interaction of these mechanisms can accelerate the surface degradation (Mow et al., 1997). Articular cartilage also experiences surface degradation due to biochemical reactions, including the loss of proteoglycans. Consequently, the collagen network and the ionic equilibrium will be affected. The identification of the main factor (biochemical or mechanical) of surface degradation and which factor precedes the other is not clearly understood (Katta et al., 2008).

### *2.2.1 Lubrication mechanism on AC*

Lubrication has an essential function in articular cartilage to conserve the optimal performance of the tissue. The boundary lubrication is estimated under contact condition of high load, low sliding speed and/ or reduced fluid viscosity (Chan et al., 2011). The adhesion of load bearing cartilage has shown to be significantly lower than that of a non-

load bearing cartilage. The load bearing cartilage behaviour is steady with low friction coefficient, contrary to the non-load bearing cartilage that has a higher friction coefficient (Chan et al., 2011).

**Figure 2.5** Adhesion and friction force of load bearing cartilage (M1) and non-load bearing cartilage (M4). (A) Friction force versus external normal load. (B) The adhesion force during the shearing, (C) cartilage surface roughness and dependence on the joint location (Chan et al., 2011). *The Figure has been removed due to copyright restrictions.*

Figure 2.5 shows the contact condition of both load bearing cartilage (M1) and non-load bearing cartilage (M4), and in Figure 2.5 (A), the friction force in load bearing cartilage (M1) is always less than non-bearing cartilage (M4) even when the normal load is increased. The adhesive force of M1 is significantly lower than M4 though their roughness is almost similar (Figure 2.5(B) and 2.5(C) respectively). Low adhesive forces between the articular cartilage surfaces reduce the wear intensity, preserving the tissue integrity. Chan et al. (2011) reported that both the load bearing surface (M1) and the non-load bearing surface (M4) had no clear morphological change under the lower and the higher normal load conditions (Figure 2.6).

**Figure 2. 6** AFM Images of (A,B) load bearing cartilage (M1) and (C,D) non-load bearing cartilage (M4) after friction testing with (A,C) lowest (1.7 nN) and (B,D) the highest (6.8

nm) external normal load (Chan et al., 2011). *The Figure has been removed due to copyright restrictions.*

Fluid film-lubricated interfaces are separated by a viscous fluid with a thickness greater than the surface roughness to prevent contact (New et al., 2008). The applied load on the cartilage surface is supported by the fluid force excited through a hydrostatic mechanism of the extremely pressurized fluid between the articulating surfaces. The thickness of a hydrodynamic film is a function of multiple factors such as fluid viscosity, geometry and roughness of the articulating surfaces, applied normal load, and sliding speed (Scherge et al., 2001).

Boundary lubrication takes place when the surface becomes rough so localized areas are in contact and/or when the lubrication property degrades to a level that the pressure in the film cannot fully support the applied load any more. Due to the lack of lubrication and protection, the cartilage experiences a high wear rate, generates wear debris and further material and property degradation. The most common particles are crystals of calcium pyrophosphate dehydrate (CPPD) and calcium hydroxyapatite (HA) (New et al., 2008).

Biological joints operate under a mixed lubrication regime where articulating surfaces are subjected to both fluid film and boundary lubrication (Mow et al., 1992). Lubrication in AC is supplied by synovial fluid; some studies have shown that synovial fluid lubrication can drastically reduce wear of cartilage pins, articulating against metal surfaces as synovial fluid lubrication has a reduced lubrication coefficient (Lipshitz, 1975). This lubricant is a dialysate of blood plasma. Its main components are the high molecular weight hyaluronate that provide the viscosity and the lubricant glycoprotein known as lubricin, which has the property of reducing the friction levels (Swann et al., 1985).

Hyaluronate (HA) was shown to penetrate the articular cartilage surface with beneficial biochemical effects, additional to the low coefficient friction. Lubricin is produced by both synoviocytes lining the joint capsule, and the superficial zone chondrocytes in articular cartilage (Schumacher et al., 1994). Lubricin functions as an effective lubricant when the glycoprotein is adsorbed to the cartilage surface via its terminals, leaving the central mucin domain free to form a low-friction, surface-protecting layer (Zappone et al., 2008).

### *2.2.2 Wear and friction of AC*

Wear on articular cartilage has preferential locations, depending on the contact area between cartilage surfaces and the loading conditions that is applied to the tissue. This wear is due to the stress levels of friction between cartilages, consequently, to the friction coefficient. Increasing contact stress in the cartilages, the friction coefficient tends to decrease. It might reduce the stress levels, allowing a more efficient rehydration of the cartilage tissue, as it has sufficient time for rehydration of previously loaded tissue, which maintain friction condition at a low level, decreasing wear (Katta et al., 2008). Figure 2.7 shows that during the start-up, which was estimated up to 20 minutes, the coefficient of friction tends to decrease when the contact stress rise, however, this coefficient is highly affected by the time that the load is still applied. During dynamic condition, the coefficient of friction remains stable with a very low value and this value is lower when the load is higher (Figure 2.8). However, this value tends to increase when the velocity is higher (Katta et al., 2007). The wear of cartilage surface might occur in a short period as a result of the failure of lubrication. When this occurs, wear gradually progresses up to a bone-bone contact occur. Joint replacement surgery can be the only option currently

(Graindorge et al., 2000). Lubrication of AC can be classified in two categories, that is, full lubrication and boundary lubrication.

**Figure 2.7** Start-up friction response of articular cartilage under three levels of load (Katta et al., 2007). *The Figure has been removed due to copyright restrictions.*

**Figure 2.8** Dynamic model of friction response of articular cartilage under three different levels of stress, sliding speed of 4 m/s (Katta et al., 2007). *The Figure has been removed due to copyright restrictions.*

### **2.3 Osteoarthritis and diagnosis**

Osteoarthritis (OA) is the most common disease in joints that involves increased loss of articular cartilage. As a result, intense pain and limited movement are experienced by the joint. Although the progressive process of OA is not fully understood, it is mainly attributed by traumatic circumstances; however, other reasons might influence in this increase, such as genetic propensity, ageing and unbalanced nutrition (Pearle et al., 2005).

#### *2.3.1 Impact of OA on society*

Most of the population affected by OA are over the age of 50 years. However, during the last decade, the number of people with OA in the age of 45 years is increasing, affecting a large population of workers (Giles et al., 2010). There is a direct correlation between OA and people occupation, and the reported activities with a high influence to increase

the risk of OA are mining, construction and agriculture. In general, the listed activities all involve a high physical demanding. 27 million Americans have OA and 632,000 joints are replaced each year due to this disease (Giles et al., 2010). The most common joint pain for adults over 45 years old is in the knee (19%). Women have a higher prevalence in the oldest age groups (Dziedzic et al., 2007). The joint pain is one of the main consequences of OA which is not clear understood. Osteoarthritis is the highest cause of disability in the UK, with consequences as pain, deformity, loss of joint mobility and stiffness, having a substantial impact on citizens, affecting their overall quality of life (Doherty, 2003). In the UK, Osteoarthritis has a negative impact in the economy with an equivalent estimated cost of 1% of the gross national product (GNP) per year (Doherty, 2003). During 1999 and 2000, more that 36 million working days were lost due to osteoarthritis with an estimated cost of £3.2 billion in lost production. At the same time, £43 million was spent on community services and £215 million was spent on social services for osteoarthritis (Doherty, 2003). Nowadays, osteoarthritis is affecting about 3 million Australians, which represent around 15% of the Australian population. An average 19000 hip and 2000 knee replacements per year are performed in Australia due to OA. The trend of the implanted joint surgery is likely to increase because of the increasing of some risk factors such as ageing, obesity and injury (March et al., 2004).

### *2.3.2 Factors influencing on the progression of OA*

Biochemical variations on the cartilage structure have an influence on the OA progress, which is related to the proteoglycan content loss, as the proteoglycan degradation reduce its chain length, affecting the formation of the cartilage structure. The inappropriate performance of the proteoglycans is also reflected in the rise of permeability which increases water content in the matrix, augmenting its volume. This event might reduce

the compressive stiffness of AC that has been identified as “the softening of early chondromalacia (Pearle et al., 2005). Figure 2.9 shows how the tissue is degraded in the superficial area where the content of proteoglycan is lower.

It is stated that ageing has an influence on the generation of shorter proteoglycan chain, making the cartilage more susceptible to fatigue fracture and OA (Felson et al., 2000). Metabolic syndrome can significantly increase the risk of knee OA which affects about 25% of the population in the USA (Yoshimura et al., 2012).

**Figure 2.9** Loss of Proteoglycan in OA. Safranin O staining cartilage. (A) healthy adult showing staining of proteoglycans in all area. (B) OA cartilage with reduced staining in superficial section, caused by proteoglycan content loss (Pearle et al., 2005). *The Figure has been removed due to copyright restrictions.*

It is estimated that obesity might increase between 9 to 13% for the onset of the knee OA. This means for every 5 kg gain in mass, the probability of developing Knee OA is increased by 35% (Hart et al., 1993). The significant differences of OA disease reported among male and female have resulted in the concept of genetic influence. Though genetic variation might influence significantly to OA, the selection and estimation of this influence is highly complex. With the advancement of modelling technology DNA and RNA analyses may explain the genetic influence over OA in a more complex trait (van Meurs et al., 2012).

### *2.3.3 Criteria and techniques for osteoarthritis diagnosis*

The understanding of cartilage degradation is essential to prevent or decrease physical disability caused by OA. Multiple factors make the diagnosis of OA a complex process (Karvonen et al., 1994; Jiang et al., 2007). In addition, discrepancies between symptoms and radiographic examination results make the diagnosis more challenging. Consequently, OA is frequently diagnosed by an overall clinical impression based on the patient's age, history of physical examination, radiographic data and magnetic resonance imaging (MRI). Articular cartilage injury has been difficult to classify due to the lack of objective measurements. Different criteria have been used to evaluate the OA intensity.

Two popularly used criteria are the International Cartilage Repair Society scale and Outerbridge scaling system. The Outerbridge classification is the most popular classification system used to describe the level of the cartilage degradation based on the size of the injured area (Outerbridge, 1961). The International Cartilage Repair Society (ICRS) classification system focuses on the depth of the cartilage injury, combined with visual measurement (Kleemann et al., 2005). The reduction of the cartilage thickness is clear evidence of the OA condition as can be seen in Figure 2.10. The cartilage thickness reduction has been used as a criterion for the OA grade assessment by using instruments such as micro-metre screw with a microscopic evaluation (Kleeman et al., 2005). Tables 2.1 and 2.2 illustrate the criteria used in these two OA classifications (Kleemann et al., 2005) and a modified international cartilage repair society system (Zilkens et al., 2011; Robert, 2007). In this modified assessment system, according to the histological assessment, the progression of the cartilage degradation is revealed by the increase on fibrillation, surface roughness and loss of proteoglycans (Kiviranta, 2009; Kleeman et al., 2005).

**Table 2.1** Classification of chondral injuries using the Outerbridge classification system (Kleemann et al., 2005). *The Table has been removed due to copyright restrictions.*

**Table 2.2** Classification of chondral injuries by International cartilage repair society (ICRS) classification system (Zilkens et al., 2011; Robert, 2007). *The Table has been removed due to copyright restrictions.*

A less common OA classification is the gait parameter, which is designed to evaluate how the variability of gait is affected by different controlled walked speeds, gender and severity of knee OA. This parameter shows a correlation of functional abilities with the intensity of OA which affect the knee motion, affecting gait complexity and muscle activity might be altered by OA (Kiss, 2011).

**Figure 2.10** Transversal section of degraded cartilages, classified according to the ICRS (Kleemann et al., 2005). *The Figure has been removed due to copyright restrictions.*

Cartilage degradation is evaluated before or after operation. The post-operative techniques can supply a higher reliability about the evaluation of morphological and structural changes of cartilage degradation than pre-operative techniques. However, some techniques such as magnetic resonance imaging (MRI) have increased the sensitivity to detect slight changes on cartilage surface morphology (Bink et al., 2013; Liess et al., 2002). This is a non-invasive technique which allows collecting information of the cartilage during the degradation process. Post-operative assessment such as histological

and biochemical are destructive procedures since a biopsy is required (Moody, 2013). Further details of widely used imaging techniques can be found in the following section.

## **2.4 Image acquisition techniques for articular cartilage surfaces**

Image acquisition techniques are widely used to obtain cartilage surface topographic data. These techniques allow qualitative and quantitative investigations of the wear characteristics of the surface at micron and nano-metre levels. Some techniques also can be used to evaluate the mechanical and biological characteristics of cartilages (Bhushan, 1995; Kumar et al., 2001). Topographic characterizations at a micron level were carried out with assistance of scanning electron microscopy (SEM), atomic force microscopy (AFM), ultrasound, laser scanning confocal microscopy (LSCM) and scanning white light interferometry (SWLI). Further information on commonly used image acquisition techniques are reviewed below.

### *2.4.1 Image acquisition of articular cartilage using scanning white light interferometry microscope (SWLI)*

White light interferometry microscopy (SWLI) combines an interferometer and microscope in one instrument (Shekhawat et al, 2009), and is an optical technique for non-contact surface topography characterization. It scans an area to produce a 3-D image of the surface. This technique has been used to evaluate the roughness on cartilage surfaces with sufficient sensitivity to detect quantitative differences in roughness (Shekhawat et al., 2009). Figure 2.11 shows the SWLI images of the surface morphologies of a healthy bovine knee cartilage at four different locations. It can be seen

that although overall the appearance of the cartilage surface is smooth, the technique reveals that there is a significant roughness difference in the four selected locations.

**Figure 2.11** 3-D image of cartilage surface topography located in four regions on the bovine knee (Shekhawat et al., 2009). *The Figure has been removed due to copyright restrictions.*

Some advantages of this technique include its fast measurement speed, ease of use, good reproducibility and high resolution of 0.01 nm or better. However, its ultimate lateral resolution is limited to 0.35  $\mu\text{m}$  (Shekhawat et al., 2009).

#### *2.4.2 Image acquisition of articular cartilage using atomic force microscopy (AFM)*

Atomic force microscopy (AFM) is considered to be one of the best methods for 3D image acquisition and for surface roughness measurements at a micron and sub-micron scale (Blunt, 2006). A typical AFM scan is over an area of 50 x 50  $\mu\text{m}$ . Thus, measurements of different spots would be required for a statistical significance, which increases the required time for the inspection. This technique also needs to be operated by a skilled operator. In addition, since a “tapping tip” needs to be used which may damage or contaminate the surface that is studied, the technique is not a fully non-destructive technique (Blunt, 2006).

AFM was used to evaluate the cartilage roughness at the sub-micron level, although this technique is more suitable to evaluate friction and mechanical response (Coles et al.,

2008). Figure 2.12 shows four surface images of articular cartilage obtained by AFM. Figure 2.12 (A) and (C) represent the topography of a healthy cartilage and Figure 2.12 (B) and (D) are the images of OA cartilages (Wen et al., 2012).

**Figure 2.12** 3D AFM images showing a banding pattern of collagen fibrils from healthy (A, C) and OA cartilage (B, D). Images C and D are a magnification of images A and C respectively (Wen et al., 2012). *The Figure has been removed due to copyright restrictions.*

#### *2.4.3 Image acquisition of articular cartilage using scanning electronic microscopy (SEM)*

Scanning electronic microscopy (SEM) is a high resolution imaging acquisition technique. A focused beam of electrons is produced and impacts the sample surface by interacting with the electrons of the sample. This interaction produces a variety of signals with the information of the sample surface that is detected through producing a surface topography image of the sample surface. To obtain the image, the surface is scanned by the electron beam which is synchronised with a detector signal. SEM can reach a resolution over 1 nm which requires to be observed in high vacuum, with a good sample preparation, an optimum calibrating condition of the microscope and a skilled operator (Suzuki, 2002). This technique can also be used with low vacuum and in environmental conditions. However, a strict samples preparation involving an ultra-thin coating of electrically conductive material is required. The most common coating materials are gold, platinum, osmium, iridium, tungsten, chromium and graphite (Suzuki, 2002). SEM has been used in the characterization of articular cartilage to evaluate the correlation between

collagen arrangements with the biomechanical properties of articular cartilage. It is known that articular cartilage have three zones where the collagen fibers change the orientation gradually from tangentially aligned in the surface to perpendicular in the deep zone. Thus the collagen structure has an influence on the biomechanical response (Changoor et al., 2011). Figure 2.13 shows the collagen fiber distribution in different zones of the cartilage. Different arrangements and collagen fiber sizes are illustrated in Figure 2.13. It can be seen that in the transitional cartilage zone the fiber orientation can be classified as oblique, non-oriented and multiple orientation, which might represent a heterogeneous biomechanical behaviour.

**Figure 2.13** SEM images of collagen fiber orientation with reference to the horizontal cartilage-bone interface. (A) Superficial zone, (B) Deep zone, (C) transitional zone-oblique orientation, (D) no predominant orientation (transitional zone), (E) organized tissues on several directions, (E), orientated and non-orientated tissues were present. The length of the scale bar is equivalent to 500 nm (Changoor et al., 2011). *The Figure has been removed due to copyright restrictions.*

#### *2.4.4 Image acquisition of articular cartilage using ultrasound technique*

Ultrasound technique has the ability to reproduce a 3D image using a high frequency of cyclic sound waves. It can reproduce the internal structure of organs with moderate clarity and resolution in a real time and without affecting the integrity of these organs. These characteristics make this technique suitable for clinical applications (Nelson et al., 1990). However, the resolution of the Ultrasound technique is normally expressed in MHz, rather than metric units, making this technique unsuitable for investigating the surface texture and the biomechanical properties of the studied issue.

Ultrasound technique has been used to evaluate the cartilage condition using a 3D reconstruction, which can supply information such as size, extension and the location of the affected area of the cartilage (Lefebvre et al, 1998). Figure 2.14 illustrates images of 3D cartilage reconstructions for a healthy and osteoarthritis (OA) cartilages. In Figure 2.14(a), the cartilage surface is smooth and the thickness is almost constant while Figure 2.14(b) and (c) present an OA cartilage with hypertrophy and an advanced cartilage degradation with evidence of holes on the surface, respectively (Lefebvre et al., 1998).

**Figure 2.14** 3D image acquisition of the cartilage. (a) Healthy cartilage, (b) cartilage with hypertrophy due to OA, (c) high degree of OA. The intensity of the colour represents the thickness of the cartilage, which is given in micrometers (Lefebvre et al., 1998). *The Figure has been removed due to copyright restrictions.*

#### *2.4.5 Image acquisition of articular cartilage using laser scanning confocal microscopy (LSCM)*

Laser scanning confocal microscopy is classified as a type of high resolution fluorescence microscopy. It is recognised as an improved imaging acquisition technique over conventional wide-field microscopy and is now an important technique for the generation of high resolution 3D images of biological samples with relatively thick sections (Jones et al., 2005). It is a non-destructive technique that requires a minimum preparation of the sample to be studied. LSCM has been used widely for biomedical purposes, including the evaluation of articular cartilage (AC) for both healthy and degraded cartilage. This technique is also employed to evaluate the cartilage structure such as the collagenous

component and articular chondrocytes using its ability of reproducing an image of specific feature from an entire gross sample (Hirsch and Hartford Svoboda, 1993). This technique has the ability of making a 3D image of a thick specimen (commonly up to 100  $\mu\text{m}$ ) using thin optical slices of around 500 nm. This characteristic allows the 3D imaging acquisition of a thick specimen with an acceptable contrast and definition (Murphy, 2001). Figure 2.15 shows a 3D OA articular cartilage surface with a predominant wavelength on the degraded surface (Tian et al., 2011).

**Figure 2.15** 3D LSCM image of an articular cartilage surface (Tian et al., 2011). *The Figure has been removed due to copyright restrictions.*

## **2.5 Surface characterization techniques**

### *2.5.1 Importance of surface morphology for OA assessment*

Due to the increase of the number of people with OA, understanding of the structure, mechanical properties and tribological conditions of cartilage is essential to identify the main factors that influence the cartilage degradation. This understanding would be reflected in the development of new methods to reduce and/or alleviate this disease (Katta et al., 2008). A diseased cartilage is characterized by the progressive loss of this tissue from the top surface to the subchondral bone. A healthy AC has an efficient lubrication system and a variation of the surface morphology affects the lubrication performance (Seror et al., 2011). Changes in the surface morphology can reveal not just the evolution of the OA condition, but also give evidence about the mechanobiology condition of cartilage (Northwood et al., 2007). The cartilage structure is affected by the OA progression. Shekhawat et al. (2009) state that the content of proteoglycan in the cartilage

is reduced with the increase of the OA. They also confirmed that the cartilage surface is rougher with the increase of OA by using the  $R_a$  parameter (see Figure 2.16).

**Figure 2.16** Roughness of osteoarthritic cartilage surfaces and the relation with the loss of proteoglycans in the cartilage structure (Shekhawat et al., 2009). *The Figure has been removed due to copyright restrictions.*

Up to date, the main surface features that describe the OA progression are not clearly understood. It is recognized that the surface morphology is the result of the surface mechanical response which is highly correlated with the structural condition of the material. AC is an anisotropic material due to the variation of its structural condition defined by the collagen orientation. This histological condition might explain the increase of the roughness morphology, since there is a correlation between the cartilage histology and the roughness condition during the OA progression (Shekhawat et al., 2009). The surface morphology is composed of several features generated by the damage mechanism and the mechanical response of the surface, and consequently, a detailed assessment of the surface morphology can lead to the main factors that generate the characteristics of the surface morphology (Kennedy, 1982).

#### *2.5.2. Numerical parameters for surface characterization*

Cartilage surface morphology has been characterized by a variety of surface texture parameters, including the most widely used amplitude parameter  $R_a$ . This parameter estimates the arithmetic average of the surface texture, and the surface information related

to shape, slope and variation of the profile cannot be evaluated by this parameter (Bhushan, 2001). Figure 2.17 shows different surface profiles with the same  $R_a$  value. This parameter is commonly used in Industries where the characteristics of the worn surfaces are similar, periodic and have been produced by the same tribological system.

**Figure 2.17** Several surface profiles with the same  $R_a$ -value (Bhushan, 2001). *The Figure has been removed due to copyright restrictions.*

The  $R_a$  parameter is included as one of the 2D parameters, which have been widely used for more than 5 decades but present limitations to describing spatial and functional surface characteristics such as the predominance of ridges or scratches. The interpretation of a 2D roughness profile might lead to misunderstanding during the surface morphology characterization since the distinction between pits and valleys can be ambiguous. Figure 2.18 shows an example. In comparison,

3D numerical parameters can describe comprehensive topographic information of a surface (Leach, 2010). In recent years, 3D surface analysis has been popularly used in the engineering and science fields by using 3D surface topography parameters to evaluate the morphologies of a surface area instead of a line (Gadelmawla et al., 2005). The areal parameters are classified into two main groups, namely, the *Field* and *Feature* parameters (Blunt and Jiang, 2003; Scott, 2009; Scott et al., 1994). Most of the parameters are field parameters. These parameters take into consideration every data point of the surface to be evaluated in comparison to the feature parameters that only take specific characteristics or limited data of the surface (Blateyron, 2013).

**Figure 2.18** The ambiguity of the characterization of a 2D profile (Leach, 2010). *The Figure has been removed due to copyright restrictions.*

The following sub-sections summarize the definitions of the field and feature parameters which are important in this project.

#### ***2.5.2.1 Field parameters***

The field parameters are composed by a set of parameters known as *S*- and *V*-parameters. The *S*-parameters evaluates the surface regarding the height amplitude and spacing frequency. The *V*-parameters are based on the Bearing area curve or *Abbott-Firestone curve* (Blunt and Jiang, 2003).

#### ***Height parameters***

These parameters characterize the amplitude properties of the surface which are classified in four categories such as dispersion, asymmetry of the height distribution, sharpness of the height distribution and extreme peaks and valleys (Blunt and Jiang, 2003). The definitions of the areal height parameters are presented in Table 2.3.

**Table 2.3** Height parameter set according to SPIP classic roughness parameters for images (Image metrology, 2012; Blateyron, 2013). *The Table has been removed due to copyright restrictions.*

### ***Spatial parameters***

These parameters characterize the spatial properties of the surface such as the peak density and directionality of the surface texture (Blunt and Jiang, 2003). These parameters are presented in Table 2.4. Among them, the texture direction parameter ( $S_{td}$ ) is the most widely used to evaluate the Fourier spectrum of the surface.  $S_{td}$  reveals the texture direction of a surface by giving the direction in angle of the texture in degrees between  $0^\circ$  and  $180^\circ$  (Leach, 2014; Blateyron, 2013) as shown in Figure 2.19.

**Table 2.4** Spatial parameters, according to SPIP Classic roughness parameters for images (Image metrology, 2012; Blateyron, 2013). *The Table has been removed due to copyright restrictions.*

**Figure 2.19** Spectrum of the polar graph representing the texture direction of a surface (Blateyron, 2013). *The Figure has been removed due to copyright restrictions.*

### ***Hybrid parameters***

The Hybrid parameters are created under the concept of both amplitude and spatial information (Stout et al., 1994). Any variation in the amplitude and/or spacing might be reflected in the hybrid property (Blunt and Jiang, 2003).

**Table 2.5** Hybrid parameters (Image metrology, 2012; Blateyron, 2013). *The Table has been removed due to copyright restrictions.*

### ***Functional parameters***

The functional parameters describe bearing characteristics and fluid retention properties using the area bearing ratio curve or *Abbott curve* (Leach, 2014; Blateyron, 2013). This curve is obtained by the accumulation of the height distribution. The definitions of the functional parameters can be found in Table 2.6.

The reduced peak height ( $S_{pk}$ ) evaluates the peak height above the core zone roughness. The core roughness depth ( $S_k$ ) evaluates the height of the core roughness presented between  $S_{pk}$  and  $S_{vk}$  parameters. The reduce valley depth ( $S_{vk}$ ) evaluates the valley depth below  $S_k$ . The peak material portion ( $S_{Mr1}$ ) is the percentage of the peak section related to  $S_{pk}$ . The valley material portion ( $S_{Mr2}$ ) is the percentage defined by the section related to  $S_{vk}$  (i.e.,  $100\%-S_{Mr2}$ ) as can be seen in Figure 2.20. The *l-h% height intervals of bearing curve* ( $S_{dcl\_h}$ ) is a set of parameters that evidence the height differences between specific bearing area ratio, from  $l\%$  to  $h\%$ , where  $l$  and  $h$  are the lower and upper values of the interval in the BAC.

**Table 2.6** Functional parameters according to SPIP Classic roughness parameters for images (Image metrology, 2012;Blateyron, 2013). *The Table has been removed due to copyright restrictions.*

**Figure 2.20** Bearing area curve with the reduced peak height, reduce core depth and reduced valley depth (Blateyron, 2013). *The Figure has been removed due to copyright restrictions.*

#### **2.5.2.2 Feature parameters**

Feature parameters are composed of nine parameters according to the International standard (ISO/TS CD 25178-2, 2006). This group of parameters characterizes specific features of the surface by using pattern recognition techniques, which involves the following steps including identifying the type of the texture feature, determining a significant feature, classifying the feature attributes and quantifying the surface features.

The surface texture is defined by many features and the feature parameters evaluate the attributes of specific features of the surface morphology, such as points, lines or areas (Blanc et al., 2011). Figure 2.21 illustrates the set of the feature parameters that describe the attributes of the specific features of the surface morphology.

**Figure 2.21** Feature parameter set, according to ISO 25178-2 (Scott, 2009). *The Figure has been removed due to copyright restrictions.*

### *2.5.3 Existing studies on cartilage morphology characterization using numerical parameters*

Cartilage surfaces contain valuable information on the cartilage wear history, and together with their mechanical properties, these features/properties are important for understanding the cartilage degradation process (Ghosh et al., 2012). With the advancement of image acquisition techniques presented in section 2.5, numerical parameters have been developed to evaluate surface textures.

Cartilage surface morphology has been characterized by a variety of surface texture parameters, being the most widely used the  $R_a$  parameter, which is a 2D amplitude parameter, representing the arithmetic average of the surface texture (Ghosh et al., 2012). Forster and Fisher (1999) stated that the  $R_{3z}$  parameter (the vertical mean from the third highest peak to the third lowest valley in each sample length over the assessment length) could supply the most accurate information about the surface morphology condition on cartilages exposed to friction in comparison to  $R_a$  and  $R_{tm}$  (mean of all the maximum peak-to-valley heights in each sampling length within the assessment length). Accardi et al. (2011) evaluated the evolution of cartilage surface condition before and after sliding tests by using both 2D and 3D parameters (e.g.,  $R_a$ ,  $R_q$ ,  $R_z$ ,  $R_t$ ,  $S_{sk}$ ,  $S_{ku}$ ). They also reported that even when morphological changes in the surface were evident after the test, the set of parameter employed did not reveal a significant change in the average surface roughness. Verberne et al (2009) studied the cartilage wear caused by sliding conditions and characterized the wear process using numerical parameters  $R_a$ ,  $R_q$  and  $R_t$  before and after the test. Some cavities on the surface were revealed after the wear test, which were attributed to lacunas where the chondrocytes were located. However, the  $R_a$  and  $R_q$  parameters did not evidence any significant change even when the surface morphological

changes were evident (Figure 2.22). These inconsistent results were reported in other studies where the  $R_q$  parameter was also used to assess the surface morphology (Chan et al., 2010; Coles et al., 2008).

**Figure 2.22** Sliding condition test of human cartilage surface; a) before and b) after test with a normal load of 60 N and 300,000 cycles (Verberne et al., 2009). *The Figure has been removed due to copyright restrictions.*

More recently, feature and field parameters were used for cartilage assessment (Tian et al., 2011). The study found that although feature parameters such as  $S_{ha}$  have not been widely used to evaluate the wear progression of AC, they have the potential to describe changes in the surface conditions which may not be revealed using commonly used roughness parameters  $R_a$  and  $R_q$ .

## 2.6 Summary

Due to the increased number of people with osteoarthritis disease that affects the well-being of humanity and the economy of nations, the understanding of the cartilage degradation process of human knee caused by (OA) has become a highly important topic. Many studies have been carried out in order to understand the causes of OA and its behaviour. However, the complexity of the cartilage tissue regarding to the biphasic composition and anisotropic properties present several challenges that need to be faced properly in order to obtain reliable results. Dehydration, for example, is one of the main

issues during the cartilage characterization, since the loss of water content in these tissues during the characterization process can significantly change the surface morphologies. The dehydration issue varies according to the employed characterization technique, as it depends on the technique requirements and limitations such as sample preparation, test condition and required time for image acquisition.

It has been widely reported that the cartilage surface morphologies evolve in the OA process. Most of the existing studies of the cartilage degradation process are conducted in a laboratory environment and the estimation of the cartilage degradation is evaluated by using conventional numerical parameters, among which the 2D parameter,  $R_a$  is widely used to assess the degraded condition of cartilage. This literature review shows the limitations of the traditional parameters commonly used to describe the surface amplitude changes and provides evidence for further studies of changes in the spatial and functional features of the surface in the OA process using advanced quantitative techniques in 3D.

## **Chapter 3 Materials and Methods**

The aim of this thesis was to identify numerical parameter(s) that could quantitatively and efficiently describe the progression of the cartilage surface degradation of human knee joints affected by osteoarthritis (OA). The cartilage surface characterization involves a careful treatment of the sample in order to obtain reliable surface morphological data by avoiding sample degradation and. The considerations for the sample treatment are from the sample extraction to image acquisition process. A procedure was developed to achieve this purpose. The steps that conformed this procedure were carefully followed in order to achieve effective and reliable results. Figure 3.1 illustrates the main steps of the procedure used in this project.

### **3.1 Sample treatment**

Cartilage samples were obtained from femoral knee condyles in total knee replacement surgeries in Queensland, Australia and under a human research ethics approval (Ethics Approval Number MHS20100401-01 approved by the Mater Health Services North Queensland Ltd Human Research Ethics Committee). A number of 12 cartilage samples were obtained from 12 patients of both genders and in an age range of 53 to 89. The OA grades of the extracted samples were identified according to the International Cartilage Repair Society Classification System (ICRS) (Kleemann et al., 2005). The OA grades presented on samples were from grades I to IV. A healthy cartilage (OA grade 0) was not obtained from the collected samples. OA grade IV was not studied in this work either, since according to the OA assessment, the subchondral

bone is exposed and the cartilage is fully removed when OA progresses reach that level. Thus, this study investigated cartilage samples with state of OA grades I, II and III.

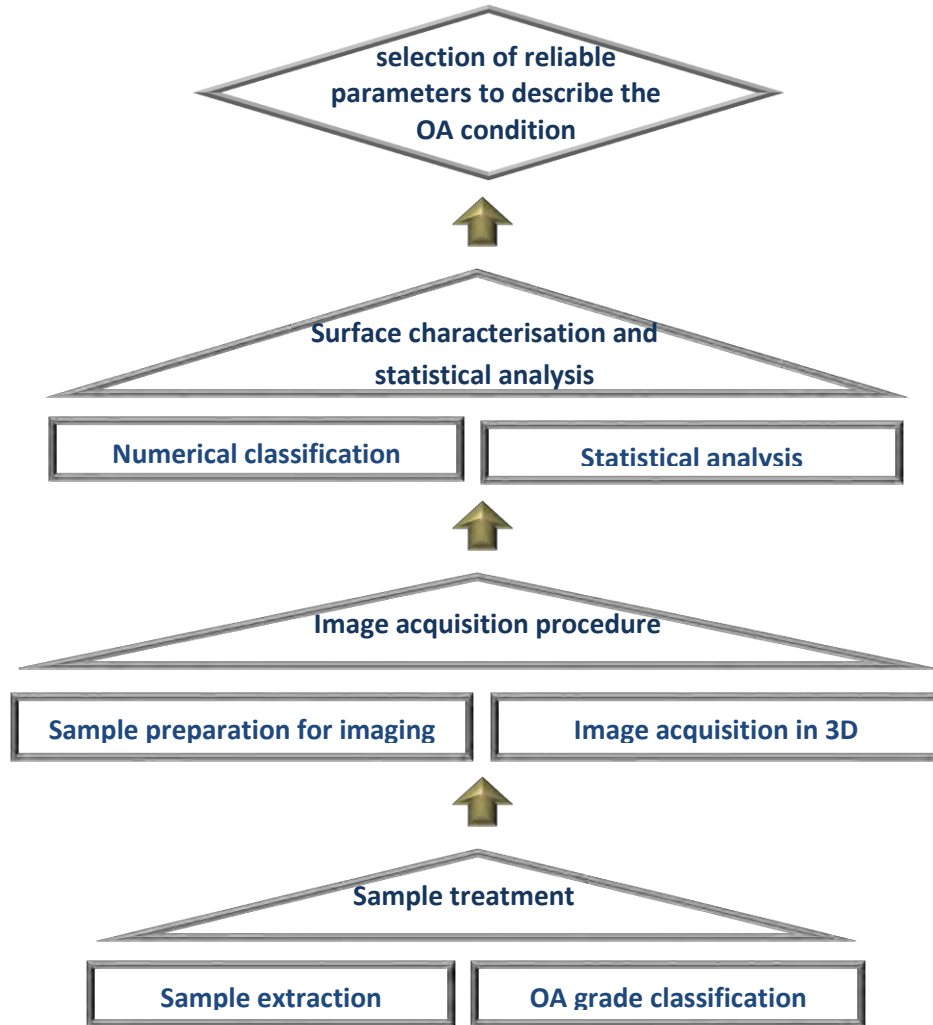


**Figure 3.1** Key steps to achieve the objectives of this thesis.

### *3.1.1 Sample extraction procedure*

The sample extraction was carried out in a PC2 lab located at the Graduate School of Biomedical Engineering, UNSW Australia. Square samples in a size of 15 mm x 15 mm were obtained from the collected samples of human knee using an electric oscillating saw with a 10 mm wide stainless steel blade. The samples were extracted in a biological hood, following a Safe Work Procedure (SWP) approved by the Graduate school of Biomedical

Engineering of such University (see Appendix A.1) to preserve the personal well-being and the integrity of surrounding areas (Figure 3.2). The electric oscillating saw is widely used in surgical procedures for the removal of human knee parts. 12 samples were obtained from the 12 patients. After the extraction procedure, the samples were placed individually in petri-dishes and immersed in a phosphate buffered saline (PBS) solution with a pH=7.4 to preserve the integrity of the sample. These samples were stored in a freezer at -20 Celsius degrees. Before the image acquisition, samples were placed in a fridge for 24 hours to thaw them from -20°C to 5°C. The cartilage change related to biomechanical properties and histological patterns during the freeze/thaw cycles are considered to be not significant (Changoor et al., 2010). The storage condition of the sample employed in this project has been reported before in other studies (Froimson et al., 1997; Wang et al., 2012).

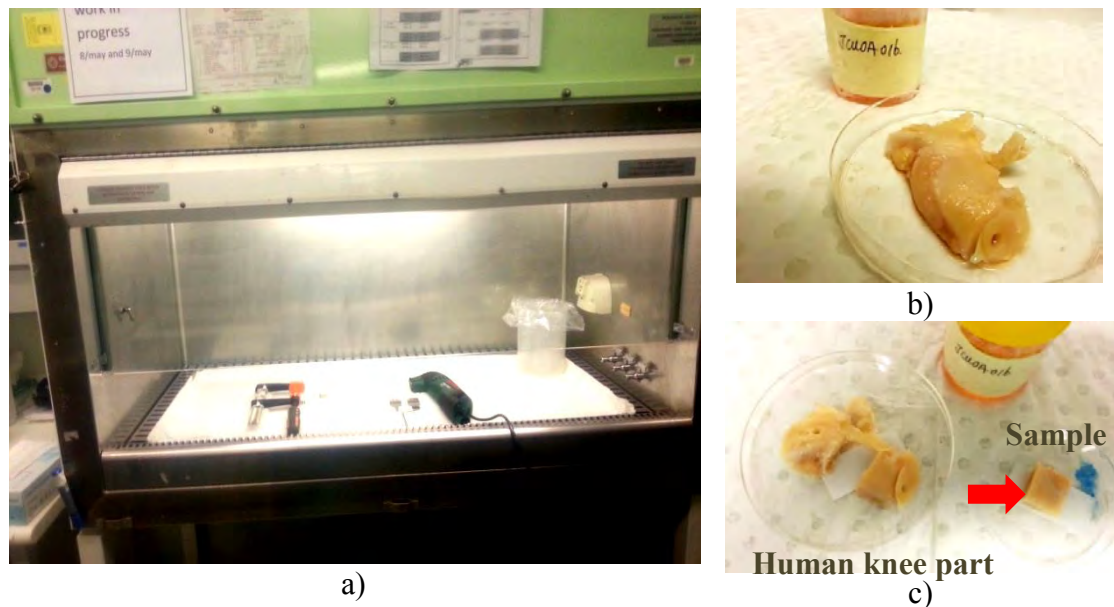


**Figure 3.2** Cartilage sample extraction procedure. a) Biological hood prepared for the sample extraction, b) Cartilage samples collected from the hospital, and c) extracted a sample of a suitable size for 3D imaging.

The small size and heterogeneous shape of the collected samples of human knee, increased the complexity of the sample extraction. During the sample extraction, the collected samples were fixed by an adapted clamp. The small oscillating angle of the blade, combined with the high frequency of oscillating, made a smooth cutting during the sample extraction, obtaining the square samples as is shown in Figure 3.2.

### *3.1.2 OA grade classification*

The OA grade classification of the studied samples was carried out primarily according to the International Cartilage Repair Society (ICRS) System (Mainil-Varlet et al., 2003). This classification is based on the depth of the cartilage injury, which was assessed by measuring the cartilage thickness of the four transversal sections of the samples by using the software *Autodesk Inventor* in this project. A digital camera was used to image the four transversal sections of the studied samples with a width of 15 mm. The ruler in the image was used to scale the image to obtain the real sample size, and the real value of the cartilage thickness. Each transversal section was measured several times along the cartilage section to identify the progression of the cartilage loss in each section. The variation of the thickness was used to identify the different OA grades presented in the sample, based on the International Cartilage Repair Society (ICRS) System as it was mentioned above.

Once the thickness data of the samples were obtained, the next step was to identify OA grade I specimens. This was because that since the cartilage thickness change according to the location in the knee (Muhlbauer et al., 2000), it is important to identify a reference point where the characterization process can be supported. Although cartilages with OA grade I reveal surface irregularities, accompanied by a yellow-white appearance with soft

and swollen characteristics (Outerbridge et al., 1961), they do not present a significant loss of material. The surface morphology is still smooth (Loken, 2010), and cartilage with OA grade I can be considered with a full thickness cartilage. It was used as a reference point for the OA cartilage classification in this project.

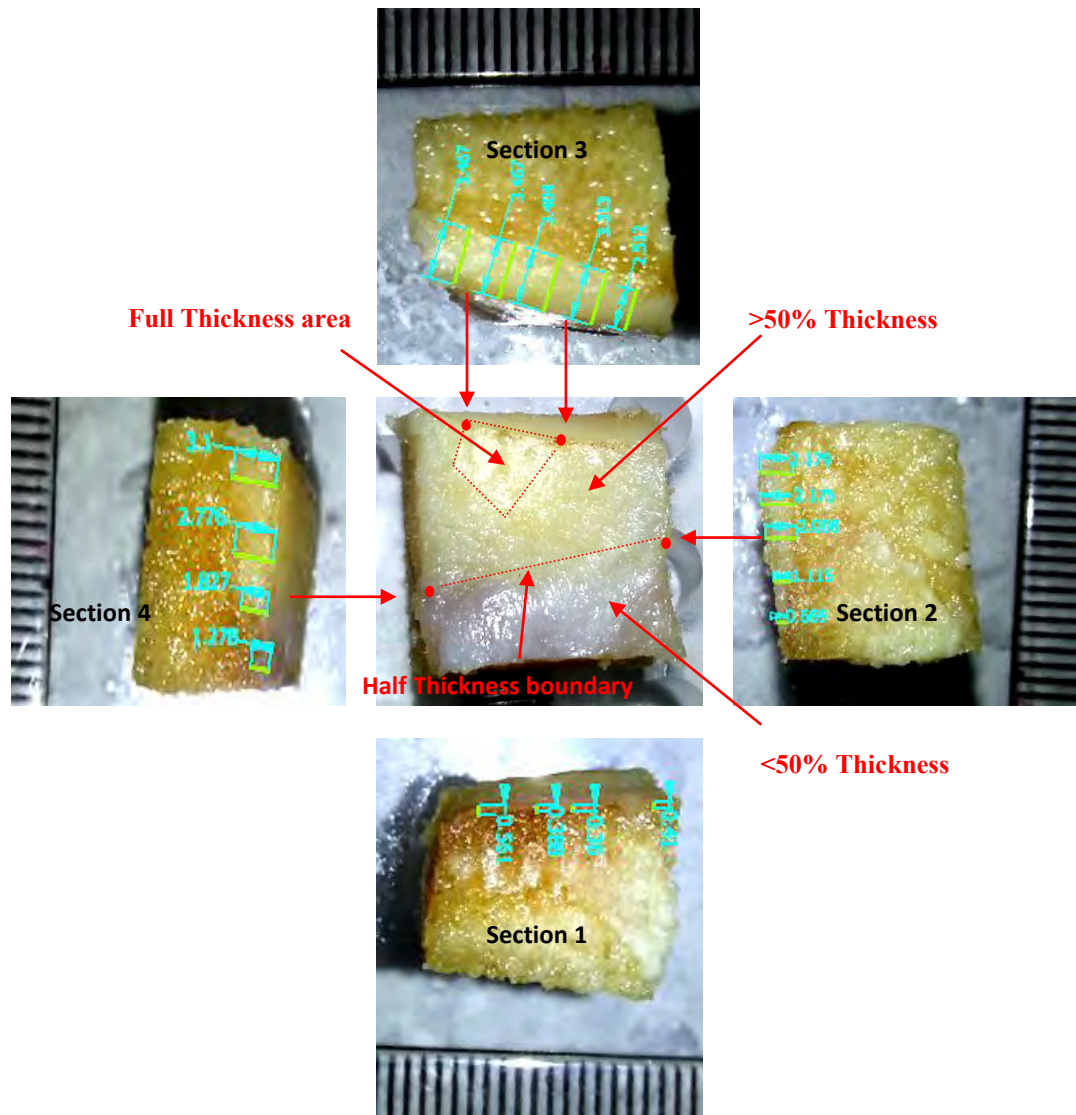


**Figure 3.3** Measurement of the cartilage thickness in the four sections of the samples to classify the OA grade condition in the cartilage sample.

Following OA grade 1 sample classification, cartilages with OA grades II and III were identified. Samples with these OA grades present a rougher surface morphology that is clearly differentiated of OA grade I by a visual inspection. The differences between OA grades II and III samples are more complex by using visual inspection. Due to difficulty in differing these two OA grades based on the surface roughness information, they were characterized using the injury depths. When the cartilage thickness has decreased less than 50%, it is considered to be OA grade II. OA grade III is identified when the material loss in thickness is higher than 50% (Mainil-Varlet et al., 2003). The same criterion was used in this project to identify OA grades II and III samples as can be seen in Figure 3.3.

### **3.2 Image acquisition procedure**

The image acquisition procedure included (a) the sample preparation for imaging, (b) setting up the microscope according to the characteristics of the surface morphology of the samples, and (c) image acquisition to obtain appropriate surface morphological data for numerical characterizations. Since cartilages are tissues conformed by around 70% of water w/w (Ewing, 1990), dehydration during the image acquisition is an issue that needs to be controlled. During the dehydration process, the volume of the cartilage is reduced, affecting the surface morphology of the cartilage. The collected data from dehydrated cartilages can lead to misunderstanding during the statistical analysis.

#### *3.2.1 Sample condition for image acquisition using laser scanning microscopy (LSM)*

Laser scanning microscopy (LSM) is an imaging technique that can provide a high resolution of 3D images at a micron scale and requires a minimal sample preparation.

However, this technique was not adapted to image biological samples for quantitative characterisation. Articular cartilage are biological tissues highly susceptible to be dehydrated during image acquisition and it is important to control such dehydration in order to obtain reliable results. The image acquisition was realized using a LSM VK-X200 Series (Keyence, 2014) Located at the School of Mechanical and Manufacturing Engineering of UNSW, Australia. A procedure for sample preparation before the image acquisition had to be realized in order to avoid the dehydration of the samples during this procedure by following the safe work procedure (SWP) designed for this purpose (see Appendix A.2). It also included the design of a sample holder device used for placing the sample on the stage of the microscope and avoiding any risk contamination related to the human sample.

The sample holder device was mainly designed to preserve the sample hydrated during image acquisition. It was introduced into a petri-dish, containing PBS solution with a pH value of 7.4 to hydrate the sample. The petri-dish was sealed to isolate the sample from the surrounded areas to avoid any disease transmission produced by the human sample. This sample was fixed to the sample holder by a screw which held the sample from the bone part, without affecting the integrity of the cartilage and allowing the cartilage surface being parallel to the objective lens of the microscope. Figure 3.4 shows the designed sample holder was in use.

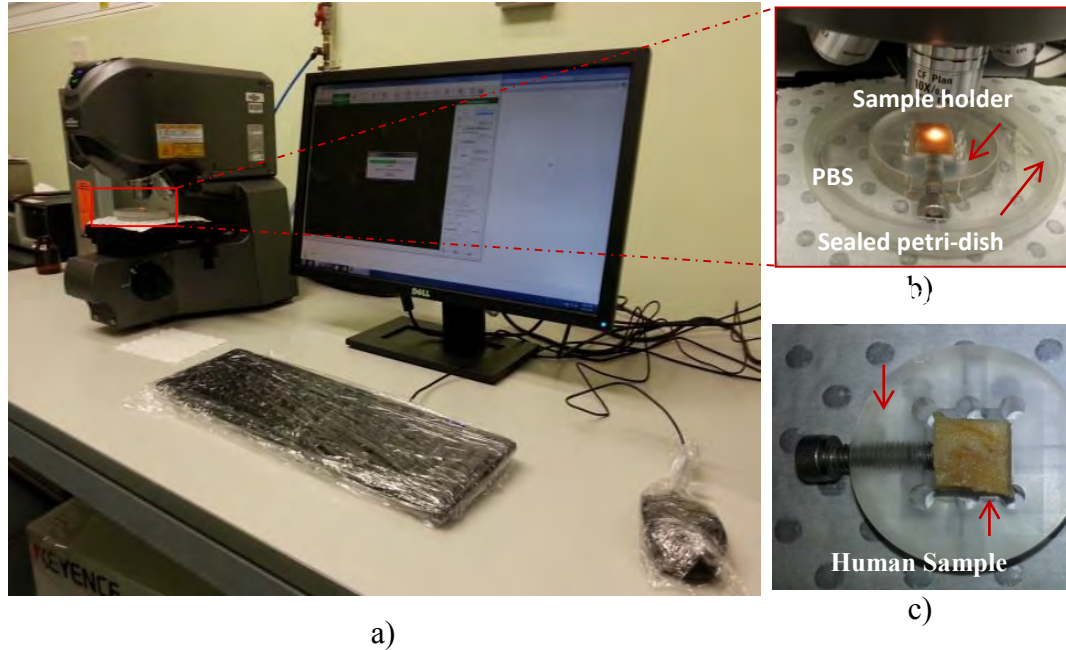


**Figure 3.4** Image acquisition procedure using LSM. (a and b). Setting up of the work area and following the Safe Work Procedure for the image acquisition process of human samples; (c) A human sample located in the sample holder (Baena and Peng, 2014).

### 3.2.2 Image acquisition using laser scanning microscopy

Samples were imaged using a 20X objective lens with a step size of  $0.05\ \mu\text{m}$  in the Z-direction. The selection of this variable was according to the texture surface of the cartilage, especially for OA grade III samples and the quality of the image supplied by the objective lens. The 10X objective lens has limitations reaching the deepest pits of a rough cartilage surface that a severe OA cartilage often has. In addition, the obtained image was normally dark, losing information about the surface condition. When the magnification was increased, the images became lighter and the resolution of the images was improved. However, the working distances decrease with an increase in magnifications. The small working distance for 50X magnification lens was an issue for imaging surfaces with OA grade III due to the roughness characteristics.

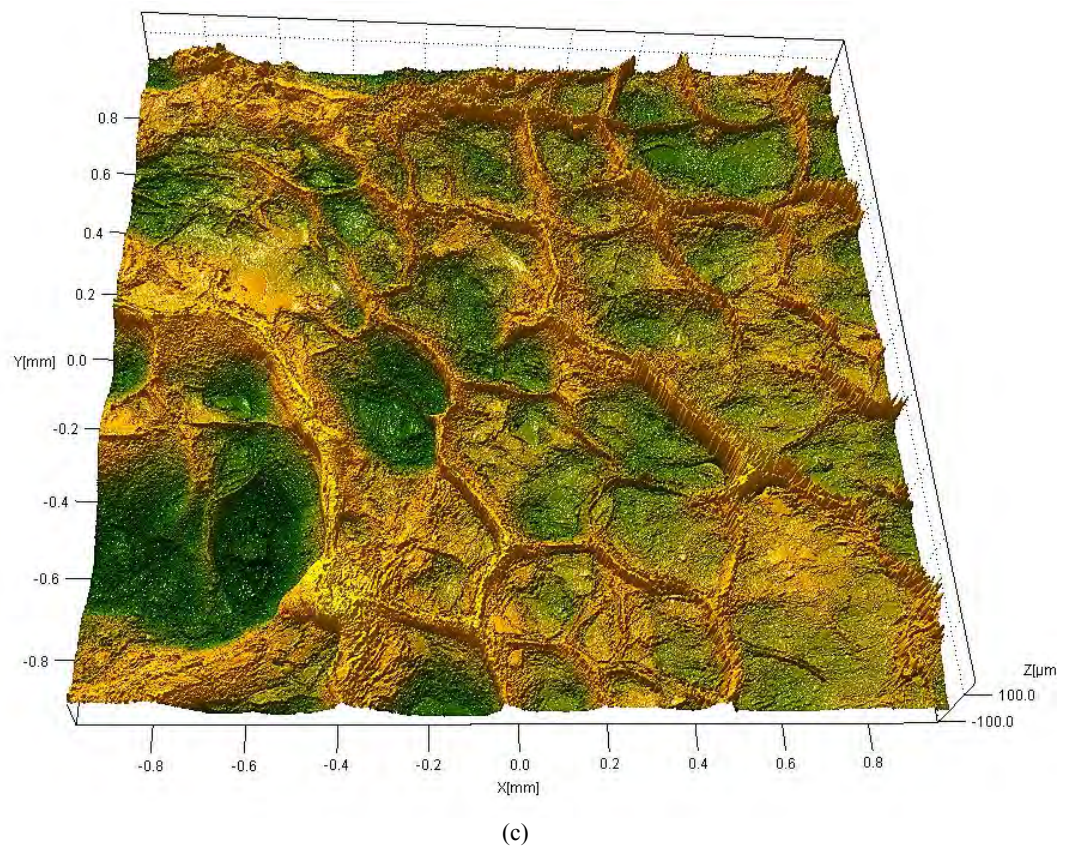
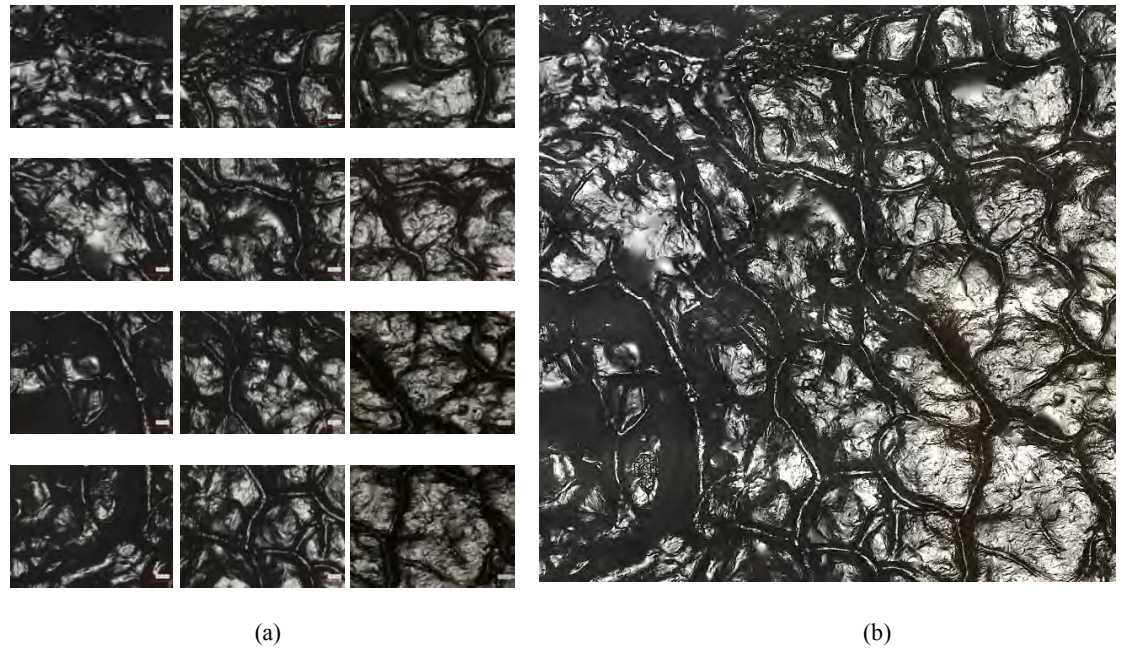


**Figure 3.5** Stitching image process of human knee cartilage with OA grade III. (a) Twelve LSM images taken using a 20X objective lens; (b) The stitched image using Topostitch; (c) 3D image of the stitched image (Baena and Peng, 2014).

Detailed information about the selection of the microscope characteristics, are mentioned in Chapter 4.. The obtained size of a 20x image taken by the LSM was 0.5 mm x 0.698 mm. Each sample was at least imaged twelve times at different locations and in a total area of 2 mm x 1.8 mm. These twelve images were stitched together with a 15% overlap so a larger image was obtained as shown in Figure 3.5 (b) and (c).

A large micro-scaled image of the surface topography can provide qualitative evidence of the OA grade progression and it can reveal specific features of the surface texture for each OA grade, which will improve the understanding about the degradation process of cartilage surfaces.

### **3.3 Surface characterization and statistical analysis technique**

The statistical analysis is the mechanism used to make inferences from the data and to evaluate the credibility of the data. The reliability of the statistical analysis depends on the treatment of the collected data, including image processing and data acquisition, but also on the selected statistical method. These criteria were employed into this project and the procedure is explained forward.

#### ***3.3.1 Image processing and characterization method***

The LSM images were processed by a standard Gaussian filter according to ISO 11562 (ISO 11562, 1996), to filter out noise and remove waviness information. A cut-off wavelength of 1/5 of the evaluated length was used. The treated images were analysed using 34 numerical parameters, including 9 height (amplitude), 9 spatial, 10 functional and 6 hybrid (see Appendix C), which are the parameters implemented in the SPIP software

of analysis of images, most of them are explained by ISO 25178-2 (ISO 25178-2, 2012). A total of 144 images from 12 samples were analysed, corresponding to 4 samples for each OA grade (I, II and III).

### *3.3.2 Criteria of evaluation and statistical procedure*

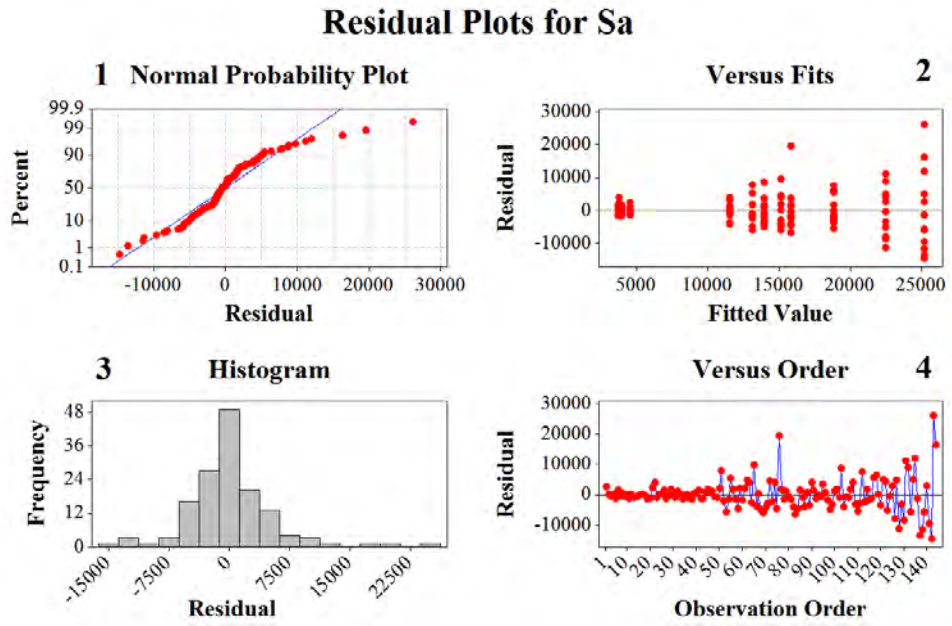
The analysis of the variance (ANOVA) model was applied to analyse the differences in the mean values of the numerical parameters between the three evaluated OA groups. The statistical conditions were a  $p$ -value of 0.05, a confidence interval of 95%, and a power ( $1-\beta$ ) of 0.9.

The ANOVA model is based on several assumptions, including the requirement about the normal distribution of the residual. When the residual is not normally distributed, a data transformation on the response is required (Montgomery et al., 2011). During the data treatment, it was observed that the residual value increases with the OA grades. This increment is related to the surface conditions of the cartilage as it is expected that the roughness value elevates with the OA grade, and consequently, the residual is also expected to increase. The trend presented by the residual suggested that the natural log (Ln) may be a suitable function to transform the data, making the residual homogeneously distributed (Montgomery et al., 2006). Figures 3.6 (a) & (b) illustrate two plots with the distribution of the residuals for both cases, before and after the data transformation, using the data of the  $S_a$  parameter. The plots of Figures 3.6(a) & (b) are composed of four graphs each. They are 1) the normal probability plot used to assess the normal distribution of the data, 2) residual versus fits for evaluating the quality of the residual dispersion and identifying the optimal transformation if it is required, 3) the histogram of the residual to confirm whether the residual follows a normal distribution, and 4) the residual vs the

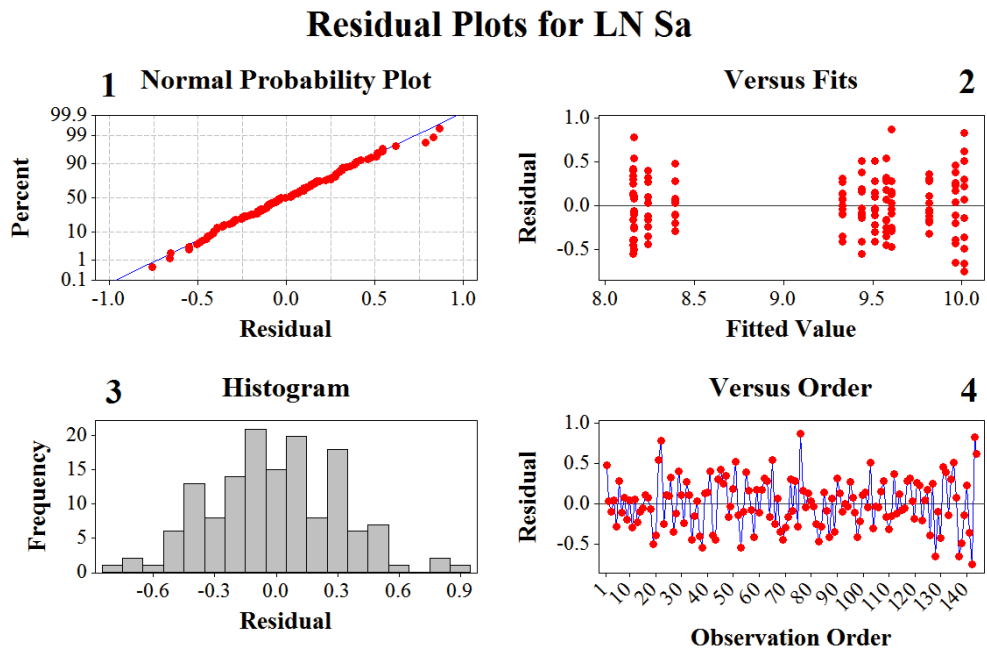
order plot to evaluate the performance of data according to the treatment combination. It can be seen from Figure 3.6 (a1) that the residual of the  $S_a$  values does not completely fit a straight line, revealing that the data does not follow a normal distribution. The dispersion of the residual (Figure 3.6 (a2)) does not uniformly spread, having a higher dispersion when the fitted value increases.

To obtain a homogeneous dispersion of the error, the data were transformed by the function Ln. Figure 3.6 (b1) shows that the line of the normal probability plot is mostly fitted by the transformed data and it has a more equal variance through the fitted values (Figure 3.6 b2).

Statistical analyses were conducted on the transformed data to select the numerical parameters which could describe the significant change in the surface conditions of human cartilage affected by OA. It is important to consider the possibility that the clinical history of patients also affects the cartilage surface condition, making every sample unique. Therefore, the surface information of the samples, even for the same OA grade, might be significantly different from each other. Consequently, each sample needs to be considered as a variable or factor. Based on the above consideration of the human samples, the two-stage nested design was used (Montgomery et al., 2003).



(a)



(b)

**Figure 3.6** Residual plot for the  $S_a$ -parameter data. (a) Original data, and (b) transformed data, using the function nature log Ln. In both (a) and (b), 1 - The normal probability plot, 2 - The residual versus fits plot, 3 - Histogram, and 4 - The residual versus the order of the data.

The factors (i.e., *OA grade* and *Samples*) were included in the experiment. The *OA grades* were considered as blocks, and the *Samples* were nested into the blocks (*OA grades*). The samples nested into each *OA grade* (i.e., blocks) are the samples where the data of the *OA grade* were taken. The linear model of the two-stage nested design is represented as (Montgomery et al., 2003):

$$Y_{ijk} = \mu + \tau_i + \beta_{j(i)} + \varepsilon_{k(ij)} \begin{cases} i = 1, 2, \dots, a \\ j = 1, 2, \dots, b \\ k = 1, 2, \dots, n \end{cases} \quad (3.1)$$

Where  $Y_{ijk}$  are the mean values of the numerical parameters of the  $K^{th}$  observation, and  $\mu$  is the overall mean (constant).  $\tau_i$  is the factor *OA grade* effect, and  $\beta_{j(i)}$  represents the  $j^{th}$  level of factor *Sample*, which is nested under the  $i^{th}$  level of factor *OA grade*.  $\varepsilon_{k(ij)}$  is used to represent the error term of the  $k^{th}$  observation from the  $j^{th}$  level of factor *Sample* within the  $i^{th}$  level of factor *OA grade*. Using this method, it is possible to identify the significant differences between levels of *OA grades* and levels of *Samples*. However, it is not possible to estimate the interaction between the *OA grade* and *Sample*, as not every level of the *Sample* is included in every level of the *OA grade*. Tukey's test was employed to make comparisons within all pairs of means, to support the obtained level of significance ( $p$ -Value) of the factors.

### 3.4 Summary

In this chapter, the procedures and techniques employed for the sample extraction, image acquisition, numerical characterizations and statistical analyses are presented. The appropriate sample size was determined to avoid sample dehydration during the sample

extraction and imaging phase. A specially designed sample holder was used in the image acquisition process to make the sample hydrated and levelled with the microscope stage. Once high quality, 3D images of the cartilage surfaces were captured, 35 numerical parameters were applied to quantitatively characterize their surface morphologies. To identify their distinctive changes with the OA progression, the statistical analyses described in section 3.3.2 were conducted to select key numerical parameter(s). The detailed procedure developments and outcomes of the above steps are reported in chapters 4-6.

## **Chapter 4 Development of Sample Extraction and Image Acquisition Procedures**

To quantitatively characterize the surface textures of human knee cartilage affected by OA, developments of sample extraction and image acquisition methods are required. This chapter focuses on the outcomes of the attempts and developed sample extraction and image acquisition process in this project.

### **4.1 Outcomes of the sample extraction procedure**

The selected sample extraction process was based on the stability of the surface topography of the sample during the image acquisition and the viability of the sample extraction process without affecting the integrity of the cartilage. Two criteria employed for determining a suitable sample size were: (a) to ensure a sufficient surface area so adequate surface data could be acquired for reliable image analyses, and (b) to avoid sample dehydration and material degradation in the sample extraction and image acquisition process. Of these two, controlling the sample dehydration was more challenging and required investigations of sample size and time effects on the dehydration. This is because cartilages are biological tissues composed by a high content of liquid (around 70%), and therefore, dehydration during image acquisition can affect the water volume in the cartilage and consequently the surface topography. For this reason, it was important to identify the behaviour of the cartilage surface for different sample conditions.

#### *4.1.1 Sample sizes and dehydration tests*

Three different sample sizes were tested in order to identify the advantage and disadvantage of each sample regarding to both, sample extraction and image acquisition procedure.

The first studied sample was a 5 mm diameter sample, manually extracted by using a puncher. This sample was extracted from a sheep cartilage by holding the bone was the cartilage was attached. The fixation of the bone was required has the slippery characteristics of the cartilage presented an impediment for the sample extraction.

5 mm samples were imaged in dry conditions in the same spot several times to evaluate morphologic changes in the surface. After 15 minutes of image acquisition, the sample had notorious changes in the surface texture caused by dehydration, which also generate a bending of the sample (Figure 4.1).

A sample of 10 mm diameter was tested in order to reduce dehydration and bending of the sample during the imaging process. The 10 mm sample was extracted by using a 10 mm hole-maker. This procedure allowed to extract the sample with a portion of bone attached to the cartilage, which can reduce the bending of the cartilage due to dehydration.

This sample was tested in a dry condition to evaluate the texture surface variation, following the same procedure realized to the 5 mm sample mentioned above. After 25 minutes of image acquisition, the variation of surface texture was not significant, according to the surface appearance and the  $R_a$ -Value. The difference on the  $R_a$ -value after the 25 minute test was 1.6%, which can be included into the error of the measurement (see Figure 4.2), This result shows that bigger samples with bone attached present a more stable surface condition and they can maintain hydrated longer than the small samples,

however, dehydration is still an issue, especially whether image acquisition for each sample last more than 30 minutes.

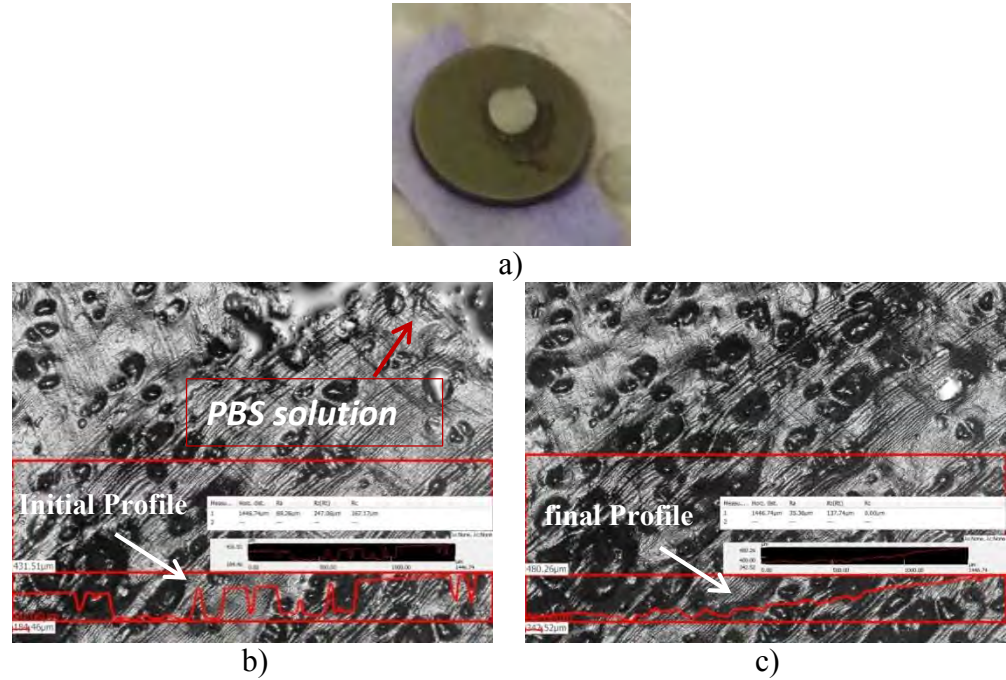


**Figure 4.1** Variation of the surface texture for a sample imaged under dry conditions for a period of 15 minutes, using LSM. a) 5 mm human sample, b) the surface of the human sample imaged just taken out from the petridish and with a magnification lens of 10X. Surface roughness  $R_a=69.26 \mu\text{m}$  measured across the red line, and c) image of the sample after 15 min of being taken out of the petridish and captured at a 10X magnification lens. Surface roughness  $R_a=35.36 \mu\text{m}$  measured on the red line.

The 10 mm samples were tested during more than one hour in two different conditions, with and without hydration. The cartilage of the sample was hydrated through the attached bone with PBS (pH=7.4). A sample holder was specially designed for this purpose. The

cartilage did not make contact directly with the PBS, as it might reach the cartilage surface, affecting the reliability of the image acquisition.

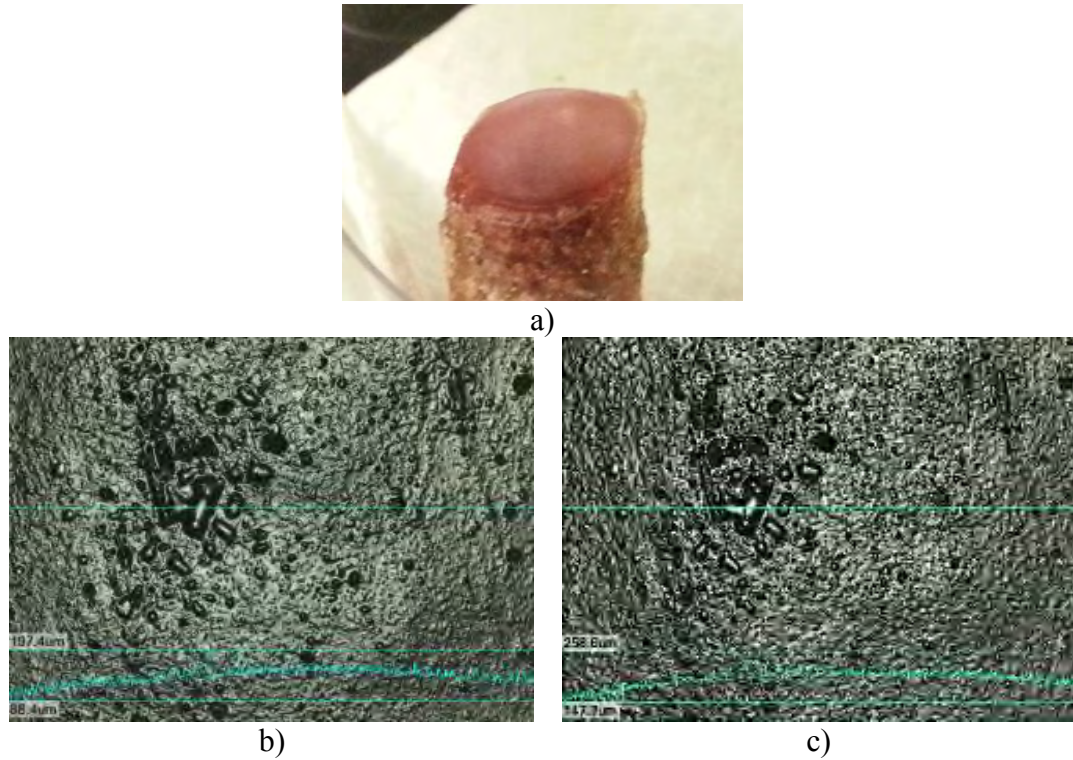


**Figure 4.2** Variation of the surface texture imaged under dry conditions for a period of 25 minutes, using LSM. a) 10 mm sheep sample, b) roughness measurement of a sheep sample, just taken out of the petri-dish,  $R_a = 12.5 \mu\text{m}$  measured across the blue line, 10X, c) roughness measurement of the sheep sample, after 25 minutes of being taken out of the petridish and captured at a 10X magnification lens. The roughness value of the blue line is  $R_a = 12.7 \mu\text{m}$ .

The sample tested in dry condition, presented a notorious appearance of dehydration after one hour, even though the sample was dehydrated, the surface appearance remained stable without evidence of bending, which was attributed to the attached bone.

The samples that were constantly in contact with PBS solution remained hydrated for a long period of time. The hydrated sample was tested for more than two hours and there was no evidence of physical appearance changes (see Figure 4.3).

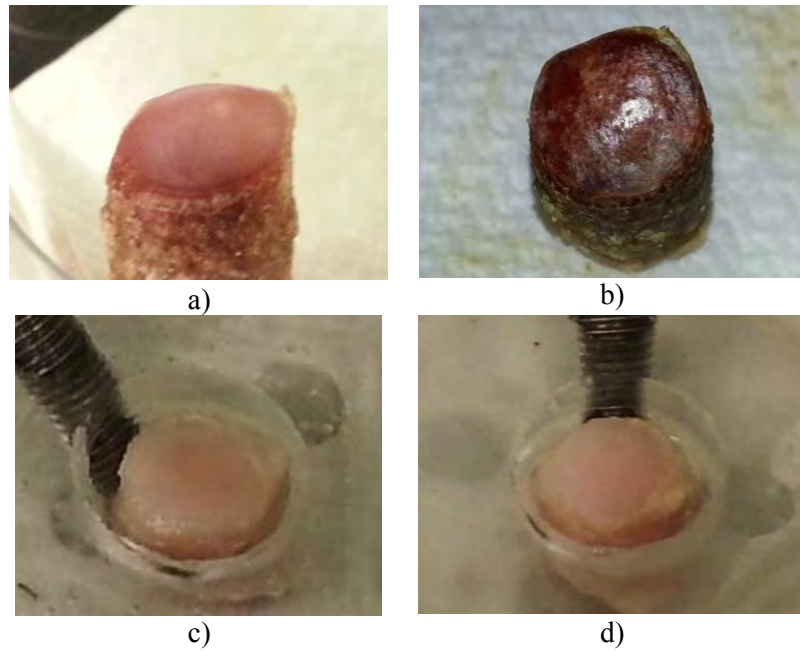


**Figure 4.3** physical appearances of the samples under both conditions, with and without hydration for around 2 hours. a) and b) sample dry condition just taken out from the petri-dish and two hours after, respectively, c) and d) hydrated sample just taken out from the petri-dish and two hours after, respectively.

The 10 mm samples presented a high performance regarding to hydration and surface topography stability during the image acquisition using the sample holder with PBS solution in. The sample extraction procedure was realized successfully by using the hole-maker connected to the drill and holding the sheep cartilage by fixing the femur with a clamp. However, the collected samples of human knee used to extract the samples in this

project, did not provide a large enough part of bone to be held without affecting the cartilage integrity, since the sample extraction by using the drill, present a significantly high holding requirements, this tool should not be used to extract the samples from the collected knee parts as the cartilage integrity can be affected due to the lack of exposed bone where the joint part could be held (see Figure 4.4). A sample extraction procedure needs to be proposed in order to protect the integrity of the human cartilage by reducing the force contact when the knee part is sized, which is mentioned below.

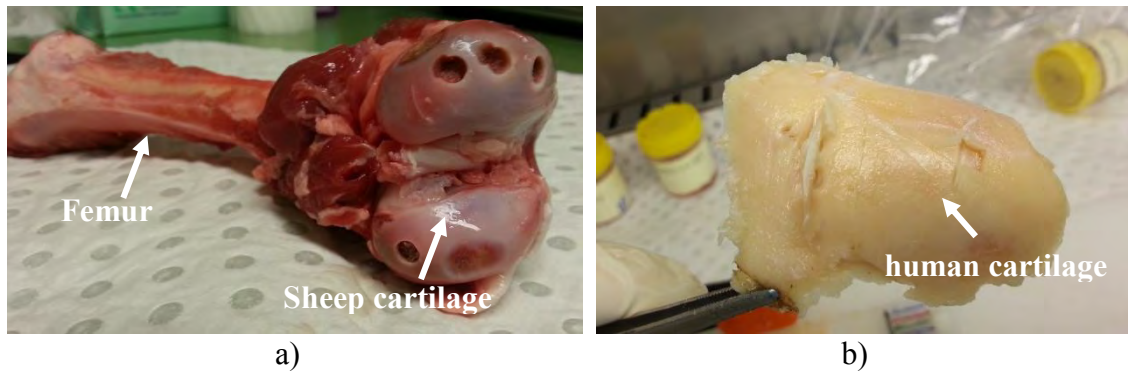


**Figure 4.4** Cartilages used for sample extraction. a) Sheep cartilage attached to the femur, and b) collected human knee samples.

#### *4.1.2 Improvement of sample extraction procedure*

The collected samples of human knee used to extract the samples for this project, were relatively small parts of bone covered with cartilage. These characteristics made the sample extraction a complex procedure to be realized with a hole-maker and a drill, since this tool presents a high fixation requirement of the collected knee part during the sample extraction which might affect the cartilage integrity. For this reason, it was important to identify another process to extract the samples with lower requirements on the knee part

fixation. These requirements were fitted by an Electrical Oscillating Saw as the small angle and the high frequency of oscillating allows cutting the cartilage softly without affect significantly the surface condition of the cartilage and presenting a low requirement for the fixation of the collected knee part. A 15 x 15 mm sample size was obtained by the electric oscillating saw, using a 10 mm stainless steel blade. Figure 4.5 shows the three different samples tested in this project by using different sample extraction procedure.

The sample extraction procedure was realized in a PC2 lab located at the Graduate School of Biomedical Engineering, UNSW, Australia, as it was mentioned in section 3.1.1. Since the samples come from human knee joints, a Safe Work Procedure was developed and approved by the Biomedical Engineering School. The samples were extracted in a safety hood, previously conditioned for this purpose (see Figure 3.2).

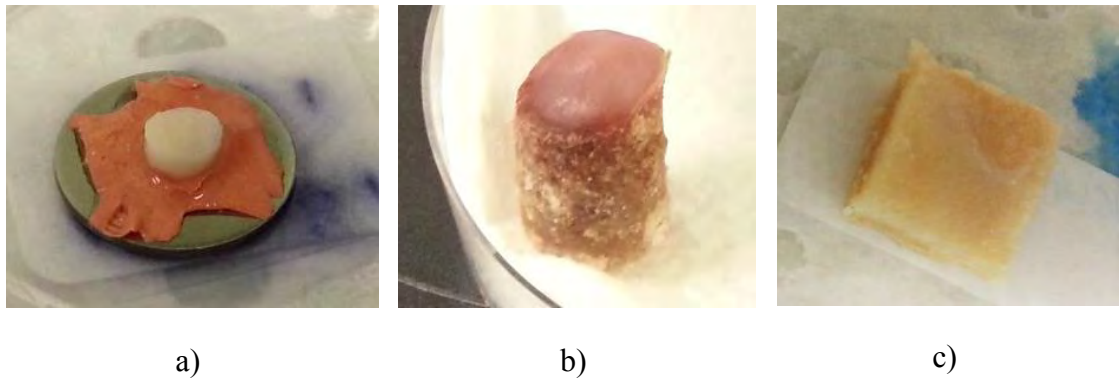


**Figure 4.5** Three different sample size extracted by different tools, a) 5 mm sample, manually extracted with a puncher, b) 10 mm sample with attached bone extracted with a hole-maker and a drill, c) 15 mm sample with attached bone, extracted with electric oscillating saw and a 10 mm stainless steel blade.

## **4.2 Outcomes of the sample holder design and its functional tests**

The Laser Scanning Microscope (LSM) allowed obtaining the 3-D images of the cartilage surface. The LSM was not adapted with a specimen holder to ensure the suitable location and the hydration condition of biological tissues during the image acquisition. The suitable location of the tested sample on the stage consisted on placing the sample with the cartilage surface parallel to the objective lens. Having a non-parallel condition of the lens and the cartilage surface, the laser might not reach the deepest regions of the surface, which will affect the data reliability.

A sample holder was designed and manufactured to face the issues presented by the sample during the image acquisition mentioned above. The sample holder allowed imaging cartilage surfaces for more than two hours without evidence of dehydration. The image acquisition process for each sample took around two hours to be completed, which made the sample hydration an important issue to be controlled during this process. The Figure 4.6 (a) shows a 10 mm sheep sample during the image acquisition under dry conditions and without an appropriate system of fixation.

The first prototype of the sample holder was designed for holding 10mm samples with satisfactory results regarding to hydration conditions and adequate positioning of the sample in the microscope. An improved sample holder device was then manufactured to hold the 15 mm x15 mm sample extracted by the Electrical Oscillating Saw. PBS solution was introduced in the device that conform the sample holder to keep the sample hydrated during the required time as can be seen in Figure 4.6 (b&c).

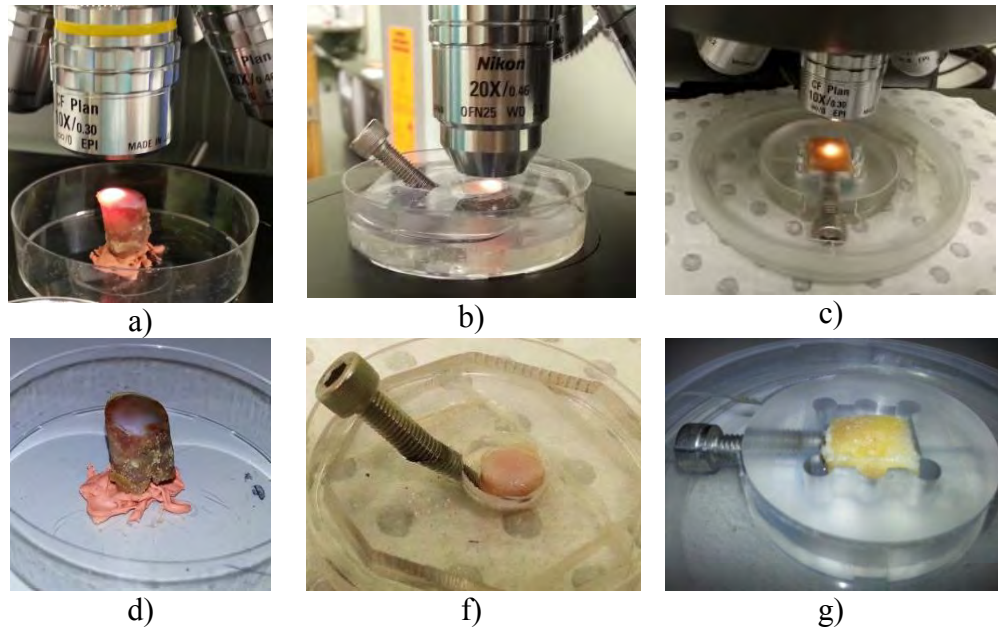


**Figure 4.6** Improvement of the sample holder used for the image acquisition, a&d) first montages for image acquisition of 10mm sample in dry condition, b and f) designed sample holder for 10mm sample with hydration, c and g) improved sample holder for 15 x 15mm human sample with hydration.

### 4.3 Setting up the laser microscope facility for image acquisition

The suitable magnification employed during the image acquisition should allow evidencing the morphological features of the surface with high resolution and reduced noise. The criterion used for determining a suitable magnification and resolution for the LSM image acquisition is mentioned in the forward sections.

#### 4.3.1 *Qualitative comparison of images taken with 10X and 20X magnification lens for OA grades III condition*

Images of a cartilage surface with three different magnifications were evaluated (10X, 20X and 50X). The three different magnifications supplied reliable images for smooth

surfaces such as OA grades 0 and I (see Figure 4.7). However, OA grade III was the most challenge surface to be imaged due to the high roughness condition of the surface texture.

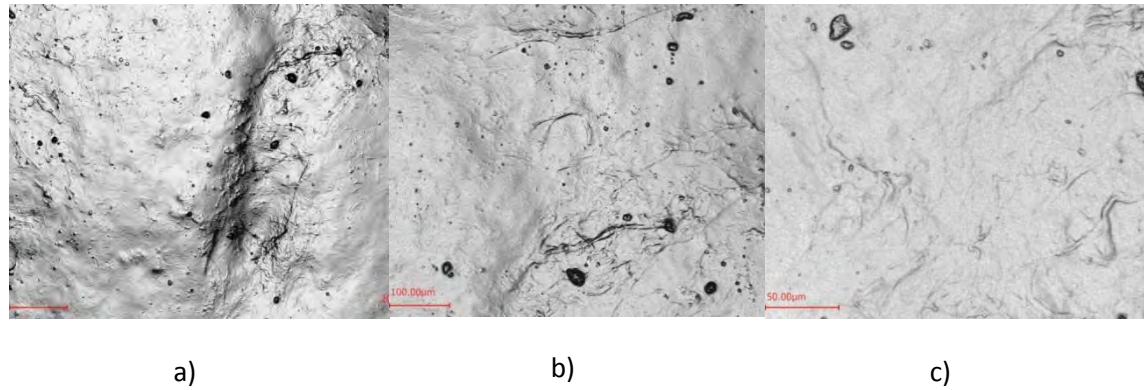


**Figure 4.7** Images of a healthy cartilage of sheep samples at three different magnifications. a) 10X, b) 20X and c) 50X.

OA grade III cartilage was imaged with a 10X magnification lens. The obtained 2D images were mainly black and a few characteristics of the surface texture could be observed. The 3D image corresponding to the 10X magnification was composed by small peaks which might be caused by noise of the image rather than a reliable description of the surface topography (see Figure 4.8 (a and c)). A 20X magnification image was taken on the same spot in order to identify and compare the characteristics revealed in both images. The 20X image presented much clearer information about the surface texture in both 2D and 3D images. The valleys and peaks are clearly defined in the 3D image, in contrast to the 10X image (Figure 4.8 (b and d)).

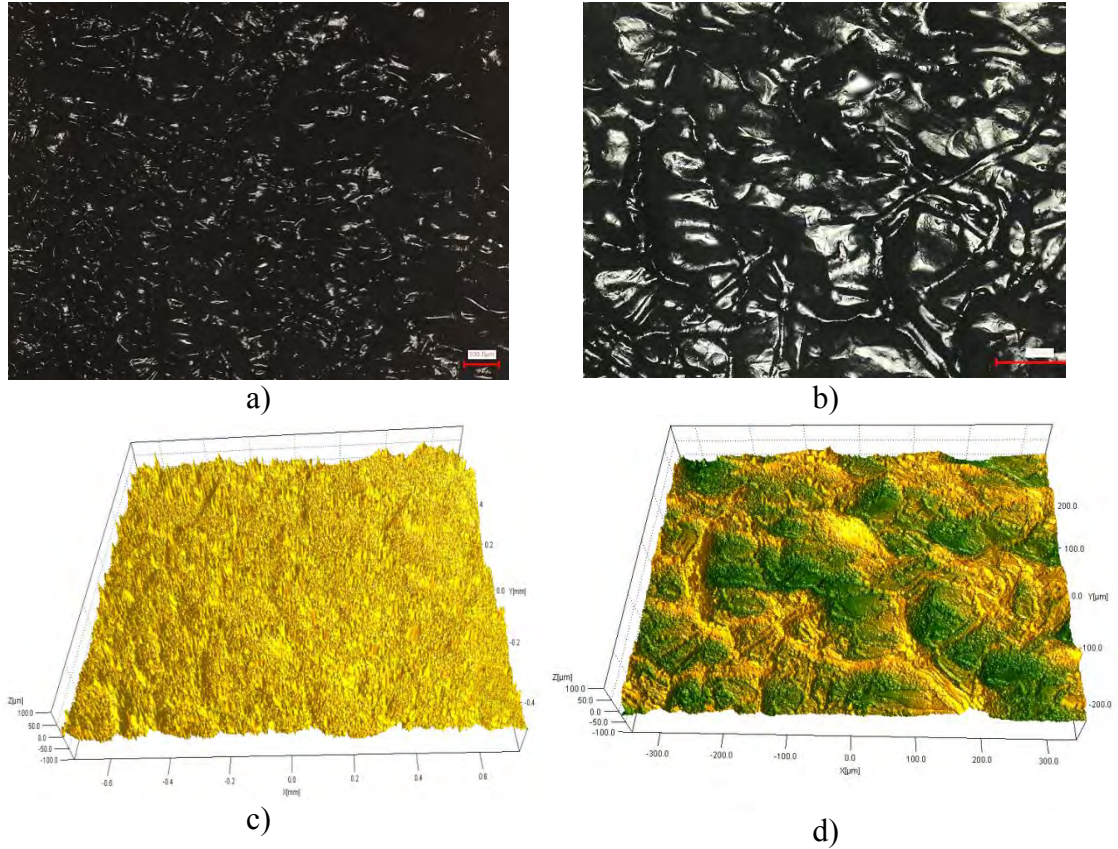


**Figure 4.8** Images of a human cartilage with OA grade III at two magnifications on the same spot of the sample; (a and b) 2D images at 10X and 20X magnification objective lens respectively; (c and d) 3D images at 10X and 20X magnification objective lens respectively.

A 50X objective lens was also evaluated in this study by acquiring images of cartilage samples in the three different OA grades. Similar to the 20X magnification, it was able to acquire appropriate surface data of the samples. However, two main issues were identified by using a 50X magnification lens for the image acquisition of cartilage with OA grade III. First, since the work distance between the lens and the sample surface is significantly reduced (0.35 mm) and the surface texture of the OA grade III cartilage is highly rough (around  $S_y$ -value=0.249 mm), imaging a rough surface becomes difficult. For some very rough surfaces, the 50X magnification objective lens was not able to scan the deepest region of the cartilage without making contact with the surface. Second, its scanning area

is smaller than that of the 20X objective lens, requiring to obtain many more images to meet the sampling areas for reliable surface measurements. Due to the above two reasons, it was determined that the 50X objective lens was not proper for imaging the samples.

Based on the qualitative criteria, the 20X magnification lens was suitable for the image acquisition in this project. Further quantitative comparisons were made below to confirm that the 20X objective lens is the most suitable for the image acquisition process.

#### *4.3.2 Quantitative comparison of the data taken with 10X and 20X magnification lens for three different OA grades*

The images taken with 10X and 20X magnification lens on the samples mentioned above were also quantified by the  $S_a$ -value in order to evaluate the reliability of the data obtained by the 10X and 20X magnification lens. The  $S_a$  parameter is used to compare the obtained values and it is not suggested that this parameter is the most suitable to describe the surface condition of degraded cartilage at this stage.

In order to compare the information presented by the images at 10X and 20X magnifications for the three different OA grades (I, II and III), the same spot of each sample was imaged twice using 10X and 20X magnifications. Table 1 shows that the values taken by 10X magnifications have stable and low coefficient of variation ( $CV$ ) for OA grade I and II but it is highly increased for OA grade III. The values of the images taken with 20X magnification have more stable  $CV$  for the three OA grade conditions with a small increase for OA grade III. The  $CV$  represents the relative standard deviation based on the mean. This  $CV$  is particularly useful to make a comparison of the standard deviation ( $SD$ ) between values with completely different means. Figure 4.9 illustrates the variation of  $S_a$  parameter with the respectively stage of OA grade and the two

magnifications of interest. It can be seen more clearly that the standard deviation for OA grade III at 10X magnification is significantly high, much higher than the *SD* reported with the 20X magnification at the same OA grade condition. This high *SD* represents an important dispersion of the data, affecting the reliability of the results. As a result, comparing the quantitative results of the data taken by the two magnifications (10X and 20X) the most reliable data obtained using 20X magnification in OA grade III samples.

**Table 4.1** Roughness value using Sa parameter for three different OA grade conditions by using two magnifications, 10X and 20X.

OA GRADE	TESTED SAMPLE	MAGNIFICATION LENS	
		10X	20X
OA I	S1	5533.02 nm	1867.25 nm
	S2	5008.28 nm	1995.63 nm
	S3	6675.88 nm	2483.37 nm
	<b>Mean±C.V</b>	<b>5739.1nm±13%</b>	<b>2115.417nm±14%</b>
OA II	S4	12135 nm	7176.09 nm
	S5	12946.6 nm	8782.04 nm
	S6	15240.6 nm	5735.91 nm
	<b>Mean±C.V</b>	<b>13440.7nm±11%</b>	<b>7231.347nm±14%</b>
OA III	S7	43001.6 nm	9886.97 nm
	S8	12441.8 nm	10197.2 nm
	S9	22368.8 nm	6747.45 nm
	<b>Mean±C.V</b>	<b>25937.4nm±54%</b>	<b>8943.873nm±19%</b>

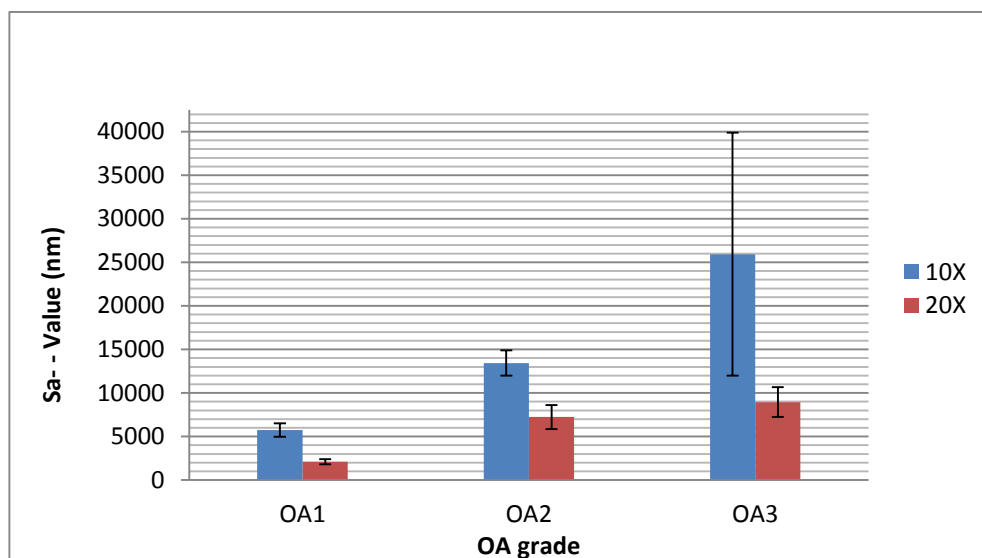


**Figure 4.9** Quantitative comparisons between the data reliability taken by 10X and 20X magnification objective lens.

#### 4.4 Summary

The susceptibility of the human cartilage to be dehydrated during the image acquisition process was assessed. The sample holder has an important contribution on the sample stability during the image acquisition process, allowing the hydration of the sample and the suitable location of this sample for image acquisition, which were essential for the acquisition of reliable information. It was evidenced how the appropriate selection of the objective lens can provide relevant information about the surface topography for numerical characterizations. The suitable sample extraction, preparation procedures and image acquisition method have been developed in this section.

## **Chapter 5 Qualitative and Quantitative Characterization Results of Cartilage Surface Affected by OA**

The characterizations of the cartilage surface textures of human knee joints affected by OA was realized using both qualitative and quantitative approaches. The distinctive surface features of the OA affected cartilages were captured and are reported below.

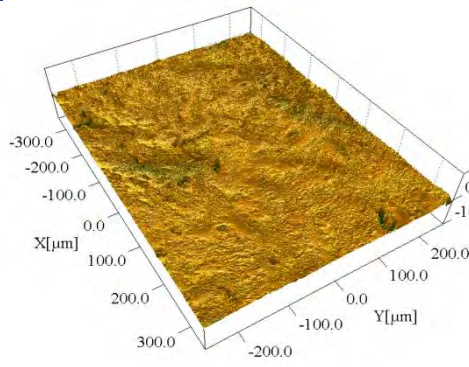
### **5.1 Qualitative characterization of cartilage affected by OA**

The qualitative information obtained from the surface topography of degraded cartilage is the first approach to the surface characterization and it can be used to formulate hypothesis required for the statistical analysis and/or to support the analysis results. The International standard ISO 4288 (1996) state that a visual test needs to be performed before the measurement test since in specific regions of the surface, the surface texture might be much rougher or smoother, being these regions a non-representative regions for the surface characterization.

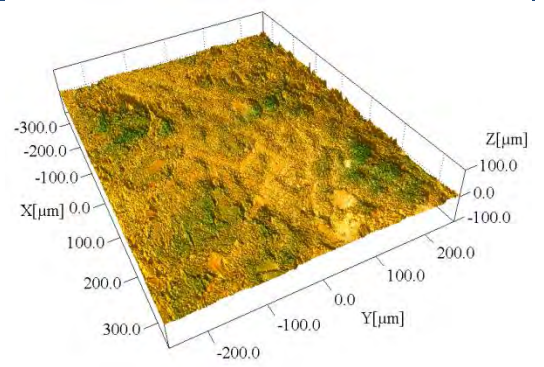
#### *5.1.1 Image acquisition by using a 20X magnification objective lens*

According to the outcome presented in chapter 4, the 20X magnification objective lens (400X magnification displayed) was the most suitable objective lens for the image acquisition of the degraded cartilage surface using a laser scanning microscope (LSM) with a step size of 0.05  $\mu\text{m}$ . This value represents less than 1% of the  $S_y$ -value for OA grade I (See Table 5.1), providing a high quality of image with displayed resolutions of both height and width measurements of 0.5 nm and 1.0 nm respectively.

O  
A  
  
G  
R  
A  
D  
E  
  
I

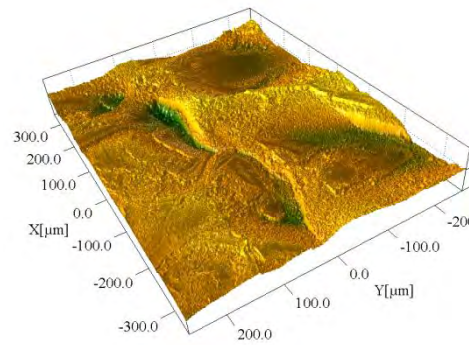


a)

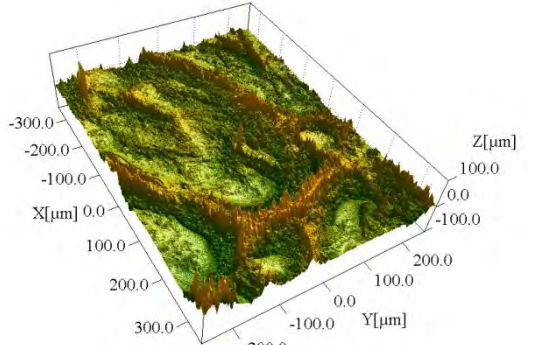


b)

O  
A  
  
G  
R  
A  
D  
E  
  
I  
I

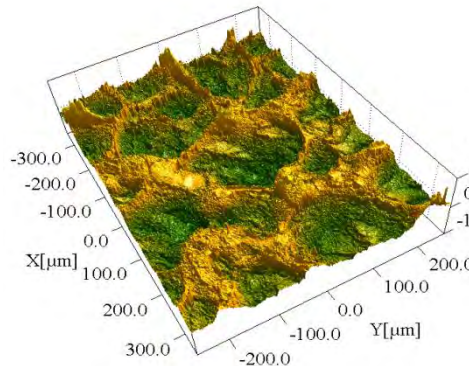


c)

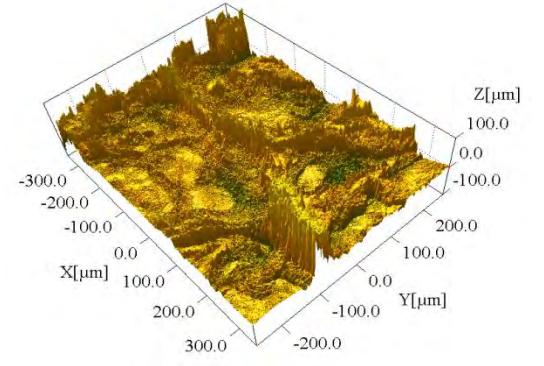


d)

O  
A  
  
G  
R  
A  
D  
E  
  
I  
I  
I



e)



f)

**Figure 5.1** Evolution of the surface morphology for degraded human knee cartilage for three different OA grade by using a 20X magnification objective lens. (a and b) OA grade I, 53 years old female and 65 years old male respectively (c and d) OA grade II, 64 years old male and 65 years old male respectively (e and f) OA grade III, 89 years old male and 76 years old female respectively.

The obtained size of a 20x image was 500  $\mu\text{m}$  x 698  $\mu\text{m}$ . The Figure 5.1 illustrates the change of the surface topography of degraded human knee cartilage for three different OA grade conditions and patients, studied in this project by using a 20X magnification objective lens. From Figure 5.1 it can be seen a relatively smooth surface for OA grade I and the roughness value is increased with the OA grade condition. From the first approach, the surface texture is basically conformed by peaks and valleys and the intensity of these specific features increases with the stage of OA, but it is not clear which of these two features are more predominant in the OA evolution. Even when the sliding condition systems are more likely to produce wear tracks on the surface caused by abrasion, orientated wear marks were not commonly evidenced in the studied cartilage surfaces. The advanced OA cartilage surface seems to have a non-periodical surface texture. This characteristic can be much clearly observed with a larger surface size.

#### *5.1.2 Qualitative information from larger image size*

In this project, it is stated that large micro-images can reveal surface characteristics that a single micro-image cannot reveal and it would be important for the understanding of the cartilage degradation evolution. During this project, a stitching image process was performed. Increasing the size of micro-images by stitching a set of images. It was not performed in previous studies of cartilages surface characterization.

At least a set of 12 images was taken for each sample by using a 20X magnification objective lens. Each image was in a size of 500  $\mu\text{m}$  x 698  $\mu\text{m}$ . These images were stitched together with a 10% overlap, resulting in a total image size of 1.93 mm x 1.85 mm. Figure 3.5 shows a stitched 2D image conformed by a set of 12 images carefully taken for the stitching process.

The large 2D image can provide an overview of the surface topography than a single image cannot meet, however, the large 3D image can provide more qualitative information regarding to the intensity of peaks and valleys than the large 2D image, allowing a clearer understanding about the morphology condition of degraded cartilage surface. Figure 5.2 illustrates the 3D stitched image of the surface presented in Figure 3.5. The 3D stitched image reveals a heterogeneous surface composes of peaks and valleys with variation in intensity between them.

This information could not be clearly identified by the single image of 400X magnifications, however, it is not possible to determinate which feature is more predominant (Peaks or valleys) as can be seen in Figure 5.2. The 3D stitched image supply an important contribution to the understanding of the surface topography of degraded human cartilage, becoming the foundation for the quantitative surface characterization assessment.

#### *5.1.3 Qualitative description between surface morphologies for 3D stitched images of OA cartilage*

The 3D stitched images have revealed useful information about the surface condition of degraded cartilage with a deeper understanding about the evolution of the surface morphology with the stage of OA grade, revealing that cartilage surfaces become rougher and more heterogeneous with the OA grade progression.

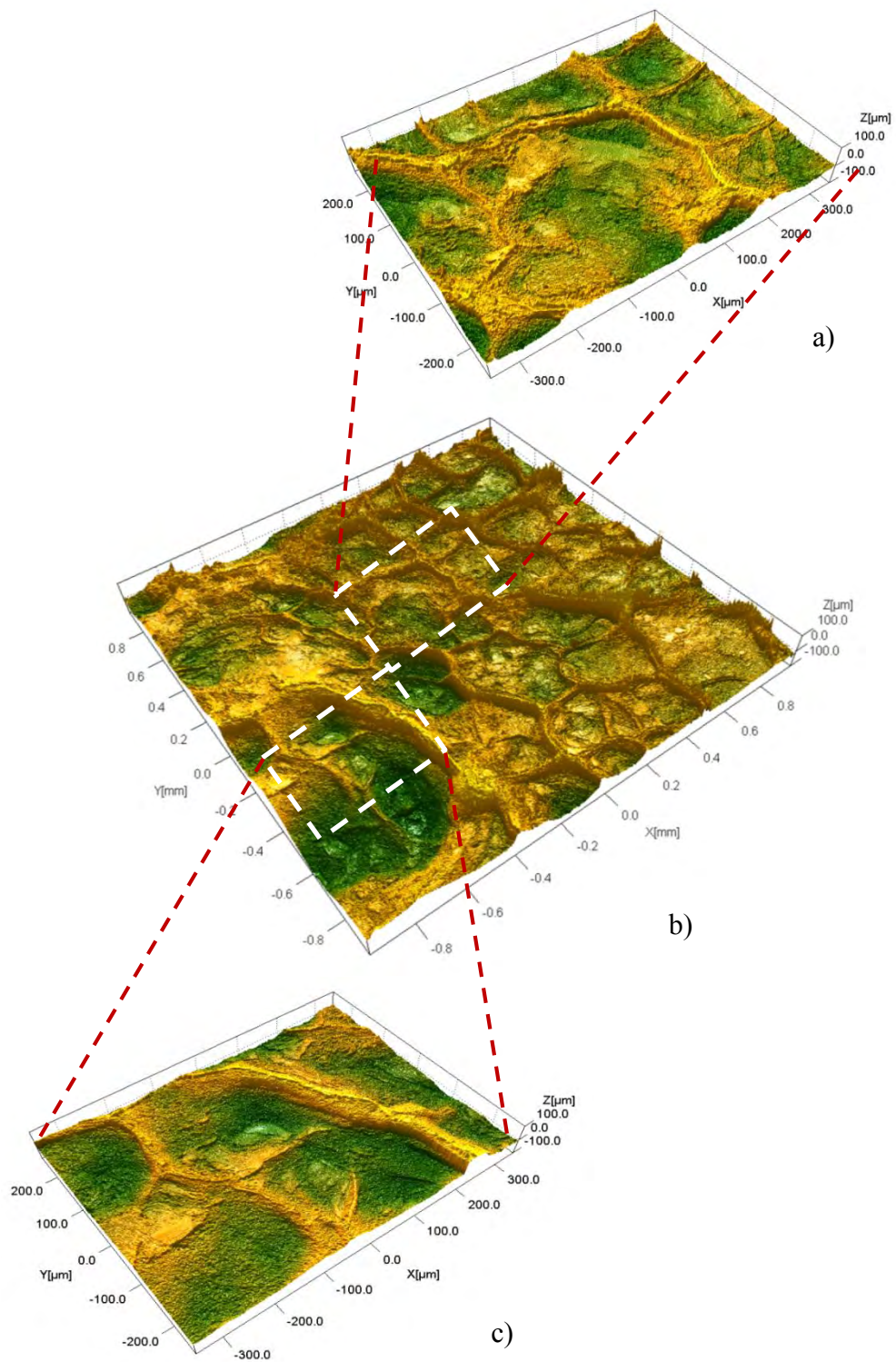


**Figure 5.2** Image process of human knee cartilage surface with OA grade III of an 89 year old male, a) and c) specific regions of the surface with different surface features (Peaks and pits respectively) (b) 3D large stitched image.

During this project, three different OA grades (I, II and III) were evaluated. The collected samples come from patients with diverse clinical history, consequently, the factors that promoted the cartilage degradation might be different for each sample and it may be reflected on the surface morphology of the samples.

Large stitched images were obtained from different OA grades and samples. Each sample was taken from a patient and/or from different location of the knee joint. The OA grade I samples still had a smooth surface to the naked eye, however, some particular features are revealed on the surface at microscale. Some areas of the cartilage surfaces with OA grade I, were slightly swollen. This characteristic is believed to be caused by the softening and swelling of the cartilage, which is a characteristic of the OA grade I cartilage (Kleemann et al., 2005).

The cartilage surfaces for both OA grades II and III are much rougher than OA grade I surfaces. Furthermore, cartilage surfaces with OA grade III tended to be rougher and more heterogeneous than that of the OA grade II. Although some samples had oriented wear marks, this feature was not a predominant characteristic of the surface, especially for OA grade II and III. Even for cartilage surfaces with the same OA grade, the surface morphology might be significantly different (see Figure 5.3 (c) and (d)).

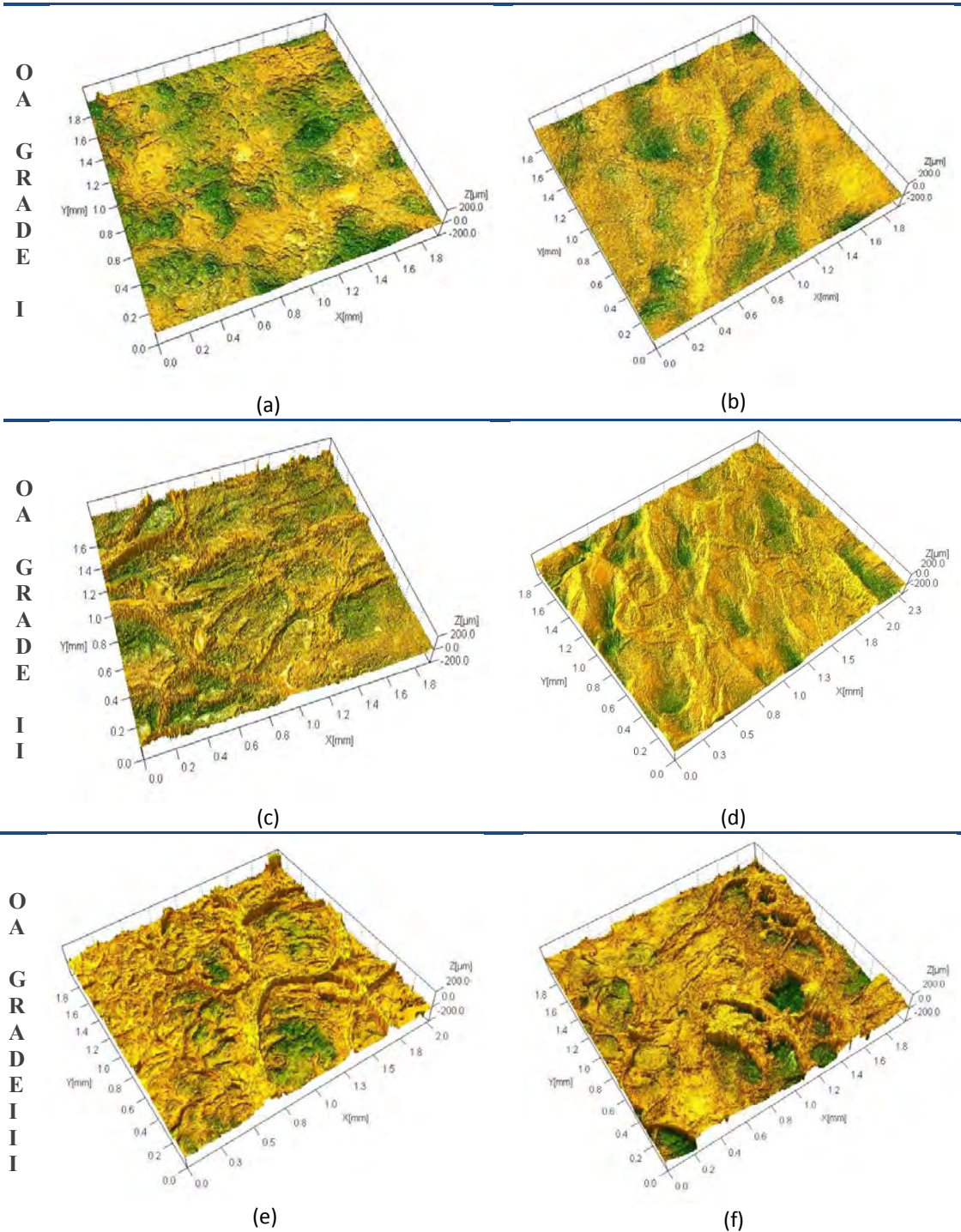


**Figure 5.3** Assembled images of diseased human knee cartilage surfaces imaged using LSM. (a) and (b) OA grade I, from 73 years old male and 53 years old female respectively, (c) and (d) OA grade II, from 65 Years old male and 65 years old male respectively, and (e) and (f) OA grade III, from 89 years old male and 53 years old female, respectively.

## **5.2 Quantitative surface characterization and statistical analysis results**

Based on the qualitative assessment, the selected numerical parameters need to identify quantitatively a significant difference between the surface morphology of the three OA grade conditions (OA grade I, II, III). It is believed that the sample condition may have an effect on the surface morphology and needs to be included in the analysis.

### *5.2.1 Classification process of the numerical parameters*

The characterizations of the cartilage surface morphology affected by OA were carried out quantitatively using 35 numerical parameters as described in Section 3.3. Following the numerical surface characterization, the classification of the numerical parameters was conducted using the two-stage nested design method with a  $p$ -value of 0.05 to identify those parameters that could describe the significant difference between the OA grades. After the first stage statistical analysis, 28 numerical parameters remained to be potential key parameters as they indicated there was a significant difference within the OA grades (Table 5.1). The Tukey's test was then used to compare all pairs of mean values of the three OA grades. The criteria for Stage 2 selection was that the parameter could tell the differences between all pairs of means of the three OA grades.

The significant difference between pairs of OA grade values was performed by the Tukey's test with 95% of Interval confidence (IC). As a result, 16 parameters, shaded in Table 5.1, were selected. To further select independent parameters from the 16 identified parameters mentioned above, Pearson correlation analysis was conducted.

**Table 5.1** Statistical results of the 28 Numerical parameters with Significant difference between OA grades (P-Value<0.05). The Standard deviation is represented by the Coefficient of Variation (CV).

Numerical parameters		OA grade								Sample		R-Sq (Adj)	Tukey's test (95% I.C)		
		OAI		OAII		OAIII		P-Value	F-Test	P-Value	F-Test		OA I	OA II	OA III
		mean	CV (%)	mean	CV (%)	mean	CV (%)								
AMP L I T U D	$S_a$ (nm)	3959.9	31.9	13900.4	35.7	20123.1	43.6	0.000	321.45	0.003	3.03	82.17	A	B	C
	$S_q$ (nm)	5317.3	36.0	18620.2	37.1	26977.0	41.7	0.000	323.57	0.002	3.11	82.28	A	B	C
	$S_y$ (nm)	73611.1	43.5	206093.8	42.5	249071.8	30.7	0.000	216.12	0.000	8.4	77.65	A	B	C
	$S_{10z}$ (nm)	66148.3	41.6	192656.4	43.4	236571.4	31.3	0.000	244.71	0.000	8.45	79.5	A	B	C
	$S_v$	32543.4	46.6	87223.2	48.0	119633.0	46.0	0.000	168.93	0.000	8.21	73.7	A	B	C
	$S_p$	41067.7	49.4	118870.4	49.3	129438.7	26.7	0.000	167.57	0.000	6.27	72.69	A	B	B
H Y B R I D	$S_{dq}$	3.13	19.5	4.56	32.7	6.77	54.1	0.000	98.55	0.000	12.7	67.75	A	B	C
	$S_{dq6}$	2.76	21.0	4.24	34.2	6.35	54.6	0.000	110	0.000	12.54	69.24	A	B	C
	$S_{dr}$	367.44	36.7	756.9	66.3	1733.56	127.3	0.000	94.26	0.000	12.97	67.3	A	B	C
	$S_{3A}$ (nm <sup>2</sup> )	1.70E+12	28.9	3.1E+12	58.6	6.7E+12	120.4	0.000	87.85	0.000	12.6	66.04	A	B	C
	$S_{Sc}$	6.92E-3	20.3	7.6E-3	19.7	9.5E-3	33.0	0.000	30.76	0.000	10.48	50.32	A	B	B
F U N C T I O N A L	$S_{bi}$	0.65	12.3	0.56	10.7	0.55	12.7	0.000	36.34	0.000	4.03	40.66	A	B	B
	$S_{ci}$	1.49	10.1	1.76	11.9	1.8	14.4	0.000	39.79	0.000	4.96	44.18	A	B	B
	$S_{vi}$	0.12	16.7	0.1	20	0.1	30.0	0.000	25.98	0.000	5.61	38.99	A	B	B
	$S_{pk}$ (nm)	8476.5	64.0	32312.8	52.2	43085.5	30.4	0.000	227.15	0.014	2.45	76.49	A	B	C
	$S_k$ (nm)	11456.9	29.1	38156.5	36.4	52898.5	45.0	0.000	273.36	0.001	3.27	79.81	A	B	C
	$S_{vk}$ (nm)	5866.1	39.0	15265.2	46.5	27257.1	83.8	0.000	158.13	0.000	10.6	73.69	A	B	C
	$S_{dc0.5}$ (nm)	32814.4	56.1	85052.7	60.0	80466.5	34.7	0.000	84.74	0.000	3.32	61.07	A	B	B
	$S_{dc5.10}$ (nm)	2280.4	58.6	10600.1	55.4	15411.6	37.4	0.000	265.58	0.418	1.03	78.73	A	B	C
	$S_{dc10.50}$ (nm)	6147.9	35.2	25605.6	41.6	36437.0	38.9	0.000	339.43	0.068	1.83	82.72	A	B	C
$S_{dc50.95}$ (nm)	8259.1	31.3	24162.4	34.4	36953.8	70.5	0.000	210.94	0.000	5.5	76.3	A	B	C	
S P A T I A L	$S_{ds}$ (μm <sup>-2</sup> )	0.14	7.1	0.11	9.1	0.11	9.1	0.000	192.39	0.000	10.5	76.61	A	B	B
	$S_{fd}$	2.37	2.5	2.23	1.8	2.22	1.3	0.000	246.44	0.000	5.74	78.88	A	B	B
	$S_{tdi}$	0.69	14.5	0.61	21.3	0.62	20.9	0.001	7.35	0.019	2.32	14.65	A	B	B
	$S_{rwi}$	0.03	33.3	0.03	33.3	0.03	33.3	0.000	8.34	0.000	6.31	30.39	A	B	B
	$S_{hw}$ (nm)	97614.7	28.9	143087.1	26.6	125181.9	17.8	0.000	41.13	0.000	8.16	50.30	A	B	C
	$S_{cl20}$	42562.4	24.1	48062.8	19.7	44749.3	19.5	0.000	5.58	0.004	5.79	26.22	A	AB	B
	$S_{cl37}$	28085.3	34.7	35392.8	24.7	32534.2	21.3	0.000	15.11	0.000	9.43	42.13	A	B	B

Two main groups with high correlation coefficients were identified. The first group is composed of 4 parameters:  $S_q$ ,  $S_{dc10\_50}$ ,  $S_k$ , and  $S_a$ . The second group contains  $S_{dq}$ ,  $S_{dr}$ ,  $S_{3A}$  and  $S_{dq6}$ , as shown in Table 5.2. This correlation reveals a statistical relationship between the numerical parameters of these two groups.

### 5.2.2 Analysis of the selected parameters

The suitable parameters used to describe the OA progression of human cartilage need to clearly and reliably identify the differences between the OA grades. The  $F$ -test evaluates the significant differences between OA grades. This test was used to rank the 16 selected parameters from the highest to the lowest level of significance. When the  $F$ -value increases, the  $p$ -value becomes smaller, and consequently, the significant difference between OA grades elevates. Due to the very small obtained  $p$ -values, the  $F$ -values become more suitable for ranking the 16 selected parameters. It can be seen from Figure 5.4, that the 4 numerical parameters with the highest  $F$ -value are  $S_{dc10\_50}$ ,  $S_q$ ,  $S_a$  and  $S_k$ . These parameters are also in the first correlated group that is displayed in Table 5.2. The parameters in the second correlated group had low  $F$ -values. The Figure 5.4 also shows that the first correlated group presents the highest adjusted coefficient of determination ( $R$ -sq Adj) and the lowest  $F$ -values for the samples (see Table 5.1).

The parameters in the second correlated group had low  $F$ -values. This study considered the differences between the samples and carried out the statistical analysis described in section 3.3 to evaluate the differences and their effects on the numerical characterizations. The statistical results revealed that the significant differences between samples varied according to the numerical parameters.

**Table 5.2** Pearson correlation coefficients between the selected numerical parameters with significant difference between pairs of OA means, using Tukey's test.

	$S_a$	$S_q$	$S_{dc10\_50}$	$S_k$	$S_{dc5\_10}$	$S_{10z}$	$S_y$	$S_{pk}$	$S_{dc50\_95}$	$S_{vk}$	$S_v$	$S_{dq6}$	$S_{dq}$	$S_{dr}$	$S_{3A}$
$S_q$	0.99														
$S_{dc10\_50}$	0.97	0.97													
$S_k$	0.98	0.96	0.94												
$S_{dc5\_10}$	0.79	0.82	0.85	0.72											
$S_{10z}$	0.87	0.90	0.86	0.81	0.79										
$S_y$	0.85	0.88	0.85	0.79	0.79	1.00									
$S_{pk}$	0.81	0.84	0.87	0.73	0.96	0.87	0.87								
$S_{dc50\_95}$	0.93	0.92	0.82	0.90	0.59	0.76	0.74	0.61							
$S_{vk}$	0.87	0.87	0.75	0.83	0.51	0.74	0.72	0.54	0.97						
$S_v$	0.84	0.85	0.80	0.81	0.66	0.91	0.92	0.70	0.79	0.79					
$S_{dq6}$	0.84	0.85	0.77	0.79	0.59	0.78	0.77	0.63	0.89	0.89	0.79				
$S_{dq}$	0.83	0.84	0.75	0.78	0.57	0.77	0.75	0.61	0.89	0.89	0.78	1.00			
$S_{dr}$	0.73	0.73	0.62	0.67	0.42	0.61	0.59	0.44	0.87	0.88	0.66	0.95	0.95		
$S_{3A}$	0.73	0.73	0.62	0.67	0.42	0.61	0.59	0.44	0.87	0.88	0.66	0.95	0.95	1.00	
$S_{hw}$	0.38	0.36	0.38	0.41	0.34	0.18	0.17	0.30	0.30	0.17	0.15	0.02	0.01	0.01	0.01

Figure 5.4 illustrates how the F-value of the samples is decreasing for the 16 selected numerical parameters when the R-Sq (Adj) and the F-value of the OA grade are increasing. The R-Sq defines how the data are well fitted by the model. The  $S_{dc10\_50}$  parameter had the highest R-sq (Adj) and a significant value for the variable samples of 0.068. This significant value ( $>0.05$ ) fails to describe the significant difference between the *samples* described by  $S_{dc10\_50}$ .

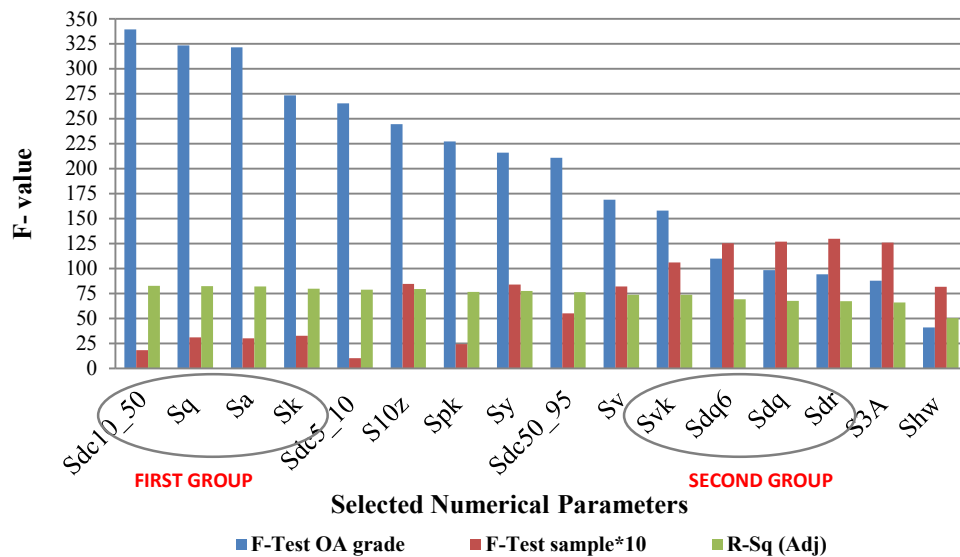


**Figure 5.4** Ranking of the 16 selected numerical parameters based on the values supplied in Table 1.

### 5.2.3 Analysis of the correlated groups

The first correlated group with the highest F-values present a clear difference between the OA grades according to the means and standard deviations (SD). Even when the parameters  $S_{dc10\_50}$ , Sq and Sa have a similar standard deviation for the three different OA

grades, the OA means represented by  $S_{dc10\_50}$  are higher and the difference between means are also higher than  $S_q$  and  $S_a$ , and thus indicating the surface feature described by this parameter has the most significant difference between the OA grades (see Figure 5.5). The second correlated group of numerical parameters can also show a significant variation on the OA grade. However, there is an increase in the relative standard deviation (RSD) or coefficient of variance (CV) compared with the first group. The CV tends to be higher when the F-value becomes lower, which explain the less significant difference between OA grades (Figure 5.6 (a) & (b)).

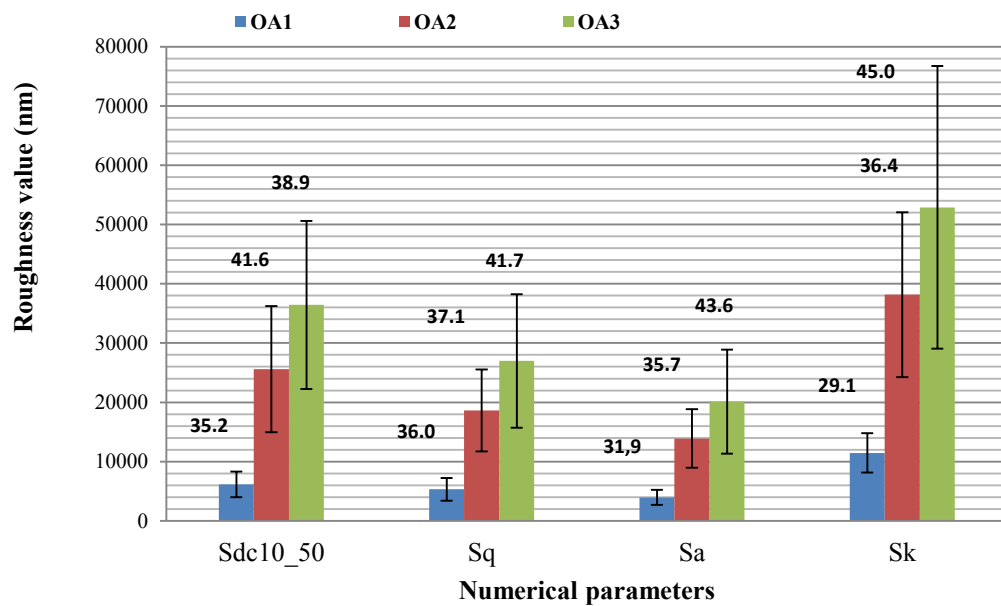


**Figure 5.5** Variations of the roughness values with the OA grades of the first correlated group of numerical parameters with the highest F-values. The numbers over the bars, represent the coefficient of variation (%).

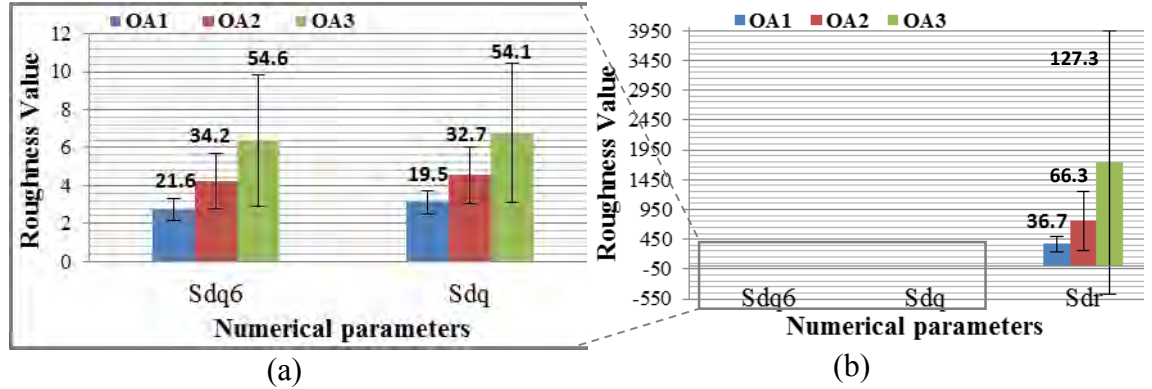


**Figure 5.6** Variation of the roughness value with the OA grades of the second correlated group of numerical parameters with the lowest F-values. The presented values are dimensionless.

#### 5.2.4 OA grade evolution described by $S_{dc10\_50}$ parameter

Based on the above statistical and correlation analyses, the  $S_{dc10\_50}$  parameter has been identified as a key parameter to describe the progression of OA. This parameter, represented by the bearing area curve (BAC or Abbott curve), depicts the height difference obtained from the interval, being between 10% and 50% of the bearing area ratio (Foster et al., 1999). The BAC illustrates a representative profile that describes the surface condition and the evolution of the profile during the OA progression. Figure 5.7 shows the BAC for three different OA grades. The peaks and valleys tended to become larger when the OA grade increased.

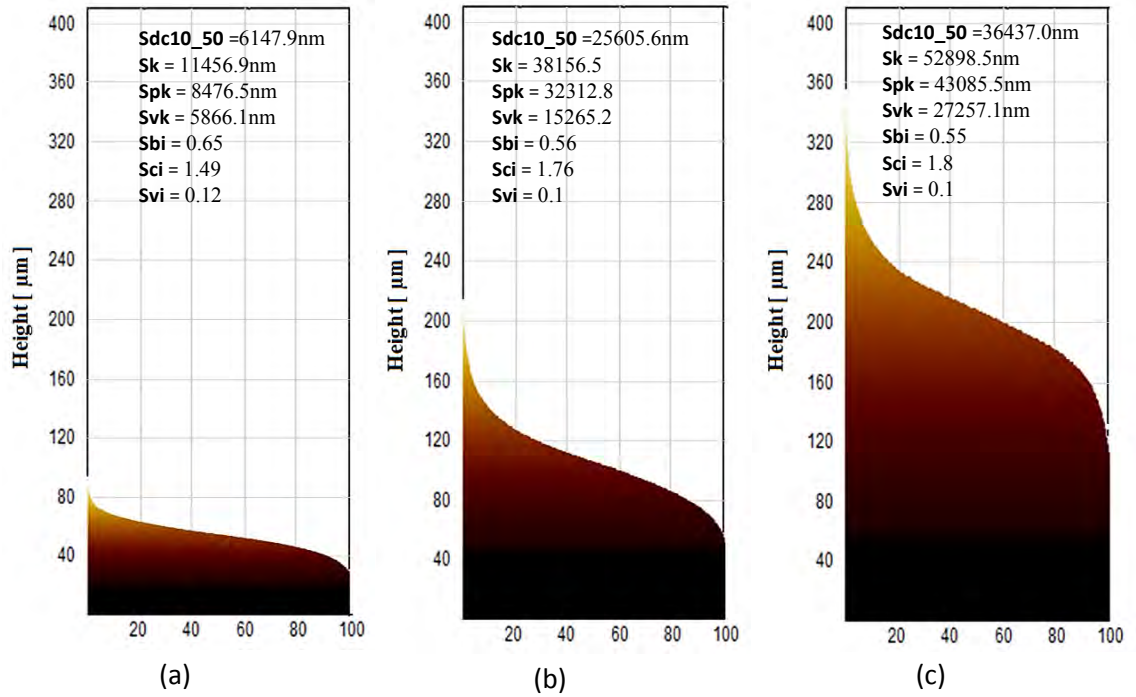


**Figure 5.7** Bearing area curves (BAC) illustrating the surface texture of three cartilage surfaces affected by OA. (a) OA grade I cartilage (73 years old male patient); (b) OA grade II (64 years old male); and (c) OA grade III (53 years old female).

### 5.3 Summary

This study has qualitatively and quantitatively characterized the surface morphologies of diseased human cartilage. Three key techniques used are laser scanning microscopy (LSM) for 3D image acquisition, numerical characterization of comprehensive surface features, and a two-stage nested design for statistical analysis allowed to select effective numerical parameters. Among the 35 parameters used in the surface characterization, functional parameter  $S_{dc10\_50}$  has been identified as the most reliable and effective descriptor. Different to the commonly used surface roughness parameter  $R_a$  in 2D or  $S_a$  in 3D, it reveals the evolution of the bearing areas of the cartilage surfaces with OA

development. The change in the BAC described by  $S_{dc10\_50}$  correlates with the deterioration of the surface and OA conditions. The numerical results reported in this work have provided further insight in the functional property of the cartilage surfaces which may be related to the collagen structures, fibrillation and the mechanical properties for better understanding of the wear process of human cartilage.

## **Chapter 6 Investigations of Micron and Sub-micron Wear Features of Diseased Human Cartilage Surfaces**

As stated before, a four year study was conducted to investigate the wear characteristics of cartilage surfaces of osteoarthritis (OA) patients in Australia. In collaboration with the University of Huddersfield, Peng's research group at UNSW Australia has carried out studies on the surface morphologies and bio-mechanical properties of articular cartilage in various OA conditions since 2010. They established imaging acquisition and analysis methods based on atomic force microscopy (AFM) with numerical characterisation techniques, in order to investigate distinctive morphologic features of human cartilage at a nano-metre scale (Wang et al., 2013). The characterization method based on LSM presented in this thesis allows making a comparison between both characterization techniques (AFM and LSM) regarding to the description of the surface morphologies of diseased human cartilage.

Sample preparation procedures were different for LSM and AFM examinations. The detailed sample preparation procedures for the LSM and AFM techniques are presented in section 3.1 of this thesis and Dr Wang's PhD thesis (2014) respectively.

The purposes of this chapter were (a) to compare the quantitative surface characterisation results in a micron and sub-micron scale, and (b) to understand distinctive changes in the surface morphologies of the cartilages in micron and sub-micron resolutions so that a better understanding of the OA process and its indicators could be achieved. Diseased cartilage samples were prepared for image acquisition using two different techniques, that is, laser scanning microscopy (LSM) in a micron scale (presented in section 3.2.1) and

atomic force microscopy (AFM) in a nano-scale described in Dr Wang's Thesis (Wang, 2014). These three-dimensional (3D), digital images were processed and analysed quantitatively.

### **6.1 Qualitative characterization of surface morphologies of human knee cartilage by using AFM and LSM techniques**

3D images of the prepared cartilage samples with three OA grade condition (OA I, II, III) were acquired using LSM and AFM separately. The key hardware settings and conditions are briefly summarised as follows.

The LSM was used to capture 3D surface information of the specimens in a non-contact mode and at a micro-metre scale, described in section 3.2.

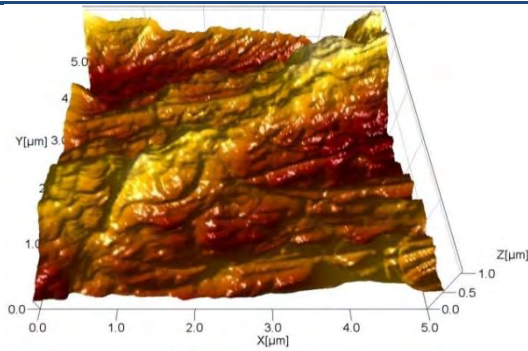
In parallel, AFM images were acquired on the diseased samples in OA grades I–III. The imaging process was carried out in a PeakForceQNM and fluid mode. DNP-10 tips with a nominal tip radius of 20 nm and a nominal spring constant of 0.35 N/m were used to image the cartilage surfaces. During the imaging process, forces in a range of 0.3 to 16.5 nN were applied to the surfaces, resulting in a constant deformation of 150 nm on the surfaces. The scanning resolution was  $256 \times 256$  pixels, and the scanning area was  $5 \times 5 \mu\text{m}^2$ . Three to four locations were imaged on each cartilage sample.

3D images of diseased cartilage in OA grades I, II and III, were acquired using LSM and AFM as described above. Figure 6.1 shows representative 3D images acquired using LSM and AFM, respectively.

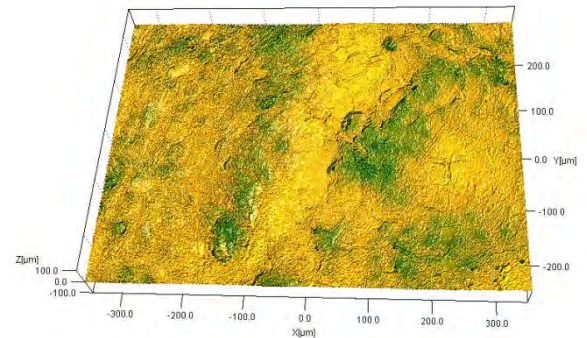
---

### OA GRADE I

---



a)

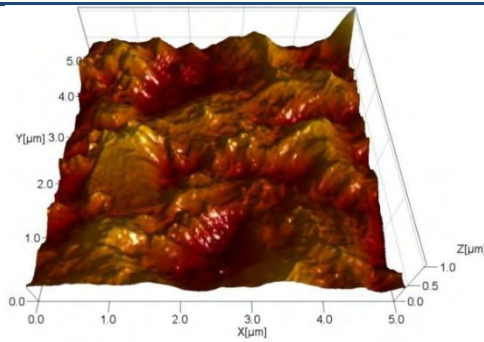


b)

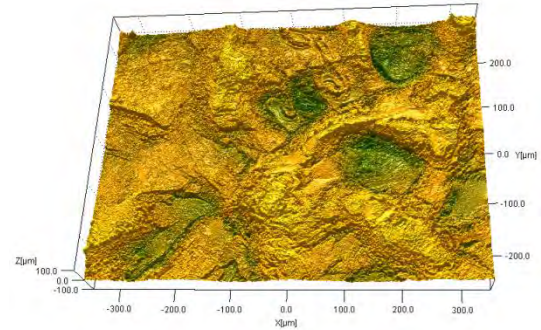
---

### OA GRADE II

---



c)

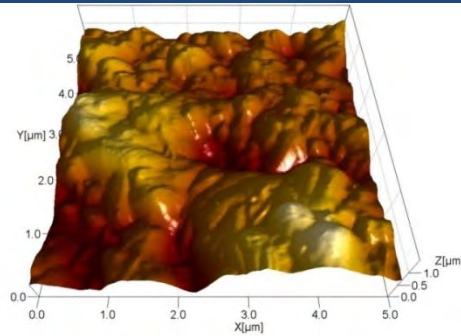


d)

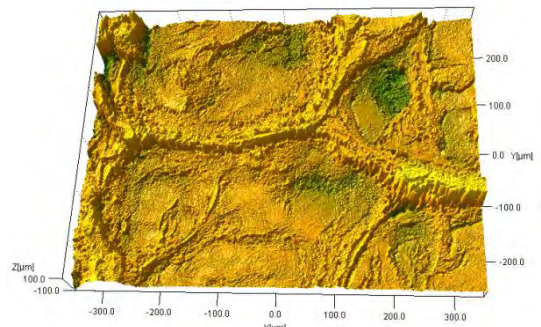
---

### OA GRADE III

---



e)



f)

**Figure 6.1** Evolution of the surface morphology with OA grade condition using both techniques, AFM and LSM; a, c and e) 3D images of cartilages in OA grades 1, 2 and 3 acquired using AFM; b, d and f) 3D images of cartilages in OA grades 1, 2 and 3 acquired using laser scanning microscopy.

From the LSM images shown in Figure 6.1 (b), (d) and (f), it can be seen that with OA progression from OA grade I to III, the cartilage surfaces became rougher with larger pits. This observation was confirmed by the AFM images obtained at the sub-micron level, revealing that the cartilage in OA grade I, knee joints became corrugated. As OA severity progressed to an advanced condition, the cartilage surfaces had gradually enlarged periodic structures and the steepened spots as shown in Figure 6.1 (a), (c) and (e).

Even when surface morphology appearance becomes rougher with the AO grade condition, according to the images obtained by both techniques, AFM and LSM, It seems that LSM can identify more features of the surface morphology for the different OA grade than AFM.

In order to have a better understanding about the surface morphology of degraded cartilage and the information of the supplied images of each technique, a larger image of the cartilage surface is used. The acquisition of this large image is the result of a stitching process described in section 5.1.2.

The large micro-image presented in Figure 6.2 (c) reveal information about the surface morphology of OA grade III condition that was not supplied by the images in Figure 6.1. The large image evidence surface features such as peaks and valleys highly heterogeneous according the intensity. Due to the intensity of the surface features, the AFM images are limited to describe the representative roughness condition of the surface (Figure 6.2 (a and b)), however, this technique might reveal the degradation process at nano-metre scale of the collagen fibers that conform the cartilage and provide its mechanical properties.

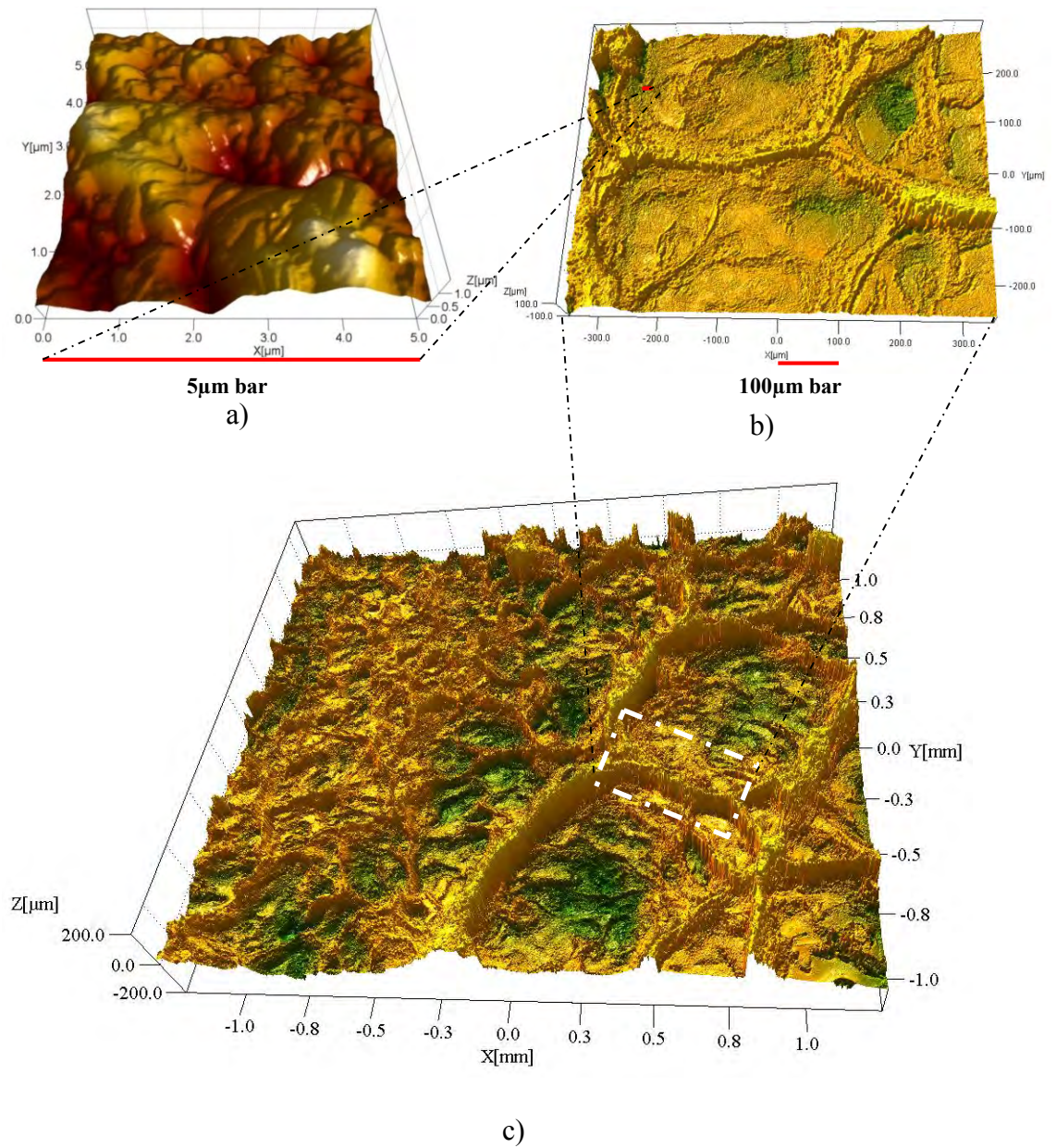


**Figure 6.2** Image of human knee cartilage surface with OA grade III a) AFM image, b) LSM image with 20x magnification objective lens and c) 3D large stitched image using LSM.

## **6.2 Quantitative characterization of surface morphologies of human knee cartilage in micro- and nano-metre scale**

Before performing quantitative image analyses, the LSM and AFM images were plane corrected to remove image bow and scan distortions. Noise was also filtered out. The images were then analysed so that the cartilage surface topographical characteristics at both the micro- and nano-metre scales could be examined for OA studies. Numerical parameters used in this study are from four sub-sets, namely, amplitude, hybrid, functional and spatial descriptors (ISO 25178-2, 2006).

Following the above quantitative characterisations, statistical analyses were conducted to evaluate and select effective numerical parameters to describe distinct surface features for OA assessment, and to seek insights into how the cartilage surfaces evolved with the OA progression and at the micro- and nano-scales. The statistical analyses were carried out in the following steps. The means and standard errors of the numerical results were calculated. For the AFM data, One way ANOVA was conducted to determine if the means of the samples in the three OA grades were statistically different. Only the parameters with a significance level of 0.05 (confidence level = 95%) or less were selected as potential significant ones. Post hoc tests ( $p < 0.05$ ) were conducted to determine where the significant differences were, i.e., to evaluate the statistical significance between the OA conditions using the selected parameters. The statistical analysis for LSM data, is described in section 3.3.2.

The LSM and AFM images were analysed separately using the same image analysis package (SPIP) and numerical parameters. The selected numerical parameters to describe the surface condition of diseased cartilages were different for both techniques, which was expected as due to the magnification level, the assessed surface features were different,

according to the qualitative analysis results mentioned above. However, in both techniques, the  $S_a$  parameter described an increase on the surface roughness with the OA grade. The  $S_a$  value at the micron scale, increased noticeably with the OA grades as can be seen in Table 6.1. These quantitative results match with the visual inspection outcome, that is, the cartilage surface became rougher when the OA grade increased. In comparison, the surface roughness changes in the nano-metre level were marginal with an overall increasing trend with OA progression.

**Table 6.1** The surface roughness ( $S_a$ ) values of the cartilage samples measured at the micro- and nano-metre scales.

Technique	Surface Roughness ( $S_a$ ) (nm)		
	OA grade 1	OA grade 2	OA grade 3
LSM	3960	13900	20123
AFM	110	111	119

In addition to the  $S_a$  results shown in Table 6.1, the numerical analyses of the LSM images showed that other amplitude parameters and functional parameters described the highest significant difference between the cartilage samples in the three OA conditions. The spatial parameters did not reveal a significant difference between the OA grades, and thus, were unsuitable to describe the OA grade progression. Based on the statistical analysis results using two-stage nested design and the Tukey's test (Montgomery, 2003)  $S_{dc10\_50}$  (10-50% height intervals of bearing curve) was identified to be an important parameter for the OA cartilage characterization, followed by  $S_q$ ,  $S_a$  and  $S_k$ . These key parameters are described in more details in section 5.2.

The nano-scaled surface texture of collagen network in the diseased cartilages was gradually damaged in the wear process as shown in Figures 6.1 (a), (c) and (e). The

change in the nano-scaled surface texture gradually progressed to the micro-level of the architecture and affects the function of cartilage (Stolz et al., 2009). The numerical results obtained by AFM revealed that some selected numerical parameters may assist in differentiating the diseased cartilage at the nano-scaled surface texture. For example,  $S_{fd}$ , fractal dimension, may discriminate the nano-scaled surface texture of OA grade II and grade III cartilages as suggested by the ANOVA analysis ( $p=0.047$ ).  $S_{tr37}$ , texture aspect ratio, revealed a statistical significance ( $p=0.050$ ) between OA grade I and III cartilages, suggesting that the nano-scaled surface texture aspect ratio tends to be different (see Table 6.2). However, The statistical analysis results at nano-meter scale did not reveal any parameters that could be used to assess the OA condition. More information about these results can be found in the Dr. Wang's Thesis (Wang, 2014).

**Table 6.2** Distinctive features the three OA grades at the micron and nano-metre scales.

Scale	Distinctive surface parameters to differentiate OA grades
Micro-metre	Amplitude (height) features including $S_a$ and $S_q$ and functional parameters $S_{dc10\_50}$ and $S_k$
Nano-metre	Spatial information including $S_{fd}$ and $S_{tr37}$

### 6.3 Summary

Numerical characterisations were conducted on the surfaces of diseased human cartilage samples at both the micro- and nano-metre scales. The surface characterizations in the sub-micron level have found that spatial changes regarding to the variation of collagen fibers at early OA grade can be revealed at this scale. In the micro-metre scale, changes to the surface roughness and functional properties of the surface were significant enough

for OA condition assessment. With support of advanced imaging facilities in 3D and quantitative analysis techniques, the results reported in this project and Dr Wang's thesis have revealed the surface morphology evolutions of cartilage surfaces affected at three OA grades. Through the nano- to micro-metre surface characterisations along with the nano-mechanical property investigations, insights into the surface changes have been achieved. Further investigations of relationships of changes in the nano-scaled surface textures and nano-mechanical properties are needed to assist in understanding the fundamental causes of OA.

## **Chapter 7 Discussion**

This research project investigates the surface morphologies of diseased cartilage of human knee affected by OA at the micron scale. Since the surface morphologies alter with OA conditions as a result of the mechanical reaction of the surface under tribological conditions and possible changes in the mechanical properties of the surface, identifying and quantitatively characterizing the main features of the surface morphologic changes help explain the OA progression and can open the door for studying the most relevant markers for OA assessments.

The qualitative and quantitative surface characterizations of the human knee cartilage with three different OA grade conditions were carried out by using laser scanning microscopy (LSM). 3D numerical parameters were used for assessing the surface conditions of the studied cartilage surfaces and reliable numerical parameters were identified to describe the main surface features associated with the OA conditions. The selection of these key parameters was achieved by the statistical method used in this project, namely the two-stage nested design. This method allows introducing in the experimental design two variables, that is, the OA grade condition (e.g., OA grades I, II, III) and the sample condition. The sample condition was introduced in the experiment as it was observed from the stitched images employed for the qualitative characterization that the surface characteristics might vary not just because of the OA condition, but also due to specific conditions of the samples, such as clinical histology and/or specific location of the human knee part where the sample came from.

This project supplied important information that can contribute to the understanding of the OA process of diseased human knee cartilage. Detailed discussions of the found results are presented below.

## **7.1 Procedures for sample extraction and image acquisition**

Setting up the sample extraction procedures prior to the image acquisition was essential for obtaining appropriate images for quantitative characterizations due to the susceptibility of biological samples to be dehydrated, affecting the reliability of the results. The susceptibility to dehydration depends on the sample characteristics and the time taken for image acquisition. More information about how the dehydration issue was addressed in this project is mentioned forward.

### *7.1.1 Identification of the required sample size*

During this study it was noticed that the cartilage surface morphology was highly affected by sample dehydration, which is influenced by the sample size and the bone attached to the cartilage. It was found that cartilage samples of 5 mm in diameter without bone attached can significantly change the surface morphology (see Figure 4.1). In comparison, samples of a diameter of 10 mm with bone attached have a more stable surface morphology during a longer period of time than the 5 mm sample (see Figure 4.2). The bone attached to the samples was essential for the stability of the surface morphology, since being the cartilage attached to the bone, the bending effect caused by dehydration is reduced. It is also believed that cartilage rehydrate can be realized by the bone fluids (Batmanghelidj, 2009). However, this surface morphology stability due to dehydration was observed to be limited, and thus a new method for sample rehydration was required.

### *7.1.2 Performance of the designed sample holder*

The biological and physical characteristics of the sample, and its location conditions on the microscope's stage influence in the quality and reliability of the collected images, which is reflected in the surface data and finally in the analysis results. The LSM employed for the image acquisition was not supplied with any specimen holder, especially for biological sample purpose, and for this reason, a sample holder was designed to guarantee a suitable location and hydration of the sample during the image acquisition. Figure 4.6 illustrates three different image acquisition procedures and outcomes. Figure 4.6 (a) is in a dry condition without the sample holder. This sample evidenced dehydration after around 30 minutes of imaging and the holding condition on the stage cannot guarantee a completely horizontal position of the cartilage surface, which is suitable for the image acquisition. These drawbacks were overcome by using the sample holder presented in Figure 4.6 (c). The bone attached to the cartilage was used to fix the sample to the specimen holder with a screw without affecting the cartilage surface. The sample holder was used during the whole image acquisition process with satisfactory results, which was reflected in the quality of the collected images.

### *7.1.3 Performance of the LSM*

Although the LSM is not widely used for quantitative surface characterizations, it is a suitable technique for examining biological tissues. This technique has a number of advantages, including (a) not requiring a special sample preparation that might affect the cartilage surface integrity, (b) the short image acquisition process to avoid sample degradation, and (c) the high resolution to provide appropriate surface data for quantitative characterizations. These advantages make this technique suitable for the OA

cartilage characterization, supplying important information about the understanding of OA cartilage surfaces.

#### *7.1.4 Criteria for the selected magnification*

Healthy cartilage presents a smooth surface that can be easily imaged using LSM (Figure 4.7). However, the sample roughness condition for advanced OA grade stage can make it difficult for capturing sufficient surface data over a large range of the depth in the Z direction. It was found that the OA grade III surface imaged at a 10X magnification objective lens did not provide clear information about the surface appearance, contrary to 20X magnification which revealed clearly the surface morphology appearance (Figure 4.8). The 50X magnification was not suitable for imaging samples with a severe condition due to the short work distance of 0.35 mm making contact with the surface during the scan process.

The reliability of the surface appearance was evaluated by the coefficient of variation (CV) which is a normalized method to evaluate the dispersion of the data (Montgomery et al., 2011). The same spot on the surface was imaged using 10X and 20X magnifications separately. The taken data at 20X magnification presented the most stable dispersion for the three OA grade conditions and the 10X magnification evidenced a high dispersion of the data for OA grade III stage (Figure 4.9). This information corroborates that the surface information can vary according the used characteristics of the microscope and confirms that the 20X magnification lens is the most suitable lens for the diseased cartilage surface characterization.

## **7.2 Qualitative and quantitative characterization of human knee cartilage at different OA grade levels**

The purpose of the qualitative assessment of the OA cartilage was to evaluate general information such as topography appearance, roughness evolution and heterogeneity of the surface texture between OA grades. The area chosen for qualitative OA assessment was based on reported studies (Loeser et al., 2003; Byers et al., 1977; Setton et al., 1993) and the obtained surface information. The entire sample surface was examined by visual inspection under an optical microscope and according to ISO 4288 (1966) before image acquisition. The image acquisition and processing techniques used in this project allowed appropriate information about the surface topography to be obtained at the micro-meter level. The selected resolution and the examined image area were higher than existing techniques reported in previous studies (Kleemann et al., 2005).

### *7.2.1 Qualitative surface assessment*

The qualitative assessment of the surface topographies of human knee cartilage affected by OA was made using stitched images at 20X magnification objective lens, which revealed information about the main patterns of the cartilage surfaces at different OA grade stages. These large images evidenced that even when OA grade I cartilages presented a smooth surface appearance in a naked-eye inspection, they had swollen regions randomly distributed at the micron scale (Figure 5.3 (a) and (b)). The swelling of the cartilage is a current characteristic of OA grade I cartilage (Outerbridge, 1961). The mechanical properties decrease on the swollen areas, therefore, becoming more susceptible to being worn out (Pearl et al., 2005). More study needs to be carried out on OA grade I cartilage to find root cause(s) of OA initiation since during this stage,

important changes in the cartilage structure, surface morphologies and mechanical properties takes place, facilitating the cartilage degradation.

The observed surfaces of OA grades II and III presented a heterogeneous morphology and the surface texture tended to be rougher with the increase of the OA. It was noticed that the surface texture became rougher with the OA progression. This change might be associated with the variation of both, orientation and density of the collagen fibers during the OA process. The heterogeneity of the surface texture is not clearly understood and it can be related to the structural change of the cartilage and/or the early OA condition. The heterogeneity and roughness condition of the cartilage surface textures need to be further studied.

The large stitched images supplied important feature information about the diseased cartilage surface that was not reported before. These large images were essential to identify the hypothesis used for the statistical analysis process and for the understanding of the statistical analysis results discussed below.

#### *7.2.2 Statistic analysis and quantitative results*

The quantitative assessment of the OA cartilage surfaces was conducted on high resolution 3D images. The collected data were sufficient to guarantee reliable results, which was confirmed by the R-Sq (Adj) values presented in Table 5.1.

The two-stage nested design based on ANOVA was the statistical method employed in this project. Although this method is not widely applied in the bio-engineering field, it was selected based on the facts that it allows two independent variables (e.g., OA grades and Samples in this study) in the experimental design, and it reveals how these variables

affect the numerical values and vice versa. Using this method, it rejected around 50% of the numerical parameters which do not describe distinctive differences between the OA grades (see Table 5.1).

This study has confirmed that the numerical parameters  $S_q$  and  $S_a$  could describe a significant variation in the surface texture between the OA grades. This study has also revealed that  $S_q$  was more reliable and effective than  $S_a$  in describing the cartilage surface roughness changes.

A group of functional parameters was found to be able to reveal the changes in the surface morphologies with OA progression. This study found that although the functional parameters,  $S_{pk}$  and  $S_{vk}$ , are not the most reliable parameters to describe the OA progression according to the F-Test (See Figure 5.4), these parameters reveal a significant evolution on peaks and valleys respectively, during the OA process.

The  $S_{pk}$  parameter reported a more accurate value than  $S_{vk}$  regarding to the R-sq (Adj) and the F-value (See Table 5.1). The accuracy of the  $S_{pk}$  respect to  $S_{vk}$  suggested that the increase of peaks was more distinctive than the increase of valleys on the surface texture during the OA process. The  $S_{pk}$  parameter evaluates the peak height above the core roughness represented on the *Bearing Area Curve (BAC)* and estimates the largest peaks of the surface texture.

The most suitable numerical parameter to characterize the cartilage surface condition, according to the analysis results was the  $Sd_{c10\_50}$  parameter as is shown in Figure 5.4. Although the samples were from different patients, the functional parameter  $Sd_{c10\_50}$  was able to describe the changes in the OA progression of human knee cartilage regarding to the satisfactory results of both R-sq (Adj) and the F-value (see Table 5.1) for different

samples with different conditions. The numerical parameter  $S_{dc10\_50}$  belongs to a set of parameters represented as  $S_{dcl\_h}$  and is named as l-h% height intervals of the *BAC*. This group of parameters describes the height differences between defined bearing area ratios, with  $l$  and  $h$  being the lower and the upper bearing area ratio of the interval (ISO 4287, 1997), respectively. The selected parameter,  $S_{dc10\_50}$  defines the height differences of the curve between 10% and 50% of the *BAC*. It revealed the OA progression based on the evolution of the peaks rather than valleys, and does not take the highest peaks of the surface texture into consideration. The variation of the cartilage surface texture during the OA grade progression is illustrated by the *BAC* (Figure 5.7). The surface texture is characterized by the increase of both peaks and pits with the severity of the OA grade, which is consistent with the visual inspection (Figure 5.3).

This parameter revealed specific functional features of the surface texture that could be used to describe the OA progression. These statistical results suggested that the  $S_{dc10\_50}$  parameter had the potential to be employed for surface characterization of the cartilage degradation process.

This study has found that the F-value of the variable samples described by the numerical parameters changed considerably between them and most of these parameters revealed a significant difference between sample (P-value < 0.05) as can be seen in Table 5.1. Therefore, the influence of the clinical histology of the samples on surface morphology needs to be studied further.

### *7.2.3 Correlation between cartilage surface texture and its structural condition*

The surface morphology of a degraded cartilage is the result of the biomechanical response, which is linked to the structure of the cartilage. The collagens of the cartilage present different orientations through the cartilage thickness. The collagen fibrils are parallel to the surface in the superficial layer with a compact structure, but these fibers become perpendicularly orientated in layers nearby to the subchondral bone (Calleghan et al., 2003). It is believed that the changes in the  $S_{dc10\_50}$  values shown in Figure 5.6 can reflect the change in the orientations of the collagen structures in the OA conditions.  $S_{dc10\_50}$  was small for OA grade I surfaces whose compact collagen structure has not been significantly disturbed. For a healthy and mild OA cartilage, as the orientation of the collagen fibers is parallel to the top surface and it is reasonable to expect the fibrillation on the surface are minimal resulting in a low  $S_{dc10\_50}$  value. With OA progress to a deep layer, the collagen changes its direction and density (Makela et al., 2012), increasing the influence of fibrillation on the surface morphology. Thus, an increase in the  $S_{dc10\_50}$  values (Figure 5.7 (b) and (c)) is expected.

Although up to date, the surface morphology evolution has not been well linked with the variation of the mechanical properties. The presented results of the functional parameter  $S_{dc10\_50}$  may open a door for studying their relation. Figure 5.7 shows that the  $S_{dc10\_50}$  values increased with the OA progression, revealing also that there was less contact or loading areas on the severe OA cartilage surfaces than on a surface with a mild OA condition.

Wear of cartilage may result from unfavourable lubrication or fatigue, or both. The qualitative and quantitative information revealed that the surface topography became rougher with the OA grade progression. An increase in the surface roughness may affect the elastohydrodynamic lubrication since these roughness have an influence on the hydrodynamic properties of the fluid film. By increasing the roughness, the contact area is reduced and the local contact pressure around the peak's area is increased considerably, resulting in a significant reduction in the lubrication capability of the fluid film (Kumar et al., 2001).

It is believed that the influence of the biphasic nature of the cartilage on the elastohydrodynamic dynamic lubrication is affected during the cartilage degradation process. The best performance of the biphasic nature of the cartilage is on the top layer, mostly associated with the soft surface and the permeability property and by maintaining a high pressure on the fluid film (Graindorge et al., 2005; Downson and Jin, 1986). During the OA progression, the roughness surface is increasing, but the permeability is reduced, affecting the performance of the biphasic nature of the cartilage, which plays an important role on the wear resistance of cartilage. This project has provided reliable quantitative evidence of the evolution of the surface topography during the OA grade process. The performance of the biphasic nature of the cartilage was not directly studied.

### **7.3 Comparison between micron and sub-micron characterization of diseased human cartilage surface**

The information supplied by the cartilage surface characterizations varies according to the employed scales. In this section, the information of cartilage surface morphology was supplied at two different scales, the micron scale using LSM and the sub-micron scale

using AFM. At the sub-micron level, the fine surface asperities of the OA grade I cartilage became larger in both the X-Y (plane) and Z (height) direction with OA progress (Wang, 2014). In contrast, at the micron level, there was an increase in both peaks and pits on the surfaces with the severity of the OA grade condition as can be seen in Figure 6.1. The asperity of the surface texture presented by both techniques (AFM and LSM) are substantially different, suggesting that the surface features revealed by these techniques are also different. The Figure 6.2 shows images of cartilage surface with OA grade III at sub-micron and micron level and the size of the sub-micron image is scaled to the size of the micron image. It is noticed that the cartilage surface characterization of sub-micron level has limitations to describe the surface morphology condition; however, it is stated that at this scale, the cartilage surface is characterized according to the cartilage structure related to collagen fiber variation (Wen et al., 2012; Stacey et al., 2013).

Numerical parameters were used to identify specific features of the cartilage surface. At the sub-micron level, the changes in  $S_a$  between the OA grades were marginal (Table 6.1), indicating that this commonly used surface roughness parameter was unable to differ the OA grades at this resolution. Furthermore, none of the amplitude parameters were assessed to be significant enough in differentiating the OA conditions. Some of them could be used to reveal distinctive changes between a healthy cartilage surface and a diseased one (Wang et al., 2013). In the micron level, the functional and amplitude parameters were identified to be the most suitable to describe the evolutions of the surfaces from OA grade I to III. The results of the amplitude parameters, in particular,  $S_a$  and  $S_q$ , were consistent with the existing OA grading criteria based on visual inspections (Outerbridge and Dunlop, 1975). For example,  $S_a$  showed a clear increasing trend with OA progress. Furthermore, the functional parameter, namely,  $S_{dc10\_50}$ , was identified as

the most reliable parameter to describe the OA condition (see Figure 5.5) from 35 parameters, where the  $S_a$  is included.  $S_{dc10\_50}$  reveals the height differences of the curve between the 10% and 50% of the bearing area curve (ISO 4287, 1997) as is mentioned in section 7.2.2. The sub-micron level shows, according to Dr Wang (2014) results that the values of  $S_{fd}$  increased steadily from an early OA condition (grade I) to a late stage (OA grade III), revealing the complexity of the surface increased when OA conditions worsened.  $S_{tr37}$  describes the anisotropic property of the surface texture. Overall, the trend of the  $S_{tr37}$  values for OA grades I to III were decreasing, indicating that the surface texture became more directional (i.e., anisotropy) as OA conditions progressed. Both  $S_{fd}$  and  $S_{tr37}$  are spatial parameters (Wang, 2014).

#### **7.4 Limitations of this project and suggestion for future work**

Although the 3D images and data obtained in this project provide valuable and reliable information about the surface morphologies of diseased cartilage and the OA progression, more work needs to be carried out on this topic. During this project, it has been found that other areas of study that will improve the understanding of the cartilage degradation process caused by OA include:

*The assessment of the surface heterogeneity of advance and early OA stage, regarding to distribution and intensity, supported by measurements of mechanical properties.*

According to the qualitative characterizations, the surface becomes rougher and more heterogeneous with the OA grade increase (Figure 5.3). The heterogeneity might be associated to anisotropic properties of the cartilage structure. It also might be associated to structure degradation process, for example, the inappropriate performance of the

proteoglycan, suggesting that the degradation of the cartilage structure might not be homogeneously distributed through the cartilage but it may start in located spots randomly distributed in the cartilage on early OA stage. Since these spots might have irregularities in the proteoglycan performance, they could experience an increase of water content (Pearle et al., 2005) producing the swollen of the mentioned spots, which may be revealed in Figure 5.3(a and b).

*The assessment of the cartilage surface with a larger number of human cartilage samples to confirm the obtained results and achieve a deeper understanding about the cartilage degradation process.* In this project, the surface morphology of the studied samples was assessed by 35 numerical parameters implemented by the software, *SPIP*, used for the microscale image processing. The assessment of the cartilage surface with these parameters, allow identifying and correlate the surface morphology of diseased cartilage with the functional properties of the surface, explained by the  $S_{dc10\_50}$  parameter. Even when this parameter explains the OA progression in the evolution of bearing functional properties, there is not a clear description of the cartilage surface given by the feature parameters and need to be studied. For further studies, more human samples need to be collected with a complete histology information of the patient.

*Investigation of the influence of the sample conditions on the surface morphologies of diseased cartilage and the factors involved in the samples that promote the morphological change.* The statistical method employed in this project allows the assessment of two variables, OA grade and Sample condition. Although the selected parameter,  $S_{dc10\_50}$ , did not evidence a significant change of the surface morphology associate to the sample condition ( $P\text{-value}_{\text{Sample}} > 0.05$ ), most of the selected parameter that described a significant difference in the OA grade stage, evidenced a significant difference in the sample

condition ( $P\text{-value}_{\text{Sample}} < 0.05$ ), as can be seen in Table 5.1, however, it was interesting how the F-test value of the variable *Sample* decrease when the F-test value of the variable *OA grade* increase (Figure 5.4).

The assessment of the influence of the sample condition in the surface morphologies of diseased cartilage in this project opens the door to further studies in the correlation of the factors involved in the sample condition.

## **Chapter 8 Conclusions**

This project has developed the procedures for sample extraction and image acquisition of the surface morphologies of diseased human knee cartilage in a hydrate condition. Based on 3D surface images acquired using LSM technique, numerical characterizations were carried out on human knee cartilage affected by OA. These developments allowed to identify and quantify main features of the diseased cartilage that explain the OA progression. Detailed outcomes of this project are presented below.

### **8.1 Outcomes of sample extraction process**

Due to the biphasic composition of cartilage with around 70% w/w of liquid, the dehydration of these tissues during image acquisition required to be controlled, since it affects highly the surface morphology of the cartilage, introducing errors in the collected data.

In this project, the sample dehydration was studied, revealing the morphological changes in the cartilage surface due to dehydration. It was found that large samples with bone attached to the cartilage, reduce the susceptibility to dehydration during image acquisition with a more stable cartilage surface. This information was essential to identify the characteristics of the sample suitable for this project. Samples of 15 mm x 15 mm with bone attached to the cartilage were used in this study.

During the sample extraction process, it was noticed that the human knee parts supplied for sample extraction were small parts of bone covered with cartilage. Those conditions presented limitation for the sample extraction, due to the restrictions of fixation presented by the small human parts without affecting the cartilage integrity as can be seen in Figure 3.2. The fixing requirements are defined by the tool employed for the sample extraction.

After testing with different tools in the Lab, it was found that the electric oscillating saw can provide smooth cuts without affecting significantly the surrounded areas of the cartilage and with minimal requirements in the fixation, due to the operation conditions such as high frequency and small angle of oscillation. A safe work procedure (SWP) was realized for the sample extraction, which was approved by the graduate school of biomedical engineering (UNSW). The obtained samples by using this procedure were successfully employed in this project, facilitating the reliability of the image acquisition process.

## **8.2 Outcomes of the image acquisition process using LSM**

The LSM was selected to capture the diseased cartilage surface data owing to its high resolution short time required for image acquisition and low requirements for sample preparation. However, this technique was not equipped with a sample holder for biological samples. In order to avoid any change in the cartilage surface during the image acquisition, a sample holder was designed in this project, allowing the sample hydration and holding the sample with the cartilage surface parallel to the objective lens (see Figure 3.4). These conditions were highly important to obtain reliable information of the surface morphology, reflected in the analysis results.

## **8.3 Qualitative assessment of cartilage surface morphology**

The qualitative information obtained from the surface morphology of the studied diseased cartilages, was essential to identify the micron scaled evolution of specific characteristics of the surface morphology with the OA progression that would be used for the hypothesis statements, required for the experimental design and support the statistical analysis

results. For the qualitative assessment, large images at the micron scale were used. At least 12 micron images taken at 20X magnification objective lens were stitched to collect appropriate surface information for quantitative characterizations. It was found in this study that the 20X magnification objective lens was the suitable magnification for the cartilage surface characterization using the LSM technique, regarding to the qualitative and quantitative information supplied from the obtained images (see Figure 4.8). The large images of the cartilage surface produced by the stitching process, allowed to evidence important characteristics of the surface morphology such as the increase of peaks and valleys with the OA grades. It was noticed that the surface morphology becomes more heterogeneous with the severity of the OA condition and the surface morphology might be also affected by the sample conditions (See Figure 5.4).

The information obtained from the observations of the cartilage surfaces were essential to identify specific characteristics of the surface morphology, allowing to state the hypothesis of this project, which were required to define the experimental design, for example, the selected numerical parameter need to identify quantitatively the OA grade conditions with significant differences between the OA grade stages and this parameter must have the potential to describe the main feature of the surface morphology that explain the OA progression, which might be associated to the picks and/or valleys, according to the obtained surface information mentioned above.

The qualitative observation also suggests that the sample condition should be included as a variable in the experiment design, since the surface morphology might be affected by the clinical histology of the patient. With these hypotheses, the statistical analysis was realized and important outcomes were obtained that corroborate the information supplied by the qualitative characterization. The large images were highly important for the

characterization and it is the first time that stitched images are used for surface analysis of human cartilage samples.

#### **8.4 Quantitative assessment of cartilage surface morphology**

The quantitative assessment of the diseased cartilage surface was performed using 35 numerical parameters. The key parameter was selected using the statistical method, namely, *two-stage nested design*, based on the ANOVA model. Although this method is not widely used in the bio-engineering field, this method allows including the experimental design two variables (i.e., OA grade and Sample condition) according to the hypothesis defined in the qualitative characterization.

Functional parameter  $S_{dc10\_50}$  has been identified as the most reliable and effective descriptor. It reveals the evolution of the bearing areas of the cartilage surfaces with OA development. The change in the BAC described by  $S_{dc10\_50}$  correlates with the deterioration of the surface and OA conditions. The numerical results reported in this work have provided further insight in the functional property of the cartilage surfaces which may be related to the collagen structures, fibrillation and the mechanical properties for better understanding of the wear process of human cartilage.

It is believed that the surface morphology of samples is the result of the tribological conditions that each sample experienced, involving variables such as external behaviour, wear mechanisms and mechanical properties of the cartilage. The mechanical properties of cartilages are related to the structure, which is affected by clinical histology of patients, consequently, the surface morphology of each sample has the potential to reveal the main factors that influence in the cartilage degradation.

This is the first project that includes the human sample condition as a factor that affect the surface morphology of cartilages, revealing evidence of the potential influence of the sample condition with the surface morphology. This evidence might build the bridge between surface morphology of diseased cartilage and the main factors that are involved in the OA progression.

### **8.5 Cartilage surface assessment at micron and sub-micron level**

Numerical characterisations were conducted on the surfaces of diseased human cartilage samples at both the micro- and nano-metre scales. The surface characterizations in the sub-micron level have found that spatial changes regarding to the variation of collagen fibers at early OA grade can be revealed at this scale. In the micro-metre scale, changes to the surface roughness and functional properties of the surface were significant enough for OA condition assessment. With support of advanced imaging facilities in 3D and quantitative analysis techniques, the results reported in this project and Dr Wang's thesis (2014) have revealed the surface morphology evolutions of cartilage surfaces affected at three OA grades. Through the nano- to micro-metre surface characterisations, insights into the surface changes have been achieved.

The information supplied at the micro-scale can describe the main surface features that compose the surface morphology of diseased cartilage. At the sub-micron scale, different surface features are revealed, being more related to the cartilage structure change in terms of the collagen fiber variation.

Further investigations of relationships of changes in the nano-scaled surface textures and nano-mechanical properties are needed to assist in understanding the fundamental causes of OA.

## **8.6 Significance and benefits of this project**

The established experimental procedures for human cartilage extraction and preparation for 3D image acquisition in a hydrate mode and the surface characterisation techniques allow the quantitative studies of human cartilage samples described in this thesis. They also enable further studies to develop reliable, objective OA markers using numerical parameters.

This work also allows further investigations of the effects of other clinical factors such as gender, age and work-related issues on OA progress. Although these issues are outside of the scope of this project, they may influence the OA process and changes in the cartilage surface textures. Once sufficient human samples are available and grouped in different age or gender groups, the presented methods can be used to study their effects on the OA progress.

Better understandings of distinctive features of and changes in the surface morphologies in the OA process have been achieved by quantitatively characterising 3D images of diseased cartilage surface at a micro-scale and comparing the results with those at a nano-scale. This study reveals that more surface morphological changes have been observed at the micrometer scale than at the sub-micron level, indicating that surface texture based OA assessment should be carried out at this resolution.

## References

- AAOS, 2011, Total knee replacement, Orthoinfo.org, Resource Available: <http://orthoinfo.aaos.org/PDFs/A00389.pdf>
- ACCARDI, M. A., DINI, D. & CANN, P. M. 2011. Experimental and numerical investigation of the behaviour of articular cartilage under shear loading—Interstitial fluid pressurisation and lubrication mechanisms. *Tribology International*, 44, 565-578.
- AIGNER, T. 2003. Collagens—major component of the physiological cartilage matrix, major target of cartilage degeneration, major tool in cartilage repair. *Advanced Drug Delivery Reviews*, 55, 1569-1593.
- AKHTAR, S., POH, C. L. & KITNEY, R. I. 2007. An MRI derived articular cartilage visualization framework. *Osteoarthritis Cartilage*, 15, 1070-1085.
- ALEXOPOULOS, L. G., WILLIAMS, G. M., UPTON, M. L., SETTON, L. A. & GUILAK, F. 2005. Osteoarthritic changes in the biphasic mechanical properties of the chondrocyte pericellular matrix in articular cartilage. *J Biomech*, 38, 509-517.
- APPLEYARD R, BURKHARDT D, GHOSH P, READ R, CAKE M, SWAIN M. & MURRELL G. 2003. Topographical analysis of the structural, biochemical and dynamic biomechanical properties of cartilage in an ovine model of osteoarthritis. *Osteoarthritis Cartilage*.11. 65-77.
- ARNO, S., WALKER, P. S., BELL, C. P., KRASNOKUTSKY, S., SAMUELS, J., ABRAMSON, S. B., REGATTE, R. & RECHT, M. 2012. Relation between cartilage volume and meniscal contact in medial osteoarthritis of the knee. *Knee*, 19, 896-901.
- ARVIDSSON, A., SATER, B. A. & WENNERBERG, A. 2006. The role of functional parameters for topographical characterization of bone-anchored implants. *Clin Implant Dent Relat Res*, 8, 70-76.

- ATESHIAN, G. A. 2009. The role of interstitial fluid pressurization in articular cartilage lubrication. *J Biomech*, 42, 1163-1176.
- BARBATO, G., CARNEIRO, K., CUPPINI, D., GARNAES, J., GORI, G., HUGHES, G., JENSEN, C. P., JØRGENSEN, J. F., JUSKO O., LIVI, S., MCQUOID H., NIELSEN, L. PICOTTO, G. B. & WILKENING, G. 1995. Scanning tunneling microscopy methods for roughness and micro hardness measurements, Synthesis report for research contract with the European Union under its programme for applied metrology, 109 pages European Commission Catalogue number: CD-NA-16145 EN-C, Brussels Luxemburg.
- BASALO, I. M., RAJ, D., KRISHNAN, R., CHEN, F. H., HUNG, C. T. & ATESHIAN, G. A. 2005. Effects of enzymatic degradation on the frictional response of articular cartilage in stress relaxation. *J Biomech*, 38, 1343-1349.
- BASTIAANSEN-JENNISKENS, Y. M., KOEVOET, W., DE BART, A. C., VAN DER LINDEN, J. C., ZUURMOND, A. M., WEINANS, H., VERHAAR, J. A., VAN OSCH, G. J. & DEGROOT, J. 2008. Contribution of collagen network features to functional properties of engineered cartilage. *Osteoarthritis Cartilage*, 16, 359-366.
- BATISTA, M. A., NIA, H. T., ONNERFJORD, P., COX, K. A., ORTIZ, C., GRODZINSKY, A. J., HEINEGARD, D. & HAN, L. 2014. Nanomechanical phenotype of chondroadherin-null murine articular cartilage. *Matrix Biol.*
- BEI, Y. & FREGLY, B. J. 2004. Multibody dynamic simulation of knee contact mechanics. *Med Eng Phys*, 26, 777-789.
- BHARAT, B. 2000. Surface Roughness Analysis and Measurement Techniques. *Modern Tribology Handbook, Two Volume Set*. CRC Press.
- BLANC, J., GRIME, D. & BLATEYRON, F. 2011. Surface characterization based upon significant topographic features. *Journal of Physics: Conference Series*, 311, 1-6

- BLATEYRON, F. 2013. The Areal Field Parameters. In Leach, R (Ed) *Characterization of areal surface texture*, Belin Heidelberg, Springer, pp. 15-43
- BLUNT, L. & JIANG, X. 2003. 2 - Numerical Parameters for Characterisation of Topography. In: BLUNT, L. & JIANG, X. (eds.) *Advanced Techniques for Assessment Surface Topography*. Oxford: Kogan Page Science.
- BORGHI, A., GUALTIERI, E., MARCHETTO, D., MORETTI, L. & VALERI, S. 2008. Tribological effects of surface texturing on nitriding steel for high-performance engine applications. *Wear*, 265, 1046-1051.
- CHAN, S. M., NEU, C. P., DURAIN, G., KOMVOPOULOS, K. & REDDI, A. H. 2010. Atomic force microscope investigation of the boundary-lubricant layer in articular cartilage. *Osteoarthritis Cartilage*, 18, 956-963.
- CHAN, S. M., NEU, C. P., DURAIN, G., KOMVOPOULOS, K. & REDDI, A. H. 2012. Tribological altruism: A sacrificial layer mechanism of synovial joint lubrication in articular cartilage. *J Biomech*, 45, 2426-2431.
- CHANG, C. F., RAMASWAMY, G. & SERRA, R. 2012. Depletion of primary cilia in articular chondrocytes results in reduced Gli3 repressor to activator ratio, increased Hedgehog signaling, and symptoms of early osteoarthritis. *Osteoarthritis Cartilage*, 20, 152-161.
- CHANGOOR, A., NELEA, M., METHOT, S., TRAN-KHANH, N., CHEVRIER, A., RESTREPO, A., SHIVE, M. S., HOEMANN, C. D. & BUSCHMANN, M. D. 2011. Structural characteristics of the collagen network in human normal, degraded and repair articular cartilages observed in polarized light and scanning electron microscopies. *Osteoarthritis Cartilage*, 19, 1458-1468.
- CHEN, J., MOSCHAKIS, T. & PUGNALONI, L. A. 2006. Surface topography of heat-set whey protein gels by confocal laser scanning microscopy. *Food Hydrocolloids*, 20, 468-474.

- CHIN, H. C., KHAYAT, G. & QUINN, T. M. 2011. Improved characterization of cartilage mechanical properties using a combination of stress relaxation and creep. *J Biomech*, 44, 198-201.
- CLAASSEN, H., SCHICHT, M. & PAULSEN, F. 2011. Impact of sex hormones, insulin, growth factors and peptides on cartilage health and disease. *Prog Histochem Cytochem*, 45, 239-293.
- COLES, J.M., BLUM, J.J., JAY, G.D., DARLING, E.M., GUILAK, F. & ZAUSCHER, S. 2008. In situ friction measurement on murine cartilage by atomic force microscopy. *J Biomech.*; 41 541-548.
- COLES, J. M., CHANG, D. P. & ZAUSCHER, S. 2010. Molecular mechanisms of aqueous boundary lubrication by mucinous glycoproteins. *Current Opinion in Colloid & Interface Science*, 15, 406-416.
- COOK, C., PIETROBON, R. & HEGEDUS, E. 2007. Osteoarthritis and the impact on quality of life health indicators. *Rheumatol Int*, 27, 315-21.
- COUPE, V. M., VEENHOF, C., VAN TULDER, M. W., DEKKER, J., BIJLSMA, J. W. & VAN DEN ENDE, C. H. 2007. The cost effectiveness of behavioural graded activity in patients with osteoarthritis of hip and/or knee. *Ann Rheum Dis*, 66, 215-221.
- DESROCHERS, J., AMREIN, M. W. & MATYAS, J. R. 2013. Microscale surface friction of articular cartilage in early osteoarthritis. *J Mech Behav Biomed Mater*, 25, 11-22.
- DOWSON D. & JIN Z.M. 1986. Micro-elastohydrodynamic lubrication of synovial joints, *Eng. Med.*, 15, 63-68.
- DZIEDZIC, K., THOMAS, E., HILL, S., WILKIE, R., PEAT, G. & CROFT, P. R. 2007. The impact of musculoskeletal hand problems in older adults: findings from the North Staffordshire Osteoarthritis Project (NorStOP). *Rheumatology (Oxford)*, 46, 963-467.

- ECKSTEIN, F., CICUTTINI, F., RAYNAULD, J. P., WATERTON, J. C. & PETERFY, C. 2006. Magnetic resonance imaging (MRI) of articular cartilage in knee osteoarthritis (OA): morphological assessment. *Osteoarthritis Cartilage*, 14, 46-75.
- EVANS, A. A. & DONAHUE, R. E. 2008. Laser scanning confocal microscopy: a potential technique for the study of lithic microwear. *Journal of Archaeological Science*, 35, 2223-2230.
- EWING, J. 1990. Articular cartilage and knee joint function. Basic science and Arthroscopy. Akron, Ohio: Raven Press.
- FELSON, D.T., LAWRENCE, R.C., DIEPPE, P.A., HIRSCH, R., JORDAN, J.M. & KINGTON, R.S. 2000. Osteoarthritis: new insights. Part 1: the disease and its risk factors. *Annals of Internal Medicine*, 133, 635-646.
- FISHER, J., INGHAM, E., JIN, Z. M., PAWASKAR, S. S. & KATTA, J. 2007. Effect of load variation on the friction properties of articular cartilage. *Proceedings of the Institution of Mechanical Engineers, Part J: Journal of Engineering Tribology*, 221, 175-181.
- FOCHT, B. C., REJESKI, W. J., AMBROSIUS, W. T., KATULA, J. A. & MESSIER, S. P. 2005. Exercise, self-efficacy, and mobility performance in overweight and obese older adults with knee osteoarthritis. *Arthritis Rheum*, 53, 659-665.
- FÖLDES-PAPP, Z., DEMEL, U. & TILZ, G. P. 2003. Laser scanning confocal fluorescence microscopy: an overview. *International Immunopharmacology*, 3, 1715-1729.
- FROIMSON M.I., RATCLIFFE, A. T.R. GARDNER, MOW, V.C. 1997. Differences in patellofemoral joint cartilage material properties and their significance to the etiology of cartilage surface fibrillation, *Osteoarthritis and cartilage*, 5, 377-386

- FORSTER, H. & FISHER, J. 1999. The influence of continuous sliding and subsequent surface wear on the friction of articular cartilage. *Proceedings of the Institution of Mechanical Engineers, Part H: Journal of Engineering in Medicine*, 213, 329-345.
- GANNON, A. R., NAGEL, T. & KELLY, D. J. 2012. The role of the superficial region in determining the dynamic properties of articular cartilage. *Osteoarthritis Cartilage*, 20, 1417-1425.
- GHOSH, S., BOWEN, J., JIANG, K., ESPINO, D. M. & SHEPHERD, D. E. 2012. Investigation of techniques for the measurement of articular cartilage surface roughness. *Micron*, 44, 179-184.
- GILES, W. & KLIPPEL, J.H., 2010. A National Public Health Agenda for Osteoarthritis. Centers for Disease Control and Prevention. Available from <http://www.cdc.gov/arthritis/docs/oaagenda.pdf>.
- GRAINDORGE, S.& STACHOWIAK, G. 2000, Changes occurring in the surface morphology of articular cartilage during wear, Department of Mechanical and Materials Engineering, University of Western Australia, *Wear* 241 (2000). 143–150.
- GRAINDORGE S., FERRANDEZ W., Z. JIN, INGHAM E., GRANT C., TWIGG P., FISHER J. 2005. Biphasic surface amorphous layer lubrication of articular cartilage. *Medical Engineering & Physics*, 27, 836–844.
- GRELLMANN, W., BERGHAUS, A., HABERLAND, E. J., JAMALI, Y., HOLWEG, K., REINCKE, K. & BIEROGEL, C. 2006. Determination of strength and deformation behavior of human cartilage for the definition of significant parameters. *J Biomed Mater Res A*, 78, 168-174.
- HAN, L., GRODZINSKY, A. J. & ORTIZ, C. 2011. Nanomechanics of the Cartilage Extracellular Matrix. *Annu Rev Mater Res*, 41, 133-168.

- HAYES, A., HARRIS, B., DIEPPE, P. A. & CLIFT, S. E. 1993. Wear of articular cartilage: the effect of crystals. *ARCHIVE: Proceedings of the Institution of Mechanical Engineers, Part H: Journal of Engineering in Medicine 1989-1996 (vols 203-210)*, 207, 41-58.
- IMAGE METROLOGY, SPIP classic roughness parameters for images, *available from* [http://www.imagemet.com/WebHelp6/Default.htm#RoughnessParameters/Roughness\\_Parameters.htm#Roughness\\_Average](http://www.imagemet.com/WebHelp6/Default.htm#RoughnessParameters/Roughness_Parameters.htm#Roughness_Average) [27 February 2013].
- ISO 11562. 1996. Geometrical Product Specifications (GPS) – Surface Texture: Profile Method -- Metrological Characteristics of Phase Correct Filters, International Organization for Standardization, Geneva.
- ISO 25178-2. 2012. Geometrical Product Specification (GPS) – Surface Texture: Areal – Part 2. Terms, Definitions and Surface Texture Parameters.
- ISO 4287. 1997. Geometrical Product Specifications (GPS) - Surface texture: Profile method - Terms, definitions and surface texture parameters, International Organization for Standardization.
- ISO 4288. 1996. Geometrical product specifications (GPS) – Surface texture: profile method-Rules and procedures for the assessment of surface texture.
- JONES, C. W., SMOLINSKI, D., KEOGH, A., KIRK, T. B. & ZHENG, M. H. 2005. Confocal laser scanning microscopy in orthopaedic research. *Progress in Histochemistry and Cytochemistry*, 40, 1-71.
- JULKUNEN, P., KIVIRANTA, P., WILSON, W., JURVELIN, J. S. & KORHONEN, R. K. 2007. Characterization of articular cartilage by combining microscopic analysis with a fibril-reinforced finite-element model. *J Biomech*, 40, 1862-1870.
- JULKUNEN, P., KORHONEN, R. K., HERZOG, W. & JURVELIN, J. S. 2008. Uncertainties in indentation testing of articular cartilage: a fibril-reinforced poroviscoelastic study. *Med Eng Phys*, 30, 506-515.

- KALEVA, E., SAARAKKALA, S., JURVELIN, J. S., VIREN, T. & TOYRAS, J. 2009. Effects of ultrasound beam angle and surface roughness on the quantitative ultrasound parameters of articular cartilage. *Ultrasound Med Biol*, 35, 1344-1351.
- KALEVA, E., SAARAKKALA, S., TOYRAS, J., NIEMINEN, H. J. & JURVELIN, J. S. 2008. In-vitro comparison of time-domain, frequency-domain and wavelet ultrasound parameters in diagnostics of cartilage degeneration. *Ultrasound Med Biol*, 34, 155-159.
- KATTA, J., JIN, Z., INGHAM, E. & FISHER, J. 2008. Biotribology of articular cartilage -a review of the recent advances. *Med Eng Phys*, 30, 1349-1363.
- KATTA, J., JIN, Z., INGHAM, E. & FISHER, J. 2009. Effect of nominal stress on the long term friction, deformation and wear of native and glycosaminoglycan deficient articular cartilage. *Osteoarthritis Cartilage*, 17, 662-668.
- KAZEMI, M., LI, L. P., SAVARD, P. & BUSCHMANN, M. D. 2011. Creep behavior of the intact and meniscectomy knee joints. *J Mech Behav Biomed Mater*, 4, 1351-1358.
- KERIN, A. J., COLEMAN, A., WISNOM, M. R. & ADAMS, M. A. 2003. Propagation of surface fissures in articular cartilage in response to cyclic loading in vitro. *Clinical Biomechanics*, 18, 960-968.
- KEYENCE. 2014. 3D Laser Scanning Microscope, VK-100/X200 Series, Kenyence corporation, Available from [http://www.keyence.com/products/microscope/laser-microscope/vk-x100\\_x200/](http://www.keyence.com/products/microscope/laser-microscope/vk-x100_x200/).
- KISS, R. M. 2011. Effect of severity of knee osteoarthritis on the variability of gait parameters. *J Electromyogr Kinesiol*, 21, 695-703.
- KIVIRANTA, P., LAMMENTAUSTA, E., TOYRAS, J., KIVIRANTA, I. & JURVELIN, J. S. 2008. Indentation diagnostics of cartilage degeneration. *Osteoarthritis Cartilage*, 16, 796-804.

- KLEEMANN, R. U., KROCKER, D., CEDRARO, A., TUISCHER, J. & DUDA, G. N. 2005. Altered cartilage mechanics and histology in knee osteoarthritis: relation to clinical assessment (ICRS Grade). *Osteoarthritis Cartilage*, 13, 958-963.
- KLIGERMAN, Y., ETSION, I. & SHINKARENKO, A. 2005. Improving Tribological Performance of Piston Rings by Partial Surface Texturing. *Journal of Tribology*, 127, 632-638
- KNUDSON, C. B. & KNUDSON, W. 2001. Cartilage proteoglycans. *Semin Cell Dev Biol*, 12, 69-78.
- KORHONEN, R. K. & JURVELIN, J. S. 2010. Compressive and tensile properties of articular cartilage in axial loading are modulated differently by osmotic environment. *Med Eng Phys*, 32, 155-160.
- KOWALSKI, R., FISHER, J. & NORTHWOOD, E. 2007. Investigation of the friction and surface degradation of innovative chondroplasty materials against articular cartilage. *Proceedings of the Institution of Mechanical Engineers, Part H: Journal of Engineering in Medicine*, 221, 263-279.
- LAASANEN, M. S., SAARAKKALA, S., TÖYRÄS, J., HIRVONEN, J., RIEPPO, J., KORHONEN, R. K. & JURVELIN, J. S. 2003. Ultrasound indentation of bovine knee articular cartilage in situ. *Journal of Biomechanics*, 36, 1259-1267.
- LANG, P., NOORBAKHSH, F., YOSHIOKA, H. 2005. MR Imaging of Articular Cartilage: current state and recent developments. *Radiol Clin Am*. 43, 629-639.
- LEACH, R. K. 2010. CHAPTER 6 - Surface topography measurement instrumentation. *In: LEACH, R. K. (ed.) Fundamental Principles of Engineering Nanometrology*. Oxford: William Andrew Publishing.
- LI, L., PATIL, S., STEKLOV, N., BAE, W., TEMPLE-WONG, M., D'LIMA, D. D., SAH, R. L. & FREGLY, B. J. 2011. Computational wear simulation of patellofemoral articular cartilage during in vitro testing. *J Biomech*, 44, 1507-1513.

- LIPSHITZ, H., ETHEREDGE, R. & GLIMCHER, M. 1975. In vitro wear of articular cartilage. *J Bone Joint Surg Am*;57, 527–534.
- LOPES, J. L., MACHADO, J. M., CASTANHEIRA, L., GRANJA, P. L., GAMA, F. M., DOURADO, F. & GOMES, J. R. 2011. Friction and wear behaviour of bacterial cellulose against articular cartilage. *Wear*, 271, 2328-2333.
- LORENZ, H. & RICHTER, W. 2006. Osteoarthritis: cellular and molecular changes in degenerating cartilage. *Prog Histochem Cytochem*, 40, 135-63.
- MAHOVIC POLJACEK, S., RISOVIC, D., FURIC, K. & GOJO, M. 2008. Comparison of fractal and profilometric methods for surface topography characterization. *Applied Surface Science*, 254, 3449-3458.
- MAINIL-VARLET, P., AIGNER, T., BRITTBERG, M., BULLOUGH, P., HOLLANDER, A., HUNZIKER, E., KANDEL, R., NEHRER, S., PRITZKER, K., ROBERTS, S. & STAUFFER, E. 2003. Histological assessment of cartilage repair: a report by the Histology Endpoint Committee of the International Cartilage Repair Society (ICRS). *J Bone Joint Surg Am*, 85-A Suppl 2, 45-57.
- MAKELA, J. T., HUTTU, M. R. & KORHONEN, R. K. 2012. Structure-function relationships in osteoarthritic human hip joint articular cartilage. *Osteoarthritis Cartilage*, 20, 1268-1277.
- MARCH, L.M., BAGGA, H. 2004. Epidemiology of osteoarthritis in Australia, The Medical Journal of Australia, 180, 6-10.
- MARTEL-PELLETIER, J., BOILEAU, C., PELLETIER, J. P. & ROUGHLEY, P. J. 2008. Cartilage in normal and osteoarthritis conditions. *Best Pract Res Clin Rheumatol*, 22, 351-384.
- MCCANN, L., UDOFIA, I., GRAINDORGE, S., INGHAM, E., JIN, Z. & FISHER, J. 2008. Tribological testing of articular cartilage of the medial compartment of the knee using a friction simulator. *Tribology International*, 41, 1126-1133.

- MCNALLY, H. A., RAJWA, B., STURGIS, J. & ROBINSON, J. P. 2005. Comparative three-dimensional imaging of living neurons with confocal and atomic force microscopy. *J Neurosci Methods*, 142, 177-84.
- MCNARY, S. M., ATHANASIOU, K. A. & REDDI, A. H. 2012. Engineering lubrication in articular cartilage. *Tissue Eng Part B Rev*, 18, 88-100.
- MILLER, G. J. & MORGAN, E. F. 2010. Use of microindentation to characterize the mechanical properties of articular cartilage: comparison of biphasic material properties across length scales. *Osteoarthritis Cartilage*, 18, 1051-1057.
- MONTGOMERY, D. C. 2003. Design and Analysis of Experiments, Sixth Edition, John Wiley and Son. Hoboken, New Jersey.
- MONTGOMERY, D.C., PECK, E.A. & VINING, G.G. 2006. Introduction to Linear Regression Analysis, fourth edition John Wiley & Sons, Hoboken, New Jersey.
- MONTGOMERY, D. C., RUNGER, G. C. & HUBELE N. F. 2011. Engineering Statistics, Fifth Edition, John Wiley and Son. Hoboken, New Jersey.
- MOORE, D. 2014. Articular cartilage, Orthobullets, Available from <http://www.orthobullets.com/basic-science/9017/articular-cartilage> [18 May 2014].
- MOW, V. & ATESHIAN, G. 1997. Friction, lubrication and wear of diarthrodial joints, Basic orthopaedic biomechanics. New York: Raven Press; 1997.
- NAKA, M. H., HATTORI, K., OHASHI, T. & IKEUCHI, K. 2005. Evaluation of the effect of collagen network degradation on the frictional characteristics of articular cartilage using a simultaneous analysis of the contact condition. *Clin Biomech (Bristol, Avon)*, 20, 1111-1118.
- NEU, C., KOMVOPOULOS, K. & REDDI, A. 2008. The interface of functional biotribology and regenerative medicine in synovial joints. *Tissue Eng Part B Rev* 14, 235, 238

- NOBLE, P., COLLIN, B., LECOMTE-BECKERS, J., MAGNEE, A., DENOIX, J. M. & SERTEYN, D. 2010. An equine joint friction test model using a cartilage-on-cartilage arrangement. *Vet J*, 183, 148-152.
- OUTERBRIDGE R, 1961, The etiology of chondromalacia patellae. *J Bone Joint Surg Br*; 43, 752-757.
- PARK, S., COSTA, K. D. & ATESHIAN, G. A. 2004. Microscale frictional response of bovine articular cartilage from atomic force microscopy. *J Biomech*, 37, 1679-1687.
- PEACH, C. A., CARR, A. J. & LOUGHLIN, J. 2005. Recent advances in the genetic investigation of osteoarthritis. *Trends Mol Med*, 11, 186-191.
- PEARLE, A. D., WARREN, R. F. & RODEO, S. A. 2005. Basic science of articular cartilage and osteoarthritis. *Clin Sports Med*, 24, 1-12.
- PEÑA, E., PÉREZ DEL PALOMAR, A., CALVO, B., MARTÍNEZ, M. A. & DOBLARÉ, M. 2007. Computational Modelling of Diarthrodial Joints. Physiological, Pathological and Pos-Surgery Simulations. *Archives of Computational Methods in Engineering*, 14, 47-91.
- PENG, Z. 2007. Osteoarthritis diagnosis using wear particle analysis technique: Investigation of correlation between particle and cartilage surface in walking process. *Wear*, 262, 630-640.
- SAARAKKALA, S., TOYRAS, J., HIRVONEN, J., LAASANEN, M. S., LAPPALAINEN, R. & JURVELIN, J. S. 2004. Ultrasonic quantitation of superficial degradation of articular cartilage. *Ultrasound Med Biol*, 30, 783-792.
- SCHERGE, M. & GORB, S. Biological Micro- and Nanotribology: Nature's Solutions. Germany: *Springer-Verlag Berlin Heidelberg*, 2001.
- SCHMIDT, T. A. & SAH, R. L. 2007. Effect of synovial fluid on boundary lubrication of articular cartilage. *Osteoarthritis Cartilage*, 15, 35-47.

- SCHUMACHER, L., BLOCK, J., SCHMID, T., AYDELOTTE, M. & KUETTNER, K. 1994, A novel proteoglycan synthesized and secreted by chondrocytes of the superficial zone of articular cartilage. *Arch Biochem Biophys*, 311, 144–152.
- SCOTT, P. J. 2003. 3 - Novel Areal Characterisation Techniques. In: LIAM, B. & XIANGQIAN, J. (eds.) *Advanced Techniques for Assessment Surface Topography*. Oxford: Kogan Page Science.
- SCOTT, P. J. 2004. Pattern analysis and metrology: the extraction of stable features from observable measurements. *Proceedings of the Royal Society A: Mathematical, Physical and Engineering Sciences*, 460, 2845-2864.
- SCOTT, P. J. 2009. Feature parameters. *Wear*, 266, 548-551.
- SEDLAČEK, M., PODGORNIK, B. & VIŽINTIN, J. 2012. Correlation between standard roughness parameters skewness and kurtosis and tribological behaviour of contact surfaces. *Tribology International*, 48, 102-112.
- SHEKHAWAT, V. K., LAURENT, M. P., MUEHLEMAN, C. & WIMMER, M. A. 2009. Surface topography of viable articular cartilage measured with scanning white light interferometry. *Osteoarthritis Cartilage*, 17, 1197-1203.
- SHIRAZI, R. & SHIRAZI-ADL, A. 2009a. Analysis of partial meniscectomy and ACL reconstruction in knee joint biomechanics under a combined loading. *Clin Biomech (Bristol, Avon)*, 24, 755-761.
- SHIRAZI, R. & SHIRAZI-ADL, A. 2009b. Computational biomechanics of articular cartilage of human knee joint: effect of osteochondral defects. *J Biomech*, 42, 2458-2465.
- SILVER, F. H., BRADICA, G. & TRIA, A. 2004. Do changes in the mechanical properties of articular cartilage promote catabolic destruction of cartilage and osteoarthritis? *Matrix Biol*, 23, 467-476.

- SOPENA JUNCOSA, J.J., CARRILLO POVEDA J.M., RUBIO ZARAGOZA M., REDONDO GARCÍA J. I., SERRA AGUADO I. & SOLERI CANET I. 2000. Estructura y función del cartilago articular. *Portada: Armas Frente a la Patología Articular*. 24-26.
- SOPHIA FOX, A. J., BEDI, A. & RODEO, S. A. 2009. The basic science of articular cartilage: structure, composition, and function. *Sports Health*, 1, 461-468.
- STACEY, M., DUTTA, D., CAO, W., ASMAR, A., ELSAYED-ALI, H., KELLY, R., JR. & BESKOK, A. 2013. Atomic force microscopy characterization of collagen 'nanostraws' in human costal cartilage. *Micron*, 44, 483-487.
- STENHAMRE, H., SLYNARSKI, K., PETREN, C., TALLHEDEN, T. & LINDAHL, A. 2008. Topographic variation in redifferentiation capacity of chondrocytes in the adult human knee joint. *Osteoarthritis Cartilage*, 16, 1356-1362.
- STOLZ, M., GOTTARDI, R., RAITERI, R., MIOT, S., MARTIN, I., IMER, R., STAUFER, U., RADUCANU, A., DUGGELIN, M., BASCHONG, W., DANIELS, A. U., FRIEDERICH, N. F., ASZODI, A. & AEBI, U. 2009. Early detection of aging cartilage and osteoarthritis in mice and patient samples using atomic force microscopy. *Nature nanotechnology*, 4, 186-192.
- STOUT, K. J., SULLIVAN, P. J., DONG, W. P. MAINSAH, E., LUO, N., MATHIA, T. & ZAHOUANI, H. 1994. The development of methods for the characterization of roughness on three dimensions. Publication no. EUR 15178 EN of the Commission of the European Communities, Luxembourg.
- SUN, Y. 2013. Sliding wear behaviour of surface mechanical attrition treated AISI 304 stainless steel. *Tribology International*, 57, 67-75.
- SUZUKI, E. 2002. "High-resolution scanning electron microscopy of immunogold-labelled cells by the use of thin plasma coating of osmium". *Journal of Microscopy* 208, 153–157.

- SWANN, D., SILVER, F., SLAYTER, H., STAFFORD, W. & SHORE, E. 1985, The molecular structure and lubricating activity of lubricin isolated from bovine and human synovial fluids. *Biochem J*, 225, 195–201.
- TEMPLE-WONG, M. M., BAE, W. C., CHEN, M. Q., BUGBEE, W. D., AMIEL, D., COUTTS, R. D., LOTZ, M. & SAH, R. L. 2009. Biomechanical, structural, and biochemical indices of degenerative and osteoarthritic deterioration of adult human articular cartilage of the femoral condyle. *Osteoarthritis Cartilage*, 17, 1469-1476.
- TEMPLE, M. M., BAE, W. C., CHEN, M. Q., LOTZ, M., AMIEL, D., COUTTS, R. D. & SAH, R. L. 2007. Age- and site-associated biomechanical weakening of human articular cartilage of the femoral condyle. *Osteoarthritis Cartilage*, 15, 1042-1052.
- THAMBYAH, A., NATHER, A. & GOH, J. 2006. Mechanical properties of articular cartilage covered by the meniscus. *Osteoarthritis Cartilage*, 14, 580-588.
- TIAN, Y., WANG, J., PENG, Z. & JIANG, X. 2011. Numerical analysis of cartilage surfaces for osteoarthritis diagnosis using field and feature parameters. *Wear*, 271, 2370-2378.
- TIAN, Y., WANG, J., PENG, Z. & JIANG, X. 2012. A new approach to numerical characterisation of wear particle surfaces in three-dimensions for wear study. *Wear*, 282-283, 59-68.
- TUMMALA, S., BAY-JENSEN, A. C., KARSDAL, M. A. & DAM, E. B. 2010. Diagnosis of Osteoarthritis by Cartilage Surface Smoothness Quantified Automatically from Knee MRI. *Cartilage*, 2, 50-59.
- VALDES, A. M. & SPECTOR, T. D. 2010. The clinical relevance of genetic susceptibility to osteoarthritis. *Best Pract Res Clin Rheumatol*, 24, 3-14.

- VAN DER KRAAN, P. M. & VAN DEN BERG, W. B. 2008. Osteoarthritis in the context of ageing and evolution. Loss of chondrocyte differentiation block during ageing. *Ageing Res Rev*, 7, 106-113.
- VAN DER KRAAN, P. M. & VAN DEN BERG, W. B. 2012. Chondrocyte hypertrophy and osteoarthritis: role in initiation and progression of cartilage degeneration? *Osteoarthritis Cartilage*, 20, 223-232.
- VAN MEURS, J. B. & UITTERLINDEN, A. G. 2012. Osteoarthritis year 2012 in review: genetics and genomics. *Osteoarthritis Cartilage*, 20, 1470-1476.
- VERTERAMO, A. & SEEDHOM, B. B. 2007. Effect of a single impact loading on the structure and mechanical properties of articular cartilage. *J Biomech*, 40, 3580-9.
- WANG, F., YING, Z., DUAN, X., TAN, H., YANG, B., GUO, L., CHEN, G., DAI, G., MA, Z. & YANG, L. 2009. Histomorphometric analysis of adult articular calcified cartilage zone. *J Struct Biol*, 168, 359-65.
- WANG, M. 2014. Development of advanced wear debris analysis techniques for osteoarthritis study. Ph.D thesis, University of New South Wales, Australia.
- WANG, M., PENG Z., WATSON, J.A., WATSON, G.S. & YIN, L. 2012. Nanoscale study of cartilage surfaces using atomic force microscopy, *Journal of Engineering in Medicine*, 226, 899-910.
- WANG, M., PENG, Z., WANG, J. & JIANG, X. 2012. Wear characterisation of articular cartilage surfaces at a nano-scale using atomic force microscopy, *Tribological International*. 63, 1-10.
- WANG, Y., LIU, H., GAO, L., XU, B. & ZHANG, C. 2011. Test the Mechanical Properties of Articular Cartilage using Digital Image Correlation Technology. *Procedia Environmental Sciences*, 8, 191-196.
- WEIDOW, J., PARK, J., KARRHOLM, J 2002. Different patterns of cartilage wear in medial and lateral gonarthrosis. *Acta Orthop Scand*, 73, 326-329.


- WEN, C. Y., WU, C. B., TANG, B., WANG, T., YAN, C. H., LU, W. W., PAN, H., HU, Y. & CHIU, K. Y. 2012. Collagen fibril stiffening in osteoarthritic cartilage of human beings revealed by atomic force microscopy. *Osteoarthritis Cartilage*, 20, 916-922.
- WILLIAMS, G. M., CHAN, E. F., TEMPLE-WONG, M. M., BAE, W. C., MASUDA, K., BUGBEE, W. D. & SAH, R. L. 2010. Shape, loading, and motion in the bioengineering design, fabrication, and testing of personalized synovial joints. *J Biomech*, 43, 156-165.
- WILSON, W., VAN DONKELAAR, C. C., VAN RIETBERGEN, R. & HUISKES, R. 2005. The role of computational models in the search for the mechanical behavior and damage mechanisms of articular cartilage. *Med Eng Phys*, 27, 810-826.
- WIRTH, W., LARROQUE, S., DAVIES, R. Y., NEVITT, M., GIMONA, A., BARIBAUD, F., LEE, J. H., BENICHO, O., WYMAN, B. T., HUDELMAIER, M., MASCHEK, S., ECKSTEIN, F. & GROUP, O. A. I. I. 2011. Comparison of 1-year vs 2-year change in regional cartilage thickness in osteoarthritis results from 346 participants from the Osteoarthritis Initiative. *Osteoarthritis Cartilage*, 19, 74-83.
- WLUKA, A. E., STUCKEY, S., SNADDON, J. & CICUTTINI, F. M. 2002. The determinants of change in tibial cartilage volume in osteoarthritic knees. *Arthritis Rheum*, 46, 2065-2072.
- WONG, B. L., KIM, S. H., ANTONACCI, J. M., MCILWRAITH, C. W. & SAH, R. L. 2010. Cartilage shear dynamics during tibio-femoral articulation: effect of acute joint injury and tribosupplementation on synovial fluid lubrication. *Osteoarthritis Cartilage*, 18, 464-71.
- YEH, A. T., HAMMER-WILSON, M. J., VAN SICKLE, D. C., BENTON, H. P., ZOUMI, A., TROMBERG, B. J. & PEAVY, G. M. 2005. Nonlinear optical microscopy of articular cartilage. *Osteoarthritis Cartilage*, 13, 345-352.

- YOSHIMURA, N., MURAKI, S., OKA, H., TANAKA, S., KAWAGUCHI, H., NAKAMURA, K. & AKUNE, T. 2012. Accumulation of metabolic risk factors such as overweight, hypertension, dyslipidaemia, and impaired glucose tolerance raises the risk of occurrence and progression of knee osteoarthritis: a 3-year follow-up of the ROAD study. *Osteoarthritis Cartilage*, 20, 1217-1226.
- ZEHBE, R., RIESEMEIER, H., KIRKPATRICK, C. J. & BROCHHAUSEN, C. 2012. Imaging of articular cartilage--data matching using X-ray tomography, SEM, FIB slicing and conventional histology. *Micron*, 43, 1060-1067.
- ZHU, H., GE, S., HUANG, X., ZHANG, D. & LIU, J. 2003. Experimental study on the characterization of worn surface topography with characteristic roughness parameter. *Wear*, 255, 309-314.
- ZILKENS, C., MIESE, F., JAGER, M., BITTERSOHL, B. & KRAUSPE, R. 2011. Magnetic resonance imaging of hip joint cartilage and labrum. *Orthop Rev*, 3, 34-41.

## Appendices

### Appendix A. Safe work procedure (SWP)

#### A.1 SWP for Sample extraction from human knee parts

OHS026  Safe work procedure	1. Completed by: <b>Juan Carlos Baena Vargas</b> Staff/Student number: <b>z339900</b>	 <b>UNSW</b> THE UNIVERSITY OF NEW SOUTH WALES

The [Writing Safe Work Procedures Guideline \(OHS027\)](#) should be consulted to assist in the completion of this form

Faculty/Division: <b>Engineering</b>		School/Unit: <b>GSBME</b>		
Document number	Initial Issue date	Current version	Current Version Issue date	Next review date

#### A.1.2 Safe work procedure title and basic description of activity

**Title:** CARTILAGE SAMPLE EXTRACTION FROM PARTS OF HUMAN KNEE, USING AN ELECTRIC OSCILLATING SAW

*Description of activity:- Extraction of samples from human knee parts. Implementing an electric oscillating saw.*

*The risk is the infection due to the human origin. The controls are training and wear personal protective equipment. Then other controls are PC 2 work practice.*

#### A.1.3 List Hazards and risk controls as per risk assessment

Task	Hazards	Controls
Using Electric saw	<ul style="list-style-type: none"><li>Electric short</li><li>Noise produced by the electric saw</li><li>Spreading of cartilage or bone particle around, during extraction</li></ul>	<ul style="list-style-type: none"><li>Being aware of leaking or wetting surfaces that may get contact with the electric connection. Ensure all leads and connections are undamaged and the device is tagged and tested. Ensure all leads are clear of the cutting blade</li><li>Wearing hearing protection and work in isolated areas or room with closed door to protect others</li></ul>

	<ul style="list-style-type: none"> <li>Cuts from the saw blade</li> </ul>	<ul style="list-style-type: none"> <li>Using a hood or cabinet to remain the particles into the hood area. Use disposable matting to retain as much particulate as possible</li> <li>Keep hands away from the blade. Clamp material where possible. First aid procedures</li> </ul>
Manipulating human samples	<ul style="list-style-type: none"> <li>Human disease</li> </ul>	<ul style="list-style-type: none"> <li>Follow PC2 work practices to reduce exposure. Contain work in a Class II biosafety cabinet. Wearing personal protective clothing. Immunisation –hep B</li> </ul>

#### A.1.3.1 Pathways for infections and control

Pathway	Hazard	Control
Sharps injuries	wounds caused by the electric saw's blade	<p><b>Minimize:</b> To Avoid handling the sample directly, using any device such as a clamp or vice</p> <p><b>Personal protective equipment:</b> two pairs of gloves, green gown and immunization.</p> <p><b>Ergonomic position:</b> Comfort during any procedure with tools involved is required to give confidence to the operator, reducing risk of injuries</p>
Generation of particles	<ul style="list-style-type: none"> <li>Ingestion</li> <li>Inhalation</li> </ul>	<p><b>Personal protective equipment:</b> eye protection, mask, immunization, hood</p>

#### A.1.4 List resources required including personal protective clothing, chemicals and equipment needed

Electric oscillating saw, petridish, clamp, paper tissues, dark green gown, gloves, PBS, Virkon, 80% Ethanol, PC hood, eye protection, mask, hear protection.

#### A.1.5 List step by step instructions or order for undertaking the task

The biological materials used in this project come from human knee joint parts that have been collected during two years for the University of James Cook (Queensland). These parts come from patients of older age that required an artificial knee joint implant. Because of the history of these joint parts, it is state that these biological samples represent a low risk of contamination.

The human cartilage will be transported to the PC2 Lab in small containers which will be introduced into a cooler to maintain the cartilage temperature around 5°C.

The human cartilage where the samples will come from, do not present a significant impediment for the requested equipment and also for the extraction procedure, which consist in the next steps.

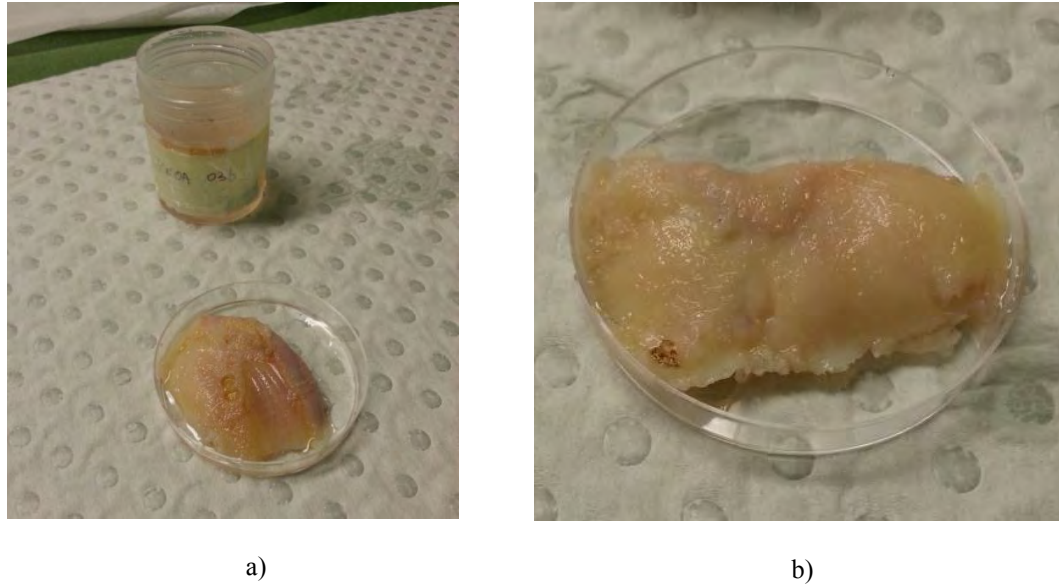


Figure A.1.1 Human knee parts obtained for sample extraction, a) Human knee cartilage and its container, b) Human knee cartilage into a 6 cm petridish.

### 1. Preparation of the work area.

To clean up the surface inside the hood before the extraction, avoiding any kind of contamination to the cartilage. After that, a sterile cloth will be used to protect the work area, especially, the surface of the hood during the sample extraction.

### 2. Setting up the electric saw

- Place the blade properly in the tool with the tool's cord unplugged
- Make sure the blade is tight to the saw
- Plug in the tool with the switch off
- Before use the tool on the sample extraction, make sure to be comfortable and safe.

### 3. Sample extraction.

The human cartilage will be located on a chopping board underneath the sterile cloth cover, which go into the hood already prepared for this purpose. The extraction of the sample will be realized using an electric oscillating saw and the cartilage will be held by a Clamp to facilitate the sample extraction and to guarantee both the cartilage surface protection and the improvement of the safe procedure in the extraction process. The PPE requested during the sample extraction consist on dark green gown, two pairs of gloves, goggles, mask and hear protection



a)



b)

Figure A.1.2 Devices used for the extraction process, a) hood, b) Electric oscillating saw

#### 4. Storing of the extracted samples.

The extracted samples will be located into a petridish with PBS to keep them free of any bacteria. The petridish will be labelled with the characteristic of the sample.

#### 5. Clean up and waste disposal requirements.

- After the sample extraction, Hood and surrounds are cleaned with a solution of Virkon and then wiped down with clean water, then 80% ethanol
- Gloves and tissues will be disposed of in the biohazard bin, using an autoclavable biohazard bag with my details on it.
- Gown will be put in the Autoclave, before being disposed.
- Hands will be washed before leaving the Lab.

#### 6. Clean up requirement for used tools.

- The used tools during the sample extraction procedure such as electric oscillating saw, blade, and clamp, are cleaned with a solution of Virkon, then, wiped down with clean water, followed by 80% ethanol and dry. All these tools, except the saw body are placed in an autoclavable bag with a biohazard warning. Labelled with personal details such as name and phone number. The saw body will be put into an oven at 60°C for three days to be decontaminated, using an autoclavable bag with Biohazard warning with personal details on it and the date when it went into the oven and was due to be taken out, before being disposed. The oven is located in the Mechanical Lab, Wiills Annexe Building

### A.1. 6 List emergency shutdown procedures

*Cover the work and turn off the hood*

#### **A.1.7 List Emergency procedures for how to deal with fires, spills or exposure to hazardous substances or tools**

*Fires: use fire extinguisher and leave the area;*

Cuts compounded with increase infection risk:

- Minor cuts, wash any injury with disinfectant (chlorhexadine ) and water for 15 minutes. Bandage. If area becomes hot and swollen seek immediate medical attention.
- Major cuts. Compress the area to stop the bleeding, seek immediate first aid. Wash the wound if possible
- If human tissue comes in contact with membranes (eyes, mouth) rinse immediately with water for 15 minutes

Spills: clean up wearing PPE and spray 80% ethanol. Then leave at least 10 mins to let the aerosols set down.

Report to lab manager;

Listed in specific SWP.'s for individual work processes

General emergencies call (938) x56666 and report the situation and follow instructions

In immediate danger / risk to yourself or others e.g. fire

break red glass alarm and activate building evacuation

- Assemble in the Michael Birt gardens in front of LOWY building or as instructed.
- Report to any available floor wardens or emergency/security personnel

Security contact 9385 6666

#### **A.1.8. List Clean up and waste disposal requirements**

- Material to be retained is placed in double containment and the exterior is wiped down to remove any contaminates.
- Items that have contact with the tissue should be separated into disposables, reusable, and tissue. Large pieces of tissue is placed in a paper autoclave bag and sealed.
- The drape surface is folded to contain any particulates and cover exposure surfaces. It is placed in a large autoclave bag.
- Any instruments should be placed in a container inside the drape.
- Gloves, contaminated towel used in clean up and any disposables have a separate bag. All items are autoclaved. Reusable protection (including the green gown) are then washed and returned to storage.
- Disposables and tissue can go into a biohazard bag and placed in the yellow bin in the cold room.
- Hood and surrounds are cleaned with a solution of Virkon and then wiped down with clean water then 80% ethanol.
- Liquid waste need to be placed into a container with Betadine

#### **A.1.9. List legislation used in the development of this SWP**

*OHS Regulation 2011*

*UNSW OHS Policy*

*OHS Training Procedure*

NSW Occupational Health and Safety Act 2000

NSW Occupational Health and Safety Regulation 2001

Australian/New Zealand Standard

2243.1:2005. Safety in Laboratories, Planning and operational aspects

2243.3:2010. Safety in Laboratories, Microbiological safety and Containment.

2243.4:1998. Safety in Laboratories, Ionizing radiations.

Worksafe WA: Guidance Note – Working Alone

UNSW OHS322 Working After-hours Guideline

EMO 049 Emergency Procedures and awareness

**A.1.10a. List competency required – qualifications, certificates, licensing, training - e.g. course or instruction:**

- *Biohazard training; Level 4 induction; Biosafety for PC2 Laboratories and quiz, blood work training*
- UNSW OHS Awareness Online: [http://www.ohs.unsw.edu.au/ohs\\_training/index.html](http://www.ohs.unsw.edu.au/ohs_training/index.html)
- UNSW Laboratory Safety Awareness: [http://www.ohs.unsw.edu.au/ohs\\_training/index.html](http://www.ohs.unsw.edu.au/ohs_training/index.html)

Knows the security phone number

Can list 3 safety considerations related to afterhours work

Is assessed as competent in the specific SWP undertaken afterhours

**A.1.10b. List competency of Assessor**

All of the above and in addition:

- OHS Supervisor Training:


Can identify Low medium and high risk work using the UNSW risk rating procedure

Has assessed and documented the task competency level of the person requesting afterhours access

Has assessed and documented the risk and hazards associated with the After hours tasks

**A.1.11. Supervisory approval, And review****Supervisor:****Signature:****Responsibility for SWP review:****Date of review:**

## A.2 SWP for image acquisition of human samples

HS026  Safe work procedure	1. Completed by: <b>Juan Carlos Baena Vargas</b>	 <b>UNSW</b> AUSTRALIA
	Staff/Student number: z3399001	

The Safe Work Procedures Guideline (HS027) should be consulted to assist in the completion of this form

Faculty/Division: <b>Engineering</b>		School/Unit: <b>Mechanical and Manufacturing Engineering</b>		
Document number <b>MECH001</b>	Initial Issue date <b>21/06/2013</b>	Current version	Current Version Issue date <b>21/06/2013</b>	Next review date <b>06/2014</b>

### A.2.2. Safe work procedure title and basic description of activity

**Title:** **Imaging acquisition procedure of human cartilage samples (biological tissues), using LSM**

**Description of activity:-** *Imaging human samples through the Laser scanning Microscopy (LSM). Samples are located in the stage of the microscopy. These samples remain all the time into a petri-dish during the image acquisition process to avoid the contamination of the microscopy and surrounding areas*

**Risk:** *infection due to the human tissues. The controls are training and use of personal protective equipment. Other controls are PC 2 work practice and immunization*

### A.2.3. List hazards and risk controls as identified during risk management

Associated risk assessment number and location:	Hazards	Controls
		Following the

Manipulating human samples	<i>Infection due to the human tissue</i>	<p><b>Personal protective equipment:</b></p> <ul style="list-style-type: none"> <li>gloves, Lab coat, enclosed shoes and safety glasses need to be used during the procedure</li> </ul> <p><b>Minimize:</b></p> <ul style="list-style-type: none"> <li>The tissues are small and they are isolated by a petri dish, which maintain into a container and a cooler to avoid any contamination.</li> <li>Clean up the microscopy and surrounded such as work bench or equipment after the image acquisition procedure with 1% Virkon soaked on toweling to wipe down, then wipe down again with 80% ethanol.</li> <li>Place any container or petridish with samples over a cloth cover.</li> <li>Samples will be transported between Labs, using double container that are placed in a Cooler to keep the samples around 5°C</li> </ul>
<b>Operating the laser scanning microscopy</b>	<p>Causing damage to the equipment</p> <p>Ergonomic issues</p>	<p><b>Minimize:</b></p> <ul style="list-style-type: none"> <li>Special training given by appropriate trainer.</li> </ul> <p><b>Minimize:</b></p> <p>The University provide the setting up your work station guide (OHS705)</p> <p>Set up workplace IAW, Uni work station guide (OHS 705)</p>

#### A.2.3.1 Pathways for infections and control

Pathway	Hazard	Control
Working with wounds	Exposed wounds during the sample handling	<p><b>Minimize:</b> To cover the wound properly and Avoid handling the sample directly, using any device such as tweezers</p> <p><b>Personal protective equipment:</b> gloves, lab coat and covered shoes</p> <p>Hepatitis B vaccination</p>

Spills and gases produced by the PBS solution, used to hydrate the samples	<ul style="list-style-type: none"> <li>• Ingestion</li> <li>• Inhalation</li> </ul>	<b>Personal protective equipment:</b> eye protection, mask
--	---	--

#### A.2.4. List resources required, including personal protective clothing, chemicals and equipment needed

*Gloves, petridish, tweezers, PBS, Lab coat, LSM, 1% Virkon solution, 80% Ethanol, paper tissues, safety glasses, cooler, small containers*

#### A.2.5. List step by step instructions or order for undertaking the task

The samples used in this project come from human knee parts that have been collected over the past two years for the University of James Cook, which belongs to the project titled “Development of Advanced Techniques to study Osteoarthritis”, UNSW’s reference No. HREC 11347/ JCU H4019

The cartilage samples will be carried from the Vibration Lab to the LSM’s room using a double container which will be located in a cooler to maintain the cartilage temperature around 5°C. The personal protection equipment (PPE) required are gloves, lab coat, covered shoes and safety glasses.

Standard PC2 work practices for the containment of biohazards are

##### **Do not**

- ☐ Eat, Drink or Smoke in the facility
- ☐ Apply cosmetics
- ☐ Mouth pipette
- ☐ Insert contact lenses
- ☐ Bring or store food
- ☐ Tongue moisten labels
- ☐ Contaminate materials (e.g. workbooks) that will be removed from the room without sterilization.
- ☐ Keep hands and pens away from your face. They may have been in contact with contaminated surfaces or aerosols
- ☐ Tie back long hair
- ☐ You must wear closed footwear
- ☐ You must notify the Lab Manager of any spills or accidents immediately
- ☐ Take care that reading and writing materials do not become contaminated.

The cartilage samples do not present any difficulty in handling as the samples are small and both the set up and the image acquisition procedure will be undertaken with extreme care. This procedure consists of the following steps and will minimize aerosol production to reduce infection risks.

### **1. Preparation of the work area.**

To clean up the surface of the microscope's stage and surrounding areas before starting with the image acquisition process, wiping down with 80% ethanol. Then, an area is arranged for the sample handling, using a bench roll with plastic backed surface cover to protect the work area of any contamination (see figure A.2.1). The microscope's stage also is protected by the bench roll during the image acquisition process.

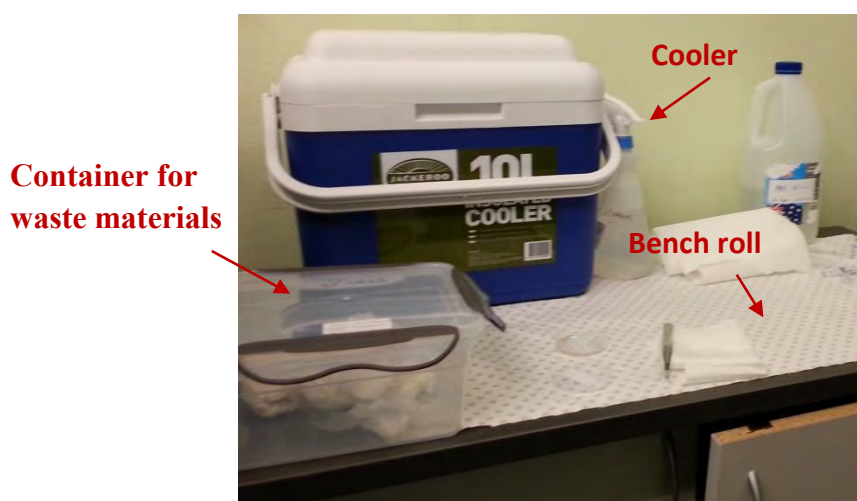


**Figure A.2.1.** Preparation of work area for handling the human samples

### **2. Sample manipulation.**

Samples will be transferred from the small container located in the cooler to a modified petri-dish that is employed for the image acquisition using tweezers. This procedure will be undertaken in an area covered with a bench roll that can absorb small spills (see figure A.2.1)

### **3. Mounting of sample for image acquisition.**

The sample will be placed sample holder which will be introduced in the modified petri-dish to allow the sample hydration during the image acquisition (see figure A.2.2 b and c). The necessary time of the image acquisition for each sample is around 2 hours. After that, the sample is returned to the small container located in the cooler that is located on the area covered with the bench roll.

The keyboard and mouse of the computer is wrapped with a plastic film during the image acquisition to avoid any contamination as can be seen in figure A.2.2-a. When the sample is under the microscope and the manipulation of the microscope is required, the gloves are changed to reduce the cross contamination.

During the image acquisition, there is no increase aerosol or gas risk produced by the Microscope's laser,

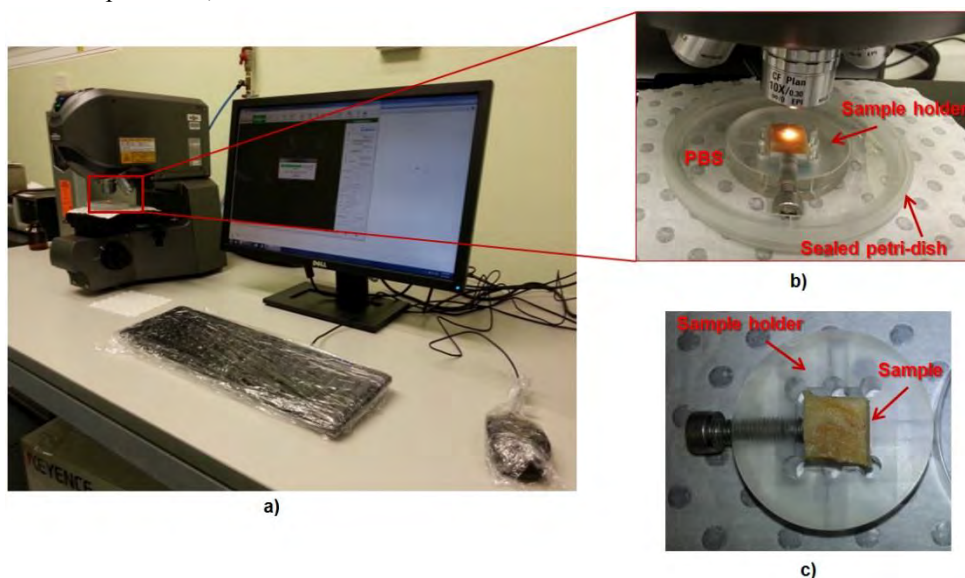


**Figure A.2.2** Risk control during the image acquisition process, a) both keyboard and mouse are wrapped down with plastic film, b) sample located in the sample holder which is introduced in a modified petridish with PBS solution for sample hydration, c) Human sample placed in sample holder.

#### 4. Turn on/off the equipment.

**Turn on the laser:** It needs to be on 20 minutes before starting with the image acquisition.

**Put the laser's opening in mode open**

**Open the image acquisition software**

To turn off the equipment, the procedure begins with closing the software up to turn off the laser. This is the opposite procedure for turning on the equipment.

#### 5. Clean up and waste disposal requirements.

- All tools such as tweezers, sample holder and modified petri-dish, are soaked in 1% Virkon for 20 minutes in a container and then wiped down with 80% ethanol. After that, they are located in a sealed container labeled as Bio-hazard material and with a phone contact number. The container also has information about the purpose of the tools and when the project is finished.

- All disposals toweling, bench roll and plastic wrap is placed in biohazard waste, sealed and then autoclaved. Placed in waste pick up point to be removed by UNSW contractors.
- Decontaminate all work benches and equipment after work has been completed with 1% Virkon soaked on toweling to wipe down any contact surfaces or spills and then 80% ethanol

#### **A.2.6. List emergency shutdown procedures**

*Turn off the laser, close the laser's opening, put samples back in the container.*

#### **A.2.7 List emergency procedures for how to deal with fires, spills or exposure to hazardous substances**

*Fires: Use fire extinguisher If practical, in case of more serious fire, use nearest break glass alarm*

*Spills: clean up wearing PPE. Cover small spills gently with 1% Virkon and large spills with Virkon powder, dispose in the contaminated waste bin, then, wipe down with 80% (V/V) ethanol.*

*If infectious material is spilt, avoid breathing in any aerosol, wait 5-10 minutes until the particles have been set down then clean up.*

*Report to lab manager;*

Listed in specific SWP.'s for individual work processes;

General emergencies call (938) x56666 and report the situation and follow instructions

In immediate danger / risk to yourself or others e.g. fire

- break red glass alarm and activate building evacuation
- Report to any available floor wardens or emergency/security personnel

Security contact 9385 6666

#### **A.2.8. List clean up and waste disposal requirements**

*Solid waste: into a biohazard bag. The biohazard bag is carried to the Biomedical Lab using a sealed container labeled biowaste. this waste material is treated in the autoclave and then, located inside a second biohazard bag sealed and labelled with a red biowaste sticker.*

#### **A.2.9. List legislation, codes of practice, manufacturers manual, industry standards etc used in the development of this SWP**

*OHS Regulation 2011*

*UNSW OHS Policy*

*OHS Training Procedure*

NSW Occupational Health and Safety Act 2000

NSW Occupational Health and Safety Regulation 2001

Australian/New Zealand Standard

2243.1:2005. Safety in Laboratories, Planning and operational aspects

2243.3:2010. Safety in Laboratories, Microbiological safety and Containment.

2243.4:1998. Safety in Laboratories, Ionizing radiations.

Worksafe WA: Guidance Note – Working Alone

UNSW OHS322 Working After-hours Guideline

EMO 049 Emergency Procedures and awareness

**A.2 10a. List competency required – qualifications, certificates, licensing, training - e.g. course or instruction:**

*Biosafety for PC2 Labs*

*Biohazard training; PC 2 induction*

- UNSW OHS Awareness Online: [http://www.ohs.unsw.edu.au/ohs\\_training/index.html](http://www.ohs.unsw.edu.au/ohs_training/index.html)
- UNSW Laboratory Safety Awareness: [http://www.ohs.unsw.edu.au/ohs\\_training/index.html](http://www.ohs.unsw.edu.au/ohs_training/index.html)

Knows the security phone number

**A.2.10b. List competency of assessor**

All of the above and in addition:

- OHS Supervisor Training:  
Can identify Low medium and high risk work using the UNSW risk rating procedure

**A.2.11. Supervisory approval, and review**

**Supervisor:**

**Signature:**

**Responsibility for SWP review:**

**Date of review:**

## Appendix B Selected 3D images of human knee cartilage surfaces affected by OA using LSM

### *B.1 Selected LSM images at 20X magnification of OA grade I.*

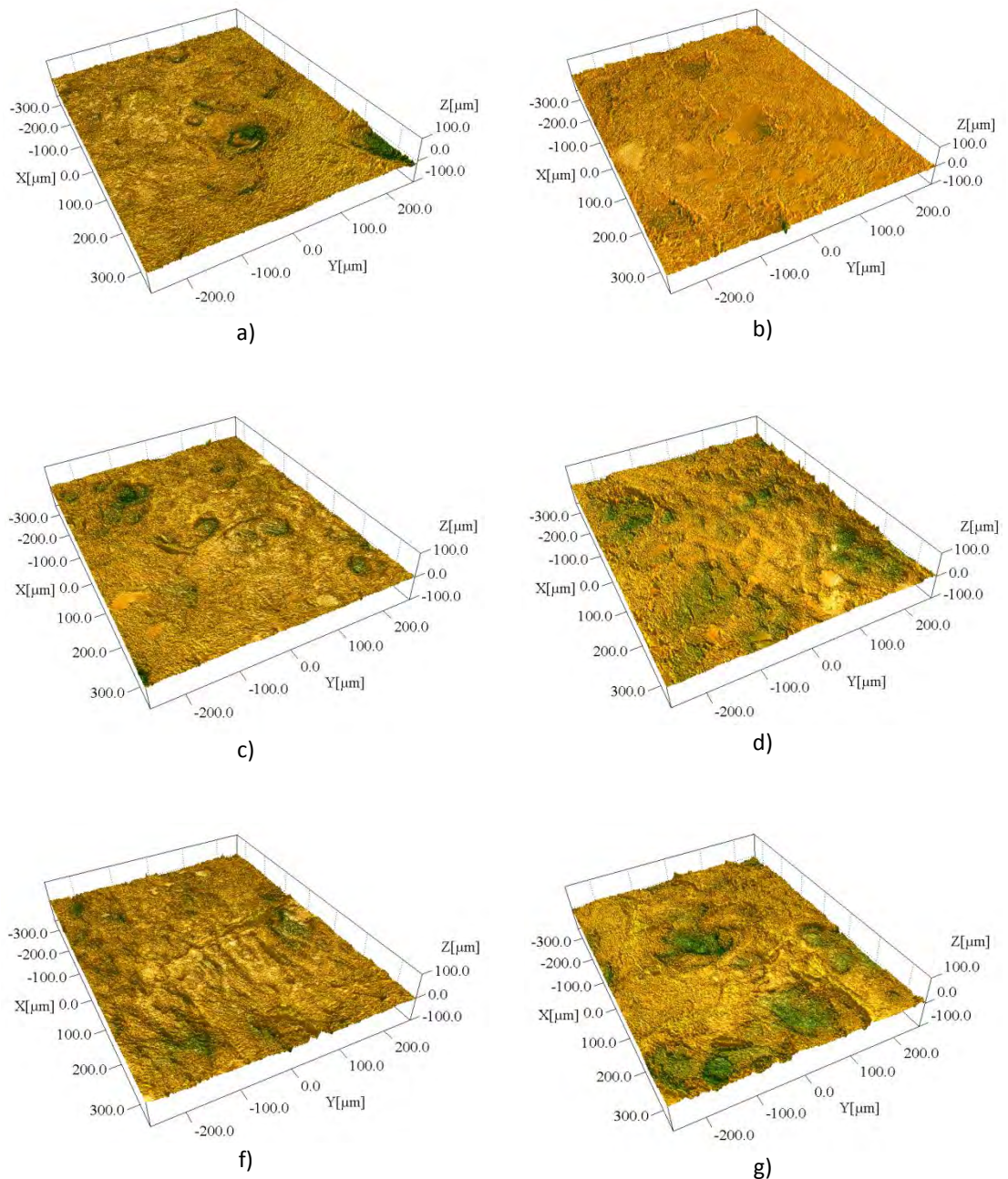


**Figure B.1.1** Representative images of Sample with OA grade I. Samples from 73 year old male patient

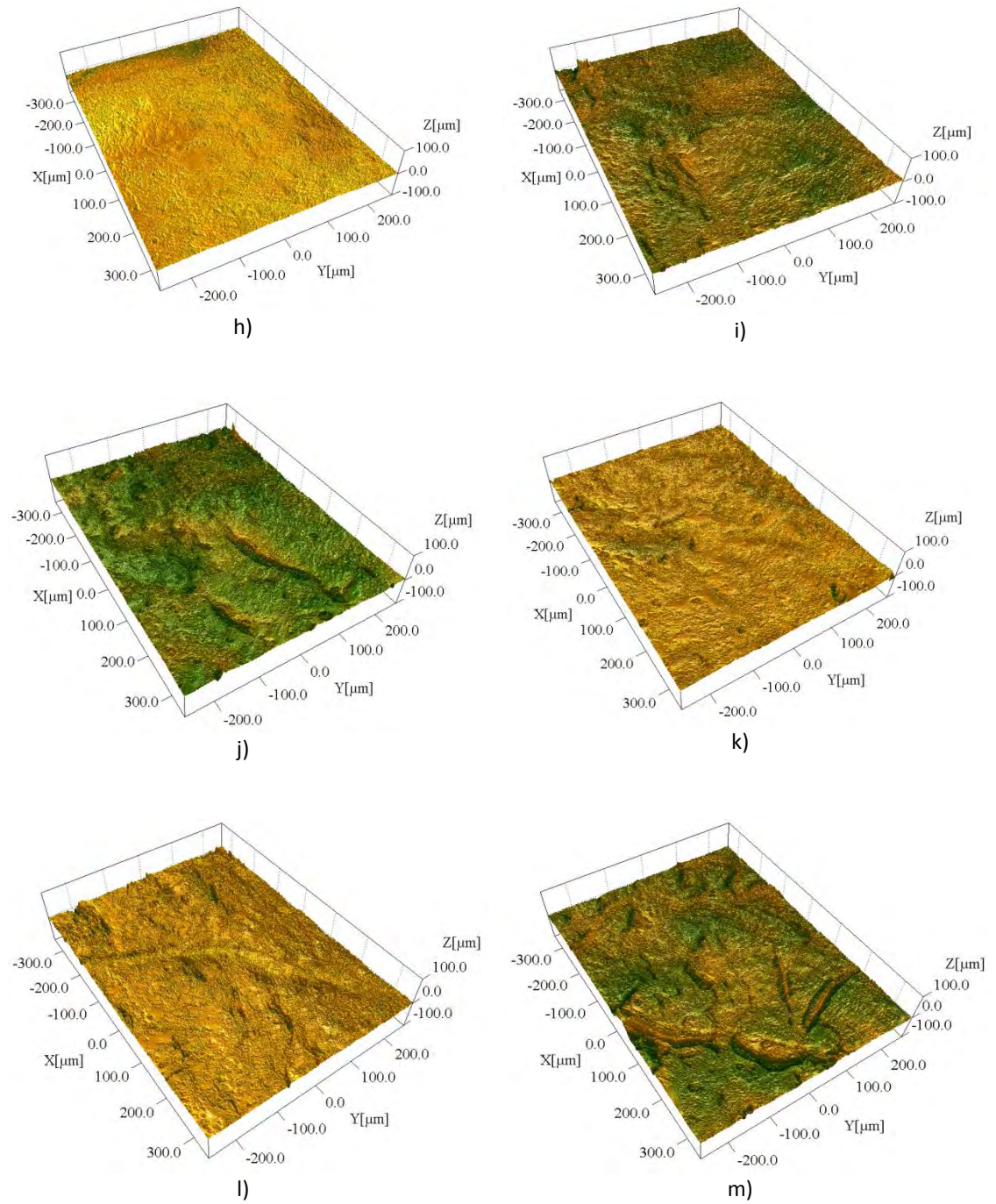
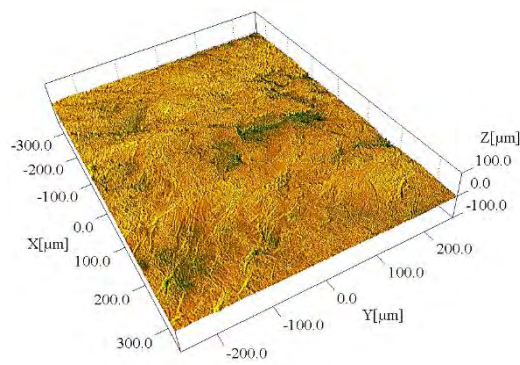
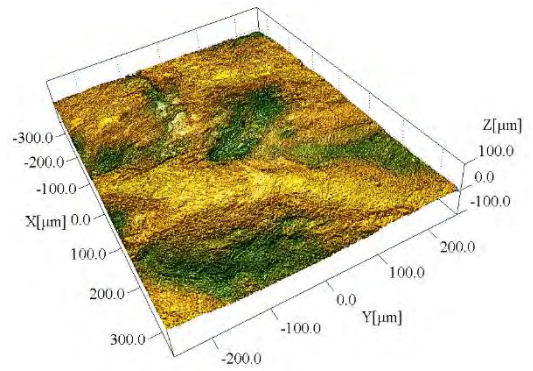


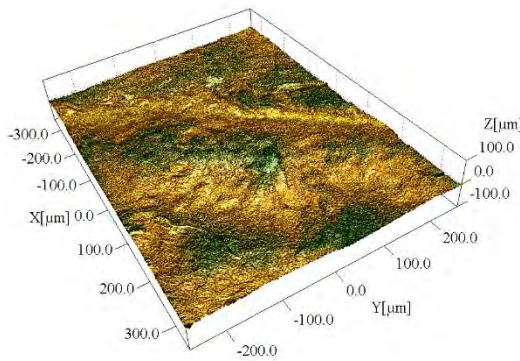
**Figure B.1.2** Representative images of Sample with OA grade I. Samples from 65 year old male patient



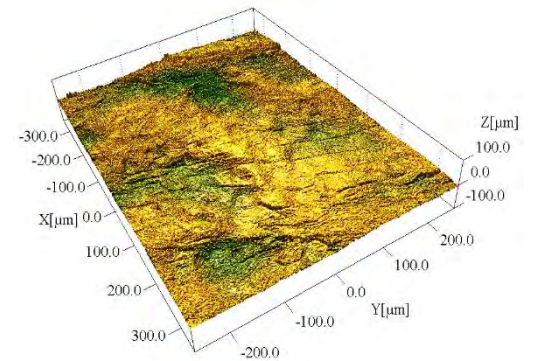
a)



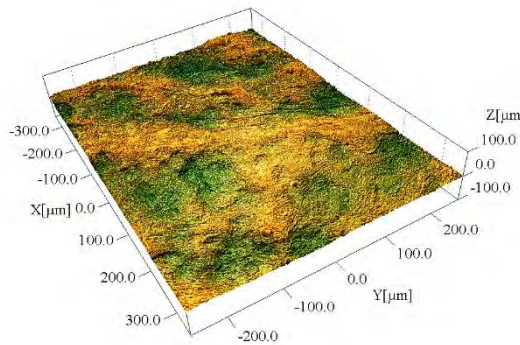
b)



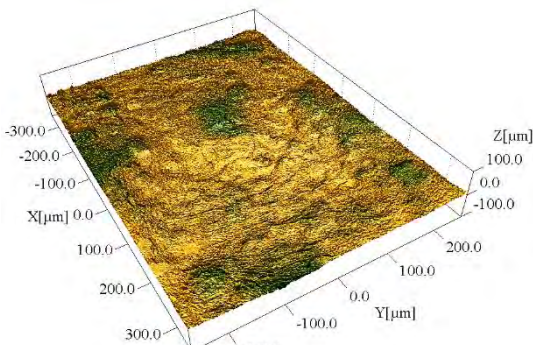
c)



d)



e)



f)

**Figure B.1.3** Representative images of Sample with OA grade I. Samples from 53 year old female patient

*B.2 LSM images at 20X magnification of OA grade II*

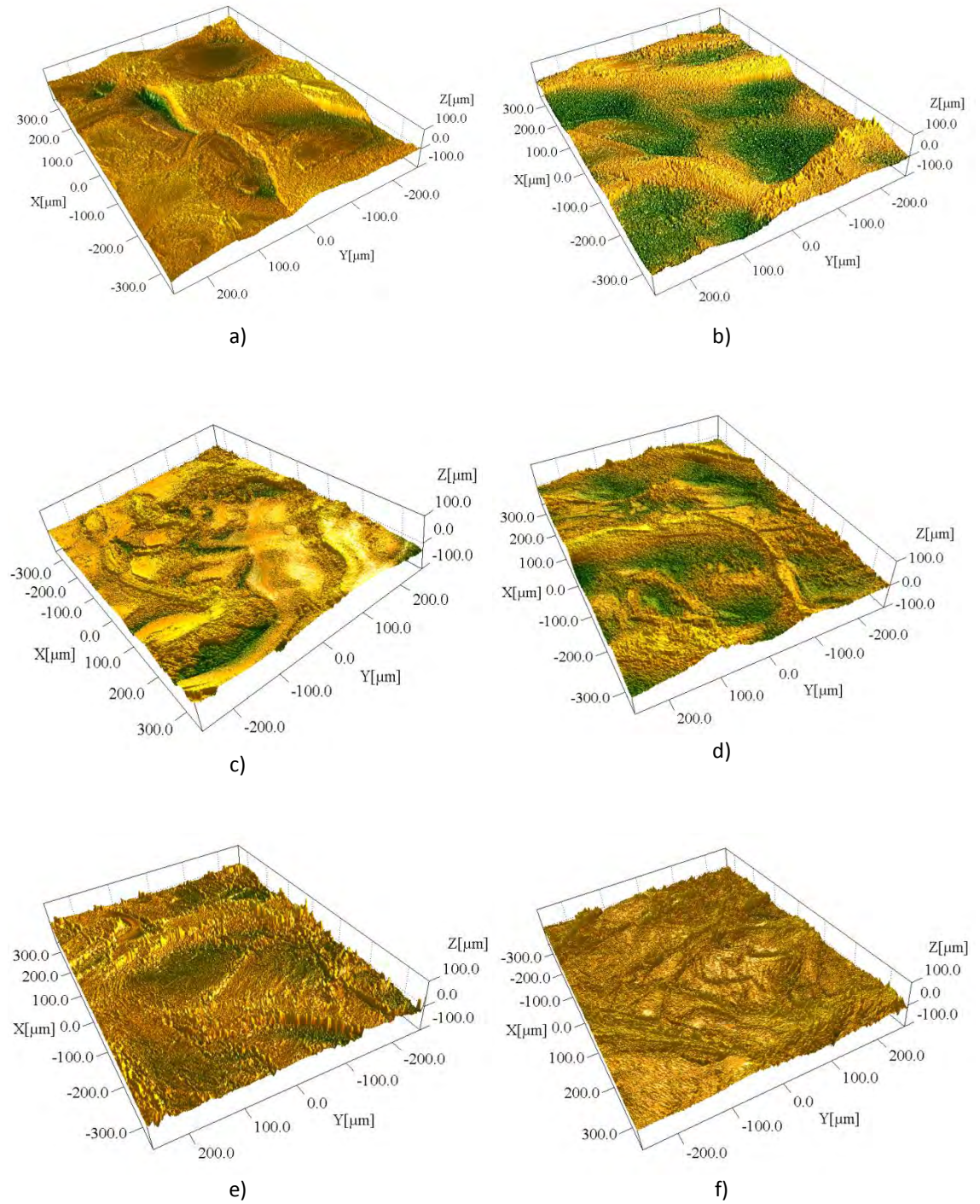


**Figure B.2.1** Representative images of Sample with OA grade II. Samples from 64 year old male patient.

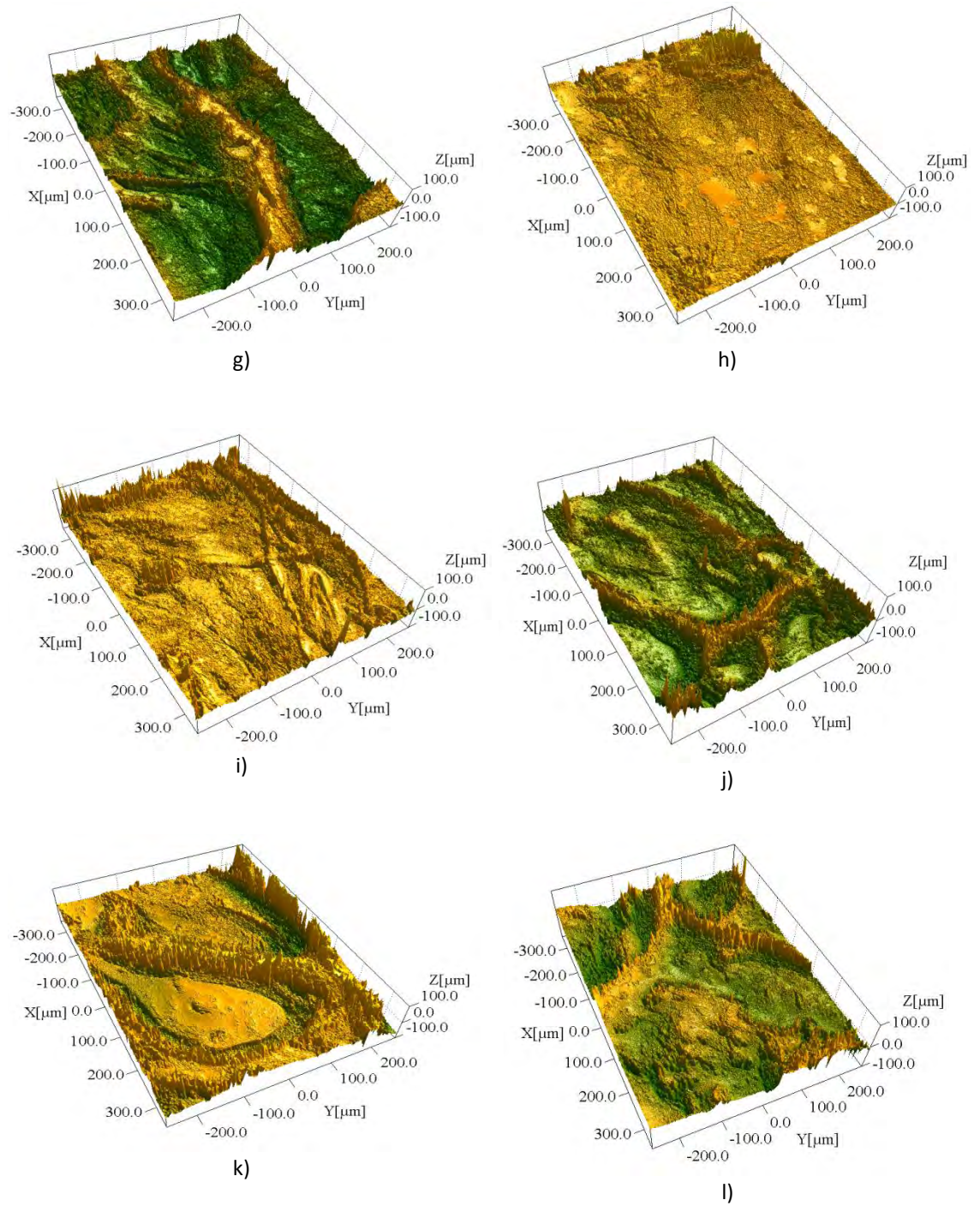
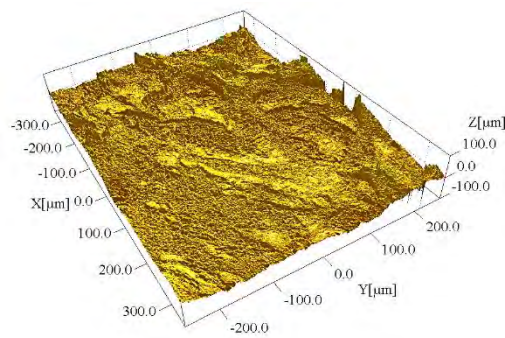
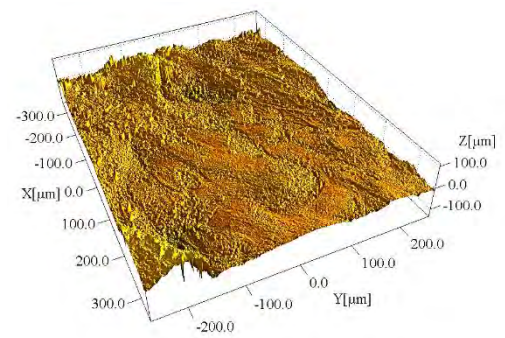


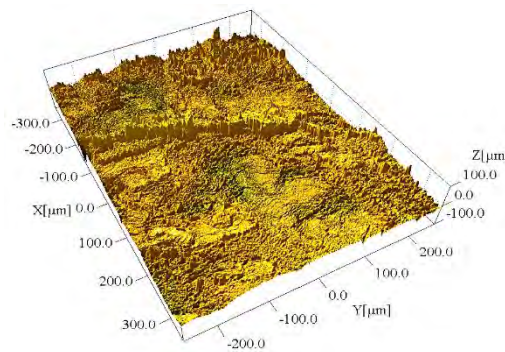
**Figure B.2.2** Representative images of Sample with OA grade II. Samples from 65 year old male patient.



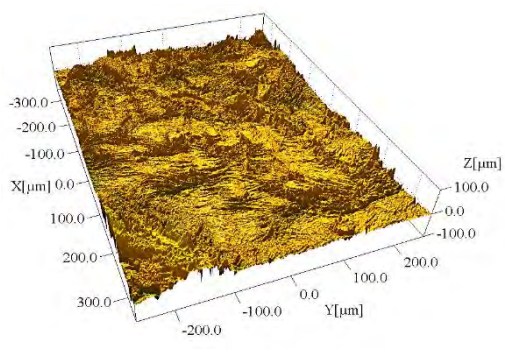
a)



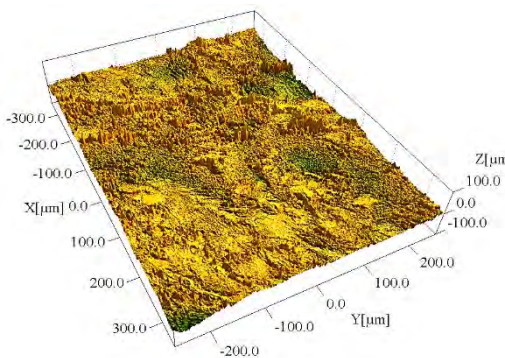
b)



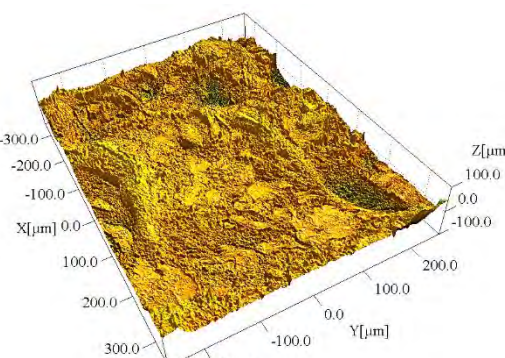
c)



d)



e)



f)

**Figure B.2.3** Representative images of Sample with OA grade II. Samples from 71 year old male patient.

*B.3 LSM images at 20X magnification of OA grade III*

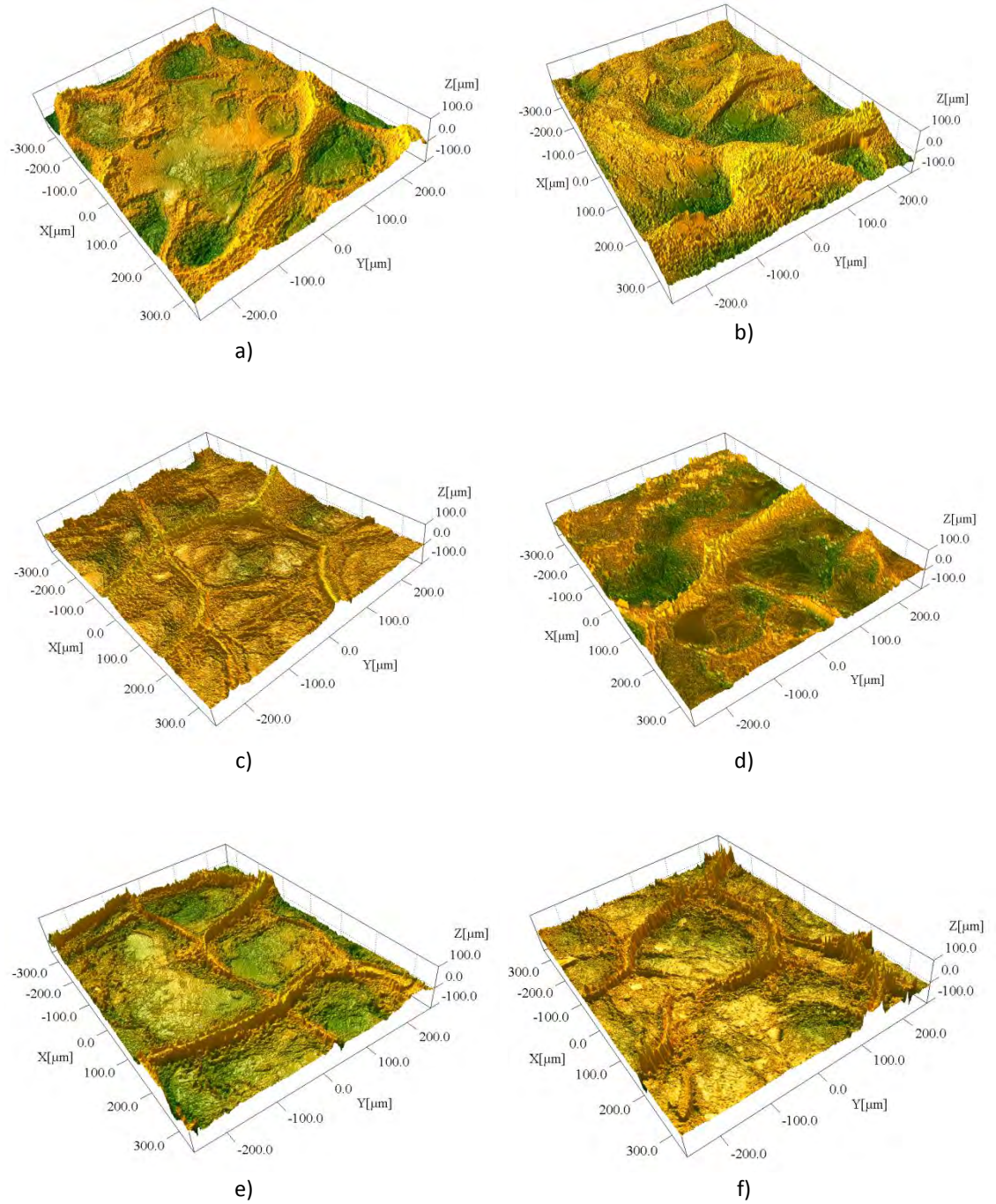
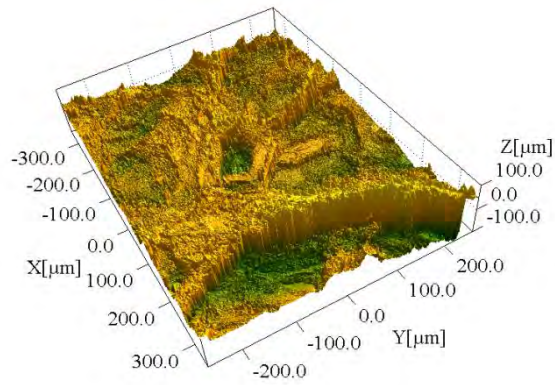
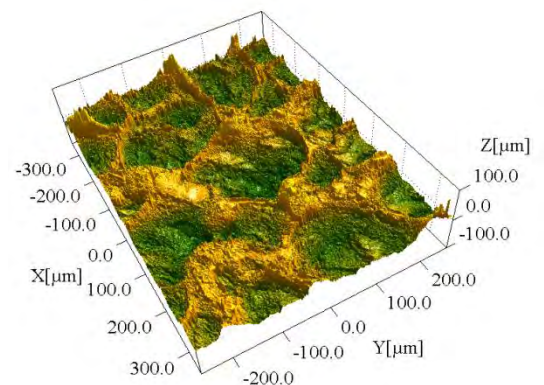


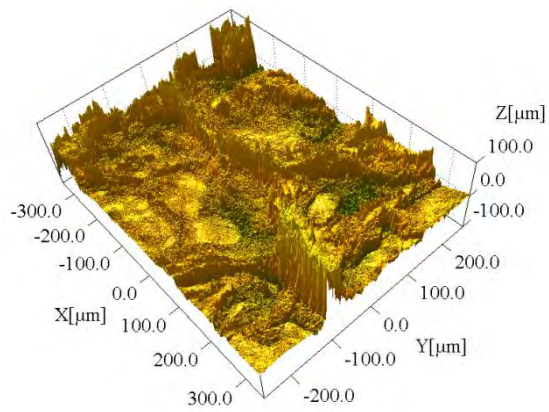
**Figure B.3.1** Representative images of Sample with OA grade III. Samples from 89 year old male patient, part 1.



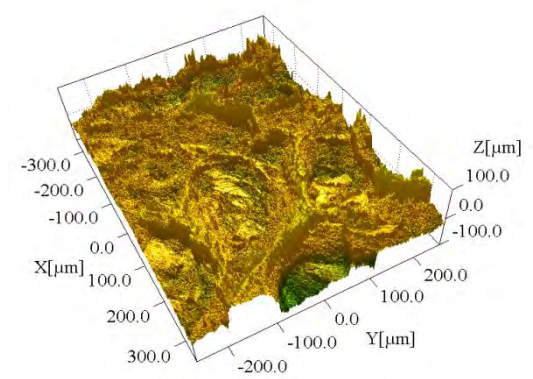
g)



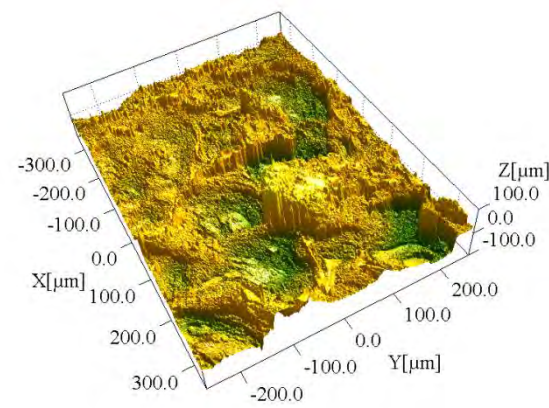
h)



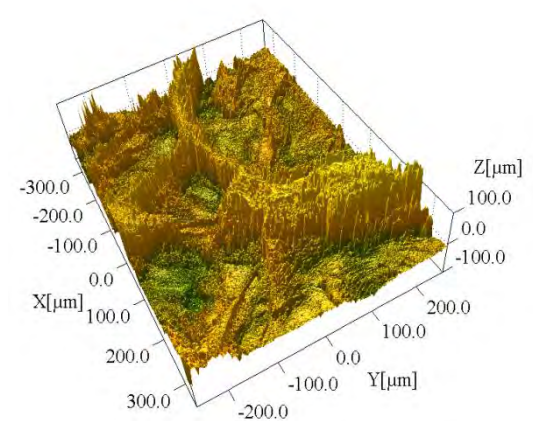
i)



j)

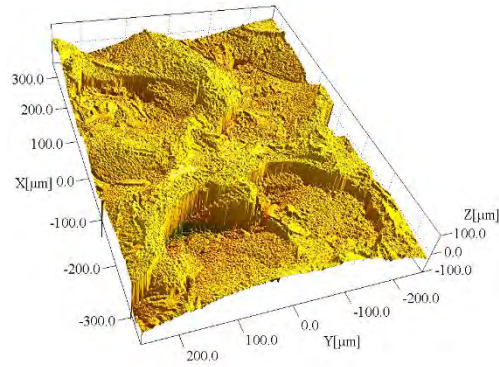


k)

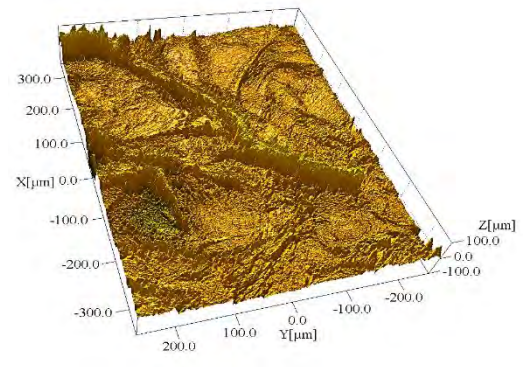


l)

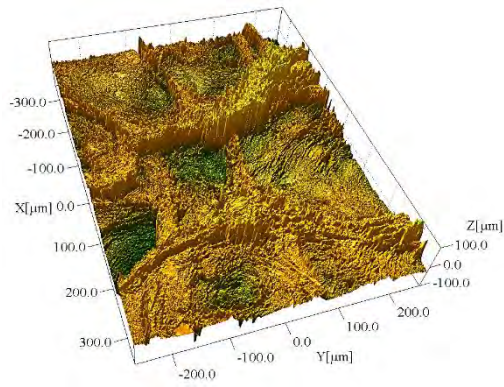
**Figure B.3.2** Representative images of Sample with OA grade III. Samples from 89 year old male patient, part 2.



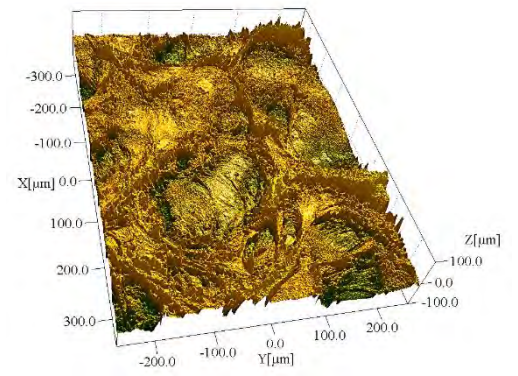
a)



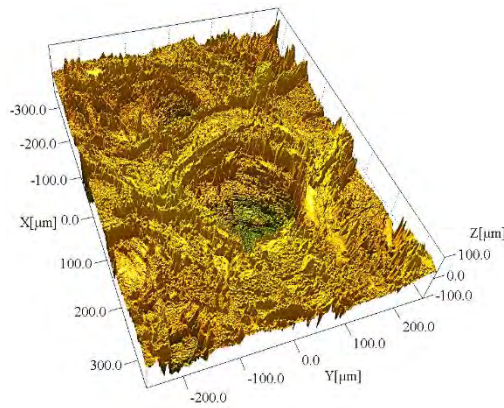
b)



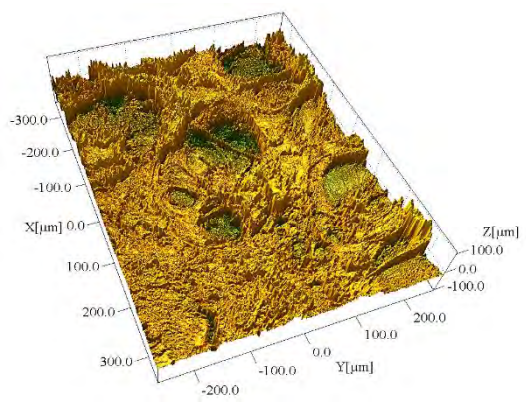
c)



d)



e)



f)

**Figure B.3.3** Representative images of Sample with OA grade III. Samples from 76 year old female patient.

## Appendix C Numerical values of the studied OA grade condition

Table C.1 Numerical values of OA grade I cartilages at the micron scale, According to the SPIP Classic surface roughness parameters implemented in SPIP

Amplitude parameters								
Sa (nm)	Sq (nm)	Sv (nm)	Sku	Sy (nm)	S10z (nm)	Ssk	Smean	Sp (nm)
7142.33	11160.5	32827.8	14.1141	134476	132504	0.044316	-3.11E-05	32633.6
4528.3	5803.87	24451	3.56946	63402.9	59733.1	0.158294	-1.04E-05	40027.9
3999.05	5227.16	52040.1	4.49896	104994	76322.3	-0.24903	8.76E-06	20781.9
4578.18	6301.92	26337.8	6.11816	89313.9	80401.1	0.140281	-3.69E-06	35711.1
3299.44	4287.04	24955.9	4.12276	53757.9	49271.9	0.229212	-4.52E-05	26141.6
5865.93	7337.22	33591.7	3.25095	740 11.3	70308.3	-0.00458	2.75E-05	27341.2
3962.9	5524.13	32663.2	5.8034	63096.8	59883.5	-0.07043	-9.11E-07	18007.7
4757.71	6100.64	37045.2	3.79304	87552.5	68022.9	0.547217	1.70E-05	30386.7
3616.15	4866.69	28491.1	5.1007	58766.5	57252.7	0.092843	1.67E-05	30354.3
4571.3	6091.57	42595.2	4.99066	89910.5	79462.2	0.189057	5.03E-07	17230.8
3283.18	4365.33	36154.2	4.71846	67204.5	57929.5	-0.13207	-1.09E-06	28137.5
4626.45	6025.59	33394	3.96086	72660.1	64619.1	0.473455	-1.23E-05	34377.8
2756.31	3630.33	21256	5.85795	77485.6	58962.1	2.07945	5.79E-08	101648
3153.3	4279.57	32724.6	5.07357	68550	59129.5	-0.04535	-4.57E-05	38951.8
3290.71	4529.05	29756	9.6685	88779.3	83837.8	-0.02319	1.37E-07	52954.4
3863.39	5066.35	36394.4	5.59477	110057	90145.5	0.406636	-1.37E-05	62976.1
3770.25	5279.29	31852.5	10.0215	95496.2	80965.7	-0.55736	-6.62E-06	28802
3262.54	4269.34	31499	5.11485	63974.2	60634.4	-0.02203	-3.41E-05	40419.6
2112.28	2718.47	19128.4	3.65997	32809.9	30397.2	-0.86574	-2.24E-05	30433.6
2362.46	3107.03	23225.1	4.76607	45469.2	41911.5	0.14398	-2.52E-06	50507.4
6005.65	9567.87	78899.5	10.0016	161544	138216	-0.38742	-1.88E-06	30275.4
7662.5	10759.6	81506.3	6.80733	171464	164542	0.136186	2.09E-06	47315.2
2700.45	3582.08	26074.2	5.82154	71082.3	62876.3	-0.54433	-1.56E-06	31050.2
3903.66	4970.89	22231	3.67122	55177.2	51064.3	0.139074	4.95E-07	39266.1
4162.11	5302.64	31609.9	3.80455	64243.5	61377.9	0.171799	2.66E-05	56229.6
5193.7	6493.94	26240.7	3.37167	66268.6	63397.5	0.172335	2.45E-05	35825.5
2656.88	3423.03	20281	3.75731	41062.9	37257.7	0.604183	-3.23E-05	59023.3
3349.5	4321.3	17529.3	4.09357	53240.4	51831.6	0.153303	3.83E-06	73662.7
5619.55	6747.29	20761.3	2.30073	46902.9	44375.3	0.575803	1.33E-05	63643.6
4178.41	5349.04	26010.2	3.29742	53351.4	51302.8	0.019891	4.72E-07	32475.2
2952.39	3643.83	18737.5	2.96218	36745.2	34587.9	-0.3629	1.52E-05	13681.5
4971.09	6268.89	22077.8	3.11464	52464.5	50627.4	-0.03715	1.28E-06	22244.1
4179.57	5611.98	26033.3	4.14234	56387.6	51940.9	0.937043	1.43E-06	82644.6
2416.93	3029.55	12586.8	2.91162	29817.6	28094	1.11406	-2.42E-05	89957.5
3224.96	4135.79	20147	3.62336	48284.5	46350.7	0.285863	-2.29E-05	45008.1

3899.21	5101.67	22051.9	4.32597	56429.7	54709	0.432276	3.78E-05	32946.2
2313.88	3134.12	25335.3	6.86462	46550.6	44743.9	-0.97185	-4.89E-07	21215.3
2000.62	2572.59	22895.6	4.52063	40145.6	37999.8	0.108887	-6.09E-07	17250
3930.33	5228.38	38104.2	4.58744	74567	68179.7	0.066118	1.50E-05	36462.7
3979.76	5223.15	37905.4	4.60009	74851.4	71289.4	-0.00795	-1.63E-05	36946
5158.86	6797.54	35095.6	4.63496	87517.4	83498	0.359764	-3.20E-06	52421.8
2339.96	3148.26	24280.1	5.92479	47894.4	45932.9	-0.47382	3.70E-06	23614.3
2213.37	3052.92	21606.6	6.36857	45691.7	44558.4	-0.90141	-2.76E-06	24085.1
4674.94	8668.34	47855.5	23.3321	130171	109398	3.92982	2.62E-05	82315.9
5289.42	7048.45	50108.3	5.19136	116648	107529	0.463628	-7.08E-05	66539.3
4465.29	5943.15	76440	5.58331	122087	82033.7	0.385765	1.42E-05	45647
4884.97	6348.1	54698.2	4.07378	93598	79487.2	0.105501	2.30E-05	38899.9
2945.74	3782.87	24597.6	3.84893	47377.7	46223.1	-0.16952	2.65E-05	22780.1

### Functional parameters

Spk (nm)	Svk (nm)	Sdc <sub>5_10</sub> (nm)	Sdc <sub>10_50</sub> (nm)	Sdc <sub>50_95</sub> (nm)	Sbi	Sci	Svi	Sk (nm)	Sdc <sub>0_5</sub> (nm)
26685.3	11832	6467.76	9432.15	16169.4	0.711746	1.39849	0.10828	15141.7	85967.3
7533.57	6454.77	2160.02	6861.23	10164.8	0.638294	1.4854	0.128494	13639.1	29859.1
8548.28	6514.3	1683.28	5681.06	9047.62	0.716495	1.33639	0.141611	11974.9	45658.9
12757.3	8136.93	2863.77	5906.53	11276.1	0.706301	1.35421	0.14091	11982	54053.7
4683.5	6158.77	1400.51	4632.45	7972.12	0.68198	1.36054	0.147998	9787.18	22515.8
9519.57	7131.91	2966.38	8157.56	12458.8	0.638167	1.50347	0.109044	18089.4	28922.3
6141.15	9485.43	1770.25	5942.98	9609.93	0.696956	1.31114	0.165412	10351.1	22507.5
8904.87	6125.9	2456.38	7544.61	9650.08	0.622413	1.54939	0.117091	14977.2	40705.8
6397.92	6906.85	1648.76	5064.04	8832.64	0.699515	1.32772	0.153383	10208.7	23318.2
9762.8	7473.37	2342.36	6666.71	10450.5	0.668169	1.43352	0.131808	13272.1	38198.4
5498.05	6786.38	1481.46	4309.7	8484.73	0.711575	1.29545	0.166423	8982.1	24915.5
9091.33	6359.84	2621.01	6698.13	10192.8	0.639947	1.49456	0.126044	13394.4	29850.3
6542.24	4353.38	1397.54	4503.17	5590.14	0.647378	1.50392	0.120725	8329.83	50621.8
7319.98	4895.44	2472.75	5632.37	5769.74	0.558426	1.73408	0.119299	8601.32	28161.8
8510.85	5333.75	1601.23	4981.61	6760.75	0.712044	1.3704	0.121504	9791.16	52662.7
8459.38	5571.94	1543.89	6837.22	7057.77	0.638305	1.53491	0.111613	11542.8	65725.5
10291	6836.19	2105.13	5358.5	8037.75	0.715413	1.35028	0.131453	10935.5	56264.3
6087.38	4379.7	1666.66	5128.2	6666.65	0.636643	1.50976	0.121053	10025.9	25769.2
2918.14	3343.02	920.52	3090.31	5062.85	0.655439	1.42408	0.144531	6252.53	9533.94
4467.68	3563.98	1366.81	3644.82	5102.75	0.630081	1.51733	0.128511	7091.42	17312.9
21378.1	14071.5	6474.71	7769.66	13596.9	0.698952	1.3928	0.142977	13262.1	68955.7
21046	10953.5	6872.3	14431.8	13401	0.551309	1.78294	0.113246	18552.1	70441
6455.7	3795.45	1709.39	4415.94	5413.08	0.613946	1.58531	0.121328	8040.2	39173.6
7195.92	4267.48	2211.51	6966.26	7076.84	0.5767	1.68616	0.100285	11877.4	24326.

5720.83	3619.3	1785.88	10433.3	9399.38	0.583041	1.66052	0.0791946	18678.6	14569
6481.51	5395.64	2352.16	7056.49	8660.24	0.576884	1.64793	0.122205	12643.6	18068. <sub>9</sub>
3569.62	3228.04	1178.21	4786.46	5743.75	0.622081	1.53582	0.107797	10109.8	12150. <sub>2</sub>
9127.04	4060.03	3364.45	9672.81	8095.72	0.518413	1.88267	0.0833769	14441.1	18294. <sub>2</sub>
8955.3	6983.75	3164.04	6667.08	9266.11	0.580045	1.64162	0.131343	11626.8	20679. <sub>2</sub>
3587.32	2391.54	1135.34	4362.09	4541.36	0.57379	1.68179	0.0990426	7535.94	11950. <sub>9</sub>
4674.4	4858.54	1257.91	4838.13	7547.48	0.659704	1.43062	0.131928	9572.27	21868. <sub>3</sub>
7886.21	4780.6	2374.8	6672.05	7463.65	0.593613	1.63424	0.107486	11485.6	25783. <sub>5</sub>
3549.75	4733.4	1026.17	3171.78	5503.98	0.70852	1.30275	0.155431	6668.15	16791. <sub>8</sub>
3482.08	2600.76	965.426	3298.54	3861.7	0.621959	1.5543	0.116413	6351.3	13113. <sub>7</sub>
8319.05	6486.68	2241.49	5678.45	8816.53	0.66006	1.44503	0.136872	11289.1	28541. <sub>7</sub>
7598.4	6017.85	1950.04	5850.11	8700.17	0.665758	1.43271	0.13212	11882.9	29100. <sub>6</sub>
11518.1	7221.46	3332.32	7892.35	10698.5	0.616232	1.57199	0.115492	15774.7	41391
4262	4057.46	1151.77	3647.27	4991	0.65561	1.44251	0.137932	6826.34	18812. <sub>2</sub>
3788.83	4997.38	1007.23	3113.26	5310.86	0.708878	1.29782	0.163174	6141.8	19778. <sub>4</sub>
27824.4	4367.24	3912.96	5739.02	6782.48	1.05321	1.05593	0.0576106	10990.4	74085. <sub>5</sub>
12163	7273.74	3272.68	8882.98	10285.6	0.607361	1.60247	0.119002	15466.7	54934. <sub>2</sub>
9544.97	6961.39	2201.97	6850.58	9541.87	0.664227	1.46279	0.133604	13198	36699. <sub>5</sub>
8860.66	7356.23	2626	7502.85	10504	0.633928	1.51327	0.128529	14785.9	28886
4691.53	4271.56	1329.23	4367.48	6456.28	0.653925	1.44959	0.129453	8954.22	16995. <sub>2</sub>
3941.84	3997.98	1234.36	4279.1	5595.75	0.625106	1.51014	0.13262	8140.12	15306
6147.04	4400.14	1813.8	5228.01	7148.51	0.616418	1.55458	0.120071	10275.4	28700. <sub>7</sub>

Spatial parameters								
Sds ( $\mu\text{m}^2$ )	Stdi	Srw (nm)	Srwi	Shw (nm)	Sfd	Scl20	Scl37	Str37
0.13029	0.593391	151171	0.028706	116362	2.26693	40949.6	30711.6	0.624813
0.140927	0.734834	151628	0.02865	99739.2	2.37164	48456.6	32759.3	0.799748
0.148718	0.733288	161503	0.030146	87271.8	2.35203	38911	26622.3	0.796085
0.135429	0.606982	159453	0.029621	87271.8	2.31315	36172.3	24569.8	0.70567
0.151529	0.803892	209524	0.036506	87271.8	2.37751	45057.6	27302.8	0.816404
0.139179	0.60192	177169	0.035494	116362	2.34353	53243.6	36179.5	0.671018
0.141351	0.782688	155969	0.028955	87271.8	2.36711	45739.1	30038.4	0.745995
0.143895	0.650828	167329	0.025577	87271.8	2.3589	53248.2	32767.4	0.738594
0.145408	0.792723	157209	0.028824	87271.8	2.3636	36863.8	23891.9	0.729188
0.140646	0.763153	169718	0.027957	87271.8	2.34509	37546.2	25257.2	0.596902
0.145197	0.857431	142440	0.04099	77574.9	2.38582	35499.8	21161.7	0.775143
0.146918	0.79643	162952	0.021332	139635	2.35845	57345.9	41643.5	0.64912
0.146234	0.786923	180827	0.044721	69817.4	2.36062	38905	22529	0.702308
0.142235	0.740548	165391	0.031079	77574.9	2.35965	34814.5	22524.8	0.634571
0.142309	0.658792	153904	0.036654	63470.4	2.33101	31403.6	18431.7	0.692483

0.137109	0.604519	173000	0.025483	87271.8	2.29775	52560.2	32081.2	0.824641
0.136285	0.644797	150279	0.037765	69817.4	2.28434	31397.4	18428.2	0.642789
0.139713	0.860708	194827	0.033496	99739.2	2.38292	42323.5	27305.1	0.548024
0.135851	0.407637	171025	0.021074	116362	2.42359	60743	40269.1	0.776119
0.152604	0.790749	157688	0.040838	87271.8	2.3383	32763	23889.9	0.648128
0.133222	0.592416	167324	0.027295	99739.2	2.21532	34132.3	24574.4	0.315833
0.117592	0.62392	165801	0.035899	87271.8	2.22454	26622	18430.6	0.346197
0.142634	0.863609	191515	0.030947	116362	2.36111	60069.2	39591.9	0.763298
0.150348	0.581367	166362	0.020486	139635	2.41641	45057.8	33452	0.377042
0.153389	0.611091	149971	0.0264	116362	2.38581	53917.5	40268.5	0.526684
0.158168	0.601876	161705	0.020123	139635	2.40884	51875.7	40953.7	0.550404
0.162044	0.677378	166494	0.029536	87271.8	2.4592	42996.2	27299.4	0.689447
0.159197	0.652796	130465	0.029826	116362	2.41137	48459.8	36175	0.576013
0.153042	0.600957	166890	0.01871	174544	2.38336	60064.6	48460	0.446481
0.156913	0.625843	157307	0.021893	139635	2.40158	50503.9	38901.7	0.508791
0.160263	0.721449	159760	0.023557	116362	2.43639	59375.6	42313.6	0.755851
0.155539	0.509946	160143	0.023251	139635	2.41074	45729	35493.2	0.262609
0.155646	0.568289	160624	0.020619	139635	2.44367	51870.8	40268.6	0.443523
0.158436	0.619813	143453	0.027477	116362	2.44292	49823	36854.4	0.606567
0.161467	0.779184	164126	0.025152	116362	2.39126	51196.4	34812.1	0.76132
0.150479	0.6409	128076	0.034847	99739.2	2.44381	36860.1	27301.8	0.555506
0.150528	0.822931	151105	0.031537	87271.8	2.4472	40957.4	24575.7	0.818398
0.152257	0.8062	159556	0.037762	87271.8	2.43734	31399.9	19795.6	0.659159
0.1346	0.739846	177771	0.051241	58181.2	2.37107	30720.3	13653.2	0.500121
0.132519	0.739856	163982	0.033753	58181.2	2.39733	25259	13652.1	0.512911
0.125823	0.687139	175074	0.058148	49869.6	2.36853	33451	9555.97	0.368427
0.155334	0.675755	120171	0.045285	77574.9	2.41965	35499.8	22526.3	0.868508
0.149421	0.816447	162779	0.028671	99739.2	2.45604	45736.8	27307.2	0.635039
0.150906	0.692325	164996	0.023092	139635	2.3048	53920.1	38901.6	0.712274
0.113134	0.695305	206627	0.048478	49869.6	2.36883	21161.7	7508.83	0.343795

Hybrid					
Sdq	Sdq6	Sdr	S3A (nm <sup>2</sup> )	S2A (nm <sup>2</sup> )	Ssc (1/(nm))
3.44283	3.12128	418.594	1.89591E+12	3.65586E+11	0.006987
3.49604	3.08318	437.442	1.96481E+12	3.65586E+11	0.00792
3.1144	2.73565	352.509	1.65431E+12	3.65586E+11	0.006867
2.97296	2.66923	320.762	1.53824E+12	3.65586E+11	0.006331
2.87924	2.49314	306.96	1.48779E+12	3.65586E+11	0.006643
3.05953	2.68401	343.105	1.61993E+12	3.65586E+11	0.00699
3.47649	3.09158	432.895	1.94819E+12	3.65586E+11	0.007741

3.13786	2.74989	360.138	1.68220E+12	3.65586E+11	0.007101
3.14105	2.75845	357.712	1.67333E+12	3.65586E+11	0.0069
2.49492	2.16432	231.392	1.21152E+12	3.65586E+11	0.005348
2.77603	2.4551	282.535	1.39849E+12	3.65586E+11	0.006015
2.68706	2.40075	264.904	1.33404E+12	3.65586E+11	0.005444
2.45376	2.21285	220.722	1.17251E+12	3.65586E+11	0.004667
2.4904	2.23246	227.696	1.19801E+12	3.65586E+11	0.004956
2.88141	2.52942	302.179	1.47031E+12	3.65586E+11	0.006516
2.0208	1.73415	154.799	9.31509E+11	3.65586E+11	0.004477
1.82581	1.58583	129.122	8.37637E+11	3.65586E+11	0.003792
2.81559	2.61193	279.439	1.38718E+12	3.65586E+11	0.004346
3.51828	3.28179	428.29	1.93135E+12	3.65586E+11	0.005746
2.21961	1.92066	185.577	1.04403E+12	3.65586E+11	0.004905
3.14011	2.73204	359.534	1.67999E+12	3.65586E+11	0.007218
3.01451	2.61765	338.653	1.60365E+12	3.65586E+11	0.007027
3.44606	2.97592	431.86	1.94440E+12	3.65586E+11	0.00805
3.27702	2.78996	393.998	1.80598E+12	3.65586E+11	0.007707
2.83207	2.44168	300.43	1.46391E+12	3.65586E+11	0.006529
2.76712	2.39342	286.41	1.41266E+12	3.65586E+11	0.006417
2.90796	2.50726	314.391	1.51495E+12	3.65586E+11	0.006819
2.80961	2.38202	294.782	1.44327E+12	3.65586E+11	0.00661
3.33836	2.89096	407.019	1.85359E+12	3.65586E+11	0.007742
3.51161	3.03624	448.129	2.00388E+12	3.65586E+11	0.008415
2.45154	2.07085	228.12	1.19956E+12	3.65586E+11	0.005815
2.80933	2.42713	295.157	1.44464E+12	3.65586E+11	0.006403
3.94157	3.44214	555.552	2.39660E+12	3.65586E+11	0.009264
2.89629	2.46271	310.897	1.50218E+12	3.65586E+11	0.006923
2.47094	2.10417	230.781	1.20929E+12	3.65586E+11	0.005757
3.58992	3.22158	460.169	2.04790E+12	3.65586E+11	0.007858
4.00107	3.5859	563.833	2.42688E+12	3.65586E+11	0.008939
4.49762	4.10534	698.43	2.91895E+12	3.65586E+11	0.00939
2.76056	2.34704	283.535	1.40215E+12	3.65586E+11	0.006264
2.81063	2.39244	293.753	1.43950E+12	3.65586E+11	0.006702
3.33964	2.96062	392.947	1.80214E+12	3.65586E+11	0.006982

Table C.2 Numerical values of OA grade II cartilages at micron scale, According to the SPIP Classic surface roughness parameters implemented in SPIP

Amplitude parameters								
Sa (nm)	Sq (nm)	Sv (nm)	Sku	Sy (nm)	S10z (nm)	Ssk	Smean	Sp (nm)
12164.4	16009	77747.1	5.05789	225085	177270	1.28248	147338	2.56E-05
15157.7	18582.5	63030.4	2.51873	120424	117226	0.581025	73606.8	2.24E-05
21033.2	33518.2	145223	22.6888	454593	450368	0.819682	83524.6	-4.6E-05
10871.1	13457.7	46799.8	2.9409	108344	104142	0.564979	133513	2.16E-06
7259.65	9261.7	36790.8	3.06259	72088.5	70623.6	0.449643	69352.4	-8.7E-05
11374.9	13890.4	52233.5	2.60441	104746	97425.7	0.430027	111803	2.36E-05
18447.2	23338.8	90508.7	3.31419	169011	165493	0.82907	113112	-1.5E-05
14773.6	18758.8	50734.1	3.17107	124650	119191	0.414948	98243.5	4.56E-05
11621.9	15045.9	49772.5	3.86189	117680	112912	0.132739	179424	1.63E-05
8308.88	10828	39999.9	3.76769	102063	99116.3	0.567874	59136.2	-7.1E-06
14971.3	18863	51831.1	3.24664	125438	123890	0.630445	62429.4	-3E-06
11273.2	15598.7	59262.2	5.34931	142787	139075	0.924354	114418	-6.3E-06
17214.8	22085.1	79769	4.11074	242584	232974	1.65251	172342	-5.63E-05
19808.1	27418.8	197647	5.72718	345580	317623	0.825642	156694	-6.78E-06
19074.4	27129.5	98573.3	8.2423	369842	349841	0.849122	162815	0.000159
12294.9	17784.6	113278	13.8119	285620	269724	1.88179	112330	-0.00011
24880.5	32869.7	141637	3.77399	325799	303922	1.11698	186565	-0.00011
11249.5	16116.2	68544.4	12.4841	264562	254475	1.74909	196018	2.84E-05
15437.6	19343.4	51849.7	3.59707	208544	193070	1.43313	179825	-4.77E-05
10153.2	14844.7	143759	9.7658	330324	302187	1.30729	148145	3.32E-05
9207.09	14202.7	112873	11.1838	225204	197408	0.702913	184162	-0.00016
10670.8	15391.7	69532.7	8.05249	249358	228696	0.933124	147933	-0.00015
12196.3	16771.1	70893.5	6.34396	219038	209045	1.4199	217851	0.000143
19608.4	28483.2	108286	5.94809	326137	300625	1.54853	271268	-0.00011
13485.2	18650.5	131271	5.71933	247731	196416	0.919445	116460	4.73E-05
19709.8	26070.1	136868	5.38705	286554	274703	1.16045	149686	-4.9E-05
11140.4	15376.9	122396	7.47429	253107	232856	1.1757	130711	2.17E-05
35354.7	47501.1	162968	4.84847	384799	380219	0.970142	221831	-0.00014
17417.6	22277.6	100996	3.57927	187742	183816	-0.11899	86745.4	5.54E-05
14179.2	18099.6	225268	4.8707	324167	297798	0.251157	98898.6	-7E-05
16943.5	22772.9	92028.3	4.47112	198615	191992	0.035024	106587	-1.7E-05
15225.5	20313.1	109823	5.97247	222566	211703	-0.64563	112744	-3.1E-05
14291.2	18074.2	82550	3.19781	164871	156417	0.347568	82320.8	7.57E-05
11566.4	15351	73272.6	4.37883	163475	157582	0.228712	90202.4	5.58E-06
9243.83	12341.2	68082.4	4.73362	158653	141730	0.774875	90571.1	1.4E-05
11162	14651.6	77064.1	4.44696	214807	189056	0.736811	137743	-1.5E-05
12956.5	16523.9	42821.4	4.34731	139690	132856	0.4013	61676.2	1.92E-05
10363.6	13641	85274.5	4.70222	169988	157859	0.090204	73969.4	-1.1E-06

7479.46	10221.8	75786.1	7.1695	156593	135791	0.135812	74667.5	1.8E-06
12048.6	15433.3	51613.7	3.38877	113290	110347	1.11828	114457	-1.5E-05
7921.28	10482.4	36513.1	4.5716	102487	95674.2	1.81178	120557	-2.8E-05
15445.6	19005.5	59799.4	2.80312	133769	128722	0.801235	90625.2	-0.00011
12853.2	17585.8	74306	7.14613	188763	176692	0.479546	65284.3	-1.6E-05
10244.5	14395.1	45930.8	7.79449	158689	147018	0.976602	96868.7	-1.8E-05
11264	14849.1	90156.2	4.75363	180781	163586	0.878104	65974	-7.3E-05
10869.7	13695.7	54681	2.92773	119965	107957	1.52885	112758	-1.3E-05
14805.8	21535.8	114718	6.53221	235275	225518	0.988147	84713.3	-8E-06
12195.9	15325.1	51954.3	2.84745	126622	114876	1.1733	80806.7	1.73E-05

Functional parameters									
Spk (nm)	Svk (nm)	Sdc <sub>5_10</sub> (nm)	Sdc <sub>10_50</sub> (nm)	Sdc <sub>50_95</sub> (nm)	Sbi	Sci	Svi	Sk (nm)	Sdc <sub>0_5</sub> (nm)
31589.8	7257.78	13532.2	23906.8	15336.4	0.475502	2.11312	0.060435	31449.9	113670
12589.6	15929.6	4826.62	25339.7	31855.6	0.616883	1.52841	0.113635	50507.1	27270. 4
68421.6	27579	20953.2	35529.3	37351.3	0.650156	1.5447	0.09164	47385.3	257815
16277.2	8587.7	5210.95	19541	19323.9	0.5715	1.69287	0.093854	35190.5	37996. 5
10390.1	9476.81	3900.58	12135.1	15602.3	0.581061	1.6292	0.122976	21815	19358. 4
11916.6	11384.3	4618.07	18892.1	22250.7	0.600663	1.59081	0.102361	39593.6	29387. 7
29598.3	21327.2	12870.5	31160.3	33531.1	0.539286	1.7885	0.094458	60305.4	35224. 6
26732.4	11349.1	10991.2	26728.6	26229	0.525505	1.85083	0.088516	43490.1	38219. 4
26514.6	8552.38	7782.45	24998.2	16744.1	0.506549	1.94397	0.07324	30300.5	38204. 8
15216.4	12079	5113.37	14112.9	16158.3	0.578991	1.65826	0.111474	24440.7	43361. 4
27199.6	10977.5	11312	27148.9	24383.7	0.525432	1.85972	0.08105	45200.6	37706. 8
29614.8	14201.1	10015.1	19457.9	20888.6	0.556851	1.75436	0.102594	29571.6	55512. 3
36612.2	15478.5	10695.1	35488.3	25279.3	0.541382	1.82421	0.079469	41735.7	122021
51377.2	22282.5	18006.2	35319.8	35319.8	0.545274	1.80506	0.099035	51808.5	97648. 8
57795.4	18412.2	17046.8	38540.6	30387.8	0.538274	1.8543	0.083351	43616.5	220867
33435.8	20426.9	8585.77	21750.6	22323	0.632886	1.55857	0.109225	31374.5	144241
61702.4	31208.8	16975.5	56149.7	41132.9	0.498129	1.95289	0.097473	56852.9	118175
32554.8	13361.4	9013.13	19616.8	20147	0.611421	1.63288	0.095555	27382.5	169659
31903.3	8407.83	9612.23	31344.2	21314.1	0.526351	1.89051	0.061976	43302.8	119944
32626.5	17300.9	10591.5	18535.2	17211.3	0.562988	1.7532	0.124877	23216.8	160197
31160.8	14745.1	5867.02	13990.6	18955	0.769465	1.30606	0.115866	22346.4	93872. 5
34630.2	14148.1	10494	21487.8	17989.8	0.532379	1.86796	0.097752	24168.2	150914
35415	12949.8	13607.6	23264.6	19314	0.506089	1.9584	0.091553	28488.1	115006
75391.1	22132	24182.5	43789.9	33986.2	0.44781	2.20924	0.085279	42942.8	154245
38721.3	18367	13404.3	20851.1	26808.5	0.572821	1.70882	0.11787	36714.8	83900. 8
50738.7	13252.7	20099	35603.9	29287.1	0.51204	1.94615	0.071576	58192.2	98772. 1
32310.7	11843.4	8115.64	17245.8	19781.9	0.635582	1.57479	0.095152	32788.1	106518
92279.9	39952.9	33930.1	69402.6	53208.6	0.494108	1.9956	0.075889	99129	125696
24822.2	22158.7	9029.66	28593.9	35742.4	0.60076	1.58543	0.111211	52945.4	49663. 1

25708.7	15374.1	7795.59	27284.6	24036.4	0.55459	1.76014	0.106195	42686.3	66262. 6
35089.2	29338.1	10746.7	24677.7	37016.5	0.644388	1.47232	0.132436	48611.4	71246. 8
22233	28861.2	6690.38	24085.3	29883.7	0.662206	1.42499	0.124739	46743.6	82068. 6
24634.1	16646.5	8590.46	26762.6	25771.4	0.551707	1.74767	0.104839	39740.4	49560. 4
22376.6	20496.5	6879.71	19328.7	23260	0.605885	1.58364	0.121536	34130	64865. 9
21879.7	9594.58	6994.74	16533	16851	0.555575	1.76944	0.096985	25406.1	68357. 7
26599.6	10237	7748.55	20662.8	19801.8	0.549156	1.79684	0.091877	32334.4	111062
26969.6	9367.68	9517.96	25754.5	18196.1	0.526864	1.87835	0.071351	32028.8	65506
24750.4	8625.74	9538.39	19758.1	16010.9	0.502576	1.97321	0.077343	29722.6	57571
19019.4	8353.5	5648.64	13180.2	12238.7	0.586905	1.69619	0.091019	21296.3	63390. 3
22671.3	12196.3	8627.28	20887.1	22930.4	0.545305	1.76983	0.10262	36949.8	33374
18487.5	7323.83	6366.93	15403.9	13144.6	0.519621	1.89201	0.085936	21406.6	45800. 8
19565.4	14110.1	6969.92	24394.7	30560.4	0.611552	1.56604	0.101788	53298.2	42891. 8
31753.8	14250.1	6809.1	20049	26479.8	0.677965	1.43998	0.114267	37532.1	88518. 3
30237.7	10439.5	10176.4	19398.9	15900.7	0.535245	1.86416	0.078118	24885.7	85863. 8
25001.4	11322.3	7970.32	20288.1	19925.8	0.560337	1.7566	0.09307	32168.9	64124. 9
18904.7	8746.39	5529.46	21877.4	18030.9	0.53971	1.79965	0.090574	29355.5	39908. 3
58716.5	8539.07	20745.7	37247.9	16030.8	0.412634	2.42567	0.053893	29108.8	68366. 5
16875.8	13777.5	5075.02	21568.8	25882.6	0.590623	1.61605	0.112187	37852.4	48720. 2

Spatial parameters								
Sds ( $\mu\text{m}^2$ )	Stdi	Srw (nm)	Srwi	Shw (nm)	Sfd	Scl20	Scl37	Str37
0.111408	0.74798	202227	0.024055	174544	2.22606	60740.5	46408.5	0.700802
0.127478	0.41454	164002	0.018067	174544	2.23664	53918.2	42315.3	0.469619
0.110655	0.6042	194278	0.029308	139635	2.1697	49825.2	32758.9	0.631386
0.123208	0.725004	177763	0.030226	174544	2.23876	60740.5	43678.9	0.761668
0.150906	0.743986	173836	0.027524	139635	2.23935	50507.6	36859.6	0.818107
0.119594	0.660088	173854	0.017034	174544	2.27968	70984.8	55966.1	0.766173
0.129764	0.693266	178769	0.024259	232725	2.20762	62798.2	49147.2	0.576057
0.125566	0.538097	190859	0.022833	232725	2.28125	54600.2	43680	0.470476
0.117879	0.612613	166257	0.018259	174544	2.27515	46411.6	37538.6	0.419757
0.135632	0.52326	157117	0.022893	139635	2.26282	45726.6	36171.7	0.546223
0.12187	0.539874	165611	0.018438	174544	2.26825	53917.1	42997.9	0.473572
0.121594	0.647577	121502	0.030104	174544	2.26454	47091.1	37536.3	0.64685
0.10684	0.717341	207691	0.024808	174544	2.1966	54612.7	38909.6	0.587737
0.082585	0.521721	155508	0.028449	99739.2	2.16821	35499.4	17748.3	0.243039
0.084413	0.795073	126163	0.036893	99739.2	2.19968	35495	23891.8	0.603571
0.108199	0.732362	157327	0.04035	63470.4	2.33303	32083.9	18431.2	0.710682
0.093562	0.576029	201053	0.033899	116362	2.1799	40957.4	28669.6	0.552634
0.101213	0.673348	153412	0.0362	87271.8	2.19796	31400.8	19798	0.483484
0.107988	0.674877	176042	0.031765	139635	2.22152	47787.4	37546.5	0.357238
0.11147	0.607996	192183	0.047658	69817.4	2.23148	30716.8	19110.4	0.848256

0.128821	0.603013	166229	0.023791	139635	2.23862	48456	36171.3	0.697142
0.104892	0.741575	124738	0.042765	87271.8	2.20331	32760.5	23887.9	0.777732
0.105382	0.730728	158578	0.030999	116362	2.16735	38913.5	28673	0.763815
0.099692	0.563435	180093	0.031514	139635	2.19562	46415	36175.7	0.344129
0.109471	0.741675	163034	0.019683	174544	2.2116	49830.3	37542.5	0.591435
0.101886	0.528223	171376	0.018801	174544	2.23258	56646.2	42314.2	0.421647
0.101451	0.610558	150351	0.032479	99739.2	2.25602	36175.4	25937.3	0.368924
0.097162	0.399652	348404	0.017475	174544	2.18807	68248.9	48458.3	0.32711
0.101645	0.597581	158659	0.024757	139635	2.2089	51195.3	37544.9	0.639644
0.107411	0.682813	181294	0.03213	139635	2.2286	50509.5	36858.3	0.593376
0.098921	0.284995	165440	0.022445	139635	2.18405	46412.3	33443.6	0.60478
0.101276	0.235971	149551	0.02572	116362	2.24417	36172.7	25252.2	0.468212
0.101418	0.55161	163726	0.024291	116362	2.2483	40952	30032.4	0.444403
0.101579	0.601915	136799	0.034401	116362	2.24185	40267.5	30030.4	0.517531
0.10868	0.616853	158741	0.022679	116362	2.30115	46414.9	34810.3	0.398428
0.10132	0.711506	169549	0.024864	116362	2.23966	47093.9	31396.4	0.589667
0.117094	0.564143	174177	0.019859	174544	2.23594	56648.8	45045	0.549843
0.111049	0.586975	158917	0.032965	99739.2	2.26648	39592.7	27301.5	0.634824
0.125016	0.595232	170290	0.044196	87271.8	2.29444	37537.3	23204.3	0.596299
0.115814	0.441738	153505	0.022317	174544	2.22232	55963.1	45043.5	0.725038
0.123391	0.60686	159192	0.025525	116362	2.26534	45045.6	31396	0.821214
0.106736	0.696359	163605	0.023765	174544	2.21345	51187.6	40268.6	0.678018
0.123996	0.823111	158110	0.018607	174544	2.23254	51880.6	39593.6	0.604291
0.121512	0.739025	164785	0.025652	139635	2.20193	51880.7	37546.7	0.809046
0.107228	0.476699	161589	0.025572	139635	2.22516	47103.8	34133.5	0.735501
0.122549	0.810089	155615	0.021928	174544	2.2551	58010.7	45043.6	0.956229
0.123268	0.474104	348404	0.021486	174544	2.21296	53236.9	40269	0.172993
0.120719	0.419127	169459	0.017548	174544	2.25028	56649.2	42316	0.607745

Hybrid parameters						
Sdq	Sdq6	Sdr	S3A (nm <sup>2</sup> )	S2A (nm <sup>2</sup> )	Ssc (1/(nm))	
3.72457	3.45577	483.23	2.13221E+12	3.65586E+11	0.006881	
3.14055	2.83754	354.056	1.65996E+12	3.65586E+11	0.006192	
7.37036	7.05236	1703.55	6.59352E+12	3.65586E+11	0.006803	
2.88161	2.59149	304.858	1.48010E+12	3.65586E+11	0.006242	
2.78127	2.46537	286.338	1.41239E+12	3.65586E+11	0.005632	
3.46608	3.15066	425.556	1.92136E+12	3.65586E+11	0.007286	
3.27091	2.94086	375.328	1.73773E+12	3.65586E+11	0.006336	
3.79259	3.42447	498.702	2.18877E+12	3.65586E+11	0.007683	
3.44813	3.13051	419.531	1.89933E+12	3.65586E+11	0.007072	
2.65417	2.38445	259.16	1.31304E+12	3.65586E+11	0.00537	
3.43006	3.10224	414.152	1.87967E+12	3.65586E+11	0.007017	
3.70148	3.36924	477.672	2.11189E+12	3.65586E+11	0.007457	

5.21666	4.90958	899.133	3.65269E+12	3.65586E+11	0.008593
6.99152	6.68519	1581.52	6.14741E+12	3.65586E+11	0.008267
8.02283	7.57531	2066.84	7.92167E+12	3.65586E+11	0.010798
9.25749	8.59103	2473.64	9.40885E+12	3.65586E+11	0.013762
7.70236	7.29579	1920.37	7.38618E+12	3.65586E+11	0.010194
4.94276	4.67794	809.605	3.32539E+12	3.65586E+11	0.00756
4.81015	4.4893	777.86	3.20933E+12	3.65586E+11	0.008643
5.48992	5.15385	994.836	4.00256E+12	3.65586E+11	0.008899
4.14148	3.81423	583.611	2.49918E+12	3.65586E+11	0.007419
4.46883	4.20639	675.879	2.83650E+12	3.65586E+11	0.007039
3.97007	3.75344	537.684	2.33128E+12	3.65586E+11	0.006089
6.46821	6.13049	1361.31	5.34234E+12	3.65586E+11	0.008211
3.92001	3.6529	518.317	2.26048E+12	3.65586E+11	0.00656
5.75323	5.3912	1079.09	4.31060E+12	3.65586E+11	0.009516
5.09332	4.77012	861.111	3.51368E+12	3.65586E+11	0.008738
7.2946	6.94844	1676.46	6.49448E+12	3.65586E+11	0.007598
4.47403	4.18607	652.5	2.75103E+12	3.65586E+11	0.007171
4.43135	4.10352	651.999	2.74920E+12	3.65586E+11	0.007181
4.23005	3.99081	584.067	2.50085E+12	3.65586E+11	0.006505
4.81652	4.50251	757.387	3.13448E+12	3.65586E+11	0.008367
5.03931	4.73868	833.241	3.41179E+12	3.65586E+11	0.008492
4.40822	4.11651	659.438	2.77640E+12	3.65586E+11	0.008236
4.39968	4.06337	655.898	2.76346E+12	3.65586E+11	0.008555
4.74067	4.44111	758.351	3.13801E+12	3.65586E+11	0.008583
3.27097	2.99577	376.176	1.74083E+12	3.65586E+11	0.006244
4.95111	4.61195	824.127	3.37848E+12	3.65586E+11	0.008907
4.3219	3.96621	636.872	2.69390E+12	3.65586E+11	0.008525
2.98421	2.72419	318.435	1.52974E+12	3.65586E+11	0.005728
3.55297	3.23529	445.198	1.99316E+12	3.65586E+11	0.007216
3.29452	3.03844	375.83	1.73957E+12	3.65586E+11	0.006092
3.71396	3.39722	476.364	2.10710E+12	3.65586E+11	0.006937
3.51842	3.25945	431.127	1.94172E+12	3.65586E+11	0.006012
4.04385	3.77432	555.467	2.39629E+12	3.65586E+11	0.007075
3.50378	3.19114	429.063	1.93418E+12	3.65586E+11	0.006878
4.61788	4.32535	712.46	2.97024E+12	3.65586E+11	0.006989
3.2732	2.96838	377.868	1.74702E+12	3.65586E+11	0.006529

---

Table C.3 Numerical values of OA grade III cartilages at micron scale, According to the SPIP Classic surface roughness parameters implemented in SPIP

Amplitude parameters								
Sa (nm)	Sq (nm)	Sv (nm)	Sku	Sy (nm)	S10z (nm)	Ssk	Smean	Sp (nm)
12083.2	16280	48456.5	4.76431	131797	128865	0.631624	170676	-0.0002087
8963.89	12059.8	44474.3	4.77779	112433	107030	0.772999	67958.2	-1.41E-05
10821.1	13777.8	80690.7	3.29068	141809	135851	0.863341	136752	-0.0001641
14985.4	20617.1	93437.9	5.20443	195245	157263	0.812116	114621	1.45E-05
15568.4	21467.5	81059.3	8.02234	251735	249099	0.321573	61117.8	-0.0001054
12876.1	18636	72382.1	6.92499	188777	173992	1.33031	103350	-8.56E-05
22624.6	29950.6	70058.1	4.0387	206811	200156	1.13036	83340.4	9.21E-06
9987.54	14228	62203.7	7.38312	161395	140585	1.31724	100378	-9.58E-06
13136	19365.3	105621	8.19403	267568	235251	1.31224	101807	-3.07E-07
12976.5	18153	50297.1	5.98648	150675	147564	1.52122	99190.9	2.87E-05
15711.6	20875.1	49064.9	4.76465	152415	144698	1.73097	116395	9.89E-05
17866.9	23842.7	83246.3	4.42737	197867	189461	2.00937	161947	6.90E-05
15636.1	20687.7	69275.2	5.28689	191122	180263	1.04445	116036	-3.79E-06
13315.2	16984.7	179225	4.24725	260476	233970	0.970082	114894	0.0001276
15687.6	21860.1	145143	8.05458	252088	246814	1.27653	121847	9.57E-06
26450.7	37127	127455	6.07339	306107	300405	0.771266	109143	-5.31E-05
16248.5	24187.7	95272.6	9.58381	268153	247281	0.504315	81251.5	8.82E-05
20627.6	26454	116530	3.70394	232306	208804	0.895063	147745	-9.02E-05
16922.6	21921.6	114627	4.22018	229521	219478	0.310613	106945	-0.0001172
17462.3	22997.5	61118.6	4.38695	177154	168428	0.730586	115776	-5.04E-05
24306.4	32320	117031	4.61986	264776	255876	0.958672	127051	-3.61E-05
25202.8	33684.7	117273	4.42462	279488	273277	0.547529	162215	1.08E-06
18893.5	24422	158539	4.47209	285589	259704	1.85225	172880	-1.53E-05
15240.4	19295.2	57938.6	3.95208	167082	159367	1.52098	178651	5.02E-06
27547.9	34694.6	189008	2.93937	321345	290100	-0.44754	101534	-3.81E-06
26814.1	32678.9	116537	2.75533	250461	238787	-0.21189	156289	-3.78E-05
17331.1	24706.1	149122	6.20695	282796	277229	0.847333	133674	-2.92E-05
22082.8	28918.7	106535	4.59536	258904	252234	0.934611	147650	4.62E-07
25163.5	32953.4	150099	3.40667	327027	302292	0.818396	105131	-1.84E-05
14409.2	19975.1	87193.1	5.51608	192324	185720	0.648447	100348	-5.12E-05
27376.8	35737.1	123228	4.05673	270878	253214	-0.24733	132337	8.81E-05
11090.2	16067	123964	10.7345	288160	272761	0.262217	133923	0.0001075
19146.9	23930.5	101835	3.03387	211167	205290	0.125906	109332	-0.0001558
13877.3	18621.3	84031.7	4.68213	184380	179442	0.715554	176928	0.0002606
33673.5	41850.5	249274	3.63312	350808	345201	1.35573	164196	-0.000125
31287.8	43007.2	232633	4.03276	388922	355680	1.2025	152369	0.0001692
19421.7	26394.4	177923	6.55397	266850	264512	-0.76096	88927.6	8.56E-05
30285.6	40721.4	158178	4.49587	325163	318617	-0.18782	166985	5.79E-05

37193.8	46883.8	159893	3.02441	326952	309764	0.027871	167058	0.0002753
23989.9	34890.6	204881	9.73728	445281	413898	1.38147	240401	-4.90E-06
11588.6	17349.4	99951.3	8.27634	203239	200486	0.271676	103287	6.47E-05
13733	18919.1	79933.7	4.85635	187073	180470	0.219314	107139	1.77E-05
19394.1	26691.9	102943	6.91001	254188	246098	1.24603	151245	1.36E-05
27963.9	36926.4	145166	3.66362	295547	291445	-0.27471	150381	-1.52E-06
15597.9	23118.9	87404	5.9002	209285	195915	1.27698	121881	-0.0001062
10512.7	15495.9	105965	8.41088	210606	195121	0.937635	104641	-8.03E-06
51330.7	68500.9	262571	3.68264	431493	427535	-0.84979	168922	-7.95E-05
41498.9	54669.1	243697	3.80968	400209	390134	-0.47289	156511	-1.50E-05

Functional parameters									
Spk (nm)	Svk (nm)	Sdc <sub>5_10</sub> (nm)	Sdc <sub>10_50</sub> (nm)	Sdc <sub>50_95</sub> (nm)	Sbi	Sci	Svi	Sk (nm)	Sdc <sub>0_5</sub> (nm)
33540.7	11062	10829	26676.3	17432.1	0.479535	2.05445	0.078474	27880.8	49390.8
21730.9	10833.5	7660.73	16898.7	16222.7	0.526745	1.84763	0.103516	23174.2	45063.1
19874.5	10680	7673.01	17903.7	21313.9	0.550532	1.75976	0.101961	33346.2	36091.5
42335.6	10873.7	20737.4	28954.2	22302.5	0.449615	2.20861	0.071178	36349.3	55952
34429.1	27578.7	8071.66	24215	33295.6	0.682822	1.4041	0.12634	45539.6	139236
45522.9	11138.8	17024	28751.7	17402.3	0.449174	2.22296	0.067468	26212.8	74905.6
55190	18712.8	24452.5	43517.3	37300.5	0.469378	2.0897	0.079499	62148.2	72943.2
33303	10211.8	11643.7	16495.2	16818.7	0.545251	1.83445	0.083527	27077.9	73096.5
51954.3	9299.03	17694.9	30563.9	15013.8	0.45131	2.23617	0.059612	27965.3	119038
38275.9	12779.3	12984	25968.1	20834.9	0.507635	1.94764	0.084793	31311	64618.3
43060.8	7151.02	17104.7	34514.8	18937.3	0.451525	2.20688	0.054672	37076.2	57117.3
42840.9	17495.8	17447.2	31722.2	30929.1	0.513649	1.90783	0.090579	49745.2	68202.7
38915.8	8191.16	12639.3	32172.8	21448.5	0.51378	1.94228	0.064835	41143.6	81581.1
25532.5	13377.3	8351.95	27143.8	19835.9	0.527739	1.86312	0.089823	37357.9	49067.6
38652.1	16982.6	15155.6	30816.4	22228.2	0.523267	1.88133	0.08107	38633.2	65169.2
84312.7	19101.4	31285.5	56436.5	36806.4	0.464742	2.14266	0.066639	63590.6	98763.8
59743.3	18099	20420.4	25794.2	27943.8	0.564683	1.77621	0.086488	42863.6	130046
42256.7	20600.1	15362.9	41433.3	28863.6	0.508763	1.93408	0.074187	57724.8	63779.3
38068.6	12140.5	12878.9	35417.1	24378	0.502784	1.96644	0.074993	45518.8	71294.1
43244.3	13756.1	17750.9	35146.8	24141.3	0.476859	2.07535	0.067615	46496.8	67808.5
59368.5	26780.2	21224.5	44571.5	42979.6	0.527627	1.85599	0.094419	66652.5	86489.9
53715	32477.2	17923.1	45367.8	48168.2	0.558827	1.72528	0.112592	66659.7	101937
40280.8	13646.1	13735.8	37773.4	26899.2	0.526869	1.88009	0.07737	50327.8	80697.6
29122	11257.5	9375.33	28460.8	23773.2	0.554298	1.77977	0.075485	44256.4	74333
33096.3	41460.9	10947.6	39926.6	65685.7	0.653039	1.43111	0.137779	82528.4	79209.2
34268.9	29241.7	10540.4	48686.7	42161.7	0.587506	1.64948	0.084823	82587.6	78300.3
47241.5	29491.1	16435	30603.2	30603.2	0.567119	1.73109	0.106173	42677.1	90109.3
56216.5	15158.5	23866.9	47733.8	25423.5	0.458097	2.16876	0.060745	49578.6	89241.5
62709.5	26922	16384.1	58982.9	38011.2	0.48363	2.01212	0.091971	58016	108791
37182.4	22708.9	13489.7	26979.4	22739.7	0.530087	1.84803	0.096966	37121.8	67448.4
60195.6	26754.1	23342.2	54827	37998.9	0.502567	1.96802	0.070703	74112.8	76540.6

33532.3	14547.3	10394.5	18479.2	18479.2	0.600475	1.66516	0.09503	28728.5	137439
26738.9	20901.4	8886.78	31315.3	36393.5	0.605726	1.58641	0.103969	61901.5	69824.7
34574.3	18153.6	12932.5	24017.5	25125.9	0.527268	1.84658	0.102384	40544.5	65031.9
30876.4	64715.6	11951.4	55538.7	64678	0.644087	1.44806	0.126612	99014.5	36557.1
62993.9	65802.2	21823.3	59234.5	71705	0.543513	1.71195	0.157481	73688.3	77160.8
28559.3	34851.7	9625.88	33155.8	36899.1	0.622472	1.50609	0.132117	56181.3	46525
48026.8	60792.5	14987.5	50175.5	64511.4	0.642534	1.45493	0.143097	83563.3	103609
50749.1	54262.2	17690.8	66831.8	72073.5	0.5819	1.63408	0.11259	110574	86488.2
64232	35086.9	18739.3	41048	41940.3	0.636776	1.55147	0.105817	56507.3	185608
33746.6	29431.2	10996.9	18735.4	21586.5	0.603398	1.60277	0.119294	30268.4	74534.4
31644.4	25779.4	10497.1	20619.2	31866.1	0.617058	1.53985	0.13843	35902.3	76478.6
44544.8	27253.9	13244.3	34638.8	29035.5	0.617102	1.61435	0.0829	49728.2	107992
41449.8	46989.5	13030.1	42644	68112	0.636817	1.47244	0.13221	68077.3	92395.4
59981.6	20938.9	32713.9	25164.6	30616.9	0.412588	2.37409	0.096478	32626.9	65847.3
28513.5	19407.6	8863.19	17304.3	21524.9	0.623014	1.55915	0.125466	25484.6	79768.7
50304.4	133171	17294.3	67447.8	164296	0.717881	1.21631	0.197678	117957	73500.8
51456.7	80295.5	21654.6	68171.8	97044.6	0.613284	1.49733	0.156862	112704	67369.8

Spatial Parameters								
Sds ( $\mu\text{m}^2$ )	Stdi	Srw (nm)	Srwi	Shw (nm)	Sfd	Scl20	Scl37	Str37
0.116331	0.426665	171945	0.024952	116362	2.23786	36857.6	27983.9	0.630708
0.122759	0.691469	157358	0.031122	139635	2.20531	35494.1	27985.5	0.49397
0.113894	0.544331	183819	0.026989	174544	2.26689	70298.1	52552.3	0.76215
0.108087	0.608624	147566	0.025325	139635	2.22169	47774.2	34806.8	0.688981
0.111405	0.44429	158672	0.027307	139635	2.18429	42324.5	29355.3	0.462504
0.107201	0.594781	156080	0.034012	99739.2	2.18311	34809.1	23887.9	0.613877
0.107589	0.437644	162912	0.016286	174544	2.2039	53234.6	42997.6	0.223353
0.116566	0.516149	166184	0.021437	139635	2.24569	44366.3	30712.7	0.499862
0.121082	0.696787	165166	0.026477	99739.2	2.20988	30033.6	21842.7	0.492283
0.111465	0.464691	156173	0.029893	116362	2.22722	33443	25252.2	0.52099
0.10679	0.747024	177035	0.032297	139635	2.21301	46417.4	32767	0.615535
0.117685	0.385372	152071	0.020958	174544	2.24367	53236.4	40266.4	0.655346
0.102028	0.574475	112296	0.031708	116362	2.21683	34806.3	25934.1	0.633147
0.098478	0.725436	158380	0.029047	116362	2.21477	40948.7	30029	0.676702
0.106963	0.644971	158743	0.028724	99739.2	2.21305	35489.1	25934.4	0.666522
0.100587	0.478107	171114	0.033557	116362	2.2017	40272.5	29352.6	0.323322
0.110092	0.494213	131493	0.035676	99739.2	2.23723	30712.4	23205	0.320681
0.098059	0.49701	141804	0.028323	116362	2.23227	44361.2	32076.7	0.839019
0.099528	0.715672	122988	0.03352	116362	2.19613	42998.1	32076.8	0.870095
0.099151	0.656415	136566	0.028581	139635	2.18851	43000.7	34126.2	0.714233
0.099741	0.445726	154891	0.025443	139635	2.22947	40948.8	31394.2	0.308644
0.089396	0.56146	142142	0.025569	139635	2.17076	51868.3	38901.2	0.770019
0.097225	0.711971	161320	0.0272	116362	2.19066	44368.5	31395.3	0.806865
0.096593	0.679204	119514	0.03487	116362	2.20787	42313.8	32759	0.799759

0.094295	0.710424	165650	0.020751	139635	2.21477	60058	41639.3	0.813248
0.100368	0.716946	147236	0.031297	99739.2	2.25884	45048.1	32077.2	0.939716
0.106369	0.664375	177813	0.044885	77574.9	2.20428	34809.3	17745.8	0.530531
0.106897	0.437805	169148	0.024429	139635	2.18911	42314.4	31394.2	0.489216
0.097849	0.537721	142751	0.025874	139635	2.18923	45736.7	34132.1	0.57485
0.114583	0.67209	168091	0.027816	116362	2.21684	46411.8	32077.5	0.870119
0.105483	0.629489	159975	0.023583	139635	2.21635	53916.2	41631.9	0.503996
0.119236	0.877445	168473	0.030813	99739.2	2.22702	43010.1	26624.1	0.684388
0.105387	0.887142	135320	0.030861	99739.2	2.24719	50519.3	31402.1	0.779858
0.110702	0.767362	152857	0.032491	99739.2	2.22208	41631.3	28664.4	0.874724
0.093095	0.541167	155886	0.022525	139635	2.17172	56659	44361.1	0.955572
0.089798	0.52102	166180	0.025886	116362	2.23014	47092.7	32759.8	0.761678
0.09964	0.678697	139853	0.031994	116362	2.19142	43682.7	32080.7	0.854641
0.088338	0.746386	161979	0.025261	139635	2.1823	43687.4	33446.5	0.742456
0.092982	0.703035	144615	0.022662	139635	2.20994	47785.6	37544.4	0.662744
0.100614	0.702996	348404	0.028936	116362	2.19693	39593.5	27305.2	0.666814
0.134953	0.70161	116225	0.038156	116362	2.27977	43684.7	32082.6	0.770559
0.135424	0.496201	153227	0.030434	116362	2.31756	38220.5	28665.2	0.482636
0.123998	0.806801	166284	0.02956	99739.2	2.26152	47091.6	30711.7	0.833117
0.116952	0.663293	348404	0.020081	174544	2.22793	73025.4	52551.6	0.681261
0.137322	0.415689	167252	0.021589	139635	2.24528	40275.9	30719.7	0.136395
0.126148	0.779974	146222	0.031977	99739.2	2.26273	38910.6	27989.4	0.707083
0.112983	0.618099	183240	0.033095	139635	2.29368	54601.6	39586.1	0.467666
0.10403	0.635601	166705	0.024715	116362	2.29696	49822.2	36854.7	0.586794

Hybrid parameters						
Sdq	Sdq6	Sdr	S3A (nm <sup>2</sup> )	S2A (nm <sup>2</sup> )	Ssc (1/(nm))	
4.0603	3.7284	565.687	2.43366E+12	3.65586E+11	0.007846	
2.44018	2.22726	219.147	1.16675E+12	3.65586E+11	0.004565	
3.51851	3.21242	432.934	1.94833E+12	3.65586E+11	0.007041	
4.57543	4.27756	702.724	2.93464E+12	3.65586E+11	0.007824	
4.09629	3.83605	507.118	2.21954E+12	3.65586E+11	0.005226	
4.52724	4.27392	680.865	2.85473E+12	3.65586E+11	0.007104	
3.40586	3.12981	393.579	1.80446E+12	3.65586E+11	0.006312	
3.80183	3.51014	493.254	2.16885E+12	3.65586E+11	0.006884	
5.42931	5.08135	977.455	3.93902E+12	3.65586E+11	0.009043	
4.16352	3.86834	568.888	2.44536E+12	3.65586E+11	0.006983	
4.97677	4.62358	817.727	3.35508E+12	3.65586E+11	0.008997	
4.59609	4.22435	667.924	2.80742E+12	3.65586E+11	0.008046	
4.6822	4.38938	719.074	2.99442E+12	3.65586E+11	0.007427	
4.38414	4.10145	653.306	2.75398E+12	3.65586E+11	0.006674	
5.2088	4.87314	902.437	3.66477E+12	3.65586E+11	0.00889	
8.26961	7.83975	2175.65	8.31944E+12	3.65586E+11	0.011037	

6.11043	5.73409	1197.59	4.74381E+12	3.65586E+11	0.009673
6.27845	5.86658	1256.63	4.95965E+12	3.65586E+11	0.010238
4.63194	4.36422	703.682	2.93815E+12	3.65586E+11	0.007044
3.93367	3.67161	526.063	2.28880E+12	3.65586E+11	0.006712
7.1753	6.7743	1601.01	6.21864E+12	3.65586E+11	0.010191
6.13552	5.83567	1192.71	4.72597E+12	3.65586E+11	0.008139
5.6072	5.28923	1032.26	4.13936E+12	3.65586E+11	0.00818
3.86112	3.5964	509.771	2.22923E+12	3.65586E+11	0.006979
9.16874	8.73251	2598.14	9.86403E+12	3.65586E+11	0.011935
10.9266	10.3023	3470.88	1.30546E+13	3.65586E+11	0.014898
8.1112	7.71957	2132.6	8.16207E+12	3.65586E+11	0.010026
6.05454	5.69849	1207.39	4.77963E+12	3.65586E+11	0.009774
7.0061	6.63483	1568.32	6.09914E+12	3.65586E+11	0.010937
5.74468	5.40423	1088.91	4.34648E+12	3.65586E+11	0.008977
8.26923	7.83039	2114.5	8.09589E+12	3.65586E+11	0.011375
5.05245	4.70358	853.026	3.48413E+12	3.65586E+11	0.00865
8.00868	7.54676	2001	7.68097E+12	3.65586E+11	0.012259
5.81844	5.47851	1114.95	4.44169E+12	3.65586E+11	0.009197
8.04969	7.60839	2025.68	7.77118E+12	3.65586E+11	0.006561
12.3224	11.6891	4449.07	1.66307E+13	3.65586E+11	0.01391
5.25887	4.94071	881.313	3.58754E+12	3.65586E+11	0.00642
7.74881	7.37762	1825.12	7.03797E+12	3.65586E+11	0.008188
8.49716	8.02566	2115.8	8.10066E+12	3.65586E+11	0.009977
9.13181	8.67796	2568.88	9.75703E+12	3.65586E+11	0.010336
5.94457	5.47809	1121.28	4.46482E+12	3.65586E+11	0.010217
7.27904	6.63939	1643.69	6.37467E+12	3.65586E+11	0.013211
9.39283	8.82004	2592	9.84156E+12	3.65586E+11	0.012414
8.44518	7.91488	2181.41	8.34051E+12	3.65586E+11	0.012685
5.6179	5.22614	1001.82	4.02810E+12	3.65586E+11	0.008629
5.30501	4.91663	919.704	3.72789E+12	3.65586E+11	0.009338
23.2301	21.9342	13431.5	4.94694E+13	3.65586E+11	0.018689
18.5677	17.3321	8806.4	3.25605E+13	3.65586E+11	0.020894

## Appendix D Statistical result, using the Engineering statistical software, Minitab.

Welcome to Minitab, press F1 for help.  
Retrieving project from file: 'D:\USERS\Z3399001\DESKTOP\UPDATED  
DATA\21-11\35 PARAM.MPJ'

### General Linear Model: LN Sa versus OA GRADE, SaSAMPLE

Factor	Type	Levels	Values
OA GRADE	fixed	3	1, 2, 3
SaSAMPLE (OA GRADE)	fixed	12	1, 2, 3, 4, 5, 6, 7, 8, 9, 10, 11, 12

Analysis of Variance for LN Sa, using Adjusted SS for Tests

Source	DF	Seq SS	Adj SS	Adj MS	F	P
OA GRADE	2	67.6649	67.6649	33.8325	321.45	0.000
SaSAMPLE (OA GRADE)	9	2.8704	2.8704	0.3189	3.03	0.003
Error	132	13.8931	13.8931	0.1053		
Total	143	84.4284				

S = 0.324424    R-Sq = 83.54%    R-Sq(adj) = 82.17%

Unusual Observations for LN Sa

Obs	LN Sa	Fit	SE Fit	Residual	St Resid
22	8.9441	8.1583	0.0937	0.7858	2.53 R
76	10.4732	9.6048	0.0937	0.8683	2.80 R
128	9.3138	9.9664	0.0937	-0.6526	-2.10 R
137	9.3578	10.0161	0.0937	-0.6583	-2.12 R
142	9.2603	10.0161	0.0937	-0.7558	-2.43 R
143	10.8460	10.0161	0.0937	0.8299	2.67 R

R denotes an observation with a large standardized residual.

Grouping Information Using Tukey Method and 95.0% Confidence

OA			
GRADE	N	Mean	Grouping
3	48	9.8	A
2	48	9.5	B
1	48	8.2	C

Means that do not share a letter are significantly different.

Tukey Simultaneous Tests

Response Variable LN Sa

All Pairwise Comparisons among Levels of OA GRADE

OA GRADE = 1 subtracted from:

OA	Difference	SE of		Adjusted
GRADE	of Means	Difference	T-Value	P-Value
2	1.254	0.06622	18.93	0.0000
3	1.594	0.06622	24.07	0.0000

OA GRADE = 2 subtracted from:

OA GRADE	Difference of Means	SE of Difference	T-Value	Adjusted P-Value
3	0.3407	0.06622	5.145	0.0000

## General Linear Model: LNSq versus OA GRADE, SqSAMPLE

Factor	Type	Levels	Values
OA GRADE	fixed	3	1, 2, 3
SqSAMPLE (OA GRADE)	fixed	12	1, 2, 3, 4, 5, 6, 7, 8, 9, 10, 11, 12

Analysis of Variance for LNSq, using Adjusted SS for Tests

Source	DF	Seq SS	Adj SS	Adj MS	F	P
OA GRADE	2	68.7202	68.7202	34.3601	323.57	0.000
SqSAMPLE (OA GRADE)	9	2.9725	2.9725	0.3303	3.11	0.002
Error	132	14.0172	14.0172	0.1062		
Total	143	85.7099				

S = 0.325870 R-Sq = 83.65% R-Sq(adj) = 82.28%

Unusual Observations for LNSq

Obs	LNSq	Fit	SE Fit	Residual	St Resid
1	9.3201	8.6820	0.0941	0.6382	2.05 R
21	9.1662	8.4610	0.0941	0.7052	2.26 R
22	9.2836	8.4610	0.0941	0.8225	2.64 R
51	10.4198	9.7014	0.0941	0.7185	2.30 R
76	10.7685	9.8861	0.0941	0.8824	2.83 R
142	9.6483	10.3391	0.0941	-0.6908	-2.21 R
143	11.1346	10.3391	0.0941	0.7955	2.55 R

R denotes an observation with a large standardized residual.

Grouping Information Using Tukey Method and 95.0% Confidence

OA GRADE	N	Mean	Grouping
3	48	10.1	A
2	48	9.8	B
1	48	8.5	C

Means that do not share a letter are significantly different.

Tukey Simultaneous Tests

Response Variable LNSq

All Pairwise Comparisons among Levels of OA GRADE

OA GRADE = 1 subtracted from:

OA GRADE	Difference of Means	SE of Difference	T-Value	Adjusted P-Value
2	1.257	0.06652	18.90	0.0000
3	1.609	0.06652	24.20	0.0000

OA GRADE = 2 subtracted from:

OA GRADE	Difference of Means	SE of Difference	T-Value	Adjusted P-Value
----------	---------------------	------------------	---------	------------------

GRADE	of Means	Difference	T-Value	P-Value
3	0.3521	0.06652	5.293	0.0000

## Residual Plots for LNSq

## General Linear Model: LNSv versus OA GRADE, SvSAMPLE

Factor	Type	Levels	Values
OA GRADE	fixed	3	1, 2, 3
SvSAMPLE (OA GRADE)	fixed	12	1, 2, 3, 4, 5, 6, 7, 8, 9, 10, 11, 12

Analysis of Variance for LNSv, using Adjusted SS for Tests

Source	DF	Seq SS	Adj SS	Adj MS	F	P
OA GRADE	2	43.0254	43.0254	21.5127	168.93	0.000
SvSAMPLE (OA GRADE)	9	9.4142	9.4142	1.0460	8.21	0.000
Error	132	16.8094	16.8094	0.1273		
Total	143	69.2490				

S = 0.356852    R-Sq = 75.73%    R-Sq(adj) = 73.70%

Unusual Observations for LNSv

Obs	LNSv	Fit	SE Fit	Residual	St Resid
21	11.2759	10.3803	0.1030	0.8956	2.62 R
22	11.3084	10.3803	0.1030	0.9281	2.72 R
46	11.2443	10.4730	0.1030	0.7713	2.26 R
51	11.8860	10.9861	0.1030	0.8999	2.63 R
62	12.1942	11.4909	0.1030	0.7034	2.06 R
78	12.3250	11.5930	0.1030	0.7320	2.14 R

R denotes an observation with a large standardized residual.

Grouping Information Using Tukey Method and 95.0% Confidence

OA GRADE	N	Mean	Grouping
3	48	11.6	A
2	48	11.3	B
1	48	10.3	C

Means that do not share a letter are significantly different.

Tukey Simultaneous Tests

Response Variable LNSv

All Pairwise Comparisons among Levels of OA GRADE

OA GRADE = 1 subtracted from:

OA GRADE	Difference of Means	SE of Difference	T-Value	Adjusted P-Value
2	0.9680	0.07284	13.29	0.0000
3	1.2851	0.07284	17.64	0.0000

OA GRADE = 2 subtracted from:

OA GRADE	Difference of Means	SE of Difference	T-Value	Adjusted P-Value
----------	---------------------	------------------	---------	------------------

3                    0.3171            0.07284            4.353            0.0001

## Residual Plots for LNSv

### General Linear Model: LNSdq versus OA GRADE, SdqSAMPLE

Factor	Type	Levels	Values
OA GRADE	fixed	3	1, 2, 3
SdqSAMPLE (OA GRADE)	fixed	12	1, 2, 3, 4, 5, 6, 7, 8, 9, 10, 11, 12

Analysis of Variance for LNSdq, using Adjusted SS for Tests

Source	DF	Seq SS	Adj SS	Adj MS	F	P
OA GRADE	2	11.4021	11.4021	5.7010	98.55	0.000
SdqSAMPLE (OA GRADE)	9	6.6126	6.6126	0.7347	12.70	0.000
Error	132	7.6365	7.6365	0.0579		
Total	143	25.6511				

S = 0.240525    R-Sq = 70.23%    R-Sq(adj) = 67.75%

Unusual Observations for LNSdq

Obs	LNSdq	Fit	SE Fit	Residual	St Resid
51	1.99747	1.25454	0.06943	0.74293	3.23 R
64	2.22543	1.74844	0.06943	0.47700	2.07 R
98	0.89207	1.40012	0.06943	-0.50804	-2.21 R
132	2.51142	2.03059	0.06943	0.48082	2.09 R
133	1.65992	2.13845	0.06943	-0.47854	-2.08 R
142	1.66865	2.13845	0.06943	-0.46980	-2.04 R
143	3.14545	2.13845	0.06943	1.00699	4.37 R
144	2.92142	2.13845	0.06943	0.78297	3.40 R

R denotes an observation with a large standardized residual.

Grouping Information Using Tukey Method and 95.0% Confidence

OA GRADE	N	Mean	Grouping
3	48	1.8	A
2	48	1.5	B
1	48	1.1	C

Means that do not share a letter are significantly different.

Tukey Simultaneous Tests

Response Variable LNSdq

All Pairwise Comparisons among Levels of OA GRADE

OA GRADE = 1 subtracted from:

OA GRADE	Difference of Means	SE of Difference	T-Value	Adjusted P-Value
2	0.3480	0.04910	7.088	0.0000
3	0.6893	0.04910	14.039	0.0000

OA GRADE = 2 subtracted from:

OA	Difference	SE of	Adjusted
----	------------	-------	----------

GRADE	of Means	Difference	T-Value	P-Value
3	0.3412	0.04910	6.950	0.0000

## Residual Plots for LNSdq

### General Linear Model: LNSdq6 versus OA GRADE, Sdq6SAMPLE

Factor	Type	Levels	Values
OA GRADE	fixed	3	1, 2, 3
Sdq6SAMPLE(OA GRADE)	fixed	12	1, 2, 3, 4, 5, 6, 7, 8, 9, 10, 11, 12

Analysis of Variance for LNSdq6, using Adjusted SS for Tests

Source	DF	Seq SS	Adj SS	Adj MS	F	P
OA GRADE	2	13.6476	13.6476	6.8238	110.00	0.000
Sdq6SAMPLE(OA GRADE)	9	7.0039	7.0039	0.7782	12.54	0.000
Error	132	8.1888	8.1888	0.0620		
Total	143	28.8402				

S = 0.249070    R-Sq = 71.61%    R-Sq(adj) = 69.24%

Unusual Observations for LNSdq6

Obs	LNSdq6	Fit	SE Fit	Residual	St Resid
51	1.95336	1.15876	0.07190	0.79460	3.33 R
98	0.80077	1.32343	0.07190	-0.52266	-2.19 R
132	2.45866	1.97326	0.07190	0.48540	2.04 R
142	1.59262	2.07215	0.07190	-0.47953	-2.01 R
143	3.08805	2.07215	0.07190	1.01589	4.26 R
144	2.85256	2.07215	0.07190	0.78041	3.27 R

R denotes an observation with a large standardized residual.

Grouping Information Using Tukey Method and 95.0% Confidence

OA GRADE	N	Mean	Grouping
3	48	1.7	A
2	48	1.4	B
1	48	1.0	C

Means that do not share a letter are significantly different.

Tukey Simultaneous Tests

Response Variable LNSdq6

All Pairwise Comparisons among Levels of OA GRADE

OA GRADE = 1 subtracted from:

OA GRADE	Difference of Means	SE of Difference	T-Value	Adjusted P-Value
2	0.4014	0.05084	7.895	0.0000
3	0.7536	0.05084	14.822	0.0000

OA GRADE = 2 subtracted from:

OA GRADE	Difference of Means	SE of Difference	T-Value	Adjusted P-Value
----------	---------------------	------------------	---------	------------------

3                    0.3522            0.05084            6.927            0.0000

## Residual Plots for LNSdq6

### General Linear Model: LNSdr versus OA GRADE, SdrSAMPLE

Factor	Type	Levels	Values
OA GRADE	fixed	3	1, 2, 3
SdrSAMPLE(OA GRADE)	fixed	12	1, 2, 3, 4, 5, 6, 7, 8, 9, 10, 11, 12

Analysis of Variance for LNSdr, using Adjusted SS for Tests

Source	DF	Seq SS	Adj SS	Adj MS	F	P
OA GRADE	2	37.2017	37.2017	18.6008	94.26	0.000
SdrSAMPLE(OA GRADE)	9	23.0400	23.0400	2.5600	12.97	0.000
Error	132	26.0471	26.0471	0.1973		
Total	143	86.2888				

S = 0.444214    R-Sq = 69.81%    R-Sq(adj) = 67.30%

Unusual Observations for LNSdr

Obs	LNSdr	Fit	SE Fit	Residual	St Resid
51	7.44047	6.07103	0.12823	1.36944	3.22 R
98	5.38974	6.31009	0.12823	-0.92035	-2.16 R
132	8.40045	7.51368	0.12823	0.88677	2.09 R
133	6.78141	7.67469	0.12823	-0.89328	-2.10 R
142	6.82405	7.67469	0.12823	-0.85064	-2.00 R
143	9.50536	7.67469	0.12823	1.83067	4.30 R
144	9.08323	7.67469	0.12823	1.40854	3.31 R

R denotes an observation with a large standardized residual.

Grouping Information Using Tukey Method and 95.0% Confidence

OA GRADE	N	Mean	Grouping
3	48	7.1	A
2	48	6.5	B
1	48	5.8	C

Means that do not share a letter are significantly different.

Tukey Simultaneous Tests

Response Variable LNSdr

All Pairwise Comparisons among Levels of OA GRADE

OA GRADE = 1 subtracted from:

OA GRADE	Difference of Means	SE of Difference	T-Value	Adjusted P-Value
2	0.6238	0.09067	6.879	0.0000
3	1.2450	0.09067	13.731	0.0000

OA GRADE = 2 subtracted from:

OA GRADE	Difference of Means	SE of Difference	T-Value	Adjusted P-Value
----------	---------------------	------------------	---------	------------------

3	0.6213	0.09067	6.852	0.0000
---	--------	---------	-------	--------

## Residual Plots for LNSdr

### General Linear Model: LNS3A versus OA GRADE, S3ASAMPLE

Factor	Type	Levels	Values
OA GRADE	fixed	3	1, 2, 3
S3ASAMPLE (OA GRADE)	fixed	12	1, 2, 3, 4, 5, 6, 7, 8, 9, 10, 11, 12

Analysis of Variance for LNS3A, using Adjusted SS for Tests

Source	DF	Seq SS	Adj SS	Adj MS	F	P
OA GRADE	2	27.9656	27.9656	13.9828	87.85	0.000
S3ASAMPLE (OA GRADE)	9	18.0513	18.0513	2.0057	12.60	0.000
Error	132	21.0088	21.0088	0.1592		
Total	143	67.0256				

S = 0.398946    R-Sq = 68.66%    R-Sq(adj) = 66.04%

Unusual Observations for LNS3A

Obs	LNS3A	Fit	SE Fit	Residual	St Resid
51	29.5171	28.3118	0.1152	1.2053	3.16 R
64	29.8727	29.1025	0.1152	0.7702	2.02 R
112	29.7496	28.9805	0.1152	0.7691	2.01 R
132	30.4423	29.5919	0.1152	0.8504	2.23 R
133	28.9085	29.7517	0.1152	-0.8433	-2.21 R
142	28.9469	29.7517	0.1152	-0.8049	-2.11 R
143	31.5324	29.7517	0.1152	1.7806	4.66 R
144	31.1141	29.7517	0.1152	1.3624	3.57 R

R denotes an observation with a large standardized residual.

Grouping Information Using Tukey Method and 95.0% Confidence

OA GRADE	N	Mean	Grouping
3	48	29.2	A
2	48	28.6	B
1	48	28.1	C

Means that do not share a letter are significantly different.

Tukey Simultaneous Tests

Response Variable LNS3A

All Pairwise Comparisons among Levels of OA GRADE

OA GRADE = 1 subtracted from:

OA GRADE	Difference of Means	SE of Difference	T-Value	Adjusted P-Value
2	0.5180	0.08143	6.361	0.0000
3	1.0792	0.08143	13.252	0.0000

OA GRADE = 2 subtracted from:

OA	Difference	SE of	Adjusted
----	------------	-------	----------

GRADE	of Means	Difference	T-Value	P-Value
3	0.5612	0.08143	6.891	0.0000

## Residual Plots for LNS3A

### General Linear Model: LNSpk versus OA GRADE, SpkSAMPLE

Factor	Type	Levels	Values
OA GRADE	fixed	3	1, 2, 3
SpkSAMPLE (OA GRADE)	fixed	12	1, 2, 3, 4, 5, 6, 7, 8, 9, 10, 11, 12

Analysis of Variance for LNSpk, using Adjusted SS for Tests

Source	DF	Seq SS	Adj SS	Adj MS	F	P
OA GRADE	2	79.6176	79.6176	39.8088	227.15	0.000
SpkSAMPLE (OA GRADE)	9	3.8260	3.8260	0.4251	2.43	0.014
Error	132	23.1331	23.1331	0.1753		
Total	143	106.5767				

S = 0.418629    R-Sq = 78.29%    R-Sq(adj) = 76.49%

Unusual Observations for LNSpk

Obs	LNSpk	Fit	SE Fit	Residual	St Resid
1	10.1919	9.0611	0.1208	1.1307	2.82 R
19	7.9787	8.9743	0.1208	-0.9956	-2.48 R
21	9.9701	8.9743	0.1208	0.9958	2.48 R
22	9.9545	8.9743	0.1208	0.9802	2.45 R
44	10.2337	8.8823	0.1208	1.3514	3.37 R
51	11.1334	10.0065	0.1208	1.1269	2.81 R
76	11.4326	10.3561	0.1208	1.0765	2.69 R
95	10.9805	10.1065	0.1208	0.8740	2.18 R

R denotes an observation with a large standardized residual.

Grouping Information Using Tukey Method and 95.0% Confidence

OA	N	Mean	Grouping
GRADE			
3	48	10.6	A
2	48	10.3	B
1	48	8.9	C

Means that do not share a letter are significantly different.

Tukey Simultaneous Tests

Response Variable LNSpk

All Pairwise Comparisons among Levels of OA GRADE

OA GRADE = 1 subtracted from:

OA	Difference	SE of	Adjusted
GRADE	of Means	Difference	P-Value
2	1.370	0.08545	16.04
3	1.724	0.08545	20.18

OA GRADE = 2 subtracted from:

OA	Difference	SE of		Adjusted
GRADE	of Means	Difference	T-Value	P-Value
3	0.3540	0.08545	4.143	0.0002

## Residual Plots for LNSpk

## General Linear Model: LNSvk versus OA GRADE, SvksAMPLE

Factor	Type	Levels	Values
OA GRADE	fixed	3	1, 2, 3
SvksAMPLE (OA GRADE)	fixed	12	1, 2, 3, 4, 5, 6, 7, 8, 9, 10, 11, 12

Analysis of Variance for LNSvk, using Adjusted SS for Tests

Source	DF	Seq SS	Adj SS	Adj MS	F	P
OA GRADE	2	47.1438	47.1438	23.5719	158.13	0.000
SvksAMPLE (OA GRADE)	9	14.2145	14.2145	1.5794	10.60	0.000
Error	132	19.6770	19.6770	0.1491		
Total	143	81.0353				

S = 0.386093    R-Sq = 75.72%    R-Sq(adj) = 73.69%

Unusual Observations for LNSvk

Obs	LNSvk	Fit	SE Fit	Residual	St Resid
21	9.5519	8.5870	0.1115	0.9649	2.61 R
51	10.2248	9.4140	0.1115	0.8108	2.19 R
76	10.5955	9.7949	0.1115	0.8005	2.17 R
101	10.2248	9.4184	0.1115	0.8064	2.18 R
131	11.0778	10.2309	0.1115	0.8468	2.29 R
132	11.0944	10.2309	0.1115	0.8635	2.34 R
143	11.7994	10.5979	0.1115	1.2015	3.25 R

R denotes an observation with a large standardized residual.

Grouping Information Using Tukey Method and 95.0% Confidence

OA	N	Mean	Grouping
GRADE			
3	48	10.0	A
2	48	9.5	B
1	48	8.6	C

Means that do not share a letter are significantly different.

Tukey Simultaneous Tests

Response Variable LNSvk

All Pairwise Comparisons among Levels of OA GRADE

OA GRADE = 1 subtracted from:

OA	Difference	SE of		Adjusted
GRADE	of Means	Difference	T-Value	P-Value
2	0.9330	0.07881	11.84	0.0000
3	1.3722	0.07881	17.41	0.0000

OA GRADE = 2 subtracted from:

OA GRADE	Difference of Means	SE of Difference	T-Value	Adjusted P-Value
3	0.4392	0.07881	5.573	0.0000

## Residual Plots for LNSvk

## General Linear Model: LNSdc5\_10 versus OA GRADE, Sdc5\_10SAMPLE

Factor	Type	Levels	Values
OA GRADE	fixed	3	1, 2, 3
Sdc5_10SAMPLE (OA GRADE)	fixed	12	1, 2, 3, 4, 5, 6, 7, 8, 9, 10, 11, 12

Analysis of Variance for LNSdc5\_10, using Adjusted SS for Tests

Source	DF	Seq SS	Adj SS	Adj MS	F	P
OA GRADE	2	103.0753	103.0753	51.5376	265.58	0.000
Sdc5_10SAMPLE (OA GRADE)	9	1.8029	1.8029	0.2003	1.03	0.418
Error	132	25.6157	25.6157	0.1941		
Total	143	130.4939				

S = 0.440520    R-Sq = 80.37%    R-Sq(adj) = 78.73%

Unusual Observations for LNSdc5\_10

Obs	LNSdc5_10	Fit	SE Fit	Residual	St Resid
1	8.7746	7.7254	0.1272	1.0492	2.49 R
21	8.7757	7.6374	0.1272	1.1383	2.70 R
22	8.8353	7.6374	0.1272	1.1979	2.84 R
51	9.9500	9.0018	0.1272	0.9482	2.25 R
76	10.4321	9.2257	0.1272	1.2063	2.86 R
95	9.9401	8.9801	0.1272	0.9600	2.28 R

R denotes an observation with a large standardized residual.

Grouping Information Using Tukey Method and 95.0% Confidence

OA GRADE	N	Mean	Grouping
3	48	9.6	A
2	48	9.2	B
1	48	7.6	C

Means that do not share a letter are significantly different.

Tukey Simultaneous Tests

Response Variable LNSdc5\_10

All Pairwise Comparisons among Levels of OA GRADE

OA GRADE = 1 subtracted from:

OA GRADE	Difference of Means	SE of Difference	T-Value	Adjusted P-Value
2	1.542	0.08992	17.15	0.0000
3	1.970	0.08992	21.91	0.0000

OA GRADE = 2 subtracted from:

OA	Difference	SE of	Adjusted
----	------------	-------	----------

GRADE	of Means	Difference	T-Value	P-Value
3	0.4283	0.08992	4.763	0.0000

## Residual Plots for LNSdc5\_10

## General Linear Model: LNSdc10\_50 versus OA GRADE, Sdc10\_50SAMPLE

Factor	Type	Levels	Values
OA GRADE	fixed	3	1, 2, 3
Sdc10_50SAMPLE(OA GRADE)	fixed	12	1, 2, 3, 4, 5, 6, 7, 8, 9, 10, 11, 12

Analysis of Variance for LNSdc10\_50, using Adjusted SS for Tests

Source	DF	Seq SS	Adj SS	Adj MS	F	P
OA GRADE	2	83.6415	83.6415	41.8208	339.43	0.000
Sdc10_50SAMPLE(OA GRADE)	9	2.0298	2.0298	0.2255	1.83	0.068
Error	132	16.2636	16.2636	0.1232		
Total	143	101.9350				

S = 0.351012    R-Sq = 84.05%    R-Sq(adj) = 82.72%

Unusual Observations for LNSdc10\_50

Obs	LNSdc10_50	Fit	SE Fit	Residual	St Resid
22	9.5772	8.6280	0.1013	0.9492	2.82 R
65	10.9358	10.2299	0.1013	0.7058	2.10 R
69	9.5461	10.2299	0.1013	-0.6838	-2.03 R
76	11.1477	10.1433	0.1013	1.0044	2.99 R
128	9.8244	10.5639	0.1013	-0.7395	-2.20 R
142	9.7587	10.4993	0.1013	-0.7405	-2.20 R

R denotes an observation with a large standardized residual.

Grouping Information Using Tukey Method and 95.0% Confidence

OA	GRADE	N	Mean	Grouping
	3	48	10.4	A
	2	48	10.1	B
	1	48	8.7	C

Means that do not share a letter are significantly different.

Tukey Simultaneous Tests

Response Variable LNSdc10\_50

All Pairwise Comparisons among Levels of OA GRADE

OA GRADE = 1 subtracted from:

OA	Difference	SE of		Adjusted
GRADE	of Means	Difference	T-Value	P-Value
2	1.416	0.07165	19.76	0.0000
3	1.762	0.07165	24.59	0.0000

OA GRADE = 2 subtracted from:

OA	Difference	SE of		Adjusted
GRADE	of Means	Difference	T-Value	P-Value

3	0.3457	0.07165	4.825	0.0000
---	--------	---------	-------	--------

## Residual Plots for LNSdc10\_50

## General Linear Model: LNSdc50\_95 versus OA GRADE, Sdc50\_95SAMPLE

Factor	Type	Levels	Values
Sdc50_95SAMPLE(OA GRADE)	fixed	12	1, 2, 3, 4, 5, 6, 7, 8, 9, 10, 11, 12
OA GRADE	fixed	3	1, 2, 3

Analysis of Variance for LNSdc50\_95, using Adjusted SS for Tests

Source	DF	Seq SS	Adj SS	Adj MS	F	P
Sdc50_95SAMPLE(OA GRADE)	9	5.9785	5.9785	0.6643	5.50	0.000
OA GRADE	2	50.9497	50.9497	25.4749	210.94	0.000
Error	132	15.9413	15.9413	0.1208		
Total	143	72.8695				

S = 0.347516    R-Sq = 78.12%    R-Sq(adj) = 76.30%

Unusual Observations for LNSdc50\_95

Obs	LNSdc50_95	Fit	SE Fit	Residual	St Resid
76	10.8820	10.2074	0.1003	0.6746	2.03 R
128	9.8244	10.5044	0.1003	-0.6800	-2.04 R
132	11.1803	10.5044	0.1003	0.6759	2.03 R
137	9.9798	10.7477	0.1003	-0.7679	-2.31 R
142	9.9770	10.7477	0.1003	-0.7708	-2.32 R
143	12.0094	10.7477	0.1003	1.2617	3.79 R
144	11.4829	10.7477	0.1003	0.7352	2.21 R

R denotes an observation with a large standardized residual.

Grouping Information Using Tukey Method and 95.0% Confidence

OA GRADE	N	Mean	Grouping
3	48	10.4	A
2	48	10.0	B
1	48	9.0	C

Means that do not share a letter are significantly different.

Tukey Simultaneous Tests

Response Variable LNSdc50\_95

All Pairwise Comparisons among Levels of OA GRADE

OA GRADE = 1 subtracted from:

OA GRADE	Difference of Means	SE of Difference	T-Value	Adjusted P-Value
2	1.068	0.07094	15.06	0.0000
3	1.392	0.07094	19.63	0.0000

OA GRADE = 2 subtracted from:

OA GRADE	Difference of Means	SE of Difference	T-Value	Adjusted P-Value
----------	---------------------	------------------	---------	------------------

3	0.3239	0.07094	4.566	0.0000
---	--------	---------	-------	--------

## Residual Plots for LNSdc50\_95

### General Linear Model: LNSku versus OA GRADE, Sku SAMPLE

Factor	Type	Levels	Values
OA GRADE	fixed	3	1, 2, 3
Sku SAMPLE(OA GRADE)	fixed	12	1, 2, 3, 4, 5, 6, 7, 8, 9, 10, 11, 12

Analysis of Variance for LNSku, using Adjusted SS for Tests

Source	DF	Seq SS	Adj SS	Adj MS	F	P
OA GRADE	2	0.0180	0.0180	0.0090	0.06	0.940
Sku SAMPLE(OA GRADE)	9	4.8118	4.8118	0.5346	3.66	0.000
Error	132	19.2765	19.2765	0.1460		
Total	143	24.1063				

S = 0.382144    R-Sq = 20.04%    R-Sq(adj) = 13.37%

Unusual Observations for LNSku

Obs	LNSku	Fit	SE Fit	Residual	St Resid
1	2.64717	1.59056	0.11032	1.05662	2.89 R
44	3.14983	1.74313	0.11032	1.40670	3.84 R
51	3.12187	1.39219	0.11032	1.72968	4.73 R
128	2.37346	1.45732	0.11032	0.91614	2.50 R

R denotes an observation with a large standardized residual.

Grouping Information Using Tukey Method and 95.0% Confidence

OA GRADE	N	Mean	Grouping
3	48	1.6	A
2	48	1.6	A
1	48	1.6	A

Means that do not share a letter are significantly different.

Tukey Simultaneous Tests

Response Variable LNSku

All Pairwise Comparisons among Levels of OA GRADE

OA GRADE = 1 subtracted from:

OA GRADE	Difference of Means	SE of Difference	T-Value	Adjusted P-Value
2	0.02258	0.07800	0.2895	0.9549
3	0.02465	0.07800	0.3161	0.9465

OA GRADE = 2 subtracted from:

OA GRADE	Difference of Means	SE of Difference	T-Value	Adjusted P-Value
3	0.002070	0.07800	0.02654	0.9996

## Residual Plots for LNSku

### General Linear Model: LNSy versus OA GRADE, Sy SAMPLE

Factor	Type	Levels	Values
OA GRADE	fixed	3	1, 2, 3
Sy SAMPLE(OA GRADE)	fixed	12	1, 2, 3, 4, 5, 6, 7, 8, 9, 10, 11, 12

Analysis of Variance for LNSy, using Adjusted SS for Tests

Source	DF	Seq SS	Adj SS	Adj MS	F	P
OA GRADE	2	42.8630	42.8630	21.4315	216.12	0.000
Sy SAMPLE(OA GRADE)	9	7.4963	7.4963	0.8329	8.40	0.000
Error	132	13.0897	13.0897	0.0992		
Total	143	63.4489				

S = 0.314903    R-Sq = 79.37%    R-Sq(adj) = 77.65%

Unusual Observations for LNSy

Obs	LNSy	Fit	SE Fit	Residual	St Resid
19	10.3985	11.2656	0.0909	-0.8671	-2.88 R
21	11.9925	11.2656	0.0909	0.7270	2.41 R
22	12.0521	11.2656	0.0909	0.7866	2.61 R
44	11.7766	11.1705	0.0909	0.6061	2.01 R
51	13.0272	11.8314	0.0909	1.1957	3.97 R
53	11.1856	11.8314	0.0909	-0.6458	-2.14 R

R denotes an observation with a large standardized residual.

Grouping Information Using Tukey Method and 95.0% Confidence

OA GRADE	N	Mean	Grouping
3	48	12.4	A
2	48	12.1	B
1	48	11.1	C

Means that do not share a letter are significantly different.

Tukey Simultaneous Tests

Response Variable LNSy

All Pairwise Comparisons among Levels of OA GRADE

OA GRADE = 1 subtracted from:

OA GRADE	Difference of Means	SE of Difference	T-Value	Adjusted P-Value
2	1.025	0.06428	15.95	0.0000
3	1.255	0.06428	19.53	0.0000

OA GRADE = 2 subtracted from:

OA GRADE	Difference of Means	SE of Difference	T-Value	Adjusted P-Value
3	0.2300	0.06428	3.578	0.0014

## Residual Plots for LNSy

## General Linear Model: LNS10z versus OA GRADE, S10zSAMPLE

Factor	Type	Levels	Values
S10zSAMPLE(OA GRADE)	fixed	12	1, 2, 3, 4, 5, 6, 7, 8, 9, 10, 11, 12
OA GRADE	fixed	3	1, 2, 3

Analysis of Variance for LNS10z, using Adjusted SS for Tests

Source	DF	Seq SS	Adj SS	Adj MS	F	P
S10zSAMPLE(OA GRADE)	9	7.1000	7.1000	0.7889	8.45	0.000
OA GRADE	2	45.6949	45.6949	22.8474	244.71	0.000
Error	132	12.3244	12.3244	0.0934		
Total	143	65.1192				

S = 0.305559    R-Sq = 81.07%    R-Sq(adj) = 79.50%

Unusual Observations for LNS10z

Obs	LNS10z	Fit	SE Fit	Residual	St Resid
1	11.7944	11.1420	0.0882	0.6523	2.23 R
19	10.3221	11.1446	0.0882	-0.8225	-2.81 R
21	11.8366	11.1446	0.0882	0.6920	2.37 R
22	12.0109	11.1446	0.0882	0.8663	2.96 R
51	13.0178	11.7828	0.0882	1.2350	4.22 R
53	11.1651	11.7828	0.0882	-0.6177	-2.11 R
76	12.8485	12.2510	0.0882	0.5975	2.04 R

R denotes an observation with a large standardized residual.

Grouping Information Using Tukey Method and 95.0% Confidence

OA GRADE	N	Mean	Grouping
3	48	12.3	A
2	48	12.1	B
1	48	11.0	C

Means that do not share a letter are significantly different.

Tukey Simultaneous Tests

Response Variable LNS10z

All Pairwise Comparisons among Levels of OA GRADE

OA GRADE = 1 subtracted from:

OA GRADE	Difference of Means	SE of Difference	T-Value	Adjusted P-Value
2	1.054	0.06237	16.90	0.0000
3	1.298	0.06237	20.81	0.0000

OA GRADE = 2 subtracted from:

OA GRADE	Difference of Means	SE of Difference	T-Value	Adjusted P-Value
3	0.2440	0.06237	3.912	0.0004

## Residual Plots for LNS10z

## General Linear Model: LNSds versus OA GRADE, SdsSAMPLE

Factor	Type	Levels	Values
OA GRADE	fixed	3	1, 2, 3
SdsSAMPLE(OA GRADE)	fixed	12	1, 2, 3, 4, 5, 6, 7, 8, 9, 10, 11, 12

Analysis of Variance for LNSds, using Adjusted SS for Tests

Source	DF	Seq SS	Adj SS	Adj MS	F	P
OA GRADE	2	2.52077	2.52077	1.26038	192.39	0.000
SdsSAMPLE(OA GRADE)	9	0.61914	0.61914	0.06879	10.50	0.000
Error	132	0.86476	0.86476	0.00655		
Total	143	4.00467				

S = 0.0809398    R-Sq = 78.41%    R-Sq(adj) = 76.61%

Unusual Observations for LNSds

Obs	LNSds	Fit	SE Fit	Residual	St Resid
22	-2.14053	-1.97045	0.02337	-0.17009	-2.19 R
45	-2.17918	-1.96943	0.02337	-0.20975	-2.71 R
53	-1.89110	-2.08576	0.02337	0.19466	2.51 R
62	-2.49392	-2.28046	0.02337	-0.21346	-2.75 R
63	-2.47204	-2.28046	0.02337	-0.19158	-2.47 R
69	-2.04933	-2.28046	0.02337	0.23113	2.98 R
134	-2.42659	-2.17830	0.02337	-0.24829	-3.20 R
135	-2.37535	-2.17830	0.02337	-0.19705	-2.54 R
137	-2.00283	-2.17830	0.02337	0.17547	2.26 R
138	-1.99934	-2.17830	0.02337	0.17895	2.31 R
141	-1.98543	-2.17830	0.02337	0.19287	2.49 R

R denotes an observation with a large standardized residual.

Grouping Information Using Tukey Method and 95.0% Confidence

OA GRADE	N	Mean	Grouping
1	48	-1.9	A
2	48	-2.2	B
3	48	-2.2	B

Means that do not share a letter are significantly different.

Tukey Simultaneous Tests

Response Variable LNSds

All Pairwise Comparisons among Levels of OA GRADE

OA GRADE = 1 subtracted from:

OA GRADE	Difference of Means	SE of Difference	T-Value	Adjusted P-Value
2	-0.2597	0.01652	-15.72	0.0000
3	-0.2977	0.01652	-18.02	0.0000

OA GRADE = 2 subtracted from:

OA GRADE	Difference of Means	SE of Difference	T-Value	Adjusted P-Value
----------	---------------------	------------------	---------	------------------

3	-0.03798	0.01652	-2.299	0.0595
---	----------	---------	--------	--------

## Residual Plots for LNSds

### General Linear Model: LNScs versus OA GRADE, ScsSAMPLE

Factor	Type	Levels	Values
OA GRADE	fixed	3	1, 2, 3
ScsSAMPLE(OA GRADE)	fixed	12	1, 2, 3, 4, 5, 6, 7, 8, 9, 10, 11, 12

Analysis of Variance for LNScs, using Adjusted SS for Tests

Source	DF	Seq SS	Adj SS	Adj MS	F	P
OA GRADE	2	2.15135	2.15135	1.07568	30.76	0.000
ScsSAMPLE(OA GRADE)	9	3.29854	3.29854	0.36650	10.48	0.000
Error	132	4.61602	4.61602	0.03497		
Total	143	10.06591				

S = 0.187002    R-Sq = 54.14%    R-Sq(adj) = 50.32%

Unusual Observations for LNScs

Obs	LNScs	Fit	SE Fit	Residual	St Resid
64	-4.28586	-4.75614	0.05398	0.47029	2.63 R
98	-5.38933	-4.95770	0.05398	-0.43163	-2.41 R
131	-5.02657	-4.55940	0.05398	-0.46717	-2.61 R
133	-5.04832	-4.49784	0.05398	-0.55049	-3.07 R
143	-3.97983	-4.49784	0.05398	0.51800	2.89 R
144	-3.86831	-4.49784	0.05398	0.62952	3.52 R

R denotes an observation with a large standardized residual.

Grouping Information Using Tukey Method and 95.0% Confidence

OA GRADE	N	Mean	Grouping
3	48	-4.7	A
2	48	-4.9	B
1	48	-5.0	C

Means that do not share a letter are significantly different.

Tukey Simultaneous Tests

Response Variable LNScs

All Pairwise Comparisons among Levels of OA GRADE

OA GRADE = 1    subtracted from:

OA GRADE	Difference of Means	SE of Difference	T-Value	Adjusted P-Value
2	0.09688	0.03817	2.538	0.0328
3	0.29378	0.03817	7.696	0.0000

OA GRADE = 2    subtracted from:

OA GRADE	Difference of Means	SE of Difference	T-Value	Adjusted P-Value
3	0.1969	0.03817	5.158	0.0000

## Residual Plots for LNScs

### General Linear Model: LNSp versus OA GRADE, SpSAMPLE

Factor	Type	Levels	Values
OA GRADE	fixed	3	1, 2, 3
SpSAMPLE(OA GRADE)	fixed	12	1, 2, 3, 4, 5, 6, 7, 8, 9, 10, 11, 12

Analysis of Variance for LNSp, using Adjusted SS for Tests

Source	DF	Seq SS	Adj SS	Adj MS	F	P
OA GRADE	2	42.3341	42.3341	21.1671	167.57	0.000
SpSAMPLE(OA GRADE)	9	7.1225	7.1225	0.7914	6.27	0.000
Error	132	16.6739	16.6739	0.1263		
Total	143	66.1306				

S = 0.355412    R-Sq = 74.79%    R-Sq(adj) = 72.69%

Unusual Observations for LNSp

Obs	LNSp	Fit	SE Fit	Residual	St Resid
1	11.5293	10.6716	0.1026	0.8576	2.52 R
19	9.5238	10.7038	0.1026	-1.1800	-3.47 R
20	10.0098	10.7038	0.1026	-0.6940	-2.04 R
22	11.4071	10.7038	0.1026	0.7033	2.07 R
38	9.7556	10.4600	0.1026	-0.7045	-2.07 R
44	11.3183	10.4600	0.1026	0.8583	2.52 R
51	12.6423	11.2543	0.1026	1.3880	4.08 R
53	10.4716	11.2543	0.1026	-0.7827	-2.30 R

R denotes an observation with a large standardized residual.

Grouping Information Using Tukey Method and 95.0% Confidence

OA GRADE	N	Mean	Grouping
3	48	11.7	A
2	48	11.6	A
1	48	10.5	B

Means that do not share a letter are significantly different.

Tukey Simultaneous Tests

Response Variable LNSp

All Pairwise Comparisons among Levels of OA GRADE

OA GRADE = 1 subtracted from:

OA GRADE	Difference of Means	SE of Difference	T-Value	Adjusted P-Value
2	1.063	0.07255	14.66	0.0000
3	1.221	0.07255	16.83	0.0000

OA GRADE = 2 subtracted from:

OA GRADE	Difference of Means	SE of Difference	T-Value	Adjusted P-Value
----------	---------------------	------------------	---------	------------------

3                    0.1574            0.07255            2.170            0.0802

## Residual Plots for LNSp

### General Linear Model: LNSbi versus OA GRADE, SbiSAMPLE

Factor	Type	Levels	Values
SbiSAMPLE(OA GRADE)	fixed	12	1, 2, 3, 4, 5, 6, 7, 8, 9, 10, 11, 12
OA GRADE	fixed	3	1, 2, 3

Analysis of Variance for LNSbi, using Adjusted SS for Tests

Source	DF	Seq SS	Adj SS	Adj MS	F	P
SbiSAMPLE(OA GRADE)	9	0.40245	0.40245	0.04472	4.03	0.000
OA GRADE	2	0.80571	0.80571	0.40285	36.34	0.000
Error	132	1.46347	1.46347	0.01109		
Total	143	2.67163				

S = 0.105294    R-Sq = 45.22%    R-Sq(adj) = 40.66%

Unusual Observations for LNSbi

Obs	LNSbi	Fit	SE Fit	Residual	St Resid
44	0.051843	-0.385717	0.030396	0.437560	4.34 R
69	-0.262060	-0.589916	0.030396	0.327856	3.25 R
72	-0.803386	-0.589916	0.030396	-0.213471	-2.12 R
91	-0.388660	-0.602995	0.030396	0.214335	2.13 R
95	-0.885194	-0.602995	0.030396	-0.282200	-2.80 R
101	-0.381521	-0.687655	0.030396	0.306134	3.04 R
141	-0.885306	-0.500835	0.030396	-0.384471	-3.81 R

R denotes an observation with a large standardized residual.

Grouping Information Using Tukey Method and 95.0% Confidence

OA GRADE	N	Mean	Grouping
1	48	-0.4	A
2	48	-0.6	B
3	48	-0.6	B

Means that do not share a letter are significantly different.

Tukey Simultaneous Tests

Response Variable LNSbi

All Pairwise Comparisons among Levels of OA GRADE

OA GRADE = 1 subtracted from:

OA GRADE	Difference of Means	SE of Difference	T-Value	Adjusted P-Value
2	-0.1441	0.02149	-6.705	0.0000
3	-0.1701	0.02149	-7.912	0.0000

OA GRADE = 2 subtracted from:

OA GRADE	Difference of Means	SE of Difference	T-Value	Adjusted P-Value
----------	---------------------	------------------	---------	------------------

3	-0.02595	0.02149	-1.207	0.4510
---	----------	---------	--------	--------

## Residual Plots for LNSbi

### General Linear Model: LNSci versus OA GRADE, SciSAMPLE

Factor	Type	Levels	Values
OA GRADE	fixed	3	1, 2, 3
SciSAMPLE(OA GRADE)	fixed	12	1, 2, 3, 4, 5, 6, 7, 8, 9, 10, 11, 12

Analysis of Variance for LNSci, using Adjusted SS for Tests

Source	DF	Seq SS	Adj SS	Adj MS	F	P
OA GRADE	2	0.96733	0.96733	0.48367	39.79	0.000
SciSAMPLE(OA GRADE)	9	0.54221	0.54221	0.06025	4.96	0.000
Error	132	1.60468	1.60468	0.01216		
Total	143	3.11422				

S = 0.110257    R-Sq = 48.47%    R-Sq(adj) = 44.18%

Unusual Observations for LNSci

Obs	LNSci	Fit	SE Fit	Residual	St Resid
44	0.054422	0.350373	0.031829	-0.295951	-2.80 R
69	0.267015	0.580633	0.031829	-0.313618	-2.97 R
72	0.792649	0.580633	0.031829	0.212015	2.01 R
91	0.364629	0.583335	0.031829	-0.218706	-2.07 R
95	0.886108	0.583335	0.031829	0.302773	2.87 R
101	0.339397	0.673532	0.031829	-0.334135	-3.17 R
124	0.774156	0.555395	0.031829	0.218760	2.07 R
141	0.864614	0.449357	0.031829	0.415257	3.93 R
143	0.195822	0.449357	0.031829	-0.253536	-2.40 R

R denotes an observation with a large standardized residual.

Grouping Information Using Tukey Method and 95.0% Confidence

OA	N	Mean	Grouping
GRADE			
3	48	0.6	A
2	48	0.6	A
1	48	0.4	B

Means that do not share a letter are significantly different.

Tukey Simultaneous Tests

Response Variable LNSci

All Pairwise Comparisons among Levels of OA GRADE

OA GRADE = 1 subtracted from:

OA	Difference	SE of		Adjusted
GRADE	of Means	Difference	T-Value	P-Value
2	0.1633	0.02251	7.254	0.0000
3	0.1828	0.02251	8.123	0.0000

OA GRADE = 2 subtracted from:

OA	Difference	SE of		Adjusted
GRADE	of Means	Difference	T-Value	P-Value
3	0.01957	0.02251	0.8695	0.6604

## Residual Plots for LNSci

### General Linear Model: LNSvi versus OA GRADE, SviSAMPLE

Factor	Type	Levels	Values
OA GRADE	fixed	3	1, 2, 3
SviSAMPLE(OA GRADE)	fixed	12	1, 2, 3, 4, 5, 6, 7, 8, 9, 10, 11, 12

Analysis of Variance for LNSvi, using Adjusted SS for Tests

Source	DF	Seq SS	Adj SS	Adj MS	F	P
OA GRADE	2	2.12474	2.12474	1.06237	25.98	0.000
SviSAMPLE(OA GRADE)	9	2.06314	2.06314	0.22924	5.61	0.000
Error	132	5.39833	5.39833	0.04090		
Total	143	9.58622				

S = 0.202229 R-Sq = 43.69% R-Sq(adj) = 38.99%

Unusual Observations for LNSvi

Obs	LNSvi	Fit	SE Fit	Residual	St Resid
44	-2.85405	-2.08908	0.05838	-0.76497	-3.95 R
49	-2.80620	-2.37447	0.05838	-0.43172	-2.23 R
67	-2.78101	-2.36789	0.05838	-0.41312	-2.13 R
95	-2.92075	-2.43460	0.05838	-0.48616	-2.51 R
101	-2.06878	-2.50947	0.05838	0.44069	2.28 R
107	-2.90641	-2.50947	0.05838	-0.39694	-2.05 R
124	-2.80107	-2.30611	0.05838	-0.49496	-2.56 R
132	-1.84845	-2.30611	0.05838	0.45766	2.36 R
139	-2.49012	-2.07525	0.05838	-0.41487	-2.14 R
143	-1.62112	-2.07525	0.05838	0.45414	2.35 R

R denotes an observation with a large standardized residual.

Grouping Information Using Tukey Method and 95.0% Confidence

OA			
GRADE	N	Mean	Grouping
1	48	-2.1	A
3	48	-2.4	B
2	48	-2.4	B

Means that do not share a letter are significantly different.

Tukey Simultaneous Tests

Response Variable LNSvi

All Pairwise Comparisons among Levels of OA GRADE

OA GRADE = 1 subtracted from:

OA	Difference	SE of		Adjusted
GRADE	of Means	Difference	T-Value	P-Value
2	-0.2615	0.04128	-6.335	0.0000
3	-0.2537	0.04128	-6.145	0.0000

OA GRADE = 2 subtracted from:

OA GRADE	Difference of Means	SE of Difference	T-Value	Adjusted P-Value
3	0.007875	0.04128	0.1908	0.9801

## Residual Plots for LNSvi

## General Linear Model: LNSk versus OA GRADE, SkSAMPLE

Factor	Type	Levels	Values
OA GRADE	fixed	3	1, 2, 3
SkSAMPLE(OA GRADE)	fixed	12	1, 2, 3, 4, 5, 6, 7, 8, 9, 10, 11, 12

Analysis of Variance for LNSk, using Adjusted SS for Tests

Source	DF	Seq SS	Adj SS	Adj MS	F	P
OA GRADE	2	59.2206	59.2206	29.6103	273.36	0.000
SkSAMPLE(OA GRADE)	9	3.1913	3.1913	0.3546	3.27	0.001
Error	132	14.2981	14.2981	0.1083		
Total	143	76.7100				

S = 0.329119 R-Sq = 81.36% R-Sq(adj) = 79.81%

Unusual Observations for LNSk

Obs	LNSk	Fit	SE Fit	Residual	St Resid
76	11.5042	10.6685	0.0950	0.8357	2.65 R
128	10.2656	10.9532	0.0950	-0.6876	-2.18 R
135	11.6134	10.9520	0.0950	0.6615	2.10 R
137	10.3179	10.9520	0.0950	-0.6341	-2.01 R
142	10.1458	10.9520	0.0950	-0.8061	-2.56 R
143	11.6781	10.9520	0.0950	0.7261	2.30 R
144	11.6325	10.9520	0.0950	0.6805	2.16 R

R denotes an observation with a large standardized residual.

Grouping Information Using Tukey Method and 95.0% Confidence

OA GRADE	N	Mean	Grouping
3	48	10.8	A
2	48	10.5	B
1	48	9.3	C

Means that do not share a letter are significantly different.

Tukey Simultaneous Tests

Response Variable LNSk

All Pairwise Comparisons among Levels of OA GRADE

OA GRADE = 1 subtracted from:

OA GRADE	Difference of Means	SE of Difference	T-Value	Adjusted P-Value
2	1.191	0.06718	17.73	0.0000
3	1.483	0.06718	22.07	0.0000

OA GRADE = 2 subtracted from:

OA GRADE	Difference of Means	SE of Difference	T-Value	Adjusted P-Value
3	0.2916	0.06718	4.340	0.0001

## Residual Plots for LNSk

### General Linear Model: LNSpk/Sk versus OA GRADE, Spk/SkSAMPLE

Factor	Type	Levels	Values
OA GRADE	fixed	3	1, 2, 3
Spk/SkSAMPLE (OA GRADE)	fixed	12	1, 2, 3, 4, 5, 6, 7, 8, 9, 10, 11, 12

Analysis of Variance for LNSpk/Sk, using Adjusted SS for Tests

Source	DF	Seq SS	Adj SS	Adj MS	F	P
OA GRADE	2	1.5119	1.5119	0.7560	5.42	0.005
Spk/SkSAMPLE (OA GRADE)	9	5.3839	5.3839	0.5982	4.29	0.000
Error	132	18.4258	18.4258	0.1396		
Total	143	25.3216				

S = 0.373617 R-Sq = 27.23% R-Sq(adj) = 21.17%

Unusual Observations for LNSpk/Sk

Obs	LNSpk/Sk	Fit	SE Fit	Residual	St Resid
1	0.56666	-0.36458	0.10785	0.93125	2.60 R
44	0.92889	-0.33720	0.10785	1.26609	3.54 R
50	-1.38924	-0.50359	0.10785	-0.88565	-2.48 R
51	0.36738	-0.50359	0.10785	0.87097	2.43 R
90	-1.00214	-0.23966	0.10785	-0.76248	-2.13 R
95	0.70168	-0.23966	0.10785	0.94134	2.63 R
131	-1.16527	-0.32174	0.10785	-0.84354	-2.36 R
141	0.60890	-0.28499	0.10785	0.89389	2.50 R

R denotes an observation with a large standardized residual.

Grouping Information Using Tukey Method and 95.0% Confidence

OA GRADE	N	Mean	Grouping
3	48	-0.2	A
2	48	-0.2	A B
1	48	-0.4	B

Means that do not share a letter are significantly different.

Tukey Simultaneous Tests

Response Variable LNSpk/Sk

All Pairwise Comparisons among Levels of OA GRADE

OA GRADE = 1 subtracted from:

OA GRADE	Difference of Means	SE of Difference	T-Value	Adjusted P-Value
2	0.1793	0.07626	2.351	0.0524
3	0.2418	0.07626	3.170	0.0054

OA GRADE = 2 subtracted from:

OA GRADE	Difference of Means	SE of Difference	T-Value	Adjusted P-Value
3	0.06245	0.07626	0.8189	0.6920

## Residual Plots for LNSvk/Sk

### General Linear Model: LNSvk/Sk versus OA GRADE, Svk/SkSAMPLE

Factor	Type	Levels	Values
Svk/SkSAMPLE (OA GRADE)	fixed	12	1, 2, 3, 4, 5, 6, 7, 8, 9, 10, 11, 12
OA GRADE	fixed	3	1, 2, 3

Analysis of Variance for LNSvk/Sk, using Adjusted SS for Tests

Source	DF	Seq SS	Adj SS	Adj MS	F	P
Svk/SkSAMPLE (OA GRADE)	9	6.85024	6.85024	0.76114	9.97	0.000
OA GRADE	2	1.60804	1.60804	0.80402	10.53	0.000
Error	132	10.07701	10.07701	0.07634		
Total	143	18.53529				

S = 0.276299 R-Sq = 45.63% R-Sq(adj) = 41.10%

Unusual Observations for LNSvk/Sk

Obs	LNSvk/Sk	Fit	SE Fit	Residual	St Resid
21	0.05924	-0.61686	0.07976	0.67610	2.56 R
29	-1.64110	-0.98208	0.07976	-0.65901	-2.49 R
51	-0.54126	-1.09612	0.07976	0.55486	2.10 R
67	-1.63905	-0.73168	0.07976	-0.90737	-3.43 R
74	-1.47955	-0.87355	0.07976	-0.60600	-2.29 R
107	-1.64572	-1.02091	0.07976	-0.62481	-2.36 R
132	-0.11319	-0.72230	0.07976	0.60910	2.30 R

R denotes an observation with a large standardized residual.

Grouping Information Using Tukey Method and 95.0% Confidence

OA GRADE	N	Mean	Grouping
1	48	-0.7	A
3	48	-0.8	A
2	48	-1.0	B

Means that do not share a letter are significantly different.

Tukey Simultaneous Tests

Response Variable LNSvk/Sk

All Pairwise Comparisons among Levels of OA GRADE

OA GRADE = 1 subtracted from:

OA GRADE	Difference of Means	SE of Difference	T-Value	Adjusted P-Value
2	-0.2579	0.05640	-4.574	0.0000
3	-0.1103	0.05640	-1.955	0.1275

OA GRADE = 2 subtracted from:

OA GRADE	Difference of Means	SE of Difference	T-Value	Adjusted P-Value
3	0.1477	0.05640	2.618	0.0265

## Residual Plots for LNSvk/Sk

## General Linear Model: LNSpk/Svk versus OA GRADE, Spk/SvkSAMPLE

Factor	Type	Levels	Values
OA GRADE	fixed	3	1, 2, 3
Spk/SvkSAMPLE(OA GRADE)	fixed	12	1, 2, 3, 4, 5, 6, 7, 8, 9, 10, 11, 12

Analysis of Variance for LNSpk/Svk, using Adjusted SS for Tests

Source	DF	Seq SS	Adj SS	Adj MS	F	P
OA GRADE	2	5.1580	5.1580	2.5790	14.43	0.000
Spk/SvkSAMPLE(OA GRADE)	9	10.1339	10.1339	1.1260	6.30	0.000
Error	132	23.5860	23.5860	0.1787		
Total	143	38.8779				

S = 0.422708 R-Sq = 39.33% R-Sq(adj) = 34.28%

Unusual Observations for LNSpk/Svk

Obs	LNSpk/Svk	Fit	SE Fit	Residual	St Resid
44	1.85178	0.30722	0.12203	1.54456	3.82 R
49	1.47076	0.59253	0.12203	0.87823	2.17 R
50	-0.23531	0.59253	0.12203	-0.82784	-2.05 R
80	-0.26092	0.56115	0.12203	-0.82207	-2.03 R
95	1.92807	0.86381	0.12203	1.06426	2.63 R
101	0.22186	1.09894	0.12203	-0.87709	-2.17 R
124	1.31065	0.40056	0.12203	0.91009	2.25 R
131	-0.74001	0.40056	0.12203	-1.14057	-2.82 R
141	1.05243	0.06910	0.12203	0.98333	2.43 R
143	-0.97354	0.06910	0.12203	-1.04264	-2.58 R

R denotes an observation with a large standardized residual.

Grouping Information Using Tukey Method and 95.0% Confidence

OA GRADE	N	Mean	Grouping
2	48	0.7	A
3	48	0.6	A
1	48	0.3	B

Means that do not share a letter are significantly different.

Tukey Simultaneous Tests

Response Variable LNSpk/Svk

All Pairwise Comparisons among Levels of OA GRADE

OA GRADE = 1 subtracted from:

OA	Difference	SE of	Adjusted
			188

GRADE	of Means	Difference	T-Value	P-Value
2	0.4372	0.08628	5.067	0.0000
3	0.3520	0.08628	4.080	0.0002

OA GRADE = 2 subtracted from:

OA	Difference	SE of		Adjusted
GRADE	of Means	Difference	T-Value	P-Value
3	-0.08520	0.08628	-0.9875	0.5861

## Residual Plots for LNSpk/Svk

## General Linear Model: LNStdi versus OA GRADE, StdISAMPLE

Factor	Type	Levels	Values
OA GRADE	fixed	3	1, 2, 3
StdISAMPLE(OA GRADE)	fixed	12	1, 2, 3, 4, 5, 6, 7, 8, 9, 10, 11, 12

Analysis of Variance for LNStdi, using Adjusted SS for Tests

Source	DF	Seq SS	Adj SS	Adj MS	F	P
OA GRADE	2	0.58173	0.58173	0.29087	7.35	0.001
StdISAMPLE(OA GRADE)	9	0.82452	0.82452	0.09161	2.32	0.019
Error	132	5.22346	5.22346	0.03957		
Total	143	6.62971				

S = 0.198926 R-Sq = 21.21% R-Sq(adj) = 14.65%

Unusual Observations for LNStdi

Obs	LNStdi	Fit	SE Fit	Residual	St Resid
19	-0.89738	-0.40549	0.05743	-0.49188	-2.58 R
50	-0.88059	-0.49018	0.05743	-0.39040	-2.05 R
79	-1.25528	-0.65578	0.05743	-0.59950	-3.15 R
80	-1.44405	-0.65578	0.05743	-0.78826	-4.14 R
124	-0.82598	-0.43095	0.05743	-0.39503	-2.07 R
141	-0.87782	-0.42715	0.05743	-0.45067	-2.37 R

R denotes an observation with a large standardized residual.

Grouping Information Using Tukey Method and 95.0% Confidence

OA	GRADE	N	Mean	Grouping
	1	48	-0.4	A
	3	48	-0.5	B
	2	48	-0.5	B

Means that do not share a letter are significantly different.

Tukey Simultaneous Tests

Response Variable LNStdi

All Pairwise Comparisons among Levels of OA GRADE

OA GRADE = 1 subtracted from:

OA	Difference	SE of		Adjusted
GRADE	of Means	Difference	T-Value	P-Value

2	-0.1443	0.04061	-3.554	0.0015
3	-0.1227	0.04061	-3.023	0.0084

OA GRADE = 2 subtracted from:

OA GRADE	Difference of Means	SE of Difference	T-Value	Adjusted P-Value
3	0.02156	0.04061	0.5311	0.8562

## Residual Plots for LNStdI

## General Linear Model: LNSrw versus OA GRADE, SrwSAMPLE

Factor	Type	Levels	Values
OA GRADE	fixed	3	1, 2, 3
SrwSAMPLE (OA GRADE)	fixed	12	1, 2, 3, 4, 5, 6, 7, 8, 9, 10, 11, 12

Analysis of Variance for LNSrw, using Adjusted SS for Tests

Source	DF	Seq SS	Adj SS	Adj MS	F	P
OA GRADE	2	0.10378	0.10378	0.05189	1.86	0.160
SrwSAMPLE (OA GRADE)	9	0.38074	0.38074	0.04230	1.52	0.148
Error	132	3.68290	3.68290	0.02790		
Total	143	4.16742				

S = 0.167035 R-Sq = 11.63% R-Sq(adj) = 4.26%

Unusual Observations for LNSrw

Obs	LNSrw	Fit	SE Fit	Residual	St Resid
42	11.6967	12.0305	0.0482	-0.3338	-2.09 R
60	11.7077	12.0488	0.0482	-0.3412	-2.13 R
76	12.7611	12.0498	0.0482	0.7113	4.45 R
95	12.7611	12.0622	0.0482	0.6989	4.37 R
136	12.7611	12.0779	0.0482	0.6832	4.27 R
137	11.6633	12.0779	0.0482	-0.4146	-2.59 R
140	12.7611	12.0779	0.0482	0.6832	4.27 R

R denotes an observation with a large standardized residual.

Grouping Information Using Tukey Method and 95.0% Confidence

OA GRADE	N	Mean	Grouping
2	48	12.0	A
1	48	12.0	A
3	48	12.0	A

Means that do not share a letter are significantly different.

Tukey Simultaneous Tests

Response Variable LNSrw

All Pairwise Comparisons among Levels of OA GRADE

OA GRADE = 1 subtracted from:

OA GRADE	Difference of Means	SE of Difference	T-Value	Adjusted P-Value
----------	---------------------	------------------	---------	------------------

2	0.03962	0.03410	1.1620	0.4780
3	-0.02564	0.03410	-0.7521	0.7329

OA GRADE = 2 subtracted from:

OA GRADE	Difference of Means	SE of Difference	T-Value	Adjusted P-Value
3	-0.06526	0.03410	-1.914	0.1387

## Residual Plots for LNSrwi

### General Linear Model: LNSrwi versus OA GRADE, SrwiSAMPLE

Factor	Type	Levels	Values
OA GRADE	fixed	3	1, 2, 3
SrwiSAMPLE(OA GRADE)	fixed	12	1, 2, 3, 4, 5, 6, 7, 8, 9, 10, 11, 12

Analysis of Variance for LNSrwi, using Adjusted SS for Tests

Source	DF	Seq SS	Adj SS	Adj MS	F	P
OA GRADE	2	0.75184	0.75184	0.37592	8.34	0.000
SrwiSAMPLE(OA GRADE)	9	2.55896	2.55896	0.28433	6.31	0.000
Error	132	5.95116	5.95116	0.04508		
Total	143	9.26196				

S = 0.212331 R-Sq = 35.75% R-Sq(adj) = 30.39%

Unusual Observations for LNSrwi

Obs	LNSrwi	Fit	SE Fit	Residual	St Resid
24	-3.88802	-3.46472	0.06129	-0.42330	-2.08 R
44	-3.76827	-3.22131	0.06129	-0.54696	-2.69 R
87	-3.11912	-3.72311	0.06129	0.60399	2.97 R
103	-4.11748	-3.65253	0.06129	-0.46495	-2.29 R
123	-3.10366	-3.58091	0.06129	0.47726	2.35 R

R denotes an observation with a large standardized residual.

Grouping Information Using Tukey Method and 95.0% Confidence

OA GRADE	N	Mean	Grouping
1	48	-3.5	A
3	48	-3.6	B
2	48	-3.7	B

Means that do not share a letter are significantly different.

Tukey Simultaneous Tests

Response Variable LNSrwi

All Pairwise Comparisons among Levels of OA GRADE

OA GRADE = 1 subtracted from:

OA GRADE	Difference of Means	SE of Difference	T-Value	Adjusted P-Value
2	-0.1756	0.04334	-4.052	0.0003
3	-0.1068	0.04334	-2.465	0.0395

OA GRADE = 2 subtracted from:

OA GRADE	Difference of Means	SE of Difference	T-Value	Adjusted P-Value
3	0.06879	0.04334	1.587	0.2548

## Residual Plots for LNSrwi

## General Linear Model: LNShw versus OA GRADE, ShwSAMPLE

Factor	Type	Levels	Values
OA GRADE	fixed	3	1, 2, 3
ShwSAMPLE (OA GRADE)	fixed	12	1, 2, 3, 4, 5, 6, 7, 8, 9, 10, 11, 12

Analysis of Variance for LNShw, using Adjusted SS for Tests

Source	DF	Seq SS	Adj SS	Adj MS	F	P
OA GRADE	2	3.79604	3.79604	1.89802	41.13	0.000
ShwSAMPLE (OA GRADE)	9	3.38834	3.38834	0.37648	8.16	0.000
Error	132	6.09083	6.09083	0.04614		
Total	143	13.27520				

S = 0.214808 R-Sq = 54.12% R-Sq(adj) = 50.30%

Unusual Observations for LNShw

Obs	LNShw	Fit	SE Fit	Residual	St Resid
24	11.8468	11.4126	0.0620	0.4342	2.11 R
44	11.8468	11.1875	0.0620	0.6592	3.21 R
61	12.0699	11.5771	0.0620	0.4928	2.40 R
64	11.0583	11.5771	0.0620	-0.5188	-2.52 R
68	11.1536	11.5771	0.0620	-0.4235	-2.06 R
87	11.3768	11.8946	0.0620	-0.5178	-2.52 R

R denotes an observation with a large standardized residual.

Grouping Information Using Tukey Method and 95.0% Confidence

OA GRADE	N	Mean	Grouping
2	48	11.8	A
3	48	11.7	B
1	48	11.4	C

Means that do not share a letter are significantly different.

Tukey Simultaneous Tests

Response Variable LNShw

All Pairwise Comparisons among Levels of OA GRADE

OA GRADE = 1 subtracted from:

OA GRADE	Difference of Means	SE of Difference	T-Value	Adjusted P-Value
2	0.3862	0.04385	8.808	0.0000
3	0.2754	0.04385	6.280	0.0000

OA GRADE = 2 subtracted from:

OA GRADE	Difference of Means	SE of Difference	T-Value	Adjusted P-Value
3	-0.1108	0.04385	-2.527	0.0337

## Residual Plots for LNShw

## General Linear Model: LNSfd versus OA GRADE, SfdSAMPLE

Factor	Type	Levels	Values
OA GRADE	fixed	3	1, 2, 3
SfdSAMPLE (OA GRADE)	fixed	12	1, 2, 3, 4, 5, 6, 7, 8, 9, 10, 11, 12

Analysis of Variance for LNSfd, using Adjusted SS for Tests

Source	DF	Seq SS	Adj SS	Adj MS	F	P
OA GRADE	2	0.129933	0.129933	0.064966	246.44	0.000
SfdSAMPLE (OA GRADE)	9	0.013743	0.013743	0.001527	5.79	0.000
Error	132	0.034797	0.034797	0.000264		
Total	143	0.178473				

S = 0.0162363 R-Sq = 80.50% R-Sq(adj) = 78.88%

Unusual Observations for LNSfd

Obs	LNSfd	Fit	SE Fit	Residual	St Resid
1	0.818426	0.854461	0.004687	-0.036034	-2.32 R
19	0.885250	0.846759	0.004687	0.038491	2.48 R
21	0.795397	0.846759	0.004687	-0.051362	-3.30 R
22	0.799550	0.846759	0.004687	-0.047209	-3.04 R
24	0.882283	0.846759	0.004687	0.035524	2.29 R
44	0.834994	0.873293	0.004687	-0.038299	-2.46 R
51	0.774589	0.808968	0.004687	-0.034379	-2.21 R
64	0.847168	0.793312	0.004687	0.053856	3.46 R

R denotes an observation with a large standardized residual.

Grouping Information Using Tukey Method and 95.0% Confidence

OA GRADE	N	Mean	Grouping
1	48	0.9	A
2	48	0.8	B
3	48	0.8	B

Means that do not share a letter are significantly different.

Tukey Simultaneous Tests

Response Variable LNSfd

All Pairwise Comparisons among Levels of OA GRADE

OA GRADE = 1 subtracted from:

OA GRADE	Difference of Means	SE of Difference	T-Value	Adjusted P-Value
2	-0.06153	0.003314	-18.57	0.0000
3	-0.06571	0.003314	-19.83	0.0000

OA GRADE = 2 subtracted from:

OA GRADE	Difference of Means	SE of Difference	T-Value	Adjusted P-Value
3	-0.004175	0.003314	-1.260	0.4205

## Residual Plots for LNSfd

## General Linear Model: LNScl20 versus OA GRADE, Sc120SAMPLE

Factor	Type	Levels	Values
Sc120SAMPLE(OA GRADE)	fixed	12	1, 2, 3, 4, 5, 6, 7, 8, 9, 10, 11, 12
OA GRADE	fixed	3	1, 2, 3

Analysis of Variance for LNScl20, using Adjusted SS for Tests

Source	DF	Seq SS	Adj SS	Adj MS	F	P
Sc120SAMPLE(OA GRADE)	9	1.81937	1.81937	0.20215	5.58	0.000
OA GRADE	2	0.41910	0.41910	0.20955	5.79	0.004
Error	132	4.78035	4.78035	0.03621		
Total	143	7.01882				

S = 0.190302 R-Sq = 31.89% R-Sq(adj) = 26.22%

Unusual Observations for LNScl20

Obs	LNScl20	Fit	SE Fit	Residual	St Resid
19	11.0144	10.5847	0.0549	0.4297	2.36 R
22	10.1895	10.5847	0.0549	-0.3952	-2.17 R
23	11.0033	10.5847	0.0549	0.4185	2.30 R
44	10.8953	10.4318	0.0549	0.4634	2.54 R
45	9.9599	10.4318	0.0549	-0.4719	-2.59 R
76	11.1309	10.7526	0.0549	0.3783	2.08 R
99	11.1605	10.6646	0.0549	0.4959	2.72 R
140	11.1986	10.7351	0.0549	0.4635	2.54 R

R denotes an observation with a large standardized residual.

Grouping Information Using Tukey Method and 95.0% Confidence

OA GRADE	N	Mean	Grouping
2	48	10.8	A
3	48	10.7	A B
1	48	10.6	B

Means that do not share a letter are significantly different.

Tukey Simultaneous Tests

Response Variable LNScl20

All Pairwise Comparisons among Levels of OA GRADE

OA GRADE = 1 subtracted from:

OA GRADE	Difference of Means	SE of Difference	T-Value	Adjusted P-Value
2	0.13211	0.03885	3.401	0.0026

3	0.06322	0.03885	1.627	0.2378
---	---------	---------	-------	--------

OA GRADE = 2 subtracted from:

OA GRADE	Difference of Means	SE of Difference	T-Value	Adjusted P-Value
3	-0.06889	0.03885	-1.773	0.1825

## Residual Plots for LNSci20

## General Linear Model: LNSci37 versus OA GRADE, Sci37SAMPLE

Factor	Type	Levels	Values
OA GRADE	fixed	3	1, 2, 3
Sci37SAMPLE(OA GRADE)	fixed	12	1, 2, 3, 4, 5, 6, 7, 8, 9, 10, 11, 12

Analysis of Variance for LNSci37, using Adjusted SS for Tests

Source	DF	Seq SS	Adj SS	Adj MS	F	P
OA GRADE	2	1.87981	1.87981	0.93991	15.11	0.000
Sci37SAMPLE(OA GRADE)	9	5.27909	5.27909	0.58657	9.43	0.000
Error	132	8.21044	8.21044	0.06220		
Total	143	15.36934				

S = 0.249400    R-Sq = 46.58%    R-Sq(adj) = 42.13%

Unusual Observations for LNSci37

Obs	LNSci37	Fit	SE Fit	Residual	St Resid
41	9.1649	9.7338	0.0720	-0.5689	-2.38 R
43	10.2149	9.7338	0.0720	0.4811	2.01 R
44	10.5688	9.7338	0.0720	0.8349	3.50 R
45	8.9238	9.7338	0.0720	-0.8100	-3.39 R
46	9.2340	9.7338	0.0720	-0.4999	-2.09 R
99	10.8696	10.3587	0.0720	0.5109	2.14 R
123	9.7839	10.3755	0.0720	-0.5916	-2.48 R

R denotes an observation with a large standardized residual.

Grouping Information Using Tukey Method and 95.0% Confidence

OA GRADE	N	Mean	Grouping
2	48	10.4	A
3	48	10.4	A
1	48	10.2	B

Means that do not share a letter are significantly different.

Tukey Simultaneous Tests

Response Variable LNSci37

All Pairwise Comparisons among Levels of OA GRADE

OA GRADE = 1 subtracted from:

OA GRADE	Difference of Means	SE of Difference	T-Value	Adjusted P-Value
2	0.2701	0.05091	5.306	0.0000

3	0.1985	0.05091	3.899	0.0005
---	--------	---------	-------	--------

OA GRADE = 2 subtracted from:

OA GRADE	Difference of Means	SE of Difference	T-Value	Adjusted P-Value
3	-0.07161	0.05091	-1.407	0.3405

## Residual Plots for LNScl37

## General Linear Model: LNSdc0\_5 versus OA GRADE, Scd0\_5SAMPLE

Factor	Type	Levels	Values
OA GRADE	fixed	3	1, 2, 3
Scd0_5SAMPLE (OA GRADE)	fixed	12	1, 2, 3, 4, 5, 6, 7, 8, 9, 10, 11, 12

Analysis of Variance for LNSdc0\_5, using Adjusted SS for Tests

Source	DF	Seq SS	Adj SS	Adj MS	F	P
OA GRADE	2	29.3245	29.3245	14.6622	84.74	0.000
Scd0_5SAMPLE (OA GRADE)	9	11.3931	11.3931	1.2659	7.32	0.000
Error	132	22.8402	22.8402	0.1730		
Total	143	63.5577				

S = 0.415971    R-Sq = 64.06%    R-Sq(adj) = 61.07%

Unusual Observations for LNSdc0\_5

Obs	LNSdc0_5	Fit	SE Fit	Residual	St Resid
1	11.3617	10.4381	0.1201	0.9236	2.32 R
19	9.1626	10.5032	0.1201	-1.3406	-3.37 R
44	11.2130	10.2302	0.1201	0.9828	2.47 R
49	11.6411	10.7275	0.1201	0.9136	2.29 R
51	12.4600	10.7275	0.1201	1.7325	4.35 R
53	9.8709	10.7275	0.1201	-0.8566	-2.15 R
136	12.1314	11.3323	0.1201	0.7991	2.01 R

R denotes an observation with a large standardized residual.

Grouping Information Using Tukey Method and 95.0% Confidence

OA GRADE	N	Mean	Grouping
3	48	11.2	A
2	48	11.2	A
1	48	10.3	B

Means that do not share a letter are significantly different.

Tukey Simultaneous Tests

Response Variable LNSdc0\_5

All Pairwise Comparisons among Levels of OA GRADE

OA GRADE = 1 subtracted from:

OA GRADE	Difference of Means	SE of Difference	T-Value	Adjusted P-Value
2	0.9280	0.08491	10.93	0.0000

3	0.9841	0.08491	11.59	0.0000
---	--------	---------	-------	--------

OA GRADE = 2 subtracted from:

OA GRADE	Difference of Means	SE of Difference	T-Value	Adjusted P-Value
3	0.05604	0.08491	0.6600	0.7870

## Residual Plots for LNSdc0\_5

### General Linear Model: LNStr37 versus OA GRADE, Str37SAMPLE

Factor	Type	Levels	Values
OA GRADE	fixed	3	1, 2, 3
Str37SAMPLE(OA GRADE)	fixed	12	1, 2, 3, 4, 5, 6, 7, 8, 9, 10, 11, 12

Analysis of Variance for LNStr37, using Adjusted SS for Tests

Source	DF	Seq SS	Adj SS	Adj MS	F	P
OA GRADE	2	0.1638	0.1638	0.0819	0.76	0.471
Str37SAMPLE(OA GRADE)	9	1.5600	1.5600	0.1733	1.60	0.121
Error	132	14.2939	14.2939	0.1083		
Total	143	16.0178				

S = 0.329071 R-Sq = 10.76% R-Sq(adj) = 3.33%

Unusual Observations for LNStr37

Obs	LNStr37	Fit	SE Fit	Residual	St Resid
32	-1.33709	-0.61953	0.09499	-0.71756	-2.28 R
62	-1.41453	-0.60454	0.09499	-0.80999	-2.57 R
95	-1.75450	-0.48306	0.09499	-1.27145	-4.04 R
103	-1.49900	-0.62753	0.09499	-0.87147	-2.77 R
113	-1.13731	-0.50382	0.09499	-0.63349	-2.01 R
117	-1.17557	-0.50382	0.09499	-0.67175	-2.13 R
141	-1.99220	-0.53824	0.09499	-1.45396	-4.61 R

R denotes an observation with a large standardized residual.

Grouping Information Using Tukey Method and 95.0% Confidence

OA GRADE	N	Mean	Grouping
3	48	-0.5	A
1	48	-0.5	A
2	48	-0.6	A

Means that do not share a letter are significantly different.

Tukey Simultaneous Tests

Response Variable LNStr37

All Pairwise Comparisons among Levels of OA GRADE

OA GRADE = 1 subtracted from:

OA GRADE	Difference of Means	SE of Difference	T-Value	Adjusted P-Value
2	-0.05628	0.06717	-0.8379	0.6802

3	0.02424	0.06717	0.3609	0.9308
---	---------	---------	--------	--------

OA GRADE = 2 subtracted from:

OA GRADE	Difference of Means	SE of Difference	T-Value	Adjusted P-Value
3	0.08052	0.06717	1.199	0.4560

## Residual Plots for LNStr37

---

**25/11/2013 10:59:25 AM**

---

Welcome to Minitab, press F1 for help.  
 Retrieving project from file: 'D:\USERS\Z3399001\DESKTOP\UPDATED  
 DATA\21-11\35 PARAM.MPJ'

## Tabulated statistics: OA GRADE

Columns: OA GRADE

1	2	3	All
2.374	2.232	2.223	2.276
0.05528	0.03614	0.03298	0.08136
48	48	48	144

Cell Contents: Sfd : Mean  
 Sfd : Standard deviation  
 Count

## Tabulated statistics: OA GRADE

Columns: OA GRADE

1	2	3	All
11457	38157	52898	34171
3330	13891	23830	23451
48	48	48	144

Cell Contents: Sk : Mean  
 Sk : Standard deviation  
 Count

## General Linear Model: LNSfd versus OA GRADE, SfdSAMPLE

Factor	Type	Levels	Values
OA GRADE	fixed	3	1, 2, 3
SfdSAMPLE (OA GRADE)	random	12	1, 2, 3, 4, 1, 2, 5, 6, 3, 7, 8, 9

Analysis of Variance for LNSfd, using Adjusted SS for Tests

Source	DF	Seq SS	Adj SS	Adj MS	F	P
OA GRADE	2	0.129933	0.129933	0.064966	42.55	0.000

SfdSAMPLE (OA GRADE)	9	0.013743	0.013743	0.001527	5.79	0.000
Error	132	0.034797	0.034797	0.000264		
Total	143	0.178473				

S = 0.0162363    R-Sq = 80.50%    R-Sq(adj) = 78.88%

Unusual Observations for LNSfd

Obs	LNSfd	Fit	SE Fit	Residual	St Resid
1	0.818426	0.854461	0.004687	-0.036034	-2.32 R
19	0.885250	0.846759	0.004687	0.038491	2.48 R
21	0.795397	0.846759	0.004687	-0.051362	-3.30 R
22	0.799550	0.846759	0.004687	-0.047209	-3.04 R
24	0.882283	0.846759	0.004687	0.035524	2.29 R
44	0.834994	0.873293	0.004687	-0.038299	-2.46 R
51	0.774589	0.808968	0.004687	-0.034379	-2.21 R
64	0.847168	0.793312	0.004687	0.053856	3.46 R

R denotes an observation with a large standardized residual.

## Residual Plots for LNSfd

## Appendix D.2 Correlation between numerical parameters

25/02/2014 10:58:11 AM

Welcome to Minitab, press F1 for help.  
Retrieving project from file: 'D:\USERS\Z3399001\DESKTOP\UPDATED  
DATA\21-11\35 PARAMETER.MPJ'

### Correlations: Sa, Sq, Sdc10\_50, Sk, Sdc5\_10, S10z, Sy, Spk, ...

	Sa	Sq	Sdc10_50	Sk	Sdc5_10	S10z	Sy
Sq	0.996 0.000						
Sdc10_50	0.970 0.000	0.967 0.000					
Sk	0.980 0.000	0.963 0.000	0.940 0.000				
Sdc5_10	0.788 0.000	0.818 0.000	0.848 0.000	0.719 0.000			
S10z	0.868 0.000	0.896 0.000	0.862 0.000	0.813 0.000	0.793 0.000		
Sy	0.851 0.000	0.880 0.000	0.848 0.000	0.794 0.000	0.788 0.000	0.996 0.000	
Spk	0.806 0.000	0.842 0.000	0.868 0.000	0.727 0.000	0.962 0.000	0.871 0.000	0.868 0.000

Sdc50_95	0.926 0.000	0.921 0.000	0.820 0.000	0.902 0.000	0.591 0.000	0.759 0.000	0.739 0.000
Svk	0.866 0.000	0.867 0.000	0.749 0.000	0.834 0.000	0.513 0.000	0.736 0.000	0.715 0.000
Sv	0.839 0.000	0.850 0.000	0.801 0.000	0.809 0.000	0.656 0.000	0.910 0.000	0.915 0.000
Sdq6	0.843 0.000	0.853 0.000	0.766 0.000	0.787 0.000	0.588 0.000	0.781 0.000	0.769 0.000
Sdq	0.833 0.000	0.842 0.000	0.753 0.000	0.776 0.000	0.571 0.000	0.765 0.000	0.752 0.000
Sdr	0.730 0.000	0.734 0.000	0.619 0.000	0.670 0.000	0.418 0.000	0.609 0.000	0.594 0.000
S3A	0.730 0.000	0.734 0.000	0.619 0.000	0.670 0.000	0.418 0.000	0.609 0.000	0.594 0.000
Shw	0.377 0.000	0.357 0.000	0.383 0.000	0.414 0.000	0.341 0.000	0.183 0.028	0.170 0.042
Sdc50_95	Spk 0.610 0.000	Sdc50_95	Svk	Sv	Sdq6	Sdq	Sdr
Svk	0.543 0.000	0.968 0.000					
Sv	0.704 0.000	0.788 0.000	0.792 0.000				
Sdq6	0.627 0.000	0.890 0.000	0.893 0.000	0.790 0.000			
Sdq	0.610 0.000	0.886 0.000	0.891 0.000	0.778 0.000	1.000 0.000		
Sdr	0.439 0.000	0.867 0.000	0.877 0.000	0.659 0.000	0.948 0.000	0.954 0.000	
S3A	0.439 0.000	0.867 0.000	0.877 0.000	0.659 0.000	0.948 0.000	0.954 0.000	1.000 0.000
Shw	0.299 0.000	0.301 0.000	0.172 0.039	0.146 0.081	0.016 0.851	0.010 0.909	0.009 0.914
Shw	S3A 0.009 0.914						

Cell Contents: Pearson correlation  
P-Value